

**Bangor University**

## **DOCTOR OF PHILOSOPHY**

### **The effect of magnetic field on the dielectric properties of DNA**

Owen, Robert

*Award date:*  
2012

*Awarding institution:*  
Bangor University

[Link to publication](#)

#### **General rights**

Copyright and moral rights for the publications made accessible in the public portal are retained by the authors and/or other copyright owners and it is a condition of accessing publications that users recognise and abide by the legal requirements associated with these rights.

- Users may download and print one copy of any publication from the public portal for the purpose of private study or research.
- You may not further distribute the material or use it for any profit-making activity or commercial gain
- You may freely distribute the URL identifying the publication in the public portal ?

#### **Take down policy**

If you believe that this document breaches copyright please contact us providing details, and we will remove access to the work immediately and investigate your claim.

The Effect of  
Magnetic Field  
on the  
Dielectric Properties of DNA

R. Brynmor Owen

February 16th 2012

PhD Thesis, Bangor University

Page i - to be replaced before binding

Page ii - to be replaced before binding

Page iii - to be replaced before binding

# Contents

<b>Abstract</b>	<b>xv</b>
<b>Acknowledgments</b>	<b>xvi</b>
<b>List of Figures</b>	<b>xvii</b>
<b>1 A Review of Relevant Literature</b>	<b>1</b>
1.1 Introduction . . . . .	1
1.2 Dielectric properties of DNA . . . . .	1
1.3 Diamagnetic Anisotropy . . . . .	6
1.4 DNA . . . . .	8
1.5 Liquid Crystalline DNA . . . . .	10
1.6 DNA at Lower concentration . . . . .	13
1.7 Orientation of Sperm nuclei . . . . .	15
1.8 Aims and Objectives of thesis . . . . .	21

1.8.1	Current knowledge . . . . .	21
1.8.2	Aims and objectives . . . . .	21
1.9	Outline of thesis . . . . .	22
<b>2</b>	<b>Theory</b>	<b>24</b>
2.1	Dielectric Relaxation Spectroscopy . . . . .	24
2.2	Dielectric Permittivity . . . . .	25
2.2.1	Polarization . . . . .	29
2.2.1.1	Electronic polarization . . . . .	29
2.2.1.2	Atomic polarization . . . . .	30
2.2.1.3	Ionic polarization . . . . .	30
2.2.1.4	Orientation polarization . . . . .	31
2.2.1.5	Interfacial or Space-Charge polarization . . . . .	33
2.2.2	Alternating Fields . . . . .	34
2.2.3	Cole-Cole distributions . . . . .	40
2.2.4	Cole-Cole Plots . . . . .	42
2.2.5	Multiple Dispersions . . . . .	44
2.2.6	D.C. Conductivity . . . . .	46

2.2.7	Electrode polarization . . . . .	46
2.2.8	Maxwell-Wagner Polarization . . . . .	49
2.3	Structure of DNA . . . . .	52
2.3.1	Structure of DNA backbone . . . . .	52
2.3.2	Construction of nucleotides . . . . .	53
2.3.3	Construction of DNA strand . . . . .	55
2.3.4	Simplification . . . . .	55
2.3.5	Denaturing DNA . . . . .	58
2.3.6	Counter-ion layer . . . . .	59
2.4	Diamagnetism . . . . .	60
2.5	Detection of small changes in dielectric properties . . . . .	62
2.6	Genetic Algorithms . . . . .	70
2.6.1	Initialisation . . . . .	70
2.6.2	Selection . . . . .	71
2.6.3	Crossover . . . . .	71
2.6.4	Mutation . . . . .	72
2.6.5	Termination . . . . .	72



2.6.6	Matlab Genetic Algorithm Toolbox . . . . .	72
2.7	Reliability of Genetic Algorithm Analysis . . . . .	73
2.7.1	Dielectric Decrement . . . . .	78
2.7.2	Frequencies . . . . .	79
2.7.3	Spreading parameter h . . . . .	80
2.7.4	D.C.Conductivity . . . . .	81
2.7.5	Conclusion . . . . .	82
<b>3</b>	<b>Experimental</b>	<b>83</b>
3.1	Introduction . . . . .	83
3.2	Equipment overview . . . . .	84
3.2.1	Design of Brass Enclosure . . . . .	84
3.2.2	The computers . . . . .	86
3.2.3	External equipment . . . . .	88
3.2.4	Computer control . . . . .	90
3.2.4.1	Introduction to RiscOS . . . . .	90
3.2.5	Wayne-Kerr Component Analyser . . . . .	92
3.2.6	Keithley Electrometer . . . . .	97

3.2.7	Multimeter . . . . .	99
3.2.8	Eurotherm . . . . .	102
3.2.9	Reading Temperature . . . . .	104
3.2.10	Reading Relative Humidity . . . . .	105
3.2.11	Control of Power Supply . . . . .	105
3.2.12	RiscPC to A3020 . . . . .	113
3.2.12.1	The GenLib library . . . . .	113
3.2.12.2	The Worker program . . . . .	118
3.2.13	Example program . . . . .	118
3.2.13.1	PROCCheckList . . . . .	120
3.2.13.2	PROCPSSetUp . . . . .	121
3.2.13.3	Set temperature . . . . .	121
3.2.13.4	Create log file . . . . .	122
3.2.13.5	Setting variables to initial values . . . . .	122
3.2.13.6	Beginning the main loop . . . . .	122
3.2.13.7	Create a folder for the data . . . . .	123
3.2.13.8	The first frequency run . . . . .	123

3.2.13.9	Increase current to Target_Current(max.i%) . . . .	124
3.2.13.10	The second frequency run . . . . .	125
3.2.13.11	Decrease current to zero . . . . .	125
3.2.13.12	The third frequency run . . . . .	126
3.2.13.13	Wait for sample to stabilize . . . . .	126
3.2.13.14	Repeating the program . . . . .	126
3.3	Calibration of Electromagnet . . . . .	130
3.4	Effect of low magnetic fields on high concentration DNA . . . . .	133
3.4.1	Introduction . . . . .	133
3.4.2	Constant concentration . . . . .	136
3.4.3	Higher concentrations . . . . .	136
3.4.4	Evaporation of DNA solution in controlled conditions . . . .	137
3.4.5	Monitoring the temperature . . . . .	139
3.5	Effect of low magnetic fields on low concentration DNA . . . . .	139
3.5.1	Preparation . . . . .	139
3.5.2	Preliminary study . . . . .	141
3.5.3	Full experiment . . . . .	141

3.5.4	Control Experiments . . . . .	143
3.5.5	Varying the concentration of DNA . . . . .	144
3.5.6	Variation of Temperature . . . . .	145
3.5.7	Variation of added Sodium Chloride . . . . .	145
3.5.8	Variation of Voltage used . . . . .	146
3.5.9	Dialysis of DNA with other salts . . . . .	147
<b>4</b>	<b>Effect of low magnetic fields on high concentration DNA - Results</b>	<b>148</b>
4.1	Introduction . . . . .	148
4.2	Constant concentration . . . . .	149
4.3	Higher concentrations . . . . .	152
4.4	Evaporation of DNA solution in controlled conditions . . . . .	154
4.5	Interpretation of Relative Humidity Graphs . . . . .	163
4.6	Monitoring the temperature . . . . .	165
4.7	Significance of Peak Gof changes . . . . .	168
<b>5</b>	<b>Effect of low magnetic fields on low concentration DNA - Results</b>	<b>173</b>
5.1	Introduction . . . . .	173
5.2	Preliminary study . . . . .	174

5.3	Full experiment . . . . .	176
5.4	Control Experiments . . . . .	181
5.5	Varying the concentration of DNA . . . . .	184
5.6	Analysis of data using Matlab . . . . .	187
5.6.1	Analysis of Dielectric Loss . . . . .	187
5.6.2	Analysis of Difference Signal . . . . .	188
5.6.3	Analysis of Change of DS with magnetic field . . . . .	190
5.6.4	Analysis of change in DS with concentration . . . . .	194
5.6.5	Variation of Temperature . . . . .	197
5.6.5.1	Discussion of effect of temperature . . . . .	201
5.6.6	Variation of added Sodium Chloride . . . . .	206
5.6.7	Variation of Voltage used . . . . .	209
5.7	Summary of factors affecting dispersion . . . . .	212
5.7.1	By investigation . . . . .	213
5.7.1.1	Magnetic field . . . . .	213
5.7.1.2	Concentration . . . . .	215
5.7.1.3	Temperature . . . . .	215

5.7.1.4	Added Sodium Chloride . . . . .	216
5.7.1.5	Voltage . . . . .	216
5.7.2	By parameter . . . . .	217
5.7.2.1	Dielectric decrement . . . . .	217
5.7.2.2	Frequency . . . . .	218
5.7.2.3	Cole-Cole spreading parameter . . . . .	219
5.7.2.4	D.C.Conductivity . . . . .	219
5.8	Dialysis of DNA with other salts . . . . .	220
5.9	Discussion of dialysis of DNA with other salts . . . . .	224
5.9.1	Diamagnetism . . . . .	225
5.9.2	Radii . . . . .	225
5.9.3	Diffusion . . . . .	228
5.9.4	Hydration . . . . .	230
5.9.5	General properties . . . . .	232
5.9.6	Conclusions . . . . .	232
5.10	Cause of dispersion . . . . .	235
<b>6</b>	<b>Conclusion</b>	<b>238</b>

<i>CONTENTS</i>	xiii
6.1 General Conclusions . . . . .	238
6.2 Further Work . . . . .	243
<b>Appendices</b>	<b>246</b>
<b>A WKLib</b>	<b>246</b>
<b>B KeithleyLib</b>	<b>253</b>
<b>C PSLib</b>	<b>256</b>
<b>D EuroLib</b>	<b>262</b>
<b>E MMLib</b>	<b>269</b>
<b>F GenLib</b>	<b>272</b>
<b>G ShowLib</b>	<b>280</b>
<b>H Main Program</b>	<b>286</b>
<b>I Worker Program</b>	<b>293</b>
<b>J MATLAB: Dielectric Data Analysis</b>	<b>309</b>
J.1 WGA3_LF.m . . . . .	309
J.2 WCC3_LF . . . . .	318

<i>CONTENTS</i>	xiv
J.3 W_Get_data(A) . . . . .	320
<b>K MATLAB: Difference Signal Analysis</b>	<b>321</b>
K.1 Diff_main . . . . .	321
K.2 Diff_calc . . . . .	331
K.3 Diff_get_data . . . . .	333
<b>L BASIC Serial Library</b>	<b>334</b>
<b>M BASIC GPIB Libraries</b>	<b>343</b>
M.1 BAS488 Library . . . . .	343
M.2 XBAS488 Library . . . . .	353
<b>N Dialysis of DNA with other salts</b>	<b>373</b>
N.0.1 Lithium Chloride . . . . .	374
N.0.2 Sodium Chloride . . . . .	376
N.0.3 Potassium Chloride . . . . .	378
N.0.4 Rubidium Chloride . . . . .	380
N.0.5 Calcium Chloride . . . . .	382
<b>Bibliography</b>	<b>384</b>



## Abstract

Previous workers have shown that high magnetic fields cause morphological changes in DNA at high concentration where it exists as the liquid crystal cholesteric phase. The aim of the present work was to identify corresponding changes in the dielectric properties of DNA in the frequency range 20 Hz to 300 kHz, at lower magnetic field intensity and lower concentrations.

Investigations were carried out with DNA solution on interdigitated electrodes, where the magnetic field was applied perpendicular to the electric field. Evidence was found of reversible changes in the dielectric properties caused by magnetic fields lower than 0.7 Tesla at high concentrations ( $\sim 170$  mg/ml). Using planar electrodes, where the magnetic field was applied parallel to the electric field, reversible changes in dielectric properties due to magnetic fields of lower than 0.7 Tesla were found in DNA solutions at lower concentrations (25 – 100 mg/ml). Replacement of the sodium in the DNA with other cations by dialysis produced similar results, though the frequencies of the responses also varied with the cations used.

A method was developed using Matlab's Genetic Algorithm toolbox to analyse the *difference* between loss spectra caused by changes in one dispersion. The method was able to extract the parameters of the dispersion before and after application of the magnetic field. Changes in these parameters with concentration, temperature, additional sodium chloride, and applied a.c.voltage are reported. Changes with temperature indicate that an Arrhenius-type process is responsible for the dispersion. Evidence was presented that the dispersion found to be susceptible to magnetic field was caused by relaxation of the counter-ions in the condensed phase surrounding the DNA chain.

# Acknowledgments

During the years I have been working on this thesis I have met many different people who have contributed, in one way or another to the final outcome.

To my fellow student Mr Gareth Thomas I would like to extend my thanks for sharing the beginning of his journey to becoming an internet entrepreneur.

I am grateful to Mr Iwan Jones for improving on my rudimentary ideas for building several parts of the apparatus used in the present work, but above all for designing and constructing the final devices with skill and accuracy.

I would like to thank Mr Aled Williams and Dr Gwyn Roberts from Industrial Development Bangor (IDB) for their help and advice with circuit design.

Above all, I wish to thank my supervisor, Dr. Stephen Bone, for his guidance, support, good humour and endless patience, and for sharing his experience of the world of scientific research.

Diolch yn fawr

# List of Figures

1.1	Diagram of DNA sample in controlled drying experiment . . . . .	11
1.2	DNA cholesteric phase with no magnetic field (Van Winkle et al., 1990)	11
1.3	DNA cholesteric phase with magnetic field (Van Winkle et al., 1990)	12
1.4	Representation of chain alignment in evaporation . . . . .	14
1.5	Intensity of the light scattering from a suspension of sperm cells at right angles . . . . .	16
1.6	Magnetic response of DNA . . . . .	17
1.7	Optical microscopic photographs of cilia in a magnetic field . . . . .	18
1.8	Optical microscopic photographs of heads extracted from bull sperms in a magnetic field . . . . .	19
1.9	Optical microscopic photographs of bull sperms with no magnetic field (Takeuchi et al., 2001) . . . . .	19
1.10	Optical microscopic photographs of bull sperms in a magnetic field .	20

2.1	Parallel plate capacitor in vacuum . . . . .	25
2.2	Parallel plate capacitor with dielectric . . . . .	27
2.3	Graphical representation of the Langevin function . . . . .	32
2.4	Variation of permittivity with frequency (Hz) . . . . .	38
2.5	Variation of dielectric loss with frequency (Hz) . . . . .	39
2.6	Permittivity vs LOG frequency (Hz) ( $h=0.2$ ) . . . . .	41
2.7	Loss vs LOG frequency (Hz) ( $h=0.2$ ) . . . . .	41
2.8	Cole-Cole plot - Single relaxation time ( $h=0$ ) . . . . .	42
2.9	Cole-Cole plot - distribution of relaxation times ( $h=0.2$ ) . . . . .	43
2.10	Loss vs LOG frequency (Hz) for multiple dispersions . . . . .	45
2.11	Cole-Cole plot for multiple dispersions . . . . .	45
2.12	Loss vs LOG frequency for 2 dispersions . . . . .	47
2.13	Loss vs LOG frequency for 2 dispersions + DC conductivity . . . . .	47
2.14	The two-layer heterogeneous system . . . . .	49
2.15	Ribose and Deoxyribose . . . . .	52
2.16	Ribose and Deoxyribose . . . . .	53
2.17	Attachment of base . . . . .	54

2.18 (a) Cytosine (b) Thymine (c) Adenine (d) Guanine . . . . .	54
2.19 Nucleotide containing Cytosine . . . . .	55
2.20 Construction of DNA strand . . . . .	56
2.21 Simplified construction of DNA strand . . . . .	56
2.22 Simplified paired DNA strands . . . . .	57
2.23 Model of Structure of DNA . . . . .	58
2.24 Simulation of Loss graphs (upper) and dLoss graph (lower) for in- crease in frequency of highest frequency dispersion . . . . .	64
2.25 dLoss graph for decrease in frequency of highest frequency dispersion	66
2.26 dLoss graph for decrease in $h$ of highest frequency dispersion . . . .	66
2.27 dLoss graph for increase in $h$ of highest frequency dispersion . . . .	67
2.28 dLoss graph for increase in $d\varepsilon$ of highest frequency dispersion . . . .	68
2.29 dLoss graph for decrease in $d\varepsilon$ of highest frequency dispersion . . . .	68
2.30 Results of Genetic Algorithm Simulation . . . . .	74
2.31 Results of Genetic Algorithm Simulation . . . . .	75
2.32 GA simulation: Dielectric Decrement . . . . .	77
2.33 GA simulation: LOG Frequencies . . . . .	79
2.34 GA simulation: Spreading parameter . . . . .	80

2.35	GA simulation: D.C.Conductivity . . . . .	81
3.1	Block diagram of Apparatus . . . . .	85
3.2	Brass enclosure . . . . .	87
3.3	Relationship between software libraries . . . . .	93
3.4	Temperature probe circuit . . . . .	97
3.5	Power supply gear system . . . . .	106
3.6	Power supply micro-switches . . . . .	106
3.7	Computer connection to micro-switches . . . . .	107
3.8	Simplified control circuit for stepper-motor . . . . .	108
3.9	Computer connection to stepper motor circuit . . . . .	108
3.10	Example program . . . . .	119
3.11	Direction of $\max_i$ . . . . .	127
3.12	Procedure to increase current . . . . .	128
3.13	Procedure to decrease current . . . . .	129
3.14	Calibration of electromagnet - current increasing . . . . .	131
3.15	Calibration of electromagnet - current decreasing . . . . .	132
3.16	Interdigitated electrode design . . . . .	134

3.17 DNA solution on interdigitated electrode . . . . .	135
3.18 Planar electrodes . . . . .	140
4.1 Change in dGof with change in magnetic field . . . . .	150
4.2 dGof at 500 Hz vs time (min), magnetic field increasing and then decreasing . . . . .	151
4.3 DNA Gof spectrum between 10-16 hours . . . . .	152
4.4 Change in single frequency Gof for first 30 hours . . . . .	153
4.5 Maximum Gof versus Time . . . . .	156
4.6 Frequency of Maximum Gof versus Time . . . . .	156
4.7 Relative Humidity versus Time . . . . .	157
4.8 Maximum Gof versus Time: Close-up . . . . .	158
4.9 Frequency of Maximum Gof versus Time: Close-up . . . . .	159
4.10 Relative Humidity versus Time: Close-up . . . . .	160
4.11 Maximum Gof versus Time: Close-up 2 . . . . .	161
4.12 Relative Humidity versus Time: Close-up 2 . . . . .	162
4.13 Local Temperature versus time (top) and Maximum Gof versus Time (bottom) . . . . .	166

4.14 Local Temperature versus time (top) and Maximum Gof versus Time  
(bottom) . . . . . 167

4.15 Local Temperature versus time (top) and Maximum Gof versus Time  
(bottom) . . . . . 171

4.16 True and Expected responses to Magnetic Field . . . . . 172

5.1 Percentage change in Loss as electromagnet current is varied. . . . . 175

5.2 Percentage change in Loss as electromagnet current is varied. . . . . 176

5.3 Change in Loss due to Magnetic field . . . . . 177

5.4 Change in Loss due to Magnetic field . . . . . 178

5.5 Change in Loss for 5000Hz (upper) and 600Hz (lower) . . . . . 179

5.6 Change in Loss vs. Magnetic field at 5000Hz . . . . . 180

5.7 Change in Loss vs. Magnetic field at 600Hz . . . . . 180

5.8 Change in Loss vs. Magnetic field at 5000Hz . . . . . 181

5.9 Change in Loss vs. Magnetic field at 600Hz . . . . . 182

5.10 DNA : Magnitude of Maximum of DS vs. Concentration . . . . . 184

5.11 DNA : Frequency of Maximum of DS vs. Concentration . . . . . 185

5.12 DNA : Magnitude of Minimum of Difference Signal vs. Concentration 185

5.13 DNA : Frequency of Minimum of Difference Signal vs. Concentration 186



5.14 Loss vs. LOG Frequency for DNA (50mg/ml) . . . . .	187
5.15 Difference Signal for DNA (50mg/ml) . . . . .	189
5.16 Dielectric decrement vs. magnetic field for DNA (50mg/ml) . . . . .	191
5.17 LOG Dispersion frequency vs. magnetic field for DNA (50mg/ml) . . . . .	192
5.18 Spreading parameter vs. magnetic field for DNA (50mg/ml) . . . . .	192
5.19 d.c. conductivity vs. magnetic field for DNA (50mg/ml) . . . . .	193
5.20 LOG Frequency vs. concentration for DNA . . . . .	194
5.21 Dielectric decrements vs. concentration for DNA . . . . .	195
5.22 d.c. conductivity vs. concentration for DNA . . . . .	196
5.23 GA:Dielectric Decrements vs. Temperature . . . . .	197
5.24 GA: LOG Frequency vs. Temperature . . . . .	198
5.25 GA: Spreading parameter vs. Temperature . . . . .	199
5.26 GA: LOG(D.C. conductivity) vs. Temperature . . . . .	199
5.27 GA: LOG Tau vs. 1/Absolute Temperature . . . . .	201
5.28 GA: LOG (Absolute temperature x Tau) vs. 1/Absolute Temperature	203
5.29 GA: Dielectric decrements vs. Added NaCl . . . . .	206
5.30 GA: LOG(Frequencies) vs. Added NaCl . . . . .	207

5.31 GA: LOG(D.C. conductivity) vs. Added NaCl . . . . .	208
5.32 GA: LOG Frequency vs. Voltage . . . . .	209
5.33 GA:Dielectric Decrements vs. Voltage . . . . .	210
5.34 GA: LOG(D.C. conductivity) vs. Voltage . . . . .	211
5.35 Summary of factors affecting dispersion . . . . .	214
5.36 Variation of Specific Dielectric Decrement with concentration for DNA (D6898 from herring testes Type XIV) . . . . .	217
5.37 All salts: Magnitude of Maximum of DS vs. Concentration . . . . .	222
5.38 All salts: Frequency of Maximum of DS vs. Concentration . . . . .	222
5.39 All salts: Magnitude of Minimum of DS vs. Concentration . . . . .	223
5.40 All salts: Frequency of Minimum of DS vs. Concentration . . . . .	223
5.41 Variation of Difference Signal Frequency parameter with Pascal's con- stants (lower), Diamagnetic susceptibility (middle), and mass suscep- tibility (top). . . . .	226
5.42 Variation of Difference Signal Frequency parameter with Covalent radius (lower), Van der Waals radius (middle) and Ionic radius in solution (top). . . . .	227
5.43 Variation of Difference Signal Frequency parameter with Diffusion Coefficient (lower) and Ion Mobility (upper). . . . .	229

5.44	Variation of the Difference Signal Frequency parameter with Ion-size parameter (lower) and the Hydration number (upper). . . . .	231
5.45	Variation of the Difference Signal Frequency parameter with Atomic number (lower), Atomic Mass (middle) and Density (upper). . . . .	233
N.1	DNA d.a. LiCl : Magnitude of Maximum of DS vs. Concentration .	374
N.2	DNA d.a. LiCl : Frequency of Maximum of DS vs. Concentration .	374
N.3	DNA d.a. LiCl : Magnitude of Minimum of DS vs. Concentration .	375
N.4	DNA d.a. LiCl : Frequency of Minimum of DS vs. Concentration .	375
N.5	DNA d.a. NaCl : Magnitude of Maximum of DS vs. Concentration	376
N.6	DNA d.a. NaCl : Frequency of Maximum of DS vs. Concentration .	376
N.7	DNA d.a. NaCl : Magnitude of Minimum of DS vs. Concentration .	377
N.8	DNA d.a. NaCl : Frequency of Minimum of DS vs. Concentration .	377
N.9	DNA d.a. KCl : Magnitude of Maximum of DS vs. Concentration .	378
N.10	DNA d.a. KCl : Frequency of Maximum of DS vs. Concentration .	378
N.11	DNA d.a. KCl : Magnitude of Minimum of DS vs. Concentration .	379
N.12	DNA d.a. KCl : Frequency of Minimum of DS vs. Concentration .	379
N.13	DNA d.a. RbCl : Magnitude of Maximum of DS vs. Concentration	380
N.14	DNA d.a. RbCl : Frequency of Maximum of DS vs. Concentration .	380

N.15 DNA d.a. RbCl : Magnitude of Minimum of DS vs. Concentration	381
N.16 DNA d.a. RbCl : Frequency of Minimum of DS vs. Concentration .	381
N.17 DNA d.a. CaCl <sub>2</sub> : Magnitude of Maximum of DS vs. Concentration	382
N.18 DNA d.a. CaCl <sub>2</sub> : Frequency of Maximum of DS vs. Concentration	382
N.19 DNA d.a. CaCl <sub>2</sub> : Magnitude of Minimum of DS vs. Concentration	383
N.20 DNA d.a. CaCl <sub>2</sub> : Frequency of Minimum of DS vs. Concentration	383

# Chapter 1

## A Review of Relevant Literature

### 1.1 Introduction

The current work investigates the effect of magnetic fields on the *dielectric* properties of DNA. Following a brief survey of the dielectric work carried out on DNA to date, this chapter describes the techniques used by various workers to investigate how the diamagnetic anisotropy of systems of molecules led to their re-orientation in magnetic fields. The availability of higher magnetic field intensities then enabled workers to investigate the effect of such fields on single macromolecules, including DNA.

### 1.2 Dielectric properties of DNA

In the past few decades the most commonly used DNA samples in dielectric investigations were calf thymus DNA and herring and salmon testes DNA, mainly because

of their ready availability in the required quantities. Workers have mainly used concentrations below 10 mg/ml, and have in some cases reduced the DNA chain length by sonication, e.g. Foster (Foster et al., 1984) used chain lengths of between 5 and 30 kilo base pairs. Despite attempts at purification, DNA chain length has not been well defined in most samples, and length distribution has usually been quite broad.

Due to the anti-parallel polarity of the strands that make up the double-helix (See Section 2.3), DNA does not have a permanent dipole moment (Pethig, 1978). Its response to an applied electrical field i.e. its dielectric response, is therefore thought to be due to the presence of the surrounding counter-ion layer (See Section 2.3.6), with the electric field creating an *induced* dipole moment (Takashima, 1989).

It is generally accepted that there are at least four dielectric dispersions in the DNA spectrum - the first at frequencies below 10 kHz, the next at frequencies between 10 and 100 kHz, a third between 1 and 100 MHz, and the fourth above 1 GHz.

Takashima (Takashima, 1963) investigated the dielectric properties of DNA with molecular weights ranging from  $0.4 \times 10^6$  to  $7.0 \times 10^6$ . He also reported on the effect of sonication, and concluded that the relaxation time was proportional to the length of the molecule. He found a dispersion in the kHz range, with a lower limit of 1700 Hz for the highest molecular weight samples. At the maximum concentration of 2 mg/ml, the dielectric decrement was found to be approximately 1000, increasing a little as the concentration was decreased. He concluded that DNA showed a dipole moment along the long axis, and that polarization involved some rotation of the whole molecule.

Sakamoto (Sakamoto et al., 1976) and Hayakawa (Hayakawa et al., 1978) used a four-electrode cell to investigate DNA in aqueous solution at frequencies ranging from 0.2 Hz to 30 kHz. They concluded that the low frequency dispersion was due to rotation of the whole DNA molecule caused by counter-ion fluctuations producing

a semi-permanent dipole moment. Molinari (Molinari et al., 1981) found that the frequency of the low frequency dispersion varied with the square of the molecular weight, and interpreted the low frequency results by movements of counter-ions along the DNA backbone.

Bonincontro (Bonincontro et al., 1984) reported on the effect of magnesium and silver ions on counter-ion fluctuations in low molecular weight DNA dielectric dispersions. He found two dispersions, one at frequencies between 7 and 40 kHz, and the other at frequencies in the range 400 – 500 kHz, for sonicated DNA with chain length varying between 500 and 2000 base-pairs, and concentration of 200 mg/ml. He proposed that the results were consistent with the model put forward by van der Touw (van der Touw and Mandel, 1974), where the movement of counter-ions surrounding a polyion could produce dispersions. That model suggested that a polyion such as DNA could be represented by a series of rigid sub-units. Counter-ion fluctuations within sub-units of the polyion could cause the high frequency dispersion, whilst similar fluctuations over the whole length of the DNA chain could give rise to the low frequency dispersion. The temperature independence of the dielectric decrement of the low frequency dispersion showed that this was due to interfacial polarization, of which counter-ion fluctuation is an example.

Sun (Sun et al., 2005) detected two dispersions at low frequencies in DNA at low temperatures (below 263K) and low concentrations (below 5mg/ml). One dispersion, denoted the Lower frequency process (LFP), was at 0.1 Hz at 173K and moved to 2.5 Hz at 213K; this was a Cole-Cole type symmetrical dispersion with activation energy equal to that of pure ice. Of relevance to the present work is the dispersion he found at low kHz frequencies, denoted HFP (Higher frequency process), which is a Debye-like process, and is “related to the bound water in the immediate vicinity of the DNA molecules”. As the temperature increased, the d.c. conductivity effects tended to encroach on both dispersions, and at the temperatures used in the present

work they would probably be overwhelmed. Sun found that the dielectric behaviour of aqueous solutions of DNA showed similar properties to those of water, and DNA dissolved in glycerol/water mixtures were similar to equivalent glycerol/water without the DNA. Because of this, Sun gives the opinion that "the dynamics of DNA solutions are dominated by the solvent".

Tomic (Tomic et al., 2007) investigated the dispersion found at frequencies between 10 and 100 kHz. He theorised that the dispersion was caused by the interaction between the fixed charges on the DNA, and mobile charges on the counter-ions and the salt ions in solution. The interaction between the DNA and the counter-ions had been described by Manning (Manning, 1969) and (Manning, 1978), where some of the counter-ions produced a condensed layer surrounding the DNA, whilst still remaining free to move within that layer. The interaction between the mobile charges themselves was then presumed to be reduced by the presence of the fixed charges on the DNA. This was described as a screening process whose intensity was, for monovalent ions, inversely proportional to the square-root of the ion concentration. Tomic concluded that at low DNA concentration and low salt concentrations, the dispersion in this frequency range was caused by the movement of counter-ions in the condensed phase close to the DNA, the displacement occurring along the whole length of the DNA molecule. At higher salt concentrations, the presence of increased numbers of free counter-ions limited the displacement of the counter-ions in the condensed layer to approximately the persistence length of the DNA, i.e. about 50 nm.

Minakata (Minakata, 1972) included the role of free counter-ions in the cause of the third dispersion found between 1 and 100 MHz, calculating that the double layer of condensed and free counter-ions surrounding the DNA would produce polarization perpendicular to the DNA chain backbone in a similar way to Maxwell-Wagner effects. Mashimo (Mashimo et al., 1989) invoked the effect of bound water, whilst



Grosse (Grosse, 1989) claimed Maxwell-Wagner interfacial processes alone could be responsible. Tomic (Tomic et al., 2007) also investigated the third dispersion, and concluded that it was produced by free counter-ions hopping between sections of the DNA chain. Bone (Bone and Small, 1995) used TDR techniques and came to similar conclusions, i.e. that the dispersion was caused by the fluctuations of counter-ions along segments of the DNA chain of length approximately 60 nm. Base-pair dipoles and Maxwell-Wagner interfacial polarization were claimed to be unlikely to cause dispersions in this frequency region with the dielectric increments found.

The dispersion found at frequencies above 1 GHz is thought to be due to the reorientation of water molecules causing polarization. Grant (Grant et al., 1978) found this to occur at approximately 17 GHz for pure water at room temperature. The presence of DNA was found to only slightly change the dielectric parameters of the dispersion. Takashima (Takashima et al., 1984) and Foster (Foster et al., 1984) confirmed that the DNA spectrum at GHz frequencies only differs marginally from the dielectric spectrum of pure water. Swicord (Swicord and Davis, 1982) and (Swicord and Davis, 1983) found that the dielectric parameters of *E. coli* DNA at 8 GHz were substantially different to those of water, and Edwards (Edwards et al., 1984) and (Edwards et al., 1985) interpreted similar results as excitation of longitudinal mechanical vibrational modes in the DNA double helix. The same *E. coli* DNA sample used by Edwards was then investigated at these frequencies by Bigio (Bigio et al., 1993) using a different method, but the resonance effects reported previously could not be reproduced.

In recent years several workers have investigated the effects of radiation in the region from 300 GHz to 10 THz on biological material. Because of the difficulty of performing impedance measurements directly at these frequencies, the absorption of thin films was studied. Wittlin (Wittlin et al., 1986) was the first to investigate the effect of these frequencies on calf thymus DNA, using thin films of thickness of

approximately  $50\mu\text{m}$ . He found several vibrational modes, and studied the variation of their frequencies with hydration. Further studies have shown that transmittance spectra at THz frequencies of the four nucleotides from which DNA is constructed were sufficiently different to form the basis of gene sequencing. The methods used in these studies included: Fischer (Fischer et al., 2002) and Shen (Shen et al., 2004) used time domain spectroscopy with laser pulses in the femtosecond range, Nishizawa (Nishizawa et al., 2005) generated frequency-tunable, high-power THz waves from GaP (Gallium Phosphide) crystals, and Globus (Globus et al., 2002) used Fourier transform spectroscopy.

The effect of magnetic fields on the dielectric properties of DNA does not seem to have been reported previously.

### 1.3 Diamagnetic Anisotropy

Many substances exhibit diamagnetic anisotropy i.e. their diamagnetic susceptibility values parallel and perpendicular to a rotational symmetry axis are different. The molecules would therefore be expected to experience a force from an externally applied magnetic field tending to change their orientation. However, the forces experienced by molecules due to the diamagnetic effect is very small, and is usually overwhelmed by thermal processes. The degree of orientation  $\beta$ , derived from Boltzmann statistics, may be calculated for a particular molecule from the following equation:

$$\beta = \frac{(\chi_{\parallel} - \chi_{\perp})H^2}{kT} \quad (1.1)$$

where  $\chi_{\parallel}$  and  $\chi_{\perp}$  are the susceptibility values parallel and perpendicular to the rotational symmetry axis,  $k$  is the Boltzmann constant,  $T$  the absolute temperature, and  $H$  the magnetic field intensity. (This equation holds for  $\beta \ll 1$ ).  $\beta$  is normally

very small at values of magnetic fields normally encountered; e.g. even for the strongly diamagnetically anisotropic benzene molecule,  $\beta \approx 10^{-7}$  for fields of 1 Tesla.

The degree of orientation is however found to be considerably increased if the anisotropic molecules are aligned parallel to each other, since the diamagnetic anisotropy of a structure consisting of many molecules is additive and directly proportional to the number of such molecules in the structure. In particular, large molecular systems are found to be almost fully aligned when they have constituent molecules which have large diamagnetic anisotropy, and are relatively fixed in position inside the system.

Such systems include the cholesteric phases of liquid crystalline compounds. As an example, Go (Go et al., 1969) and Tohyama (Tohyama and Miyata, 1974) found that cholesteric liquid crystalline Poly-Y-benzyl-L-glutamate tended to orient its axes perpendicular to the direction of an externally applied magnetic field, and that this was due to the anisotropy of diamagnetic susceptibility of the cholesteric structure. Finer (Finer and Darke, 1975) slowly cooled Poly-L-Lysine Hydrobromide solutions in the magnetic field of an n.m.r. spectrometer, and found that the long axes of the Poly-L-Lysine $\alpha$ -helices were aligned parallel to the magnetic field of the n.m.r. magnet. He found that this was because of the anisotropy of the diamagnetic susceptibility of the hexagonally-packed  $\alpha$  helices.

Biological systems show similar alignment in magnetic fields. As an example, Arnold (Arnold et al., 1958) visually observed the orientation of muscle fibres suspended between the poles of a magnet with field of intensity approximately 0.3 Tesla. Similarly, Chalazonitis (Chalazonitis et al., 1970) observed that rod outer segments from frog retinas in suspension re-orientated in a constant magnetic field of approximately 1 Tesla; the rods tending to align themselves with their long axes parallel to the magnetic field. Hong (Hong et al., 1971) explained that the retinal rods

were oriented in a steady magnetic field because they contained a regular array of disc membranes, and that if there were any molecules with diamagnetic anisotropy present, then their effect would be magnified, and have an orientating effect on the whole structure. He argued that rhodopsin, which has a high degree of diamagnetic anisotropy, could be the constituent responsible for the alignment.

Becker (Becker et al., 1973) found that *Chlorella pyrenoidosa* cells in aqueous solution were oriented by normal magnetic fields because of the anisotropy in the diamagnetic susceptibility of oriented chlorophyll molecules. He concluded that the alignment was due to the presence of porphyrin rings in the structure, which aligned themselves parallel to the magnetic field. He followed this work with studies of bovine visual rod outer segments oriented in homogenous magnetic fields (Becker et al., 1978), where he showed that the diamagnetic susceptibility anisotropy of rhodopsin aromatic residues were sufficient to account for the magnetic orientation of the rods.

## 1.4 DNA

Maret (Maret et al., 1975) used the availability of higher magnetic field intensities (up to 14 Tesla) to investigate the effect of such fields on the orientation of single macromolecules in dilute solutions. Amongst the molecules he used in his experiments, the high-molecular weight nucleic acids such as DNA are of relevance to the current work. The method employed the Cotton-Mouton effect, i.e. the birefringence induced in the DNA solution by the magnetic field. The birefringence  $\Delta n_B$  is defined as being equal to  $n_{\parallel} - n_{\perp}$ , where  $n_{\parallel}$  and  $n_{\perp}$  are the refractive indices of the solution parallel and perpendicular to the direction of the applied magnetic field. The degree of orientation of the DNA ( $\beta$ ) was proportional to  $\Delta n_B$  for small values of  $\beta$ , and could thus be calculated. For native calf thymus DNA with con-

centration of 10mg/ml, the method led to the determination of the small value for the orientation of 0.88%, when the magnetic field intensity was equal to 12 Tesla. The tendency was for the DNA to orient with the axis of the DNA double helix *perpendicular* to the direction of the magnetic field.

When the temperature was increased to above 70°C, the magnetically induced orientation decreased to zero. In this temperature range, the relatively rigid DNA double helix begins to divide into two separate single DNA strings. In the double helix, the base pairs are all parallel to each other and perpendicular to the axis of the DNA filament. However, the single strand DNA filaments are much more flexible, and the bases are no longer parallel; they are relatively free to rotate. Maret therefore concluded that the base-pairs were responsible for the magnetic orientability of the DNA molecules, since they consist partly of aromatic rings which are diamagnetically anisotropic. The rings tend to align their planes parallel to the magnetic field, and since in the DNA structure, these rings will all be parallel to each other, their additive anisotropy will ensure that the DNA molecule as a whole will try to orient with the filament perpendicular to the field direction. Maret (Maret and Dransfeld, 1977) further demonstrated using similar techniques that the rigidity of DNA may also be explained by the coplanar stacking of successive base-pairs.

Brandes (Brandes and Kearns, 1986) reported that calf thymus DNA, reduced to approximately 100 base-pairs in length and dissolved in  $D_2O$  (deuterium oxide) at a concentration of 250 mg/ml, formed a cholesteric liquid crystal. Shortly after preparation of the solution on a slide, it turned opaque due to the formation of small domains which were in the order of a few micrometers in magnitude. Viewing between crossed polarizers revealed strong birefringence in the solution, and varying colours in the domains. When the solution was left for several days, small rod-like crystals were seen to develop, with diameter less than  $3\mu\text{m}$ , and length up to  $40\mu\text{m}$ . However, when the slide was placed between the poles of an NMR magnet (5.9 Tesla)

with the field perpendicular to the face of the slide, the entire solution turned clear within seconds. The structure induced by the magnetic field was stable for several weeks even when the slide was removed from the magnet. When the slide was placed with the magnetic field parallel to the face of the slide, a granular structure was seen. This slowly turned over the course of approximately a day to a pattern consisting of alternating dark and bright lines with separation of approximately  $1.2\mu\text{m}$ , all perpendicular to the direction of the magnetic field. The lines were so uniform that the slide could be used as a diffraction grating, clearly indicating the formation of a highly ordered system.

## 1.5 Liquid Crystalline DNA

Strzelecka (Strzelecka and Rill, 1988) and (Strzelecka et al., 1988) and Van Winkle (Van Winkle et al., 1990) and (Van Winkle et al., 1997) investigated the liquid crystalline structure of DNA, and the effect of magnetic fields on that structure.

Strzelecka (Strzelecka and Rill, 1988) used NMR spectroscopy to determine the concentrations at which DNA formed different types of structures - isotropic at lower concentrations, followed by biphasic regions, with fully cholesteric liquid crystalline structure above a certain concentration. For the 146 base-pair length DNA studied, the biphasic region was between 125 and 155 mg/ml, and fully liquid crystalline above 155 mg/ml. The appearance of the cholesteric liquid crystalline phase showed a highly birefringent aligned fringe structure when a magnetic field was applied.

Van Winkle (Van Winkle et al., 1990) refined the technique of using controlled drying experiments, where a small volume of concentrated DNA solution (100 mg/ml in 0.25 M ammonium acetate buffer) was placed on a microscope slide. The liquid was then surrounded by a polyacrylate mounting medium, leaving a gap of approx-

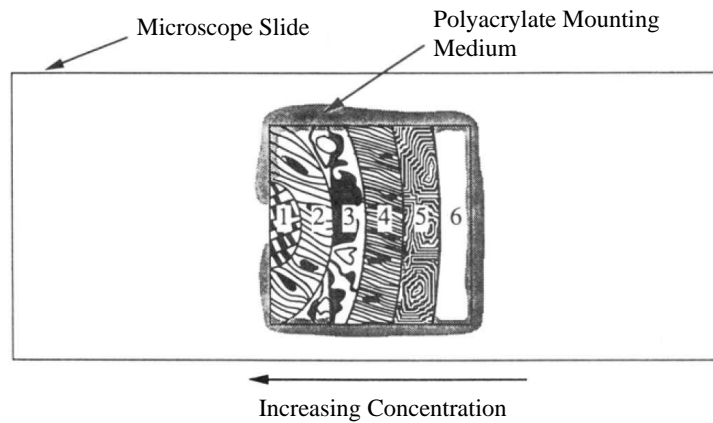


Figure 1.1: Diagram of DNA sample in controlled drying experiment. The phases which appear are: (1) High density phase (2) Unwinding cholesteric phase (3) A phase of complicated structure only seen in these experiments (4) Fully cholesteric phase (5) Biphasic region (6) Isotropic phase (Van Winkle et al., 1990)

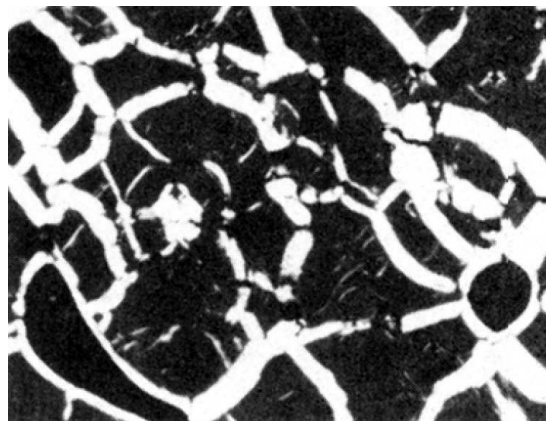


Figure 1.2: DNA cholesteric phase with no magnetic field (Van Winkle et al., 1990)

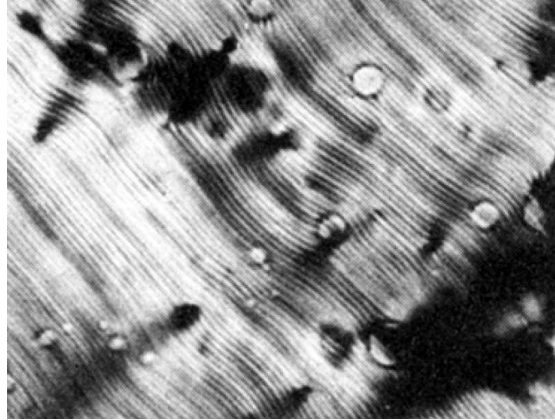


Figure 1.3: DNA cholesteric phase with magnetic field (Van Winkle et al., 1990)

imately 3 mm on one side, and then a coverslip placed over it. (See Figure 1.1) As the sample dried, a concentration gradient was established, with maximum concentration on the left of the diagram. Although the system is a dynamic one, the phases shown across the slide were found to be broadly similar to those found with stabilized samples.

As the sample slowly evaporated, the different phases shown in Figure 1.1 appeared in the following order (from right to left i.e. from low to high concentration): isotropic  $\rightarrow$  precholesteric (probably nematic liquid crystalline)  $\rightarrow$  cholesteric  $\rightarrow$  unwinding cholesteric  $\rightarrow$  multiple phases of high density. The same sequence was observed in those samples not exposed to magnetic field and in those placed in a 3.5 Tesla field. The appearance of the isotropic, precholesteric and high density phases were identical with and without magnetic fields. However, application of the magnetic field changed the appearance of the cholesteric and unwinding portions of the solution. Figure 1.2 shows the appearance of the cholesteric phase with no magnetic field; the bright areas are referred to as “oily streaks”, whilst the dark areas



are cholesteric with twist axis perpendicular to the plane of the image. Figure 1.3 shows the cholesteric phase when the magnetic field was applied. It can be seen that there is a high degree of alignment in the morphology of the cholesteric liquid crystalline structure under these conditions. For the approximately 150 base-pair length DNA studied, Van Winkle found that the solution was only fully cholesteric above 200 mg/ml.

Van Winkle (Van Winkle et al., 1997) went on to further investigate the behaviour of cholesteric liquid crystalline DNA in various magnetic fields. No evidence of alignment was found in a magnetic field produced by a 1.1 Tesla electromagnet. Re-orientation of the cholesteric phase was however found in 3.5 T, 6.4 T and 9.4 T NMR magnets, with fingerprint stripes of width approximately  $1.1\mu\text{m}$  aligned *perpendicular* to the direction of the magnetic field. With the 9.4 Tesla magnet however, there appeared to be larger scale distortions in the fingerprint structure, with longer wavelength stripes aligning *parallel* to the field direction. When the sample was removed from the magnet, these stripes annealed away over several days.

## 1.6 DNA at Lower concentration

Morii (Morii et al., 2004) used the re-orientating effect of magnetic fields on DNA to create a highly homogeneously oriented membrane of DNA. He surmised that many applications which use nano-functional materials could conceivably show enhanced operation if anisotropic materials, such as a film with molecular orientation, could be easily developed. Several samples of DNA were prepared with varying average molecular weights, and the initial concentration of each DNA solution sample was adjusted to 60 mg/ml. A sample was placed on a 25 x 25 x 0.10 mm clean silica plate, so that the solution could spread out as a 0.05 mm thick layer over a 20 x 20

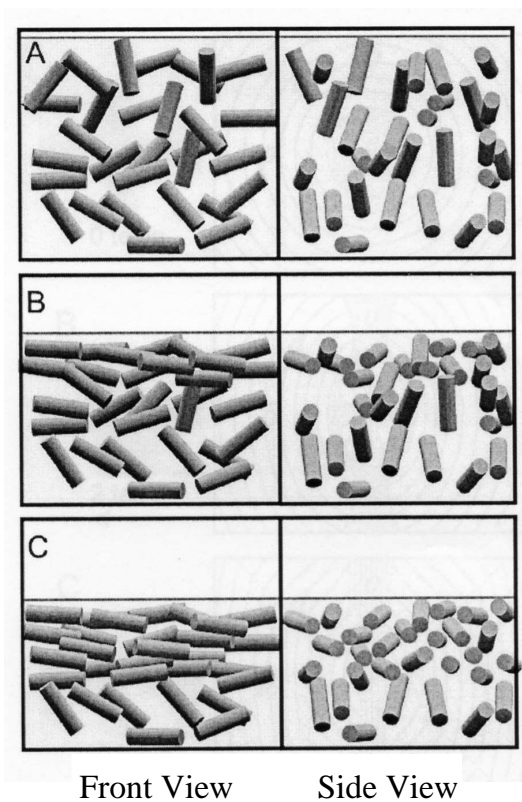


Figure 1.4: Representation of chain alignment. The magnetic field direction is perpendicular to the Front View. Each cylinder is a straight region of the DNA filament. The order of the diagrams A, B then C shows the direction of evaporation with time. (A) The magnetic field is orienting the DNA at right-angles to the field. (B) After some evaporation, condensation occurs near the surface. (C) Further condensation leads to formation of the liquid crystal stage. (Morii et al., 2004)

mm area. The plate was immediately placed horizontally between the poles of a 10 Tesla magnet so that the magnetic field was *parallel* to the plate surface, and the film allowed to dry. When dry, the film was found to be highly ordered, with the DNA aligned perpendicular to the magnetic field direction.

It was suggested that the mechanism for the formation of the film involved both the action of the magnetic field and the interfacial effect of the air-liquid interface (See Figure 1.4). The magnetic field alone acting in a direction parallel to the plate surface would induce the DNA to align perpendicular to that direction as seen in A, but with no preferred alignment in a vertical plane. The condensation which occurred at the air-liquid interface induced the DNA to align parallel with the surface. Further condensation near the surface led to the formation of a liquid crystal structure in that area. As the solution evaporated further, the concentration of the liquid reached the point where the whole volume formed liquid crystals, but by that time, the alignment of the DNA filaments had already occurred.

Previous workers had reported that a substantial re-orientating effect of magnetic fields on DNA i.e. where the result was obvious under a microscope, was confined to concentrations above 150 mg/ml, i.e. where the DNA formed a cholesteric liquid crystal structure. Morii however used solutions with initial concentration of only 60 mg/ml, and found that the magnetic field was still having a re-orientating effect which resulted in films showing obvious alignment. He still required a large magnetic field of 10T for this to occur however.

## 1.7 Orientation of Sperm nuclei

Suzuki (Suzuki and Nakamura, 1996) investigated the effect of very low magnetic fields ( $< 0.1\text{T}$ ) on insect (*Gryllus bimaculatus*) sperm nuclei. He found that when

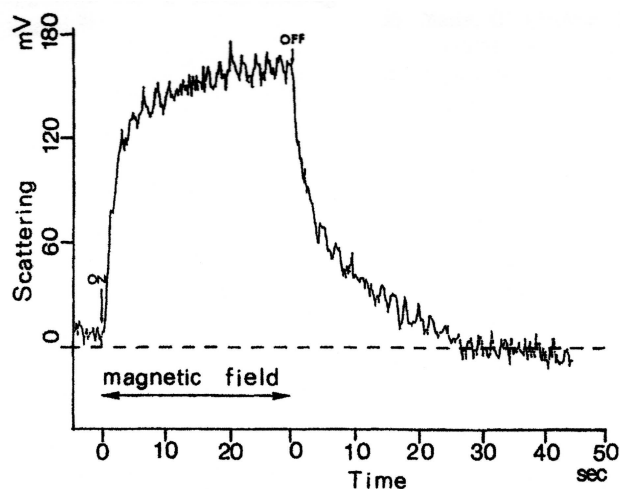


Figure 1.5: Intensity of the light (measured by photo-multiplier) scattering from the suspension of sperm cells at right angles. When the magnetic field was applied for 30 seconds (shown with an arrow) the scattering was enhanced, while when the field was switched off the response returned to its original value. (Suzuki and Nakamura, 1996)

the magnetic field was applied to a suspension of insect sperm of concentration  $10^5$  cells/ml, the intensity of 600nm light scattering from the suspension at right angles was increased. When the field was switched off, the intensity, as measured by a photo-multiplier, returned to its original value in approximately 30 seconds. (See Figure 1.5)

The response of single DNA molecules to strong magnetic fields had been explained by the presence of  $\pi$  electrons on the bases, which induce a magnetic field at right angles to the planes of the bases (See Figure 1.6). When a strong external magnetic field was applied, the DNA helix rotated to minimize the diamagnetic energy, i.e. so that the helix axis was perpendicular to the direction of the external field. The

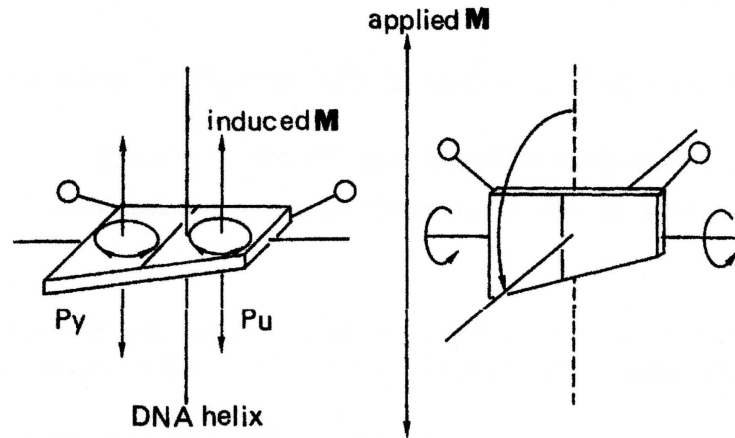


Figure 1.6: Magnetic response of DNA. Left - a pyrimidine (Py) and a purine (Pu) in a base-pair have  $\pi$  electrons circling on the plane of the base-pair, and thus can induce a diamagnetic field towards the direction which is perpendicular to the plane (induced M) and thus essentially parallel to the DNA helix axis. Right - when an external magnetic field is applied (applied M), the DNA is oriented so that its helix axis becomes perpendicular to the applied magnetic field, in order to minimize the energy created by the two magnetic fields. (Suzuki and Nakamura, 1996)

regular arrangement of the base-pairs in the DNA structure magnified the effect. Even so, it had previously required larger magnetic fields (14T) to orientate DNA strands (Maret et al., 1975).

Suzuki surmised that the response of the sperm nuclei to the relatively small magnetic fields used ( $< 0.1\text{T}$ ) was explained by the arrangement of the DNA inside the nucleus. Such sperm nuclei have  $4.7 \times 10^4$  DNA double strands inside a  $20\mu\text{m}$  needle-like package; the DNA strands are highly oriented with their helix axes parallel to the sperm nucleus' long axis. The response of each DNA strand is thus in

the same direction as all other strands, and the nuclei would thus be expected to tend to re-orient at right angles to the magnetic field direction.

Emura (Emura et al., 2001) studied bull sperm cells using similar methods. He measured how the degree of orientation varied with the intensity of the external magnetic field, and found that the cells were fully orientated with the whole body perpendicular to the field direction when the intensity was just below 1 Tesla.

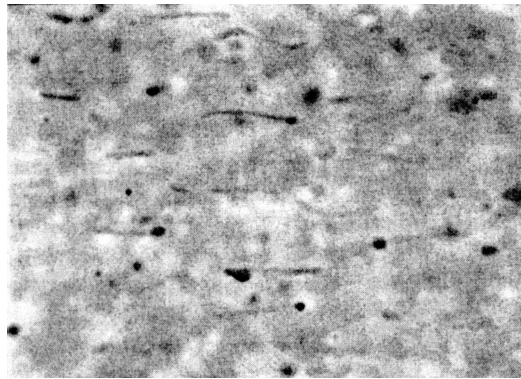


Figure 1.7: Optical microscopic photographs of cilia in a magnetic field of 8 Tesla (direction from left to right) (Takeuchi et al., 2001)

Takeuchi (Takeuchi et al., 2001) also studied bull sperm, but looked too at the response of the heads of bull sperms and cilia containing microtubules similar to those found in the tail (flagellum) of the sperm. He found that the cilia, and hence the microtubules orient *parallel* to the applied magnetic field (See Figure 1.7), whilst the heads orient *perpendicular* to the field (See Figure 1.8). The complete bull sperms would therefore be expected to orient with their heads perpendicular to the magnetic field direction, and their tails at right angles to this. In fact, it appears

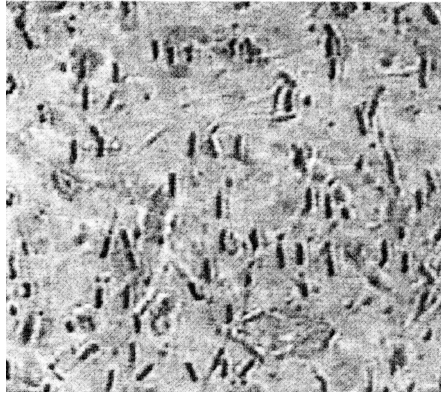


Figure 1.8: Optical microscopic photographs of heads extracted from bull sperms in a magnetic field of 1.5 Tesla (direction from left to right) (Takeuchi et al., 2001)

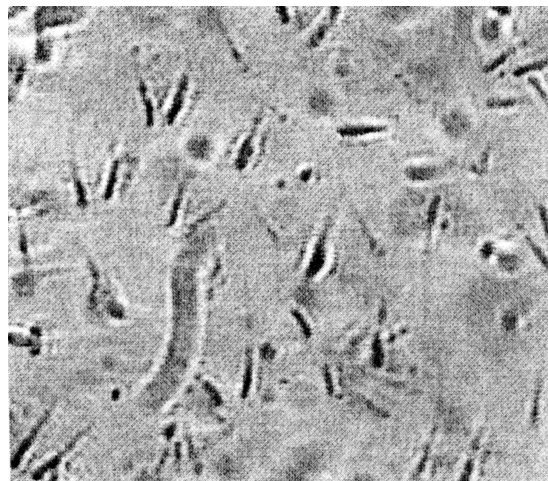


Figure 1.9: Optical microscopic photographs of bull sperms with no magnetic field (Takeuchi et al., 2001)

that the whole sperm cells orient perpendicular to the field direction; compare the microscopic photographs of sperm with *no* magnetic field (Figure 1.9) and that of sperm *with* magnetic field (Figure 1.10). The direction of the magnetic field is from left to right in all diagrams *with* magnetic field.

The arrangement of the DNA in the heads of bull sperm could therefore be deduced from these results of Emura (Emura et al., 2001) and Takeuchi (Takeuchi et al., 2001).

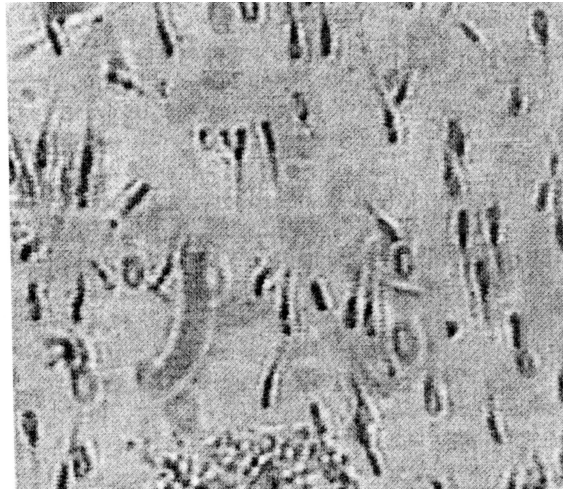


Figure 1.10: Optical microscopic photographs of bull sperms in a magnetic field of 1.5 Tesla (direction from left to right) (Takeuchi et al., 2001)



## 1.8 Aims and Objectives of thesis

### 1.8.1 Current knowledge

As described in the Literature Review, high magnetic fields ( $> 3.5$  Tesla) have been shown to cause morphological changes in DNA at high concentration ( $> 170$  mg/ml) where it exists as the liquid crystal cholesteric phase.

### 1.8.2 Aims and objectives

1. To identify corresponding changes in the *dielectric* properties of DNA
  - with lower intensity magnetic fields ( $< 0.7$  Tesla).
  - at high concentrations ( $> 150$  mg/ml), where DNA would be expected to exist in the liquid crystal cholesteric phase.
  - using interdigitated electrodes, where the magnetic field is applied perpendicular to the electric field.
2. To identify corresponding changes in the *dielectric* properties of DNA
  - with lower intensity magnetic fields ( $< 0.7$  Tesla).
  - at low concentrations ( $25 - 100$  mg/ml) where DNA is unlikely to have cholesteric liquid crystal structure.
  - using planar electrodes, where the magnetic field is applied parallel to the electric field.
  - where the sodium in the DNA solution is replaced with a range of other cations by dialysis.
  - where the temperature, amount of added sodium chloride and a.c.voltage are varied.

3. Describe the Difference Signal (See Section 2.5) as a useful method of visualising small changes in dielectric loss spectra.
4. Develop a method to analyse Difference Signals using Matlab's Genetic Algorithm toolbox in terms of the modification of one dispersion by magnetic field.
5. Identify the mechanisms by which the dielectric properties of DNA are modified by external magnetic field.

## 1.9 Outline of thesis

In Chapter 1, this thesis presents a review of the relevant literature concerning dielectric measurements on DNA, together with reported magnetic effects.

Chapter 2 presents the basis of dielectric theory and a description of the structure of the DNA molecule. The concept of the Difference Signal is introduced, and an outline of the general principles of Genetic Algorithm programs is described. An assessment of the reliability of Matlab's Genetic Algorithm toolbox as a method of analysing the difference signal is presented.

Chapter 3 gives a description of the experimental equipment used in the present work, together with an outline of the computer programs which communicate with and control the different components. Descriptions are then given of the experimental studies carried out on the effects of magnetic fields on DNA solutions under varying conditions.

Chapter 4 describes and discusses the results of studies carried out on DNA solutions using interdigitated electrodes, where evaporation of the solution enabled high concentrations to be achieved. The effect of low magnetic fields on DNA solutions

at concentrations at which it forms cholesteric liquid crystals is reported.

Chapter 5 describes and discusses the results of studies carried out on DNA solutions using planar electrodes. The effect of low magnetic fields on DNA solutions at lower concentrations is reported. The results of Genetic Algorithm analysis of the results of various studies is given.

Chapter 6 discusses the conclusions reached as a result of this thesis, and lists possible future work.

The appendices list all the computer programs used in the present work, and finally a comprehensive bibliography is included.

# Chapter 2

## Theory

### 2.1 Dielectric Relaxation Spectroscopy

Spectroscopy is the term normally used for the variation in the absorption of light over the frequency range  $10^{14}\text{Hz}$  -  $10^{16}\text{Hz}$ . Analysis of this frequency-dependent absorption in the infra-red, visible and ultraviolet parts of the electromagnetic spectrum gives information on the atomic and molecular composition of the substance under investigation. When electromagnetic radiation at lower frequencies ( $10^{-5}\text{Hz}$  to  $10^{11}\text{Hz}$ ) is used in a similar way, this is called Dielectric Relaxation Spectroscopy. In this case, investigation of the relaxation absorptions is able to provide information on the charge-transport and rotational properties of materials.

## 2.2 Dielectric Permittivity

Consider a parallel plate capacitor consisting of two parallel plates each of area  $A$  separated by a distance  $d$  placed in a vacuum. If a potential difference  $V$  is applied across the plates, then the total charge on the plates  $\pm q_0$  will all be free charges  $+Q_F$  and  $-Q_F$ . These then produce the electric field between the plates. (See Figure 2.1)

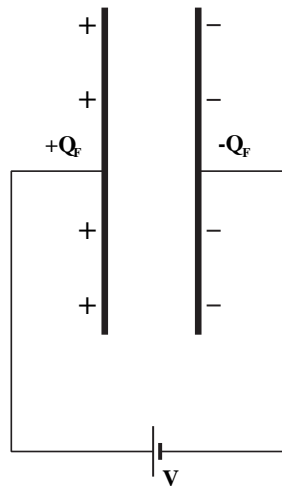


Figure 2.1: Parallel plate capacitor in vacuum

The capacitance of this system can then be calculated from the equation:

$$c_0 = \frac{Q_F}{V} \quad (2.1)$$

Assume that the space between the plates of the capacitor is filled with a dielectric material. Each molecule in a polar dielectric is a dipole which has a moment defined according to this equation:

$$\text{moment } \mu = Ql \quad (2.2)$$

where  $Q$  is the charge in coulombs, and  $l$  is the distance separating the charges in metres. The magnitude of the dipole moment is usually measured in Debye units. ( 1 Debye =  $3.33 \times 10^{-30}$  coulomb metres.)

Considering the dielectric macroscopically, the sum of the dipole moments in an element of volume  $\Delta v$  may be determined from:

$$\sum_{i=1}^{N\Delta v} \mu(i) = N\mu\Delta v = P\Delta v \quad (2.3)$$

where  $\mu$  is the mean dipole moment of the molecules, and  $N$  is the number of molecules per unit volume. The quantity  $P$  is then the dipole moment per unit volume, and is denoted the electric polarization. It can also be useful when considering capacitors to interpret the electric polarization as a surface charge density.

Normally, in the absence of an electric field, the permanent dipole moments of the molecules will be randomly orientated, and thermal motion will cause their directions will be changing continuously . When an electric field is applied, the dipoles tend to align themselves with the direction of the field, although the extent of this alignment is small in fields of the magnitude normally used. The electric field is then said to have polarised the material.

Because of this polarization, the surfaces of the material next to the plates will carry bound charges of opposite polarity  $+Q_B$  and  $-Q_B$ . These bound surface charges neutralise part of the charges on the plates. The remainder of the charge is called the free charge  $Q_F$  - this is what produces the field in the material. (See Figure 2.2)

The capacitor can now hold a total charge  $q_T$  equal to  $Q_F + Q_B$  at the same applied voltage  $V$ . The capacitance of the system has now increased to  $c_T$ , where:

$$c_T = \frac{Q_T}{V} \quad (2.4)$$

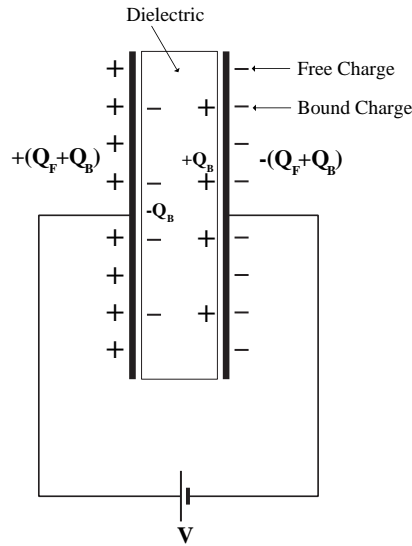


Figure 2.2: Parallel plate capacitor with dielectric

Since  $Q_T$  is larger than  $Q_F$  in Equation 2.1, this capacitance is obviously larger than the capacitance without the dielectric, and is caused by the polarizability of the material. A quantity called the (static) relative permittivity of the dielectric material may now be defined as the ratio of these capacitances, i.e.

$$\epsilon_r = \frac{c_T}{c_0} = \frac{Q_T}{Q_F} \quad (2.5)$$

Ignoring edge effects, the capacitance of the original capacitor in vacuum may be calculated from the following equation:

$$c_0 = \frac{\epsilon_0 A}{d} \quad (2.6)$$

where  $A$  is the Area of the capacitor plates in  $m^2$ ,  $d$  is the separation of the plates in  $m$ , and  $\epsilon_0$  is a constant called the permittivity of free space. Its value is  $8.854 \times 10^{-12}$  farad/m. The capacitance of the capacitor filled with dielectric is then larger than

this by a factor equal to the relative permittivity of the material  $\epsilon_r$  . i.e.

$$c_T = \frac{\epsilon_0 \epsilon_r A}{d} \quad (2.7)$$

$\epsilon_r$  is also the ratio of the total charge to the free charge:

$$\epsilon_r = \frac{Q_T}{Q_F} \quad (2.8)$$

The bound charge  $Q_B$  is given by:

$$Q_B = \int_s \sigma_p ds = \int_s P ds \quad (2.9)$$

where  $\sigma_p$  is the surface charge density of the bound or polarization charges, and  $s$  is the area of the surface. Similarly, the free charge is given by:

$$Q_F = \int_s \sigma_f ds = \int_s \epsilon_0 E ds \quad (2.10)$$

where  $\sigma_f$  is the surface charge density of the free charges, and  $E$  is the intensity of the Electric field between the plates. By substituting in Equation 2.8, and summing over the surfaces, we get:

$$\begin{aligned} \epsilon_r &= \frac{Q_F + Q_B}{Q_F} \\ \epsilon_r &= 1 + \frac{Q_B}{Q_F} \\ \epsilon_r - 1 &= \frac{Q_B}{Q_F} \\ \epsilon_r - 1 &= \frac{P}{\epsilon_0 E} \end{aligned} \quad (2.11)$$



## 2.2.1 Polarization

This increase in capacitance is due to the polarization of the molecules of the dielectric between the plates. This polarization can be produced by five separate effects:

- Electronic polarization;
- Atomic polarization;
- Ionic polarization;
- Orientation polarization;
- Interfacial or Space-Charge polarization.

### 2.2.1.1 Electronic polarization

In a non-polar substance the neutral molecules have their effective centres of positive and negative charge at the same point. When the material is placed between the plates of a capacitor, the electric field will exert a force on the electrons in one direction, and an equal force in the opposite direction on the positive nucleus. The centres of the positive and negative charges are no longer at the same point, a process called electronic polarization. The electronic or induced dipole moment per molecule  $\mu_e$  is:

$$\mu_e = \alpha_e E$$

where  $\alpha_e$  is called the electronic polarizability of the molecule.

### 2.2.1.2 Atomic polarization

Atomic polarization is caused by the movement of the atoms relative to each other, and is greatest when the material is ionic, and the atoms have excess charges of opposite polarities. The electric field exerts opposite forces on the two kinds of atoms, thus inducing a further dipole moment. The atomic dipole moment per molecule  $\mu_a$  is:

$$\mu_a = \alpha_a E$$

where  $\alpha_a$  is called the atomic polarizability of the molecule.

### 2.2.1.3 Ionic polarization

If the material consists of molecules which have a charged outer surface, then a cloud of counter-charged ions may be attracted towards them. An electric double-layer is thus created, since the counter-ions will be attracted electrostatically to the molecules. An external electric field may then exert sufficient force on the counter-ions to make them migrate to other positions on the molecule. The displacement of these counter-ions caused by an externally applied electric field results in an induced ionic polarization. The ionic dipole moment per molecule  $\mu_i$  is:

$$\mu_i = \alpha_i E$$

where  $\alpha_i$  is called the ionic polarizability of the molecule.

### 2.2.1.4 Orientation polarization

In a molecule of a polar substances, the total of the positive and negative charges is equal, i.e. the molecule is neutral. But the distribution of these charges is different, so that the effective centres of the positive and negative charges may be separated by distances which are of the same order of magnitude as the size of the molecule. This creates a permanent electric dipole. Typically, polar molecules are those which have no centre of symmetry, e.g. water, acetone and methanol.

If polar molecules are exposed to an electric field, they tend to orientate themselves with the direction of the field, while thermal effects try to restore random orientations. This is called orientation polarization, and it may be calculated from the following equation:

$$\frac{\mu_o}{\mu} = \coth x - \frac{1}{x} = L(x) \quad (2.12)$$

where  $\mu$  is the permanent dipole moment of the molecule,  $\mu_o$  is the average component of the dipole moment in the direction of the applied field, and  $L$  is the Langevin function. The variation of the Langevin function with  $x$  is shown in Figure 2.3. The term  $x$  is given by:

$$x = \frac{\mu E}{kT} \quad (2.13)$$

where  $E$  is the electric field,  $T$  is the absolute temperature, and  $k$  is the Boltzmann constant. Normally the electric field intensity is less than  $1 \times 10^7$  V/m and dipole moment values are typically of the order of  $1 \times 10^{-30}$  C/m. The value of  $x$  is therefore much less than 1, and as can be seen from Figure 2.3, the Langevin function reduces to approximately  $\frac{1}{3}$ . Equation 2.12 can then be written:

$$\frac{\mu_o}{\mu} = \frac{\mu E}{3kT} \quad (2.14)$$

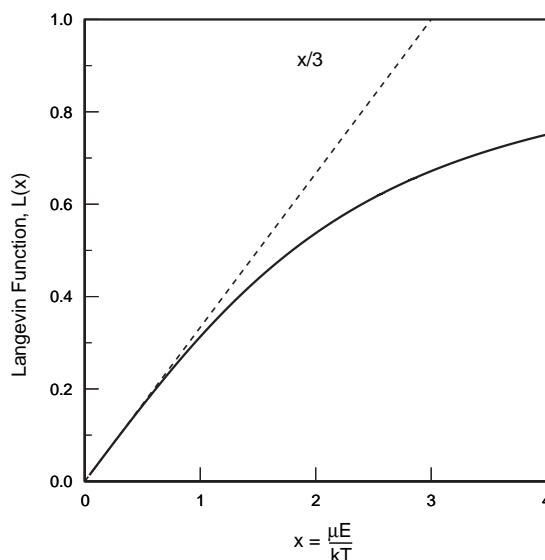


Figure 2.3: Graphical representation of the Langevin function

The extent to which dipoles align with an electric field is given by this ratio. It is very small for the magnitude of field intensity usually found, thus implying that dipoles are only very weakly aligned with the direction of the electric field, and that the tendency to random orientation due to thermal effects is predominant.

$$\mu_o = \frac{\mu^2 E}{3kT} = \alpha_o E \quad (2.15)$$

where  $\alpha_o$  is the orientation polarizability of the molecule.

If the above four polarizabilities are added together, an expression for the total dipole moment per molecule is obtained:

$$\mu = \left( \alpha_e + \alpha_a + \alpha_i + \frac{\mu^2 E}{3kT} \right) E \quad (2.16)$$

This is known as the Langevin-Debye formula.

### 2.2.1.5 Interfacial or Space-Charge polarization

If a material contains ions or electrons which are able to move significant distances on a macroscopic scale, these charge carriers will tend to accumulate wherever there are significant discontinuities. These can include phase boundaries, centres of impurity, lattice defects and electrode surfaces, leading to non-uniform charge distribution in such areas.

If a substance is non-homogeneous, e.g. it consists of layers of different materials, or of particles of one material suspended within the bulk of another, then different parts may have different conductivities. Charge carriers will be able to move relatively easily through the regions of lower resistance, and will build up at the interfaces to regions of higher resistance. The areas of high conductivity will therefore become more polarized, increasing the apparent mean moment of the molecules.

$$\mu_s = \alpha_s E \quad (2.17)$$

where  $\alpha_s$  is the interfacial or space-charge polarizability. Interfacial polarization can be frequency dependent and can often create effects which appear to be due to orientation polarization. (See Section 2.2.8 for details.)

If interfacial polarization is included, the total polarization can be produced by up to five processes, depending on the nature of the charges in the material. The average dipole moment per molecule is found from:

$$\mu = \alpha E \quad (2.18)$$

where  $\alpha$  is the total polarizability ( $\alpha_e + \alpha_a + \alpha_i + \alpha_o + \alpha_s$ ).

### 2.2.2 Alternating Fields

Consider the effect of applying a slowly changing alternating electric field to a capacitor with a polar material between its plates. As the field increases or decreases, all the polarization effects have time to react to the field, and they will reach values equal to those they would achieve in a steady field of magnitude equal to the instantaneous value of the alternating field. The permittivity would in these circumstances be independent of the frequency, and would be equal to that in a static field.

The movement of the dipoles produces an alternating current in the dielectric - this is called the displacement current. When the frequency is low and the dipoles are able to follow the variations in the field, the current will be  $90^\circ$  out of phase with the voltage which produces the electric field. The power absorbed in the circuit is equal to  $VI \cos \phi$ , where  $\phi$  is the phase difference between the voltage and current. At low frequencies therefore, the power absorbed is zero, and the energy is transmitted without loss.

If the frequency of the alternating field is increased, the dipoles are no longer able to follow the changes in the field, since they cannot rotate quickly enough. The amplitude of their oscillations decreases, and the amount of charge stored by the dielectric, and hence the permittivity falls. There is now a phase difference of less than  $90^\circ$  between the voltage and the displacement current, from which it follows that power is absorbed by the dielectric. Thus Joule heating of the dielectric occurs - and this is known as Dielectric Loss.

As the frequency of the voltage is increased further, a point is reached when the dipoles are totally unable to respond to changes in the field. The orientation polarization thus no longer makes a contribution to the permittivity of the material, and it is effectively equivalent to a non-polar dielectric in its ability to store charge.

The fall in permittivity of a dielectric substance as frequency is increased is usually referred to by the term *dielectric dispersion*. A dispersion which occurs as the orientation polarization falls from its value at low frequency to its negligible value at high frequency is referred to as a dielectric relaxation.

At the frequencies at which dielectric polarizations are seen, the effects which give rise to the ionic, atomic and electronic polarizations are able to fully respond to the changes in the voltage. When however the frequency is increased to the infra-red region ( $10^{11}\text{Hz}$  to  $10^{14}\text{Hz}$ ), it is found that atoms and ions are no longer able to follow the changes in the field, since the frequency of the field is above their natural frequency of vibration - a phenomenon called resonance absorption. Above these frequencies, the permittivity is due completely to the electronic polarization.

At the frequencies at which dielectric relaxations are observed, the contributions of the ionic, atomic and electronic polarizations are found to be constant and do not depend on frequency. Let the polarization due to these effects be denoted  $P_\infty$ . From equation 2.11, it can be inferred that:

$$P_\infty = \varepsilon_0(\varepsilon_\infty - 1)E \quad (2.19)$$

$P_\infty$  is the polarization at frequencies above those at which dipoles are able to follow the field, and  $\varepsilon_\infty$  is the relative permittivity at these frequencies. The polarization at low frequency, denoted  $P_s$ , will be larger than  $P_\infty$ , since there will be an additional contribution from the orientation polarization. Therefore:

$$P_s = \varepsilon_0(\varepsilon_s - 1)E \quad (2.20)$$

where  $\varepsilon_s$  is the permittivity at low frequency, sometimes referred to as the static permittivity. The orientation polarization  $P_o$  is therefore equal to:

$$P_o = \varepsilon_0(\varepsilon_s - 1)E - \varepsilon_0(\varepsilon_\infty - 1)E \quad (2.21)$$

$$\therefore P_o = \varepsilon_0 E (\varepsilon_s - \varepsilon_\infty) \quad (2.22)$$

If a certain fixed field were to be applied to the dielectric, then  $P_\infty$  would reach its equilibrium value almost instantaneously. The orientation polarization however would take time to reach its equilibrium value, varying from  $10^{-10}$  seconds to a period of years. The variation of  $P_o$  with time is exponential, so the value of the orientation polarization at a time  $t$  after the fixed field has been applied is:

$$P_o(t) = P_o \left(1 - e^{-\frac{t}{\tau}}\right) \quad (2.23)$$

where  $\tau$  is a constant related to the rate at which the polarization changes, and is called the relaxation time of the dielectric material. If this equation is differentiated with respect to time, it follows that:

$$\frac{dP_o(t)}{dt} = \frac{1}{\tau} [P_o - P_o(t)] \quad (2.24)$$

$$\frac{dP_o(t)}{dt} = \frac{1}{\tau} [\varepsilon_0 E (\varepsilon_s - \varepsilon_\infty) - P_o(t)] \quad (2.25)$$

If instead of a fixed field, we consider an alternating field of field intensity  $\hat{E} = E_0 e^{j\omega t}$ , then the above equation becomes:

$$\frac{d\hat{P}_o(t)}{dt} = \frac{1}{\tau} \left[ \varepsilon_0 \hat{E} (\varepsilon_s - \varepsilon_\infty) - \hat{P}_o(t) \right] \quad (2.26)$$

Its solution for a steady-state is:

$$\hat{P}_o(t) = \frac{\varepsilon_0 (\varepsilon_s - \varepsilon_\infty)}{1 + j\omega\tau} \hat{E} \quad (2.27)$$

The complex total polarization is therefore:



$$\hat{P}(t) = \hat{P}_o(t) + \hat{P}_\infty(t) \quad (2.28)$$

$$\hat{P}(t) = \frac{\varepsilon_0(\varepsilon_s - \varepsilon_\infty)}{1 + j\omega\tau} \hat{E} + \varepsilon_0(\varepsilon_\infty - 1) \hat{E} \quad (2.29)$$

But, from equation 2.11, it may be inferred for an alternating field that:

$$\hat{\varepsilon}_r = \frac{\hat{P}(t)}{\varepsilon_0 \hat{E}} + 1 \quad (2.30)$$

$\hat{\varepsilon}_r$  is referred to as the complex permittivity.

$$\therefore \hat{\varepsilon}_r = \frac{(\varepsilon_s - \varepsilon_\infty)}{1 + j\omega\tau} + (\varepsilon_\infty - 1) + 1 \quad (2.31)$$

$$\hat{\varepsilon}_r = \varepsilon_\infty + \frac{(\varepsilon_s - \varepsilon_\infty)}{1 + j\omega\tau} \quad (2.32)$$

$$\hat{\varepsilon}_r = \varepsilon_\infty + \frac{(\varepsilon_s - \varepsilon_\infty)(1 - j\omega\tau)}{1 + \omega^2\tau^2} \quad (2.33)$$

$$\hat{\varepsilon}_r = \varepsilon_\infty + \frac{(\varepsilon_s - \varepsilon_\infty)}{1 + \omega^2\tau^2} - j \frac{(\varepsilon_s - \varepsilon_\infty)\omega\tau}{1 + \omega^2\tau^2} \quad (2.34)$$

Separating the real and imaginary parts of equation 2.34, we get:

$$\varepsilon'_r = \varepsilon_\infty + \frac{(\varepsilon_s - \varepsilon_\infty)}{1 + \omega^2\tau^2} \quad (2.35)$$

$$\varepsilon''_r = \frac{(\varepsilon_s - \varepsilon_\infty)\omega\tau}{1 + \omega^2\tau^2} \quad (2.36)$$

These are referred to as the Debye equations. The real component  $\varepsilon'_r$  is the relative permittivity which is usually denoted simply  $\varepsilon'$ . Its magnitude varies with frequency from a maximum of  $\varepsilon_s$  at low frequencies to a minimum of  $\varepsilon_\infty$  at high frequency. Figure 2.4 shows the variation with frequency of  $\varepsilon'$  for a dispersion with  $\tau = 0.00015915$ ,  $\varepsilon_s = 12$  and  $\varepsilon_\infty = 4$ .

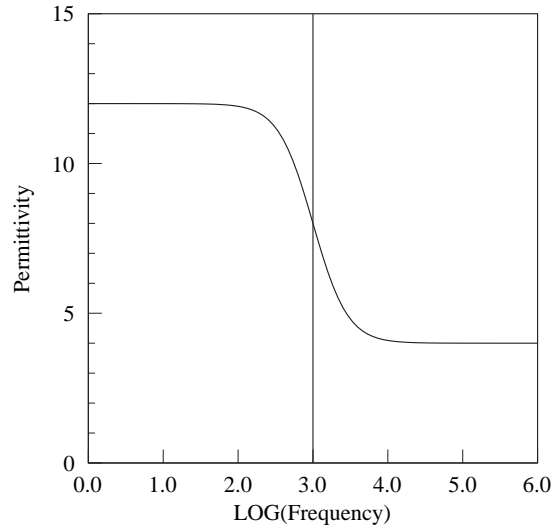


Figure 2.4: Variation of permittivity with frequency (Hz)

The imaginary component  $\varepsilon''_r$  is referred to as the dielectric loss, and usually denoted simply  $\varepsilon''$ . Figure 2.5 shows the variation of loss with frequency for the same dispersion as in Figure 2.4. It can be seen that the magnitude of the loss initially increases with frequency until it reaches a maximum value when  $\omega\tau$  is equal to 1. This occurs when the frequency reaches the value given by:

$$f_c = \frac{1}{2\pi\tau} \quad (2.37)$$

which for this dispersion is 1000Hz. At this frequency, the values of  $\varepsilon'$  and  $\varepsilon''$  are:

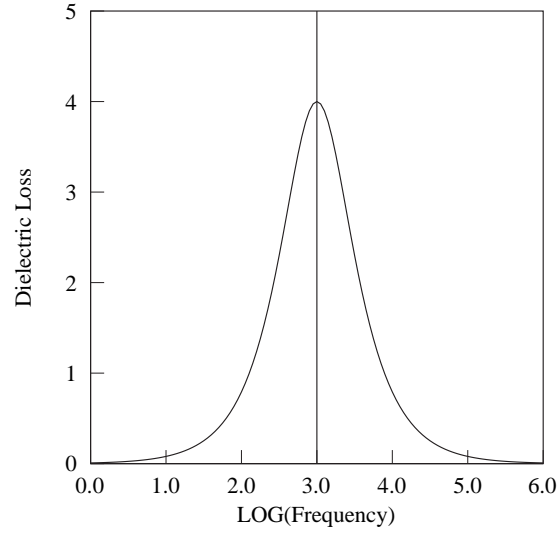


Figure 2.5: Variation of dielectric loss with frequency (Hz)

$$\epsilon' = \frac{\epsilon_s + \epsilon_\infty}{2} \quad (2.38)$$

$$\epsilon'' = \frac{\epsilon_s - \epsilon_\infty}{2} \quad (2.39)$$

i.e. at 1000Hz the permittivity is 8, and the dielectric loss is 4.

When experimental data is analysed, the relaxation time  $\tau$  can be determined by finding the frequency at which  $\epsilon''$  is a maximum. At higher frequencies, the loss decreases to a negligible value.

The Debye equations (2.35 and 2.36) are able to describe a system in which all the components have identical relaxation times, and where the width of the  $\epsilon''$  peak at the half-height value is 1.14 decades. In practice however, most experimental spectra are found to have broader absorption curves and lower maximum dielectric loss. It is thought that each dipole may have a relaxation time which is slightly

different to other dipoles, thus giving in each material a range of relaxation times distributed around a mean value.

### 2.2.3 Cole-Cole distributions

To take account of this distribution of relaxation times, Cole and Cole (Cole and Cole, 1941) modified equation 2.34 by introducing a parameter  $h$ , as shown below:

$$\hat{\varepsilon}_r = \varepsilon_\infty + \frac{(\varepsilon_s - \varepsilon_\infty)}{1 + (j\omega\tau)^{1-h}} \quad (2.40)$$

Where  $0 \leq h < 1$ , and  $\tau$  is now considered to be the mean effective relaxation time. Obviously, when  $h = 0$ , Equation 2.40 is equivalent to Equation 2.34. As the distribution of relaxation times tends towards infinity,  $h$  tends towards 1. For most experimental results therefore, the values of the permittivity and loss can be derived from Equation 2.40 by separating the real and imaginary parts to give:

$$\varepsilon' = \varepsilon_\infty + \frac{(\varepsilon_s - \varepsilon_\infty) (1 + (\omega\tau)^{(1-h)} \sin \frac{\pi h}{2})}{1 + 2(\omega\tau)^{(1-h)} \sin \frac{\pi h}{2} + (\omega\tau)^{2(1-h)}} \quad (2.41)$$

$$\varepsilon'' = \frac{(\varepsilon_s - \varepsilon_\infty) ((\omega\tau)^{(1-h)} \cos \frac{\pi h}{2})}{1 + 2(\omega\tau)^{(1-h)} \sin \frac{\pi h}{2} + (\omega\tau)^{2(1-h)}} \quad (2.42)$$

Figures 2.6 and 2.7 show the variations of permittivity and loss with frequency. The values of all the parameters are the same as in Figures 2.4 and 2.5, except that  $h$  is now equal to 0.2. The value of  $h$  was, of course, effectively equal to 0 in the previous figures. It can be seen that the loss peak is now broader and the maximum value of the loss is lower. The permittivity graph has a shallower gradient near the mean value of the relaxation frequency, and the permittivity value reaches its low and high frequency limits further away from that frequency.

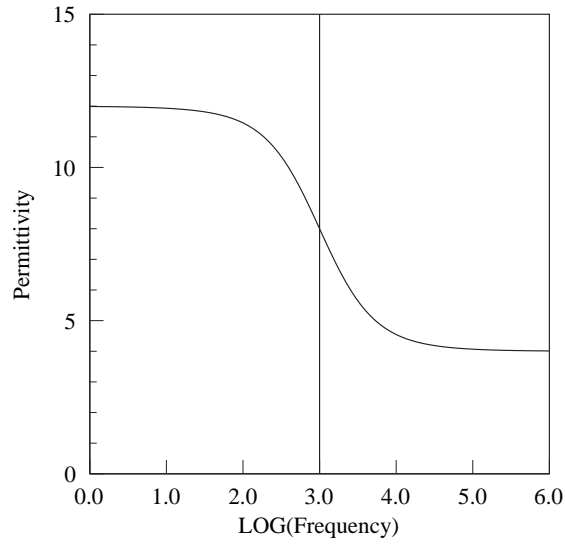


Figure 2.6: Permittivity vs LOG frequency (Hz) ( $h=0.2$ )

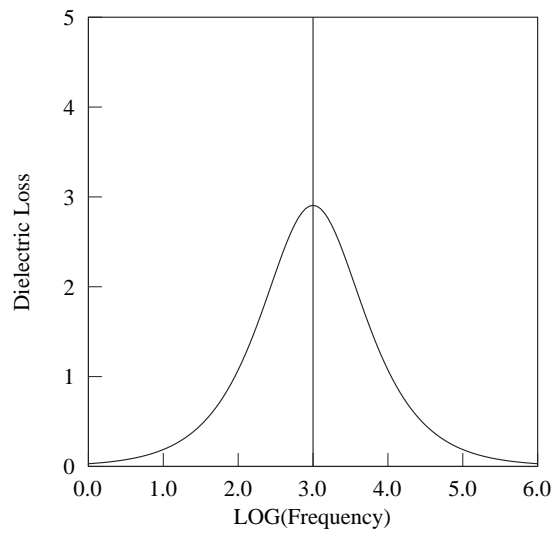
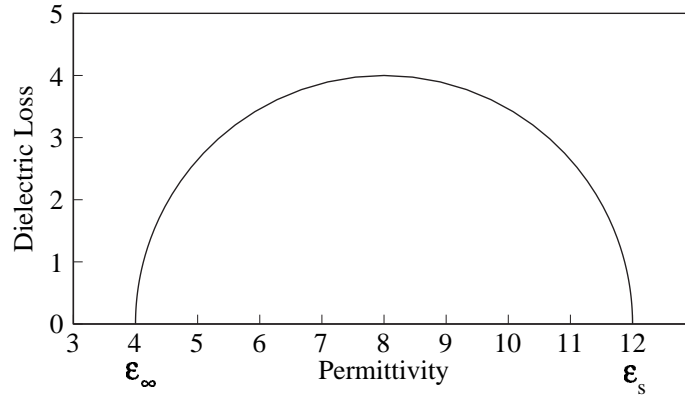


Figure 2.7: Loss vs LOG frequency (Hz) ( $h=0.2$ )

Figure 2.8: Cole-Cole plot - Single relaxation time ( $h=0$ )

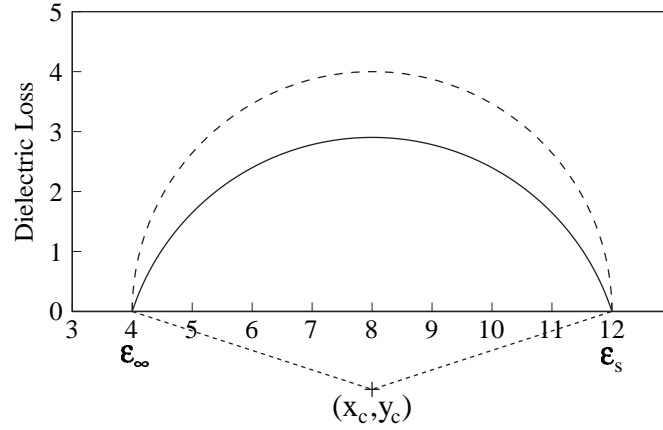
### 2.2.4 Cole-Cole Plots

The Debye equations (2.35 and 2.36) may be rearranged to give the equation:

$$\left[ \varepsilon' - \frac{(\varepsilon_s + \varepsilon_\infty)}{2} \right]^2 + [\varepsilon'']^2 = \left[ \frac{(\varepsilon_s - \varepsilon_\infty)}{2} \right]^2 \quad (2.43)$$

This is of the form  $(x - a)^2 + y^2 = r^2$ , which is the equation for a circle. Equation 2.43 can therefore be thought of as representing a circle of radius  $(\varepsilon_s - \varepsilon_\infty)/2$  with its centre point at  $(\varepsilon_s + \varepsilon_\infty)/2, 0$ , on a graph of  $\varepsilon''$  against  $\varepsilon'$ . Only positive values of  $\varepsilon''$  and  $\varepsilon'$  are possible, so the graph is a semicircle, as shown in Figure 2.8. This is called a complex permittivity plot, or more commonly a Cole-Cole plot (after its originators).

For a dispersion with a single relaxation time, the plot of  $\varepsilon'$  against  $\varepsilon''$  intersects with the  $\varepsilon'$  axis at the points  $(\varepsilon_\infty, 0)$  and  $(\varepsilon_s, 0)$ , and the centre of the semicircle is on the  $\varepsilon'$  axis. When however a Cole-Cole plot is drawn for a dielectric in which there is a distribution of relaxation times, the centre of the semicircle will be below the  $\varepsilon'$  axis, as shown in Figure 2.9. (The Cole-Cole plot for  $h = 0$  is shown as a

Figure 2.9: Cole-Cole plot - distribution of relaxation times ( $h=0.2$ )

dotted line for comparison). The equation for the case where  $h > 0$  is:

$$\left[ \epsilon' - \left( \frac{\epsilon_s + \epsilon_\infty}{2} \right) \right]^2 + \left[ \epsilon'' + \left( \frac{\epsilon_s - \epsilon_\infty}{2} \right) \tan \left( \frac{\pi h}{2} \right) \right]^2 = \left[ \left( \frac{\epsilon_s - \epsilon_\infty}{2} \right) \sec \left( \frac{\pi h}{2} \right) \right]^2 \quad (2.44)$$

This represents a circle of radius  $\left[ \left( \frac{\epsilon_s - \epsilon_\infty}{2} \right) \sec \left( \frac{\pi h}{2} \right) \right]$  with its centre at  $(x_c, y_c)$ , where:

$$x_c = \frac{(\epsilon_s + \epsilon_\infty)}{2} \quad (2.45)$$

$$y_c = -\frac{(\epsilon_s - \epsilon_\infty)}{2} \tan \frac{h\pi}{2} \quad (2.46)$$

A lower semicircular Cole-Cole plot corresponds to a material with a wide distribution of relaxation times. Values of  $\epsilon_s$  and  $\epsilon_\infty$  taken from the intercepts, enable the value of  $h$  to be calculated from Equation 2.46.

### 2.2.5 Multiple Dispersions

In practical experimental situations, dielectric spectra are usually more complex than those produced in systems derived from either a single relaxation time, or a spread of such dispersions centred on one frequency.

Assuming that the relaxation processes producing a multiple dispersion plot are independent, then the high frequency permittivity of the lower frequency dispersion will be equal to the low frequency permittivity of the neighbouring high frequency dispersion. The principle of superposition may then be used to resolve the dispersions, and Equations 2.41 and 2.42 can be modified to give the total permittivity and total loss from multiple dispersions as follows:

$$\varepsilon' = \varepsilon_{\infty,1} + \sum_{i=1}^{i=n} \frac{(\varepsilon_{s,i} - \varepsilon_{\infty,i}) (1 + (\omega\tau_i)^{(1-h_i)} \sin \frac{\pi h_i}{2})}{1 + 2(\omega\tau_i)^{(1-h_i)} \sin \frac{\pi h_i}{2} + (\omega\tau_i)^{2(1-h_i)}} \quad (2.47)$$

$$\varepsilon'' = \sum_{i=1}^{i=n} \frac{(\varepsilon_{s,i} - \varepsilon_{\infty,i}) ((\omega\tau_i)^{(1-h_i)} \cos \frac{\pi h_i}{2})}{1 + 2(\omega\tau_i)^{(1-h_i)} \sin \frac{\pi h_i}{2} + (\omega\tau_i)^{2(1-h_i)}} \quad (2.48)$$

Figure 2.10 shows a graph of dielectric loss against LOG Frequency made up of three dispersions - the dotted lines show the separate contributions. Figure 2.11 shows the corresponding Cole-Cole plot, again with the individual dispersions.

Attempts can be made to analyse the data in order to resolve the individual dispersions; Section 5.6 includes a discussion on the use of Genetic Algorithms in Matlab for this purpose. Davidson (Davidson, 1961) reported on how useful such methods are for various combinations of dispersions. He commented that the successful resolution of dispersions is only possible if the relaxation times are substantially different to each other. Even then, he says that “results may sometimes be analysed in more than one way.” In such circumstances, it is difficult to justify drawing conclusions



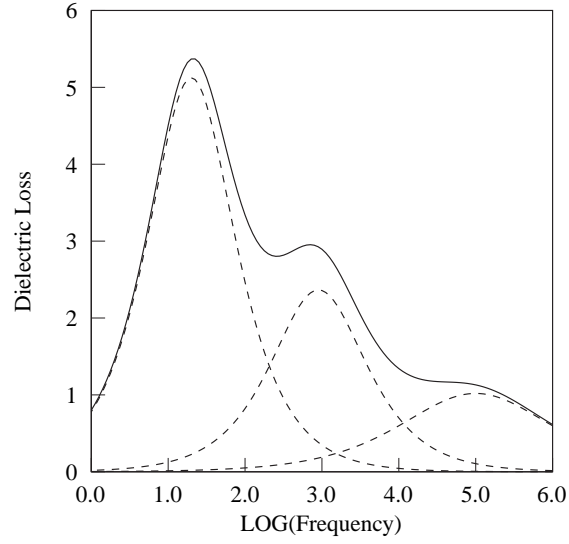


Figure 2.10: Loss vs LOG frequency (Hz) for multiple dispersions

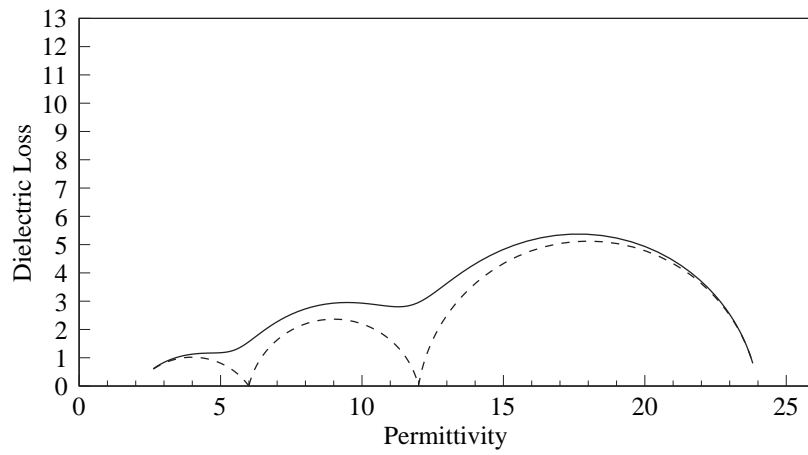


Figure 2.11: Cole-Cole plot for multiple dispersions

from such analyses.

### 2.2.6 D.C. Conductivity

As noted above, the process of dielectric absorption is related to the dissipation of energy in a material. Such energy losses can also be produced by processes related to the d.c. conductivity  $\sigma$ , and these make a contribution to the total dielectric absorption. Therefore the total dielectric loss  $\varepsilon''_T$  at a frequency  $f$  is made up of the ordinary loss as discussed above, plus a term due to the d.c. conductivity:

$$\varepsilon''_T = \varepsilon'' + \frac{\sigma}{2\pi f \varepsilon_0} \quad (2.49)$$

Whilst the contribution of the d.c. conductivity will probably be negligible at high frequencies, at very low frequencies the second term can become predominant. This can be seen in Figures 2.12 and 2.13. Both these figures show two dispersions - one labelled D1 at approximately 10Hz and the other labelled D2 at approximately 1000Hz - the individual dispersions are shown as dotted lines. In both cases the solid line shows the combined loss from both dispersions. In Figure 2.12, the presence of the two dispersions is obvious in the combined loss plot. But in Figure 2.13, D.C. conductivity completely masks the presence of the lower frequency dispersion.

### 2.2.7 Electrode polarization

When a metallic electrode is placed into a solution, a d.c. potential is set up between the electrode and the liquid in contact with it. Application of an electric field, as in measurement of the dielectric properties of a solution, will cause a change in that d.c. potential over a time interval which is dependent on the nature of the solution and of the metal of the electrode. This effect is called Electrode Polarization, and was

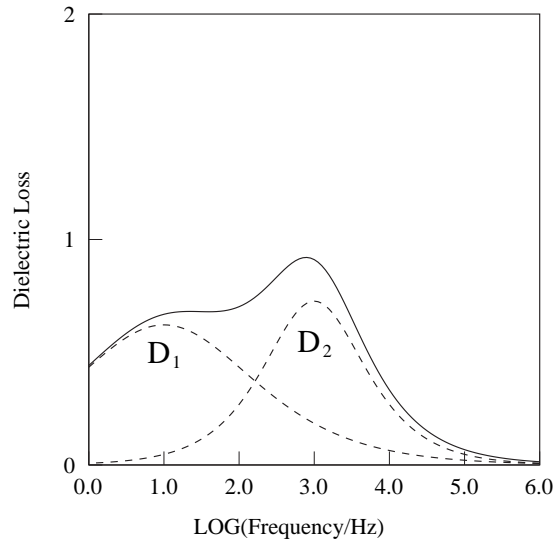


Figure 2.12: Loss vs LOG frequency for 2 dispersions

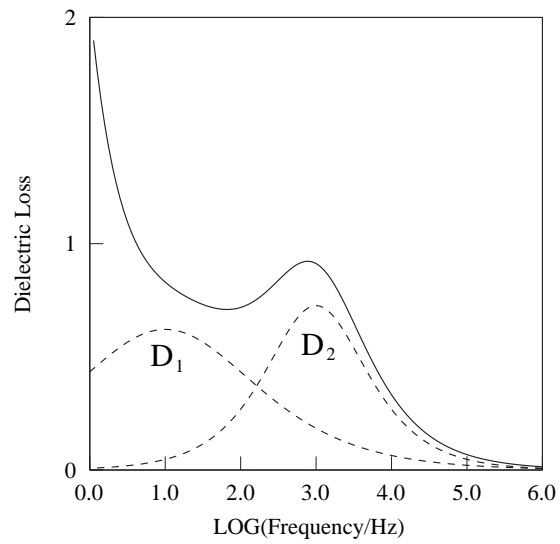


Figure 2.13: Loss vs LOG frequency for 2 dispersions + DC conductivity

extensively described by Schwan (Schwan, 1966). Electrode polarization can modify dielectric spectra, especially at low frequencies, and the effect can vary from one experiment to another, even when using the same electrode and the same solution.

In this thesis, the data is analysed mainly by considering the Difference Signal, i.e. the *difference* between dielectric loss plots of DNA solution, with and without applied magnetic field (See Section 2.5). The difference signal is composed only of those parts of the dielectric loss spectrum which change with magnetic field, and completely ignores those parts which are unaffected by magnetic field. The measurements of the two spectra whose difference is used to calculate the Difference Signal are separated by a time interval of at most three minutes. All other factors apart from magnetic field, including electrode polarization, are unchanged in that time. It may be concluded therefore that, although electrode polarization will modify loss spectra unpredictably, the difference signal will remain unaffected.

### 2.2.8 Maxwell-Wagner Polarization

In a heterogeneous material composed of a range of different substances each with its own conductivity and permittivity, charge carriers are able to move more easily through some parts than others. When an electric field is applied to such a material, charge will concentrate at points of discontinuity which are due to change in dielectric property, or due to structural defects

Should an alternating electric field be applied to such a heterogeneous material, the rate at which charge carriers congregate at boundaries will vary with the frequency of the applied field. Since the distribution of the charge carriers will then be time-dependent, this can lead to frequency dependence in the dielectric properties of the material, even though the dielectric properties of the individual substances show no such dependence. The dispersions which can be observed in such a heterogeneous material are called Maxwell-Wagner or interfacial polarizations.

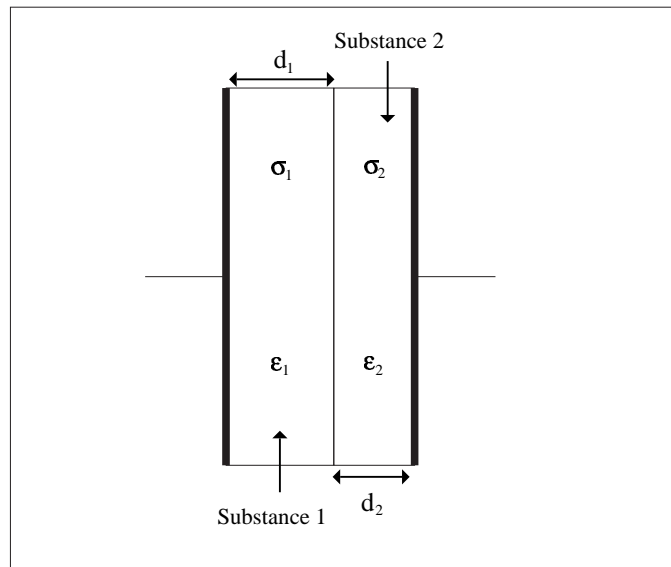


Figure 2.14: The two-layer heterogeneous system

As an example of a simple system which shows interfacial polarization, consider Fig-

ure 2.14. Two slices of dielectric both of cross-sectional area  $A$  and of thicknesses  $d_1$  and  $d_2$  are placed between two electrodes, and an electric field of frequency  $f$  applied. The permittivities of the two substances are  $\varepsilon_1$  and  $\varepsilon_2$ , and their conductivities are  $\sigma_1$  and  $\sigma_2$ .

Volger (Volger, 1960) derived equations for the Maxwell-Wagner dispersions in multi-layered systems of different materials. He assumed that each layer could be modelled by a capacitor with a resistance in parallel. For a system of  $n$  layers, the dispersion could be described in terms of the Debye equations:

$$\varepsilon' = \varepsilon_\infty + \frac{(\varepsilon_s - \varepsilon_\infty)}{1 + \omega^2\tau^2} \quad (2.50)$$

$$\varepsilon'' = \frac{(\varepsilon_s - \varepsilon_\infty)\omega\tau}{1 + \omega^2\tau^2} \quad (2.51)$$

where  $\varepsilon_s$  and  $\varepsilon_\infty$  may be calculated from:

$$\varepsilon_s = \frac{\sum_{i=1}^n d_i \sum_{i=1}^n \frac{\varepsilon_i d_i}{\sigma_i}}{\left(\sum_{i=1}^n \frac{d_i}{\sigma_i}\right)^2} \quad (2.52)$$

$$\varepsilon_\infty = \frac{\sum_{i=1}^n d_i}{\sum_{i=1}^n \frac{d_i}{\varepsilon_i}} \quad (2.53)$$

For the two-layer system, using  $d = d_1 + d_2$ , these may be simplified to the following:

$$\varepsilon_s = \frac{d(\varepsilon_1 d_1 \sigma_2^2 + \varepsilon_2 d_2 \sigma_1^2)}{(\sigma_1 d_2 + \sigma_2 d_1)^2} \quad (2.54)$$

$$\varepsilon_{\infty} = \frac{d\varepsilon_1\varepsilon_2}{\varepsilon_1d_2 + \varepsilon_2d_1} \quad (2.55)$$

For a system of  $n$  layers, the number of dispersions will appear to be  $n - 1$ . Thus for two layers there will appear to be one dispersion, with  $\tau$  given by:

$$\tau = \frac{\varepsilon_0 (\varepsilon_1d_2 + \varepsilon_2d_1)}{\sigma_1d_2 + \sigma_2d_1} \quad (2.56)$$

It is thought that more complex systems such as a cylinder surrounded by a shell with different dielectric properties can also produce Maxwell-Wagner type dispersions.

## 2.3 Structure of DNA

(Part of this section has been adapted from the web-page <http://www.chemguide.co.uk/organicprops/aminoacids/dna1.html>. The diagrams have been redrawn to include all the atoms in the structure.)

### 2.3.1 Structure of DNA backbone

One part of the backbone of a DNA strand is deoxyribose, which as the name suggests is the sugar ribose after the removal of an oxygen atom. Figure 2.15 shows ribose and deoxyribose. The ring structure is made up of one oxygen atom and four carbon atoms. These are numbered as shown in Figure 2.15 1' to 4'. The carbon atom denoted 5' is part of the  $CH_2OH$  group attached to the main ring carbon atom denoted 4'.

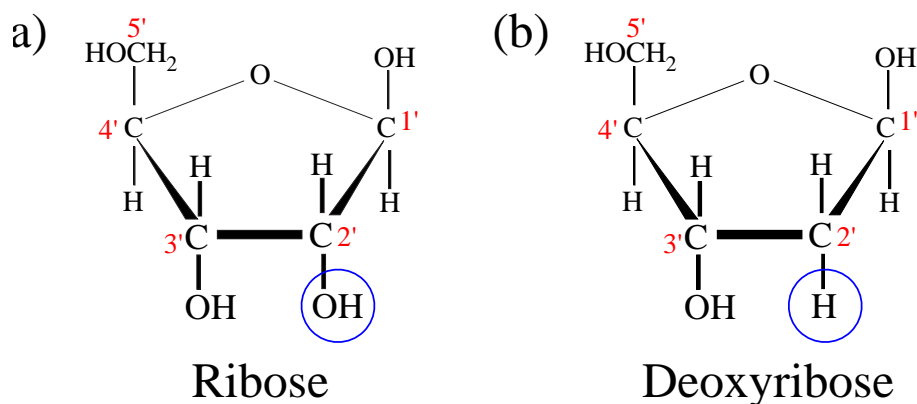


Figure 2.15: Ribose and Deoxyribose

A phosphate group is now attached to the sugar molecule as shown in Figure 2.16, where it can be seen that the phosphate has replaced the OH group attached to the



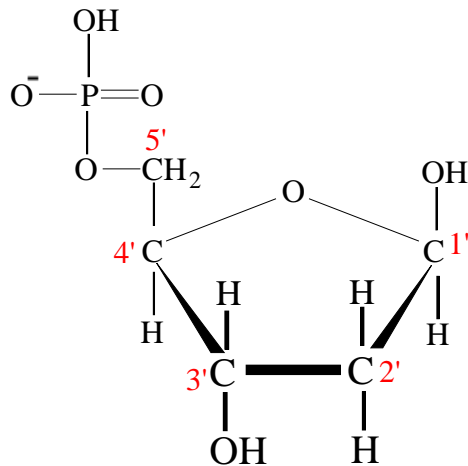


Figure 2.16: Ribose and Deoxyribose

5' carbon atom.

### 2.3.2 Construction of nucleotides

A nucleotide is made up of the sugar-phosphate molecule seen in Figure 2.16, together with an organic base, which is attached to the 1' carbon atom, as shown in Figure 2.17. The OH group on the 1' carbon is lost in the process.

The four possible bases which form part of the DNA structure are shown in Figure 2.18. (a) shows the base Cytosine, (b) Thymine, (c) Adenine and (d) Guanine. As can be seen, Cytosine and Thymine have one ring, and are known as Pyrimidines. Adenine and Guanine have two rings, and are called Purines. The hydrogen atom shown in red in each of these structures is discarded when the base is attached to the 1' carbon atom of the sugar-phosphate molecule via the Nitrogen atom shown in blue. Thus the nucleotide containing Cytosine would have the structure shown

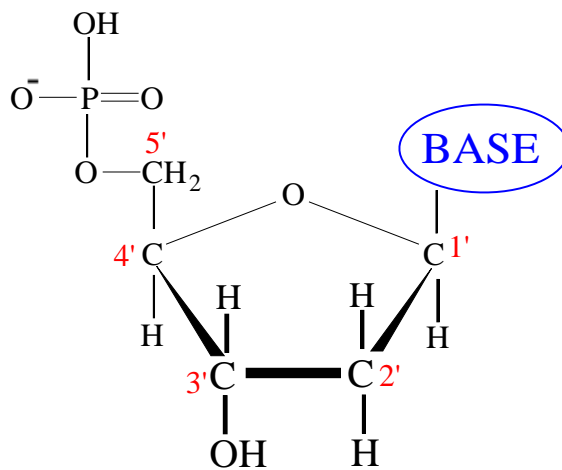


Figure 2.17: Attachment of base

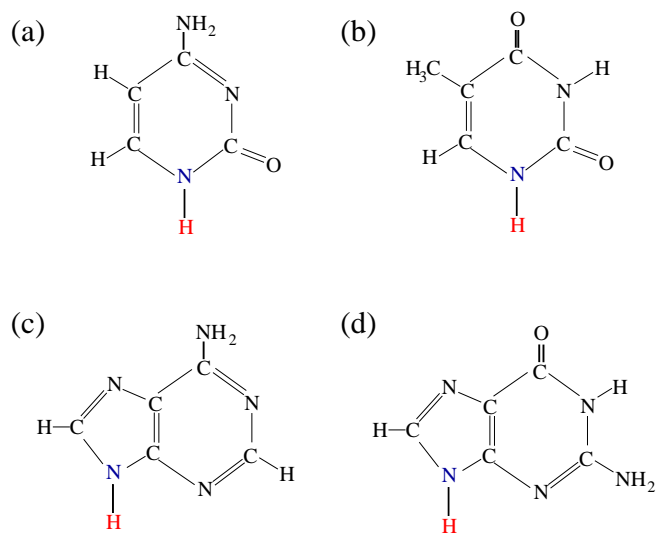


Figure 2.18: (a) Cytosine (b) Thymine (c) Adenine (d) Guanine

in Figure 2.19.

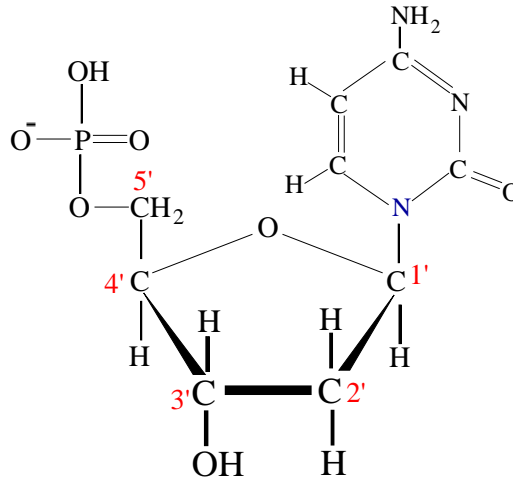


Figure 2.19: Nucleotide containing Cytosine

### 2.3.3 Construction of DNA strand

Nucleotides can be joined together in a string, by linking the phosphate group of one nucleotide to the 3' carbon atom of the next nucleotide, as shown in Figure 2.20. As can be seen, a molecule of water is discarded as each nucleotide is attached to the string.

### 2.3.4 Simplification

If we illustrate the phosphate group by a diamond labelled P, the deoxyribose ring by a pentagon with the oxygen atom indicated, and the base by a rectangle labelled with the initial letter of its name (C,T,A or G), then Figure 2.20b can be redrawn, and extended as shown in Figure 2.21. Note that since the bases Adenine and

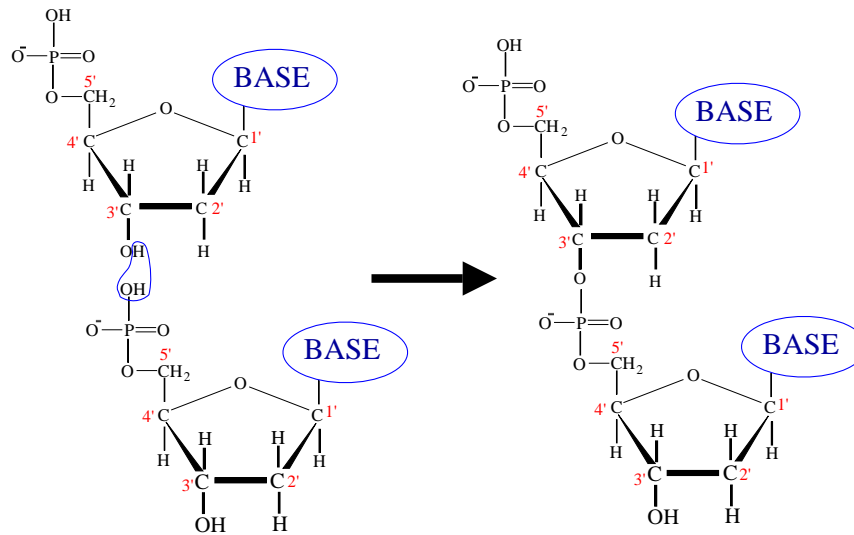


Figure 2.20: Construction of DNA strand

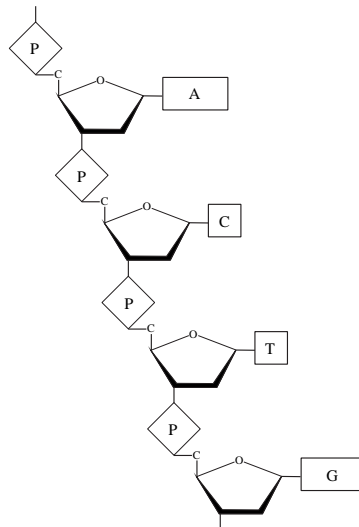


Figure 2.21: Simplified construction of DNA strand

Guanine has two rings, whereas Cytosine and Thymine have only one ring, the A and G rectangles are shown larger than the C and T rectangles.

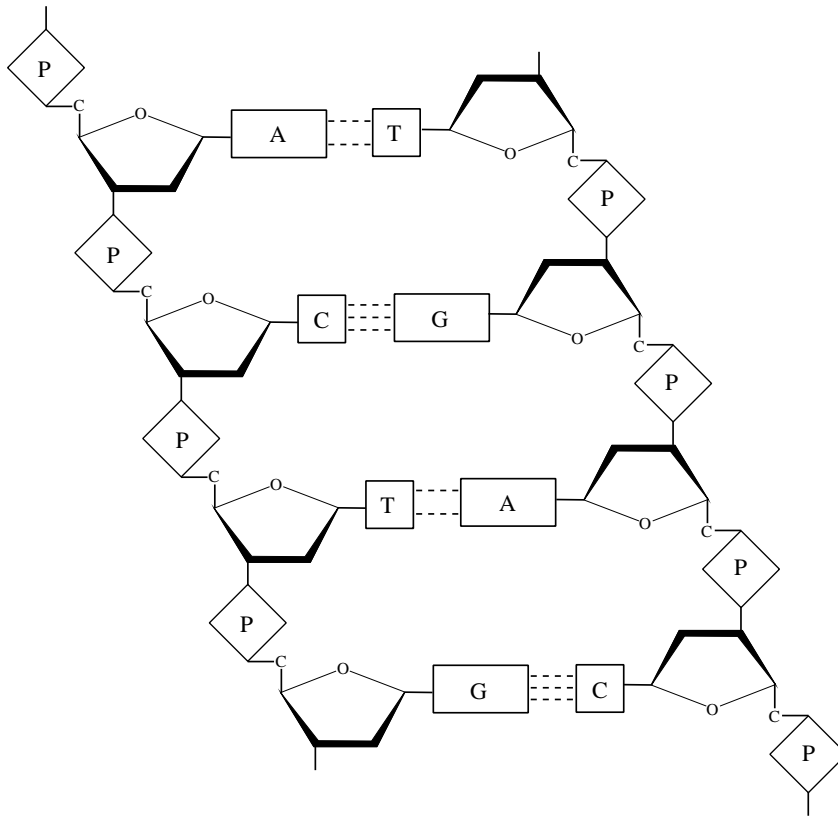


Figure 2.22: Simplified paired DNA strands

The DNA strand shown in Figure 2.21 is paired with a similar strand, when the bases of the first strand connect to the bases of the second strand via hydrogen bonds. Because of the structure of the bases, Adenine always pairs with Thymine using two hydrogen bonds, and Cytosine and Guanine connect using three hydrogen bonds. (Figure 2.22). The AT and CG combinations are known as base-pairs.

The two strands of DNA form a right-handed double helix, i.e. they twist around each other with approximately 10 base-pairs per helical turn, each of which measures

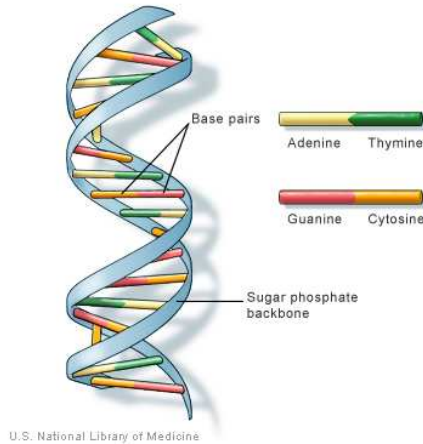


Figure 2.23: Model of Structure of DNA

approximately 3.4nm. (See Figure 2.23) The double helix has a constant diameter of 2nm, and the two chains have anti-parallel polarity i.e. one is effectively upside-down compared to the other.

### 2.3.5 Denaturing DNA

The base-pairs in DNA can be separated by breaking the hydrogen bonds seen in Figure 2.22; the DNA then takes up a random coil configuration as separate strands. This *denatured* state can be achieved by breaking the bonds with heat, increasing the pH, or by using chemicals such as urea or formamide. When heat is used and the two strands begin to separate, the melting point is defined as the temperature at which half of the DNA has denatured; i.e. when half of the base pairs have had their hydrogen bonds broken.

### 2.3.6 Counter-ion layer

The phosphate groups which form part of the sugar-phosphate backbone, seen in Figure 2.23, are on the outside of the DNA double-helix, and carry a net negative charge (See Figure 2.20). In aqueous solutions, particularly in saline solutions, some of this negative charge is neutralized by cations from the solution. These cations, (e.g. positive sodium ions if the DNA is dissolved in sodium chloride) are therefore attracted to the negative phosphate groups, and form a counter-ion layer around the DNA helix. Manning (Manning, 1978) proposed that the binding of the counter-ions was non-localized, i.e. the positive ions in the counter-ion layer are able to move freely up and down the outside of the DNA helix and inside the layer itself. Apart from these counter-ions, which he denoted *condensed counter-ions*, he suggested that the other positive ions in the saline solution could be separated into *diffuse counter-ions* which neutralize the remainder of the charge, and the *bulk* ions in the rest of the saline solution.

Bonincontro (Bonincontro et al., 1984) described counter-ion fluctuation in the condensed phase as an example of interfacial polarization. The dielectric decrement of a dispersion caused by such fluctuations should therefore be independent of temperature.

## 2.4 Diamagnetism

If a magnetic field is applied to a molecule, those electrons which have their orbits perpendicular to the field direction will experience a very small change in their angular momentum. This may be predicted by Faraday's Law, which states that moving charged particles in a magnetic field will experience a force.

Should the molecule contain paired electrons whose angular momenta are opposite, then in the *absence* of a magnetic field, their angular momenta will cancel exactly - the molecule has no net magnetic moment. When a magnetic field is applied to such a molecule however, the change in angular momentum will be different for each pair of electrons, and this produces an *induced* magnetic moment. This condition, where the direction of the induced moment is *opposite* to the direction of the applied field is referred to as *Diamagnetism*. Diamagnetic substances include hydrogen, ammonia, bismuth, copper and graphite - they will all be *repelled* by a magnet, though with very little force. Diamagnetism is present in *all* materials, but is extremely weak and is often masked by stronger magnetic effects.

For a magnetic material, its *Permeability* is defined from the following equation:

$$\mu = \frac{B}{H} \quad (2.57)$$

where B is the magnetic flux density in the material, measured in Tesla, and H is the magnetic field strength in Henry. For a vacuum, this is called the permeability of free space, and is denoted  $\mu_0$ . It has a value of  $4\pi \times 10^{-7}$ .

The *relative* permeability of a material is defined as:

$$\mu_r = \frac{\mu}{\mu_0} \quad (2.58)$$



where  $\mu$  is the material's permeability, and  $\mu_0$  is the permeability of free space. For diamagnetic substances, their permeability is almost equal to  $\mu_0$ . It is therefore more useful to define the material's *Susceptibility*, which is:

$$\chi = \mu_r - 1 \tag{2.59}$$

where  $\mu_r$  is the material's relative permeability. Diamagnetic materials have relative permeability slightly smaller than one; their susceptibilities are therefore *negative*. Examples of some susceptibility values are:

- $\chi$  for Bismuth =  $-16.7 \times 10^{-5}$
- $\chi$  for Copper =  $-0.92 \times 10^{-5}$
- $\chi$  for Hydrogen =  $-0.0002 \times 10^{-5}$

## 2.5 Detection of small changes in dielectric properties

This section introduces the concept of the *Difference Signal* - a plot which shows the effect of small changes in the parameters of a dispersion much more clearly than superimposed plots of the dielectric loss before and after the changes.

In this simulation, let there be two contributions to a dielectric loss spectrum i.e. a plot of dielectric loss against LOG(frequency):

- The first is a *fixed* contribution which is not affected by the application of magnetic field. The nature of the fixed component may consist of other dispersions, d.c. conductivity or some other cause. For the purpose of this simulation, the only important quality of the fixed contribution is, as its name suggests, that it is independent of changes in magnetic field. For this simulation, the fixed component is made up of two dispersions. This should not however be taken to imply that the low frequency spectrum of DNA could be modelled as three dispersions.
- The second contribution to the dielectric loss spectrum is a *single dispersion* which is modified in some way by a magnetic field, and in this simulation is assigned an initial relaxation frequency of 1900 Hz.

The complete loss spectrum, made up from the two components is shown as the solid line plot in the upper graph in Figure 2.24. The left-hand vertical line indicates the initial relaxation frequency of the dispersion, i.e. 1900 Hz.

Let the parameters of the single dispersion be changed as if by the application of an external magnetic field; e.g. let the relaxation frequency be increased from 1900

Hz to 2400 Hz, indicated by the right-hand vertical line. The fixed contribution to the loss graph is of course constant, whilst the dispersion moves slightly towards higher frequencies. The resultant loss graph made up of the fixed contribution and the modified dispersion can be seen as a dotted line in the upper graph in Figure 2.24. Detailed examination shows that the loss values increase in magnitude at high frequencies, whilst decreasing at low frequencies. There is no change in the loss value at some intermediate frequency.

The change in the dielectric loss plots is so small however that it is difficult to see exactly what has occurred, and analysis of both curves with programs using Matlab's Genetic Algorithm toolbox fails to indicate reliably the parameters of the dispersions before and after application of the magnetic field. This is where the concept of the Difference Signal is introduced.

If the Loss *without* magnetic field is denoted  $Loss_1$ , and the Loss *with* magnetic field is denoted  $Loss_2$ , then the change in Loss  $dLoss$  is found from:

$$dLoss = Loss_2 - Loss_1 \quad (2.60)$$

Note that quantities such as  $Loss_1$  should be properly denoted  $Loss_1(f)$ , where  $f$  represents frequency, since they are all functions of frequency, even though the nature of those functions would be difficult to determine. For brevity however, the simpler form will be used.

$Loss_1$  was made up of the fixed component (FC) and the dispersion with relaxation frequency 1900 Hz, denoted D1900; therefore:

$$Loss_1 = FC + D1900 \quad (2.61)$$

Similarly,  $Loss_2$  is made up of the fixed component (FC) and the dispersion with relaxation frequency 2400 Hz, denoted D2400; therefore:

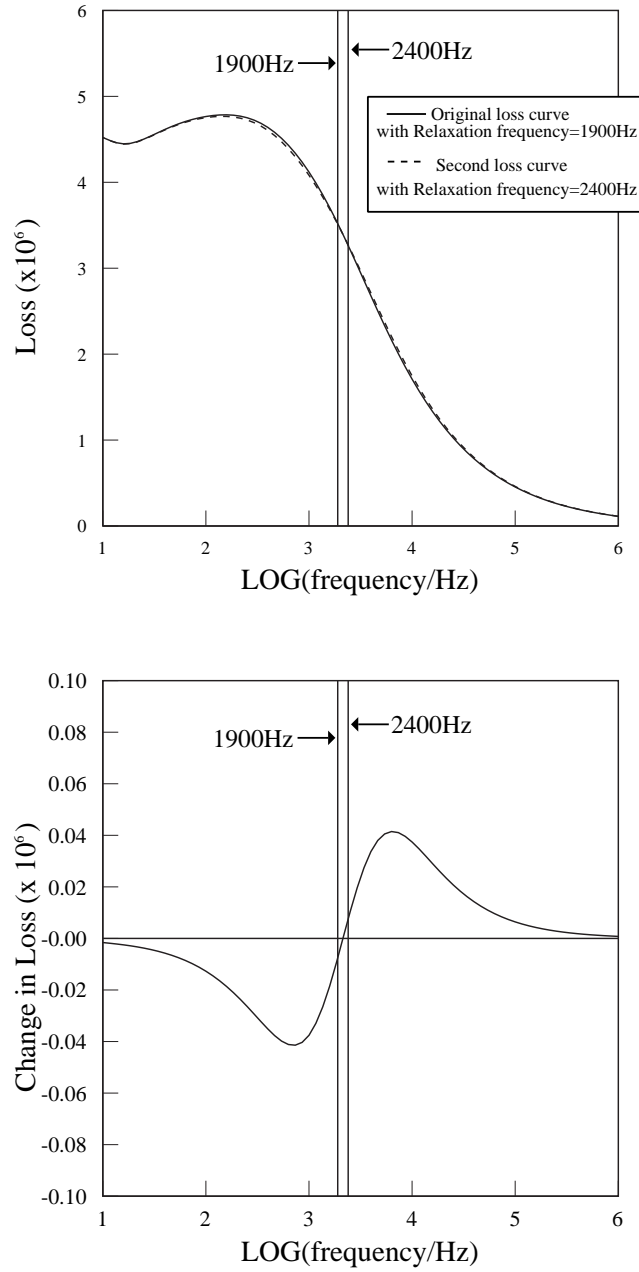


Figure 2.24: Simulation of Loss graphs (upper) and dLoss graph (lower) for increase in frequency of highest frequency dispersion

$$Loss_2 = FC + D2400 \quad (2.62)$$

Substituting for  $Loss_1$  and  $Loss_2$  in Equation 2.60, the following is derived:

$$dLoss = FC + D2400 - (FC + D1900) \quad (2.63)$$

$$dLoss = D2400 - D1900 \quad (2.64)$$

The lower graph in Figure 2.24 shows dLoss against LOG Frequency for the same parameters as used in the upper graph; it will be denoted the *Difference Signal*. In this case the result of the change is much easier to see than in the upper graph. The shape of the curve is indicative of an *increase* in the relaxation frequency of the dispersion. The point at which dLoss is zero has moved to a frequency slightly higher than the original frequency. This point, where the dLoss plot crosses the LOG(Frequency) axis, will be denoted the *null point*.

From Equation 2.64, it can be seen that the Difference Signal does not include any contribution from the fixed component of the dielectric loss spectrum. As such the Difference Signal isolates only those components of the dielectric loss spectrum which change with magnetic field. It should be noted that analysis of the Difference Signal can shed no light on the nature or magnitude of the fixed component.

Just as the lower graph in Figure 2.24 shows the Difference Signal for increasing frequency, Figure 2.25 shows the Difference Signal for the case where the frequency is *decreased* from 1900Hz to 1500Hz, whilst keeping all other parameters constant. The shape of the dLoss plot is completely different to the case where the frequency is increased - it is almost a mirror image in the LOG(frequency) axis. The point at which dLoss is zero i.e. the null point, has moved to a frequency slightly lower than the original frequency.

Figure 2.26 shows the dLoss plot for the case where  $h$ , the Cole-Cole parameter from

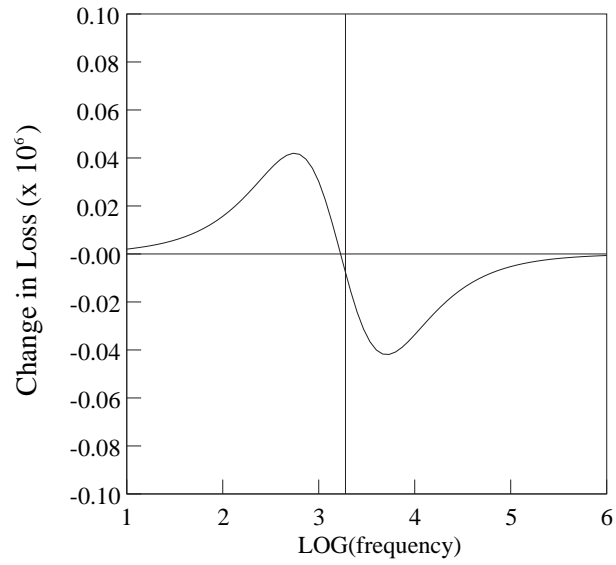


Figure 2.25: dLoss graph for decrease in frequency of highest frequency dispersion

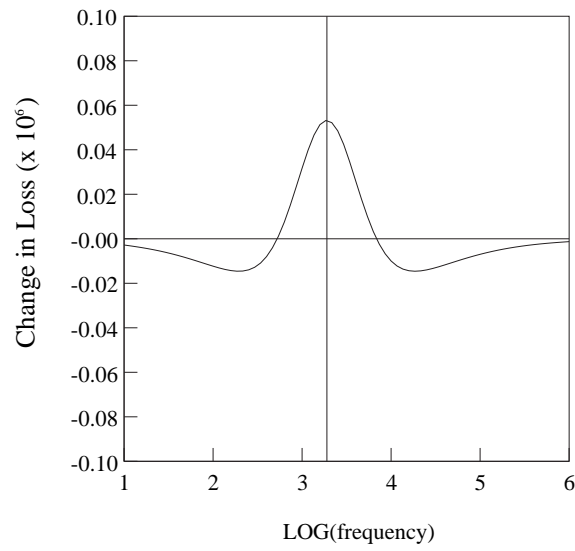


Figure 2.26: dLoss graph for decrease in  $h$  of highest frequency dispersion

Equation 2.40 is *decreased* for the affected dispersion, keeping all other parameters constant. The shape of the plot is completely different to those seen in Figures 2.24 and 2.25. Figure 2.27 shows the dLoss plot for the case where  $h$  is *increased* for the affected dispersion, keeping all other parameters constant.

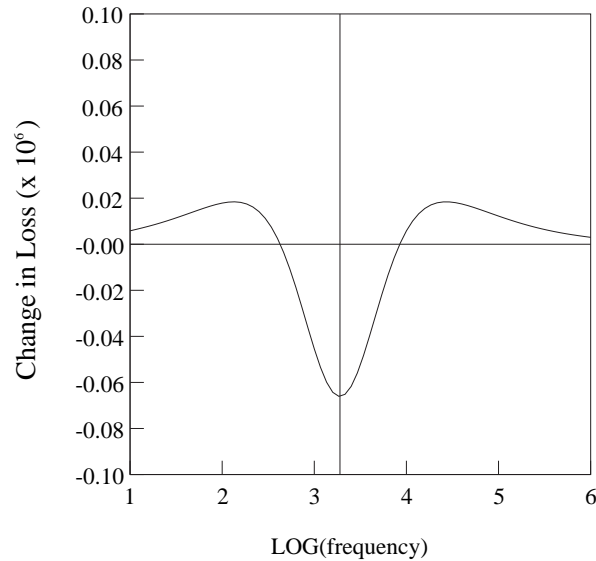


Figure 2.27: dLoss graph for increase in  $h$  of highest frequency dispersion

Figure 2.28 shows the dLoss plot for the case where the dielectric decrement  $d\varepsilon = \varepsilon_s - \varepsilon_\infty$  for the affected dispersion, is *increased*, keeping all other parameters constant. Similarly, Figure 2.29 shows the dLoss plot for the case where the dielectric decrement  $d\varepsilon$  for the affected dispersion, is *decreased*, keeping all other parameters constant.

In practice, the difference between the dielectric loss spectrum of DNA solution with *no* magnetic field and that *with* a magnetic field i.e. the Difference Signal, is similar in general shape to the lower graph in Figure 2.24. Analysis indicates however that whilst only frequency is changed to create that plot, *all* the dielectric parameters associated with one dispersion change with application of the magnetic field (See Section 5.6.2). The detailed structure of the Difference Signal is dependent on the

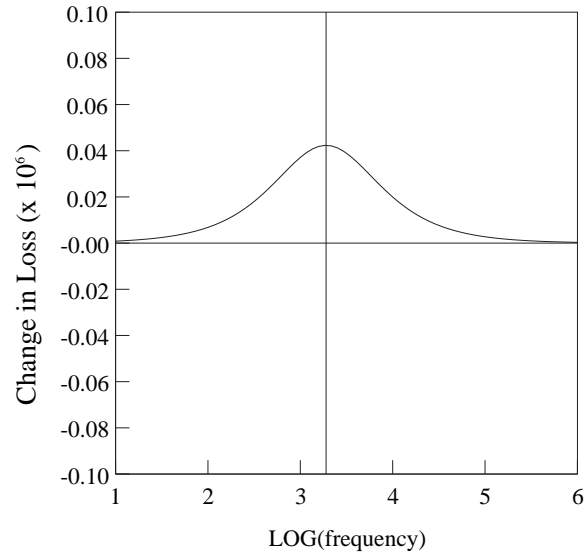


Figure 2.28: dLoss graph for increase in  $d\varepsilon$  of highest frequency dispersion

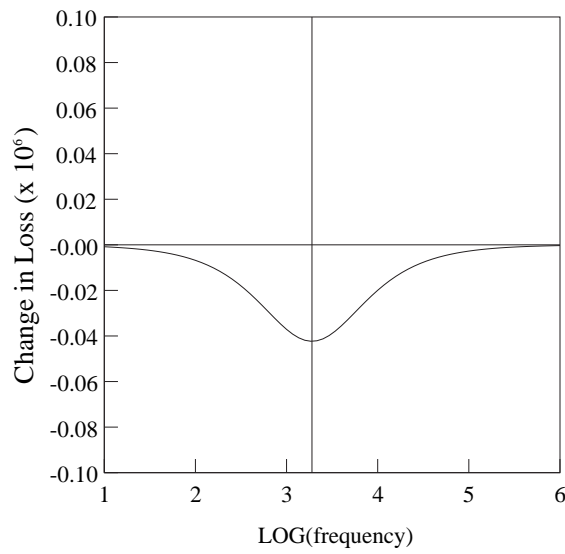


Figure 2.29: dLoss graph for decrease in  $d\varepsilon$  of highest frequency dispersion



magnitudes and directions of the relative changes in all the parameters which define a dispersion. As such, analysis must use advanced techniques such as Genetic Algorithm programming, as described in Section 2.6 to separate the Difference Signal into the dispersions which produced it.

It can be concluded that the Difference Signal is a useful way of visualising small changes in loss spectra, and that in general terms the shape of the plot can indicate whether the relaxation frequency has increased or decreased.

## 2.6 Genetic Algorithms

The Genetic Algorithm is a method for finding a global best solution for an optimisation problem; e.g. in the current work the technique is used to fit the parameters of two dispersions to data representing the experimental results of the difference between dielectric loss values before and after applying a magnetic field. The process mimics biological evolution by simulating natural selection - it repeatedly changes a group of individual solutions using methods derived from biological processes.

At each step in the process, the genetic algorithm selects individual solutions from the current generation as “parents” and combines them to produce “children” or “offspring” for the next generation. The process continues until the best solution satisfies specific criteria, such as the difference between the theoretical and experimental values being less than a certain value.

In general, genetic algorithms can be divided into several sections:

### 2.6.1 Initialisation

In the initialisation stage, the number and type of variables used in the process are decided on. These must be coded, usually using binary notation, to create a string of symbols which is termed a “chromosome”. The number of bits describing the chromosome obviously varies depending on the problem. The initial population is usually generated completely at random with each bit of the chromosome having equal probability of being assigned to 0 or 1.

## 2.6.2 Selection

Each chromosome in the current population is then evaluated for its “fitness”, i.e. how well it satisfies the requirements of the problem. The probability that the chromosome will participate in creating the next generation then depends on this fitness value. Although the selection of “parents” is random, this selection based on fitness criteria tends to eliminate those solutions which are least able to lead to a good solution.

## 2.6.3 Crossover

Crossover is the method by which two “parents” are combined to produce “offspring”. The simplest kind of crossover is called one-point crossover, and can be described as follows. Suppose two parent chromosomes each of length  $L$  are to be combined to produce two child chromosomes of the same length. The process starts by generating a random number  $r$  (where  $1 < r < L$ ). The first offspring chromosome is created by combining the first  $r$  bits of the first parent with the last  $L - r$  bits of the second parent. Similarly, the second offspring is generated by adding the last  $L - r$  bits of the first parent to the first  $r$  bits of the second parent. Bit  $r$  is then obviously the point at which the offspring swap from one parent to the other, hence the term “crossover”. The crossover operation is performed randomly with a probability usually between 0.6 and 0.95. One-point crossover is only one type of crossover function used in Genetic Algorithms - in practice there are many other types which have been devised.

### 2.6.4 Mutation

Mutation is also used in Genetic Algorithm processes and operates on single chromosomes. It consists of changing a random bit in the chromosome string either from 0 to 1 or from 1 to 0. The probability of mutation occurring is usually between 0.001 and 0.01.

### 2.6.5 Termination

The three processes of Selection, Crossover and Mutation are repeated for many generations. At each stage the “child” chromosomes are evaluated, and if there are any which satisfy the optimisation criteria, then the process terminates, and the chromosome or solution which is deemed to be the *best* is returned as the solution.

The generation of successive populations by random computations usually enables Genetic Algorithms to avoid local minima which classical derivative-based optimisation methods often produce.

### 2.6.6 Matlab Genetic Algorithm Toolbox

The Genetic Algorithm Toolbox, which is available as an optional add-on to Matlab, performs the above processes in the background, and is optimised to perform the complex calculations as quickly as possible. Even so, the programs used in the present work (See Appendices J and K) require many days to satisfy the optimisation criteria. The Toolbox enables the programs to operate on data in multi-dimensional arrays rather than the one-dimensional strings described above, whilst simplifying the process for the user. (See <http://www.mathworks.com/help/toolbox> for details.)

## 2.7 Reliability of Genetic Algorithm Analysis

The concept of the Difference Signal was introduced in Section 2.5. A method was developed to analyse these Difference Signals using Matlab and the Genetic Algorithm toolbox. The method is based on the proposition that the Difference Signal can be produced when a single dispersion in the dielectric spectrum of DNA is modified by the application of magnetic field. The Genetic Algorithm program is able to analyse the Difference Signal and give values for all the parameters defining the dispersion both before and after the application of the magnetic field. The Matlab programs used to carry out this analysis are shown in Appendix K.

In order to assess the reliability of this analysis process, the production of Difference Signals was simulated theoretically using Equation 2.48, modified to reflect the fact that the Difference Signal is produced by subtracting the dielectric losses of two dispersions rather than adding them. These difference signals were produced from known parameters, which could be compared with the results generated from the Genetic Algorithm analysis of the theoretical data.

The theoretical Difference Signals analysed were generated from the following data, with the suffix "1" denoting the parameter *before* applying the field, and the suffix "2" denoting the parameters *after* applying the field. The values of the parameters were chosen to approximately reflect the results found in the experimental sections, except that each individual parameter could be changed separately, as required.

- Test 1: Dielectric decrement constant: i.e.  $d\varepsilon'_1 = 5.70 \times 10^5$ ,  $d\varepsilon'_2 = 5.70 \times 10^5$ . Frequency increasing:  $f_1 = 1800\text{Hz}$ ,  $f_2 = 2500\text{Hz}$ . Spreading parameter constant :  $h_1 = 0.09$ ,  $h_2 = 0.09$ . D.C. conductivity constant:  $\sigma_1 = 3.3 \times 10^{-9}$ ,  $\sigma_2 = 3.3 \times 10^{-9}$ .
- Test 2: As with Test 1, except Dielectric decrement decreasing: i.e.  $d\varepsilon'_1 = 5.70$

	f1	f2	dE1(x10 <sup>5</sup> )	dE2(x10 <sup>5</sup> )	h1	h2	sigma1	sigma2
1(True)	5.70	5.70	1800	2500	0.09	0.09	3.3E-9	3.3E-9
1(GA)	5.60 ±0.63	5.60 ±0.61	1786 ±75	2480 ±71	0.089 ±0.002	0.089 ±0.002	1.26E-8 ±0.83E-8	3.56E-8 ±3.06E-8
2(True)	5.70	5.60	1800	2500	0.09	0.09	3.3E-9	3.3E-9
2(GA)	5.63 ±0.98	5.53 ±0.87	1794 ±54	2470 ±52	0.088 ±0.002	0.088 ±0.002	9.22E-9 ±4.24E-9	2.87E-8 ±2.18E-8
3(True)	5.70	5.70	1800	2500	0.09	0.06	3.3E-9	3.3E-9
3(GA)	5.61 ±0.94	5.61 ±0.92	1778 ±74	2464 ±72	0.092 ±0.002	0.061 ±0.002	1.31E-8 ±0.90E-8	2.56E-8 ±1.95E-8
4(True)	5.70	5.70	1800	2500	0.09	0.09	3.3E-9	3.3E-7
4(GA)	5.62 ±0.36	5.62 ±0.42	1787 ±65	2474 ±68	0.089 ±0.002	0.089 ±0.002	3.54E-9 ±2.33E-9	4.76E-7 ±4.09E-7

Figure 2.30: Results of Genetic Algorithm Simulation: Tests 1-4, True values and GA results. dE1 and dE2 are the dielectric decrements, f1 and f2 are the frequencies, h1 and h2 are the spreading parameters, and sigma1 and sigma2 the d.c. conductivities

	f1	f2	dE1(x10 <sup>5</sup> )	dE2(x10 <sup>5</sup> )	h1	h2	sigma1	sigma2
5(True)	5.70	5.70	1800	2500	0.09	0.09	3.3E-9	3.3E-6
5(GA)	5.64 ±0.82	5.64 ±0.86	1779 ±56	2472 ±71	0.088 ±0.002	0.088 ±0.002	6.35E-9 ±5.02E-9	6.09E-6 ±3.71E-6
6(True)	5.70	5.70	1800	2500	0.09	0.09	6.6E-9	6.6E-6
6(GA)	5.62 ±0.86	5.62 ±0.85	1794 ±56	2484 ±67	0.089 ±0.002	0.089 ±0.002	5.47E-9 ±4.60E-9	1.22E-5 ±1.05E-5
7(True)	5.70	5.70	1800	2500	0.09	0.06	6.6E-9	6.6E-6
7(GA)	5.66 ±0.75	5.66 ±0.75	1792 ±62	2485 ±63	0.091 ±0.002	0.062 ±0.002	5.50E-9 ±4.12E-9	1.13E-5 ±0.81E-5
8(True)	5.70	5.60	1800	2500	0.09	0.06	3.3E-9	3.3E-6
8(GA)	5.65 ±1.04	5.55 ±0.98	1776 ±69	2461 ±67	0.091 ±0.002	0.062 ±0.002	5.28E-9 ±3.96E-9	5.97E-6 ±4.12E-6

Figure 2.31: Results of Genetic Algorithm Simulation: Tests 5-8, True values and GA results. dE1 and dE2 are the dielectric decrements, f1 and f2 are the frequencies, h1 and h2 are the spreading parameters, and sigma1 and sigma2 the d.c. conductivities

$$\times 10^5, d\varepsilon'_2 = 5.60 \times 10^5.$$

- Test 3: As with Test 1, except Spreading parameter decreasing :  $h_1 = 0.09$ ,  $h_2 = 0.06$ .
- Test 4: As with Test 1, except D.C. conductivity increasing:  $\sigma_1 = 3.3 \times 10^{-9}$ ,  $\sigma_2 = 3.3 \times 10^{-7}$ .
- Test 5: As with Test 4, except D.C. conductivity increasing to a different value:  $\sigma_1 = 3.3 \times 10^{-9}$ ,  $\sigma_2 = 3.3 \times 10^{-6}$ .
- Test 6: As with Test 4, except D.C. conductivity increasing, with both values different:  $\sigma_1 = 6.6 \times 10^{-9}$ ,  $\sigma_2 = 6.6 \times 10^{-6}$ .
- Test 7: As with Test 6, except Spreading parameter decreasing :  $h_1 = 0.09$ ,  $h_2 = 0.06$ .
- Test 8: As with Test 7, except Dielectric decrement decreasing: i.e.  $d\varepsilon'_1 = 5.70 \times 10^5$ ,  $d\varepsilon'_2 = 5.60 \times 10^5$ .

The full results can be seen in Figures 2.30 and 2.31, showing the “True” parameters used to generate the theoretical Difference Signals, and the Genetic Algorithm (GA) results for each test, together with the uncertainty in the results reported by the Matlab program. The effectiveness of the Genetic Algorithm process may be assessed by comparing the “True” parameters with the GA results.

In the following sections, the reliability of the process will be discussed for each of the parameters of the dispersion in turn.



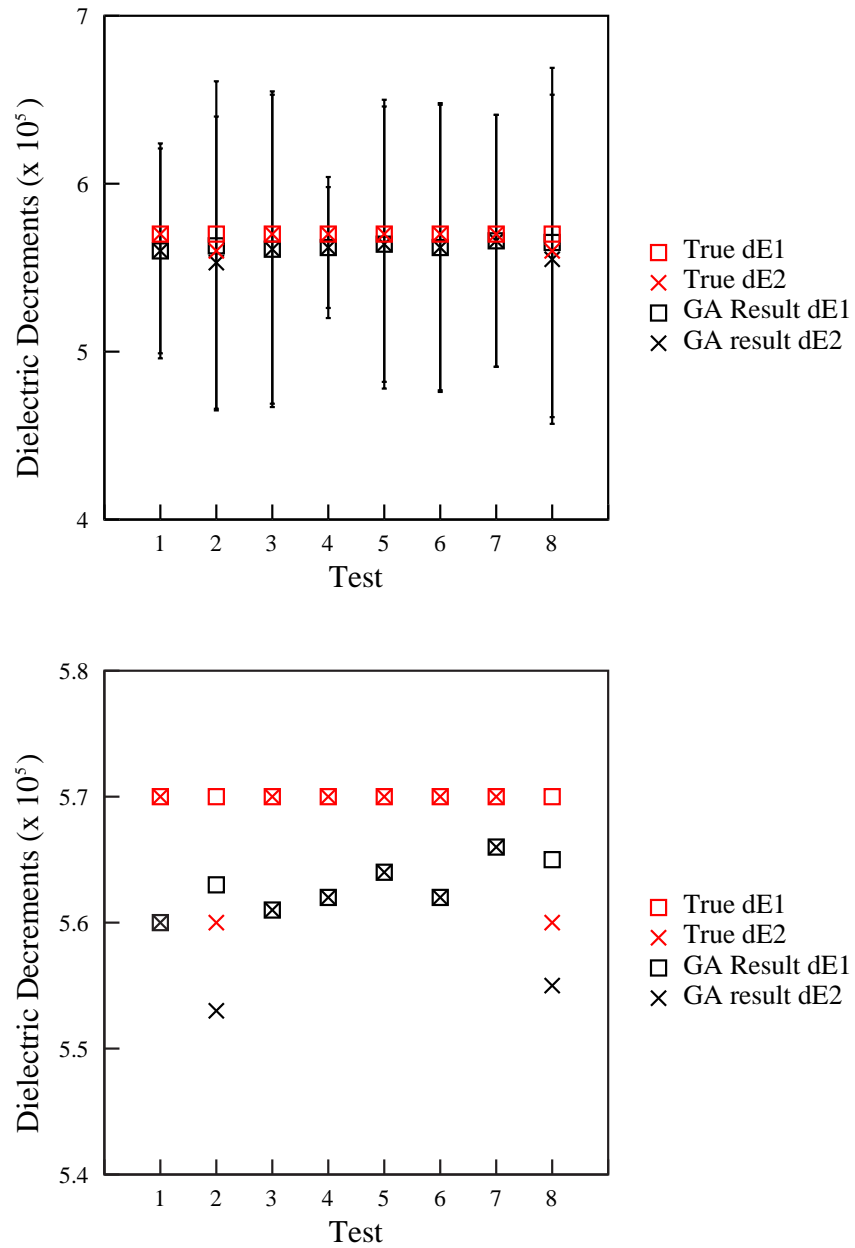


Figure 2.32: Results of Genetic Algorithm Simulation - Dielectric Decrement, showing true values used in simulation, together with the equivalent results found from Genetic Algorithm analysis. Top graph shows error bars for GA results. Lower graph shows magnified view, separating values which are close together in top graph.

### 2.7.1 Dielectric Decrement

Figure 2.32 shows the “true” dielectric decrements (denoted dE1 and dE2) used in each of the eight tests, together with the equivalent results found by analysis using the Matlab program.

The top graph in Figure 2.32 shows the error bars for the dielectric decrement results found for each of the tests. The “true” results, shown in red, are clearly well within the uncertainty given by the program.

The lower graph in Figure 2.32 shows a magnified view of the same data without the error bars. Where the “true” values of  $d\varepsilon'_1$  and  $d\varepsilon'_2$  are equal (Tests 1,3,4,5,6 and 7), the equivalent mean results from the analysis can also be seen to be equal, though slightly smaller than the true values - the difference however being less than 2%. Examination of the results from individual games shows that if the true decrements are equal, the GA program is able to confirm this, i.e. the GA decrements are also equal. But the *actual* values found by the GA program vary, as shown by the error bars in the top graph in Figure 2.32. The distribution of the results is slightly biased towards values lower than the true value.

Where the value of  $d\varepsilon'_1$  is larger than  $d\varepsilon'_2$  (Tests 2 and 8), the GA analysis confirms this, with the difference in the true parameters being reflected in the difference in the equivalent mean parameters. Examination of individual games shows that this difference is present in every game, though the individual values vary considerably. Again the difference between the true values of the dielectric decrements and the mean values found by the GA program represent a difference of less than 2%.

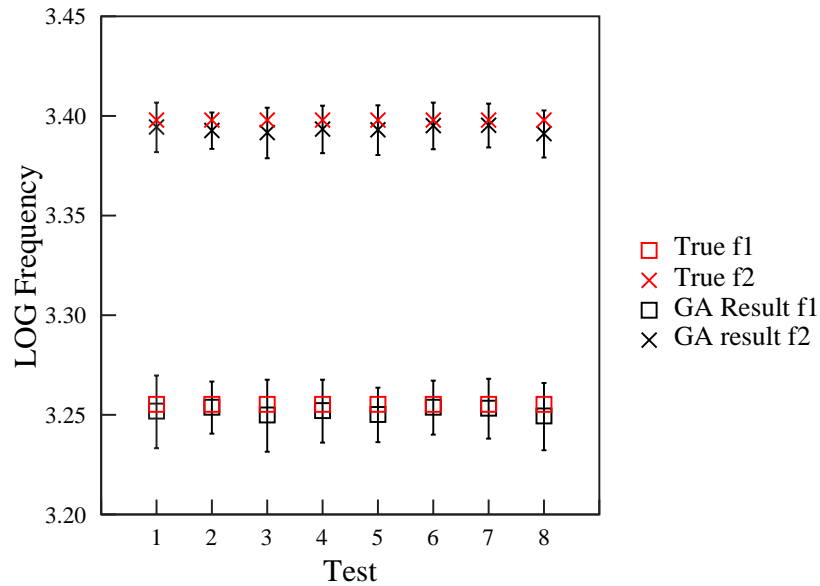


Figure 2.33: Results of Genetic Algorithm Simulation - LOG Frequencies, showing true values used in simulation, together with the equivalent results found from Genetic Algorithm analysis

## 2.7.2 Frequencies

Figure 2.33 shows the “true” frequencies (denoted f1 and f2) used in each of the eight tests, together with the equivalent results found by analysis using the Matlab program.

For each of the eight tests, Figure 2.33 clearly shows that true values of the frequencies are within 1% of the mean values found by the Genetic Algorithm analysis. The uncertainty in the results represents up to approximately 5% of the mean values.

### 2.7.3 Spreading parameter $h$

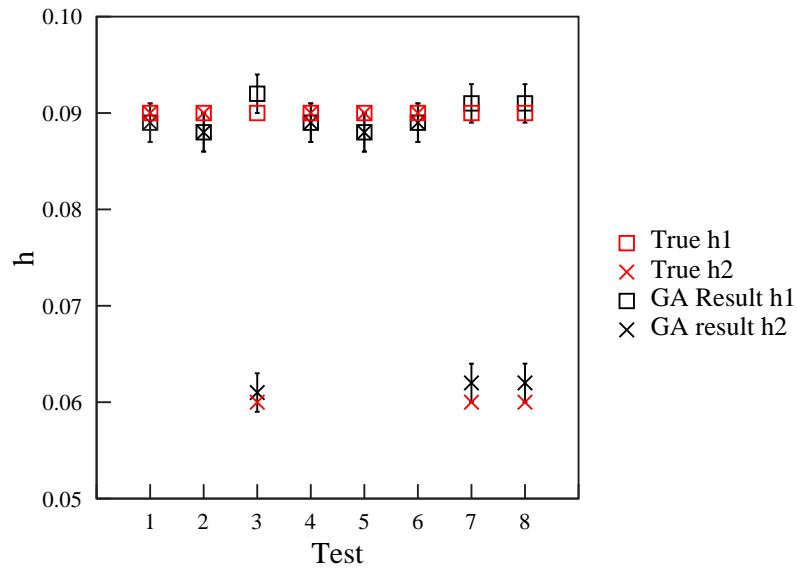


Figure 2.34: Results of Genetic Algorithm Simulation - Spreading parameter  $h$ , showing true values used in simulation, together with the equivalent results found from Genetic Algorithm analysis

Figure 2.34 shows the “true” spreading parameters (denoted  $h1$  and  $h2$ ) used in each of the eight tests, together with the equivalent results found by analysis using the Matlab program.

Where the true spreading parameters used in generating the theoretical difference signals are equal (Tests 1,2,4,5 and 6), the equivalent mean values found by genetic algorithm analysis are also equal, though slightly lower by less than 2%. Examination of each of the games shows that the program gives results for the spreading parameter which are slightly biased towards values lower than the true value, resulting in the mean being slightly smaller.

Where the true spreading parameter decreases from  $h_1=0.09$  to  $h_2=0.06$  (Tests 3, 7 and 8) the mean values found by genetic algorithm analysis are slightly larger than the true values (by 2 to 3%). The true values are often at the limit of the uncertainty in the GA program results.

#### 2.7.4 D.C.Conductivity

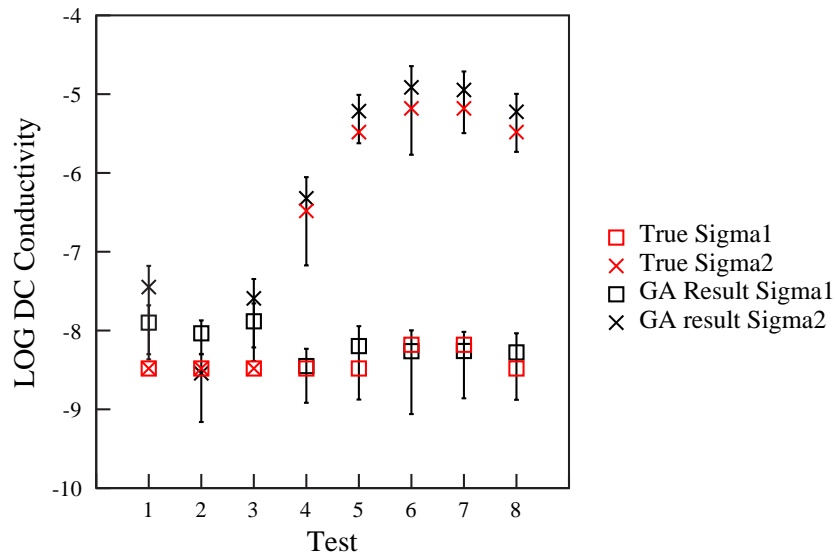


Figure 2.35: Results of Genetic Algorithm Simulation - D.C.Conductivity, showing true values used in simulation, together with the equivalent results found from Genetic Algorithm analysis

Figure 2.35 shows the “true” D.C.Conductivities (denoted Sigma1 and Sigma2) used in each of the eight tests, together with the equivalent results found by analysis using the Matlab program.

Where the true d.c. conductivities used in generating the theoretical difference signals are equal (Tests 1,2 and 3), the mean results found by genetic algorithm analysis can imply that  $\text{Sigma}2$  is larger than  $\text{Sigma}1$  (Tests 1 and 3) or that  $\text{Sigma}2$  is smaller than  $\text{Sigma}1$  (Test 2). In tests 1 and 3, the true values are outside the uncertainty limits determined by the program. In cases such as this, the analysis could perhaps imply that the d.c. conductivity has changed when in reality it has stayed the same.

In the remainder of the tests, where the d.c. conductivity is increased in the generation of the Difference Signal, in general the genetic algorithm analysis is quite effective in detecting this change. The variation in the actual values found however is quite wide, representing up to 90% uncertainty in the mean values found by the program. The LOG scale tends to conceal the wide variation.

### 2.7.5 Conclusion

This simulation tends to overestimate the reliability of the genetic algorithm analysis process because the theoretical Difference Signals used are exact values at all frequencies. The experimental Difference Signals show noise especially at low frequencies; this would affect the determination of the variation of d.c. conductivities in particular. However, the simulation has confirmed that the Matlab Genetic Algorithm program is able to extract the parameters of the two dispersions from the Difference Signal fairly accurately. The results of the analyses quoted in Sections 5.6.2 to 5.6.7 may therefore be taken to be representative of changes in dispersion parameters which could produce the difference signals observed.

# Chapter 3

## Experimental

### 3.1 Introduction

This chapter is divided into:

- Equipment overview: A description of the apparatus and how computers control and communicate with each component;
- A description of the method for investigating of the effect of low magnetic fields ( $< 0.7$  Tesla) on solutions of DNA at high concentrations ( $> 150$  mg/ml). To achieve the high concentrations required, DNA solutions were allowed to evaporate on interdigitated electrodes until the concentration range was consistent with the DNA forming a cholesteric liquid crystal phase. The magnetic field was applied perpendicular to the electric field.
- A description of the method for investigations which examine the effect of low magnetic fields ( $< 0.7$  Tesla) on DNA solutions at lower concentrations (25–100 mg/ml) using planar electrodes, where the magnetic field was parallel

to the electric field.

The high concentrations of DNA solution could only be achieved by evaporation, which meant that only interdigitated electrodes could be used. The rate of evaporation using planar electrodes was too slow to reach the required concentrations in a suitable time.

## 3.2 Equipment overview

Figure 3.1 shows a block diagram of the apparatus used. The components will first be briefly described individually, before explaining in detail how each part interfaces to the computers, and how the controlling program uses procedures and functions to communicate via that interface.

### 3.2.1 Design of Brass Enclosure

In order to be able to control and measure the relative humidity surrounding the sample when it placed between the poles of the electromagnet, it is necessary to isolate the sample. This is achieved by designing an air-tight brass enclosure to completely surround the poles of the electromagnet. The design of the enclosure can be seen in Figure 3.2.

In use, the enclosure is placed so that the pole-pieces are vertical, and the gap between them, where the planar electrode cell is inserted (See Figure 3.18) is horizontal. The pole-pieces are held in position between the coils of the electromagnet by two screws, one at the top of the apparatus holding the top pole-piece, and the other holding the lower pole-piece. The position and therefore the separation of the





pole-pieces can be changed by adjusting these screws.

For maximum flexibility three ports are built into the enclosure. Using these ports, the sample cell and various sensors can be placed *inside* the enclosure whilst maintaining electrical contact with external equipment. The ports use Ultra-Torr NW10 and NW12 attachments, through which electrical connections are made with PET-sockets. The advantage of PET sockets is that they are able to pass electrical signals through air-tight vacuum connectors. Port 3 can be seen in the Figure with its Ultra-Torr attachment which has 3 PET sockets passing through it. The other two ports are similar, though have only two PET sockets each. Alternatively, one port can be used to connect the brass enclosure to the vacuum system, should that be necessary.

For most experiments, port 2 is used to hold the sample cell, port 3 connects the LM35 temperature sensor (See Section 3.2.6), and for some experiments, port 1 is used to connect the vacuum system.

### 3.2.2 The computers

The main computer, the RiscPC, is the main controller of all the apparatus shown. The second computer, the A3020, acts as a slave device under the control of the RiscPC. Some of the components are directly connected to the RiscPC, e.g. the Wayne-Kerr component analyser, whilst others are connected to the A3020, e.g. the power supply.

Two extension cards, referred to as podules, are fitted to the RiscPC; the first is a GPIB card and the second a dual serial port expansion card. GPIB (General Purpose Interface Bus), also known as IEEE-488, is a short-range digital communications bus specification used to interface with laboratory instruments. In this case

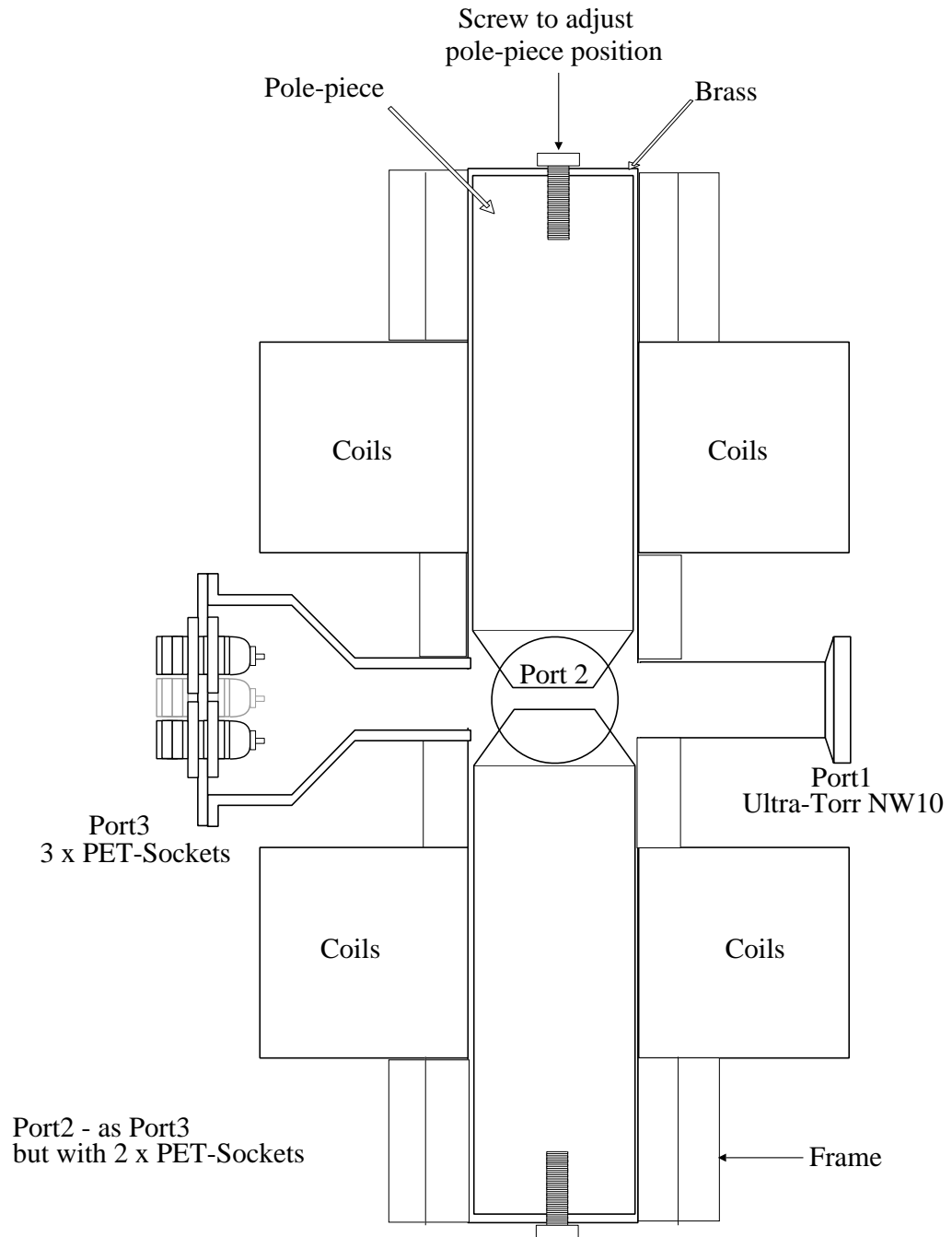


Figure 3.2: Brass enclosure

it is used to control and communicate with the Wayne-Kerr component analyser and the Keithley 670 Programmable Electrometer. One port of the dual serial port card communicates with the Eurotherm temperature controller, and the second port communicates with the multimeter.

The A3020 was fitted with an extension card comprising a combined Analogue port and User port as part of previous work. The Analogue port is connected to a sensor which reads the relative humidity in the vacuum system, and also to a probe which reads the temperature in the cabinet which holds the electromagnet and associated equipment. (See Sections 3.2.9 and 3.2.10 for details). The interface to these sensors and the scaling circuit were designed by a previous worker (Horsey, 2001), and enables more accurate measurement of the relative humidity than would direct connection of the ADC to the sensor.

The User port is used with apparatus designed as part of the present work, to send commands to the stepper motor controlling the current from the power supply. The User port is also used to detect the closing of two micro-switches which indicate the extreme range through which the stepper motor rotates the power supply rheostat. (See Section 3.2.11)

The two computers are connected together via their serial ports; commands are sent from the RiscPC to the A3020 e.g. to read the temperature sensor via the analogue port. The readings are then sent from the A3020 back to the RiscPC along the same connection. (See Section 3.2.12)

### 3.2.3 External equipment

The Wayne-Kerr component analyser is connected to the sample which is placed between the poles of the electromagnet. The analyser is able to measure the con-

ductance and capacitance of the sample at any one of the forty-two frequencies available (20Hz to 300kHz). The measurements are taken when requested by the main computer via GPIB, and the values are transferred to the controlling program using the same protocol. (See Section 3.2.5 for details)

The Keithley 617 Programmable Electrometer is connected to an LM35 temperature sensor, which is placed in close proximity to the sample inside the electromagnet enclosure. The electrometer is set up to measure the d.c. voltage across the sensor, which is directly proportional to the temperature in degrees celsius. Thus the temperature of the sample may be monitored by the controlling program at any time via GPIB. The temperature probe circuit simply supplies the sensor with a five volt power supply. (See Section 3.2.9)

It should be noted that the Wayne-Kerr Component Analyser and the Keithley 617 Programmable Electrometer are both connected to a single port on the computer's GPIB extension card. Each device has allocated to it a 'Device Address', which is 6 for the Wayne-Kerr and 27 for the Electrometer. Every command transmitted by the computer over the GPIB bus includes a reference to the address of the device with which the program is initiating communication. In this way the two devices are able to share a common connection to the computer.

The Multimeter measures the current flowing through the coils of the electromagnet, the value of that current may be read by the main computer using serial protocols. (See Section 3.2.7 for details)

The Eurotherm controls a fan heater under the control of the main computer using serial protocols, with its thermocouple sensor being attached to the outside of the brass electromagnet enclosure. Thus the controlling program is able to transmit the required temperature to the Eurotherm, which switches the heater on or off as required to maintain that temperature. (See Section 3.2.8 for details.)

### 3.2.4 Computer control

The following sections describe in detail how the main computer, the RiscPC, is able to communicate with each component in Figure 3.1. Details of the principal parts of the computer programs used are shown, in order to illustrate their use.

#### 3.2.4.1 Introduction to RiscOS

The RiscPC is a computer based on the StrongArm microprocessor and the RiscOS operating system. The RISC (Reduced Instruction Set Computer) in the name refers to the fact that the microprocessor uses fewer machine-code instructions than normal processors. This means that the instructions execute fairly quickly, and that the power used is very low. Further development of this microprocessor have led to the ARM processors used in the majority of current mobile phones.<sup>1</sup>

The programs are written in BBC BASIC VI, which is an interpreted language incorporated within the RiscOS operating system.<sup>2</sup> Control of low-level commands is achieved by the use of Software Interrupts (SWI's), using the BASIC "SYS" command. There are many hundreds of these interrupts available in the operating system, and they simplify tasks such as communicating via the serial port. The StrongArm processor's registers can be directly assigned through these SYS commands, enabling the machine-code routines called by the software interrupts to access values passed to them by the BASIC program. Similarly, the low-level machine code routines can themselves pass values back to the BASIC program via these registers.

An example of this would be `SYS"OS_SerialOp",3,65 TO ;C%` This command trans-

---

<sup>1</sup>See [http://en.wikipedia.org/wiki/ARM\\_architecture](http://en.wikipedia.org/wiki/ARM_architecture)

<sup>2</sup>See [http://en.wikipedia.org/wiki/BBC\\_Basic](http://en.wikipedia.org/wiki/BBC_Basic)

mits the byte 65 (ASCII code for upper-case A) from the serial port; 3 is placed in register R0, and diverts the call to the machine code for ‘serial port send’, whilst the byte to be sent (65) is placed in register R1. If the byte has been successfully sent, the machine code writes a zero to the register C%, which is the clear flag. When control is returned to BASIC, the value of C% is available to the program, and enables it to respond appropriately depending on its value.

The two extension cards fitted to the RiscPC are from Intelligent Interfaces Ltd. The company supplies program libraries with the cards, which include procedures using their own specially-written SWI calls - this means that software communicating through these cards can take advantage of these calls, often simplifying the code. The High-Speed Serial Card comes with the library referred to as BasicLib.Serial, and is listed in Appendix L. The GPIB card is accompanied by the libraries BASICLib.BAS488 and BASICLib.XBAS488 which are listed in Appendix M. (The XBAS488 library contains the same procedures as BAS488, but modified to trap errors, making program development easier.)

Before these libraries can be used, the relevant block drivers have to be loaded in the computer’s Boot sequence. The system variables “IIDual\$ Dir” and “IEEE488\$ Dir” have also to be defined in the Boot sequence as the location of the libraries. Every program using the BasicLib.Serial library must then begin with the following line:

- LIBRARY “<IIDual\$Dir>.BasicLib.Serial”

Every program using the GPIB libraries must have the following lines:

- LIBRARY “IEEE488\$Dir.BASICLib.BAS488”
- and LIBRARY “IEEE488\$Dir.BASICLib.XBAS488”

Procedures and functions are written and assembled in individual libraries, each library being dedicated to one piece of apparatus. The libraries are:

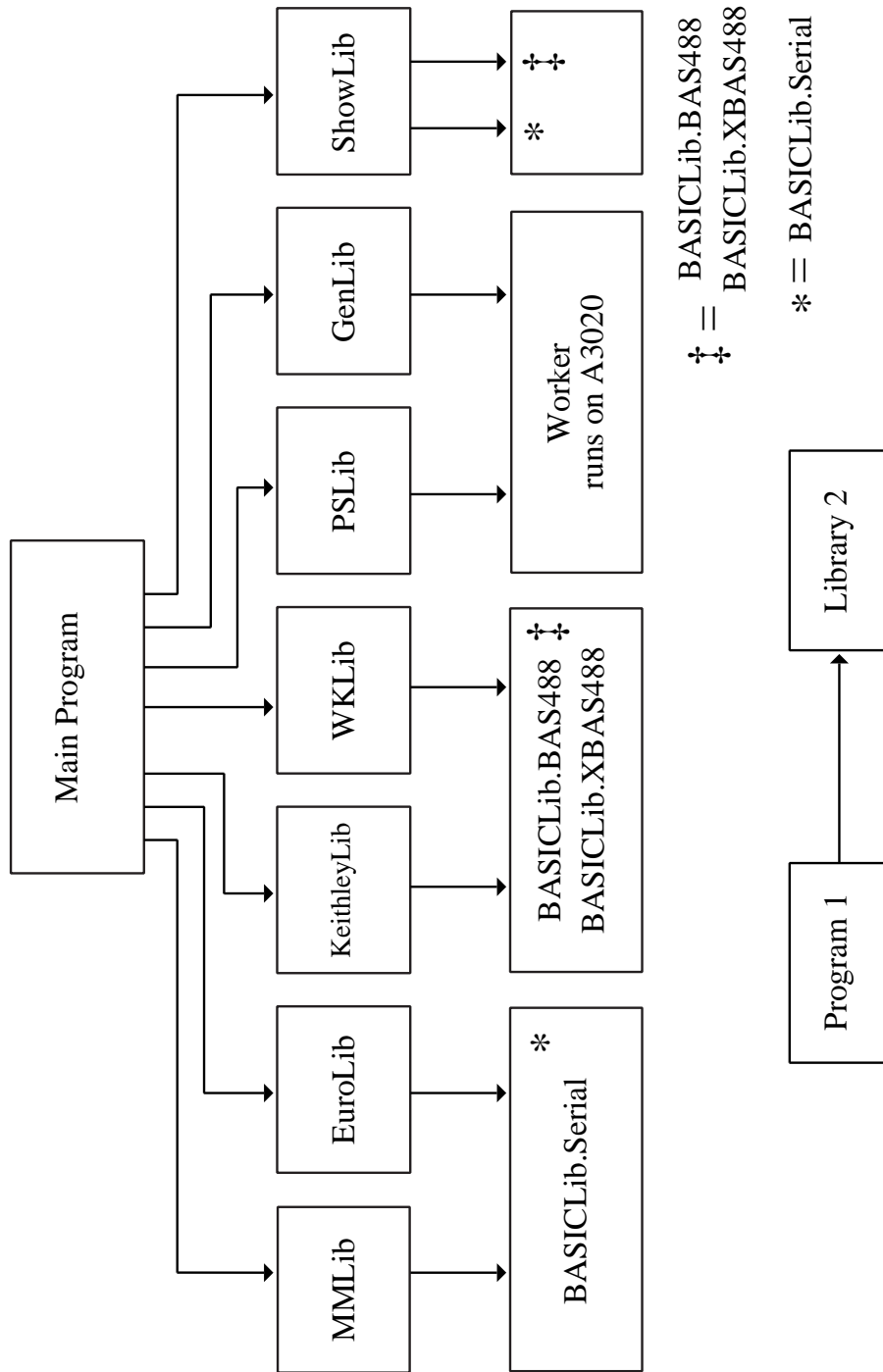
- WKLib: A library containing those functions and procedures used to communicate with the Wayne-Kerr component analyser.
- KeithleyLib): A library used to communicate with the Keithley 617 Programmable Electrometer.
- PSLib: A library to control the Power Supply stepper motor (via the A3020).
- EuroLib: A library to communicate with the Eurotherm temperature controller.
- MMLib: A library to read values from the multimeter.
- GenLib: A library to communicate with the A3020.
- ShowLib: A library initialising communications with all the above apparatus, together with any general screen printing procedures required.

The relationship between the libraries is illustrated in block form in Figure 3.3, showing how a program uses procedures in one library, which in turn relies on procedures in a second library. Only the essential parts of the procedures and functions included in these libraries will be described in the sections below. The full contents of the libraries are listed in Appendices A to G.

### 3.2.5 Wayne-Kerr Component Analyser

The Wayne-Kerr Component Analyser applies an alternating voltage across the electrodes of the sample cell at a particular frequency, and then reads the capacitance and conductance of the sample at that frequency. The WKLib library (See





Key: Arrow Direction means : Program 1 uses procedures in Library 2

Figure 3.3: Relationship between software libraries

Appendix A) contains the procedures and functions used. Note that the name of every procedure in this library starts with ‘W\_’, in order to make it obvious which apparatus is being referred to. Note also that the line numbers are added here as an aid to their referencing in the following explanation - they are not part of the program.

The procedure PROCW\_SetUpTheGPIBSystem shown below sets up the GPIB system to communicate with the Wayne-Kerr by choosing the correct device address (6) in line 20. Line 50 sets a suitable time-out period, i.e. the time after which control returns to the computer if no reply has been received from the Wayne-Kerr. Lines 90 and 100 set the ‘end-of-string’ character code to 10 both for strings which are input and output. Other procedures setup the voltage to be used (0.4 volts in most cases), the ‘speed’ of the connection (“NORMAL”), and read the frequencies used by the Wayne-Kerr into a string array Global\_f\$(f%), where f% varies from 1 for 20Hz to 42 for 300kHz.

```

10 DEFPROCW_SetUpTheGPIBSystem
20 w_device_adr% = 6
30 sysctrl_adr% = 0
40 w_mode% = 0
50 PROCtimeout_period(40.0)
60 PROCtimeout_on
70 PROCescape_on
80 PROCinit          :REM Sends REN, IFC, ATN=false
90 PROCeos_out_1chr(10)
100 PROCeos_in_1chr(10)
110 ENDPROC

```

The procedure most used from this library is PROCW\_OneFrequency(f%). This procedure is listed below, and will be described in some detail as an example of how

a program communicates on the GPIB bus.

```

200 DEFPROCW_OneFrequency(f%)
210 LOCAL freq,freq$,ft%,a$,status1%,status2%,cap$,con$
220 REPEAT
230  freq$="FREQ"+Global_f$(f%)
240  PROCadrandoutput(w_mode%,w_device_adr%,freq$)
250  PROCadrandoutput(w_mode%,w_device_adr%,"TRIGGER")
260  ft%=TIME:REPEAT:UNTIL TIME>=ft%+1
270  a$ = FNadrandinput(w_mode%,w_device_adr%,255)
280  ft%=TIME:REPEAT:UNTIL TIME>=ft%+1
290  @%="+E10.5"
300  status1%=FNXadrandinput(cap$,w_mode%,w_device_adr%,255)
310  status2% = FNXadrandinput(con$,w_mode%,w_device_adr%,255)
320  @%="+E10.5"
330  Global_freq$=Global_f$(f%)
340  Global_cap$=cap$
350  Global_con$=con$
360  freq=VAL(Global_freq$)
370  con=VAL(con$)
380  Global_cdbf=con/freq  :REM cdbf=Conductance Divided by Frequency
390  Global_cdbf$=STR$(Global_cdbf)
400 UNTIL INSTR(con$,"E")>0 AND INSTR(cap$,"E")>0
410 ENDPROC

```

This procedure takes a single parameter  $f\%$ , which represents the index of the frequency required in the `Global_f$` array. Within the procedure, `PROCadrandoutput` (from the `BASICLib.BAS488` library) takes three parameters - the mode (which is always 0), the device address, and the ASCII string to be sent to the Wayne-Kerr. To apply an a.c. voltage to the sample, the strings to be sent are “FREQ” and the frequency wanted e.g. “FREQ2000” for 2000Hz, followed by “TRIGGER”. (See lines 240 and 250) Lines 260 and 280 introduce a short delay into the program, and

are found to be helpful for correct communication on the GPIB bus.

FNadrandinput is the function used to read the values of the quantities measured from the Wayne-Kerr into the program. Line 270 simply commands the Wayne-Kerr to return a string up to 255 characters in length, until the "end-of-string" character is detected. The first string returned is simply the frequency as sent in line 240, and is discarded. In lines 300 and 310, FNXadrandinput is the version of the input function from the BASICLib.XBAS488 library, and will return an error code in status1% and status2% if an error is detected. The function also reads values of capacitance and conductance into the cap\$ and con\$ variables. These are used to assign values to Global\_con\$, Global\_cap\$ and Global\_cdbf\$ which are available as global variables to other parts of the program. (The "cdbf" in Global\_cdbf\$ is an acronym for "Conductance Divided by Frequency", which for any given sample is directly proportional to the dielectric loss.)

The output and input commands are repeated until the cap\$ and con\$ variables both contain the string "E", which indicates that they both contain a number expressed in exponent format.

The simple one-line command PROCW\_OneFrequency with the appropriate parameter, can therefore be used within another program to instruct the Wayne-Kerr to measure the capacitance and conductance of a sample at a given frequency, and to make those values available to that program. (See Section 3.2.13 for examples). PROCW\_Sweep repeats PROCW\_OneFrequency for each of the 42 frequencies available to the Wayne-Kerr and enables a complete dielectric spectrum to be determined.

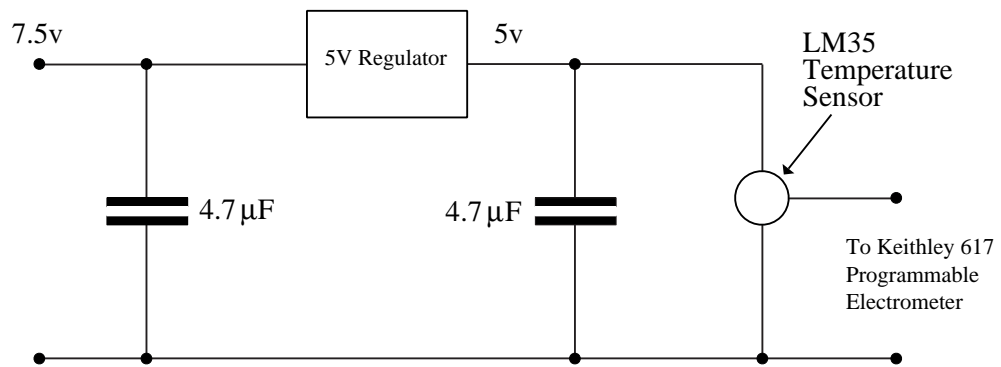


Figure 3.4: Temperature probe circuit

### 3.2.6 Keithley Electrometer

The Keithley 617 Programmable Electrometer is used to measure the temperature as close as possible to the sample. The transducer used is a LM35 temperature sensor, and produces a d.c. voltage directly proportional to the temperature in degrees celsius. The LM35 is supplied with a regulated 5volt d.c.voltage, and connected to the Keithley Electrometer as shown in the circuit in Figure 3.4.

The Keithley Electrometer is connected to the RiscPC using GPIB, and is set up to measure d.c. voltage in the range 0 – 20 volts as shown in the following procedure:

```

500 DEFPROCG_SetUpTheGPIBSystem
510 g_device_adr% = 27
520 sysctrl_adr% = 0
530 g_mode% = 0
540 PROCtimeout_period(40.0)
550 PROCtimeout_on

```

```

560 PROCescape_on
570 PROCinit      :REM Sends REN, IFC, ATN=false
580 PROCadrandoutput(g_mode%,g_device_adr%,"FOX") :REM F0=Volts
590 PROCadrandoutput(g_mode%,g_device_adr%,"G1X") :REM G1=No prefix
600 PROCadrandoutput(g_mode%,g_device_adr%,"R3X") :REM R0=Auto R3=20volts
610 PROCadrandoutput(g_mode%,g_device_adr%,"C1XZ1XC0X") :REM Zero meter
620 PROCadrandoutput(g_mode%,g_device_adr%,"BOX") :REM Electrometer
630 PROCadrandoutput(g_mode%,g_device_adr%,"DOX") :REM Electrometer display
640 ENDPROC

```

As can be seen, this procedure, in common with all others in this library, is given a name starting with the string "G\_" (for GPIB). The device address is set to 27 and the timeout period to 40 seconds. The commands in lines 580 to 630 set up the electrometer to read d.c. voltage up to 20 volts, the string sent in line 610 being essential to set the zero value on the electrometer.

The function most often used from this library is FNG\_GetVoltage which is listed below.

```

700 DEFFNG_GetVoltage
710 LOCAL data$,voltage$
720 PROCeos_out_1chr(13)
730 PROCeos_in_1chr(13)
740 data$ = FNadrandinput(g_mode%,g_device_adr%,255)
750 voltage$=FNG_ChangeFormat(data$)
760 PROCeos_out_1chr(10)
770 PROCeos_in_1chr(10)
780 voltage=VAL(voltage$)
790 =voltage

```

The two GPIB devices sharing the connection to the computer can be controlled from the same program, since the individual commands such as PROCadrandoutput and FNadrandinput include parameters which refer to the device address of the

apparatus being communicated with, i.e. `g_device_adr%` or `w_device_adr%`. However, when the program transmits the strings to the device, or receives strings as input, the program itself must be ready to send or read those strings in the correct format. The only difference between the Wayne-Kerr component analyser and the Keithley Electrometer is in the “end of string character” (eos) used by each device. The Wayne-Kerr ends its strings with ASCII 10 (Line Feed), and the Keithley uses ASCII 13 (Carriage Return). The program is set up to use the Wayne-Kerr format as default, in order to be able to read data from this device as often and as quickly as possible, e.g. in `PROCW_OneFrequency(f%)`.

When the temperature is read from the Keithley using `FNG_GetVoltage`, lines 720 and 730 first set the eos character to the Keithley format. Line 740 then reads the voltage from the Electrometer, before lines 760 and 770 reset the eos character to the default Wayne-Kerr format. In this way, communication with the Wayne-Kerr can assume that the eos format is already set up correctly. Line 750 changes the voltage reading from the exponent format transmitted from the Keithley to a decimal format.

The main program can therefore use a line such as “`temp=FNG_GetVoltage`” as often as necessary to monitor the temperature of the sample.

### 3.2.7 Multimeter

The multimeter is connected in series with the Farnell D100 Power Supply and the coils of the electromagnet, and is set up to measure the current flowing up to a value of 10 Amps. (Note that the maximum value of the current used in these experiments is 1.1 Amps) The multimeter includes a serial port, which can be connected to a computer using normal serial protocols. The RiscPC communicates with the multimeter via port 1 of the High-Speed Serial Card, using the procedures

in the MMLib library. (Note that the names of all the procedures in this library start with “MM”) The procedures in the MMLib in turn use the procedures in the BasicLib.Serial library listed in Appendix L. Only the essential parts of the MMLib library will be described here; the full listing can be seen in Appendix E.

Before communication can begin, the serial port must be initialized, as shown in the procedure below:

```

100 DEFPROCMMInitialize_Serial_Port(MMport%)
110 SYS"IIDual_ReadWriteSerialStatus",MMport%,&96,&FFFFFF00
120 SYS"IIDual_ReadWriteDataFormat",MMport%,&5
130 SYS"IIDual_ReadWriteRxBaudRate",MMport%,12
140 SYS"IIDual_ReadWriteTxBaudRate",MMport%,12
150 WHILE FNSerial_ReadEntriesInBuf(MMport%)>0
160 b$=FNMMReceive(MMport%)
    REM b$ is a string containing any data in the serial buffer
170 ENDWHILE
180 ENDPROC

```

The variable MMPort% must be set to the port number i.e. 1, before this procedure is called. Line 120 sets various states of the serial system, in particular it switches off handshaking. Line 120 sets the serial port data format to 7 data bits, 2 stop bits with parity check disabled. Lines 130 and 140 set the serial port baud rate for receive and transmit to 600 Baud. Lines 150 to 170 simply ensure that the serial port buffer is empty.

Two further procedures are defined to transmit data from the RiscPC to the multi-meter i.e. PROCMMSend, and to receive data as a string from the multimeter, i.e. FNMMReceive. They are listed below:

```

100 DEFPROCMMSend(A%,MMport%)

```



```

110 LOCAL F1
120 REPEAT
130 SYS"IIDual_SendByte",MMport%,A% TO ;F1
140 UNTIL (F1 AND &2 )=0
150 ENDPROC

160 DEFFNMMReceive(MMport%)
170 LOCAL byte%,flags%,att%
180 data$=""
190 REPEAT
200   REPEAT
210     SYS"IIDual_GetByte",MMport% TO ,byte% ;flags%
220     UNTIL (flags% AND %0010) = %0000
230     IF byte%>31 data$+=CHR$(byte%)
240     att%=TIME:REPEAT:UNTIL TIME>=att%+5
250 UNTIL FNSerial_ReadEntriesInBuf(MMport%)=0
260 =data$

```

PROCMMSSend sends the byte A%, and repeats the action if necessary until successful transmission is achieved, signified by the flag F1 being cleared in line 140. FNMMReceive reads all the data in the serial port buffer until that buffer is empty. It builds a string holding the value of the current being measured from every byte with an ASCII code in the appropriate range (Line 230). These two procedures are used in the most commonly used procedure in the MMLib library, which is FNMMGetCurrent, as listed below.

```

300 DEFFNMMGetCurrent(MMport%)
310 LOCAL Flag%,a$
320 Flag%=0
330 REPEAT
340   PROCMMSSend(ASC("P"),MMport%)
350   a$=FNMMReceive(MMport%)
360   IF LEFT$(a$,2)="DC" AND RIGHT$(a$,1)="A" Flag%=1

```

```
370 UNTIL Flag%=1  
380 =FNMMValueOfCurrent(a$)
```

In line 340, the ASCII code for “P” is sent to the multimeter. This instructs it to measure the current, and to transmit a string including the value of that current from its serial port. The received string starts with “DC” and ends with “A” for Amps. The function `FNMMValueOfCurrent` strips these extraneous letters, leaving the result which is the numeric value of the current.

The main program is then able to measure the current through the electromagnet at any time, simply with code such as “`I = FNMMGetCurrent(1)`”.

### 3.2.8 Eurotherm

The Eurotherm controller is connected to a thermocouple attached to the outside of the brass electromagnet enclosure. It reacts to the temperature detected by that thermocouple by switching a fan heater on or off. In this way, it tries to maintain the enclosure at a steady temperature. That temperature, called the set point, can be selected by the software running on the RiscPC. Once set by the program, the Eurotherm can then be left to maintain the temperature with no further intervention from the software. The Eurotherm is connected to port 2 of the High-Speed Serial Card, using the procedures and functions in the `EuroLib` library. The procedures in this library in turn use the procedures in the `BasicLib.Serial` library listed in Appendix L. (The `EuroLib` library was first developed for previous work, but a shortened description is included here for completeness.)

Since the Eurotherm is connected to port 2 of the High-Speed Serial Card in the same way that the Multimeter is connected to port 1, the procedures in `EuroLib` are similar in principle to those found in `MMLib`. Only the general outlines of the

library will be described here - the full listing can be seen in Appendix D.

The serial port is initialized in a similar way to Section 3.2.7, except that the baud rate is set to 9600, and the data format to 1 start bit, 7 data bits, 1 Stop bit and Even Parity. PROCESend is essentially the same as PROCMMSSend, except for the method of assigning the port, which is a global value in EuroLib, and a parameter of the procedure in MMLib.

PROCESendNewValue(t\$) is used to send a combination of two-letter mnemonic command and a numeric value; e.g. “SL25.0” means “let the set-point be 25.0 °C”. However, in the same way that the GPIB system requires the assignment of a device address, the Eurotherm serial protocol also requires a Group address Identifier (GID) and an Unit address Identifier (UID) to be sent as part of any command. Error detection is also included in the protocol by terminating the transmitted string with a block check character (bcc)<sup>3</sup>

Similar two-letter mnemonics are used in the procedure FNESENDenquiry, which asks the Eurotherm to return the current value of one of its variables. e.g. FNESENDenquiry(“SP”) will return the value of the set-point; FNESENDenquiry(“PV”) gives the current value of the temperature detected by the Eurotherm’s thermocouple. FNESENDenquiry uses FNEReplyReceived to read the data returned from the Eurotherm; device and block addresses are again sent, together with bcc error checking.

Thus the main program can with a simple command such as PROCESendNewValue(“SL25.0”) change the set-point temperature which the Eurotherm will subsequently try to maintain. FNESENDenquiry(“PV”) will, if necessary, then allow the program to monitor the actual temperature.

---

<sup>3</sup>See [http://en.wikipedia.org/wiki/Block\\_check\\_character](http://en.wikipedia.org/wiki/Block_check_character).

### 3.2.9 Reading Temperature

As noted above, the A3020 had been already fitted with a combined analogue port and user port extension card. Only the analogue port of this card had been used in previous work to measure temperature and relative humidity. For completeness, these uses will be briefly described here.

The analogue port is connected to a LM35 Precision Centigrade Temperature Sensor (as in Section 3.2.6) in order to measure the temperature of the cabinet holding most of the equipment.

```

DEFNTemperature(tttotal%)
LOCAL ch%,t
ch%=3
t=FNVoltage(ch%,tttotal%)
t=t*100
=t

```

The function FNTemperature running on the A3020 is shown above, and can be seen to take a parameter tttotal%. Because the analogue port readings display some variation due to noise, it is necessary to repeat the readings a number of times (typically 1000), and take the mean value - this number is the parameter tttotal%. Each reading takes less than 0.5ms, so the total time taken is acceptable. A more serious problem is caused by long-term drift in the analogue to digital converter; this is overcome by connecting one of the analogue port's four channels (Channel 2) to the output from an ICL8069 voltage reference chip, which gives a constant 1.227volts. When the value of a voltage connected to one of the other channels is required, the channel's reading is compared with that of channel 2, and the true voltage thereby calculated. The temperature probe's output is connected to Channel 3; hence the variable ch% is set to 3. The function FNVoltage incorporates these

corrections, and applies them to the ADC reading obtained by the `ADVAL(ch%)` command (See `FNReadAdval` in the `Worker` program.)

### 3.2.10 Reading Relative Humidity

Channel 1 of the analogue port is connected to a Honeywell HIH-3610 Humidity Sensor, which measures the relative humidity in the vacuum system which can be attached to the brass enclosure surrounding the electromagnet. The relative humidity value is then measured in a similar way to the temperature. One difference however is that the voltage from the humidity sensor is modified before it reaches the analogue port. This modification is achieved by a circuit designed by a previous worker (Horsey, 2001); the circuit adjusts the input voltage from the humidity sensor by removing the offset. It thus improves the resolution of the measurement.

### 3.2.11 Control of Power Supply

The electromagnet coils are connected to a Farnell D100 Power Supply (100 volts, 1.1 Amps). In order to be able to control the current supplied to the electromagnet in software, the power supply's current-adjusting rheostat is connected to a stepper motor (5 volts, 7.5 degree step-angle bi-polar stepper motor, Rapid electronics order code 37-0525) via a three-step gear system (See Figure 3.5). The gear system reduces the speed of rotation of the stepper motor by a factor of 64, and improves the resolution of rotation of the rheostat to approximately 7 minutes of an arc. The stepper motor is controlled from the User port extension card fitted to the A3020.

The final gear attached to the rheostat is extended outwards and attached to a rotating bar (See Figure 3.6). At the extreme clockwise and anti-clockwise positions of this bar's rotation, it engages with two micro-switches. These are activated when

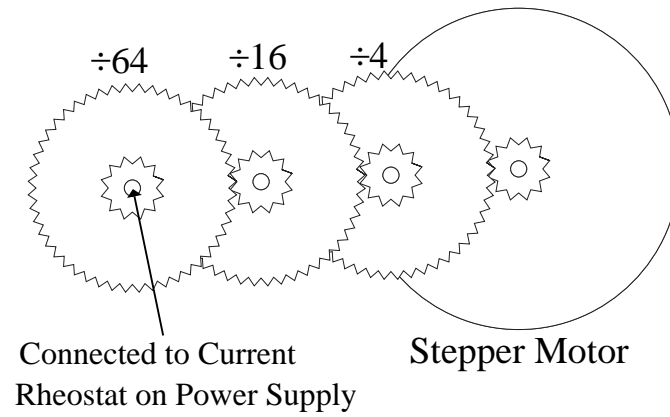


Figure 3.5: Power supply gear system

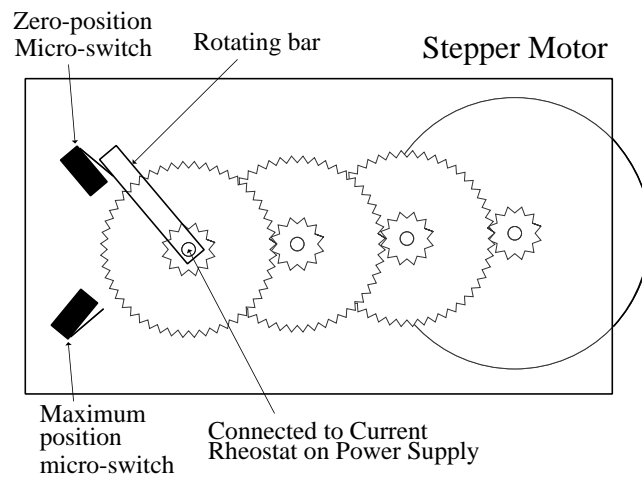


Figure 3.6: Power supply micro-switches

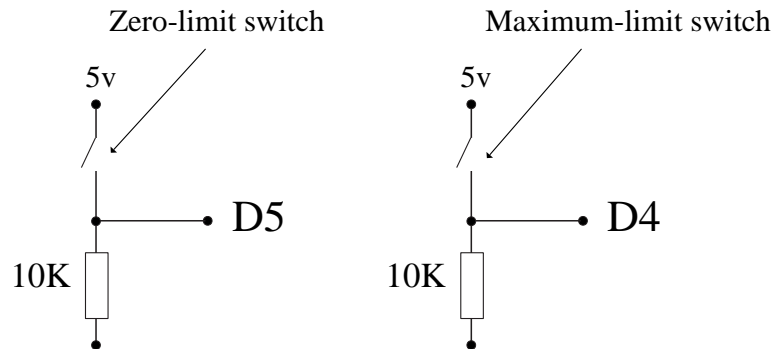


Figure 3.7: Computer connection to micro-switches

the current is at its minimum and maximum values, and are directly connected to the D4 and D5 user port inputs of the A3020, as shown in Figure 3.7. The procedure to read the state of these micro-switches is described below.

The stepper motor is connected to a circuit based on the L297 and L298N chips (See simplified circuit Figure 3.8). The L298N has four outputs which are directly connected to the stepper motor's coils; The L297 requires four inputs which are DIR (Direction), ENB (Enable), CLK (clock), PWR (Power). These signals are supplied by the user port outputs D0,D1,D2 and D3, via ZVN4306 mosfets and an opto-isolator circuit, based on the TL074 quad opto-coupler. Figure 3.9 shows a single opto-isolator circuit connected to D0 - its output is connected to pin 17 of the L297, i.e. the direction pin. The other three outputs D1, D2 and D3 are connected through similar circuits. The opto-isolators are used to protect the computer from potential damage by the large back-emfs produced by the stepper motor. The L297 is able to control the stepper motor in half-step mode, where the coils are energized

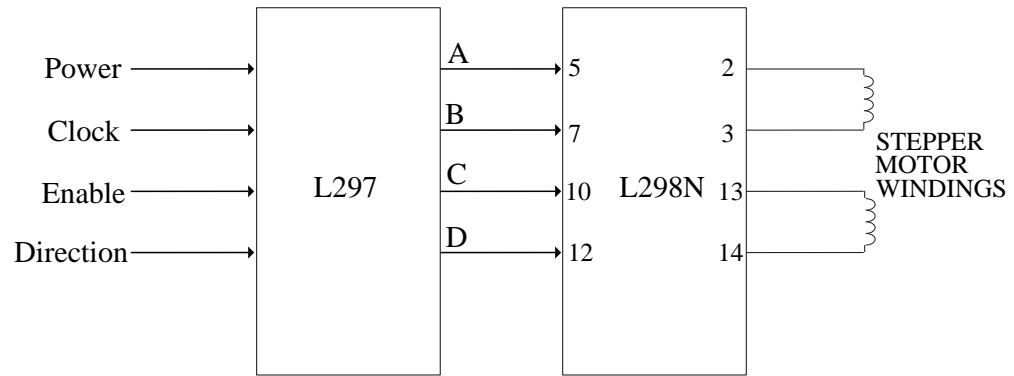


Figure 3.8: Simplified control circuit for stepper-motor

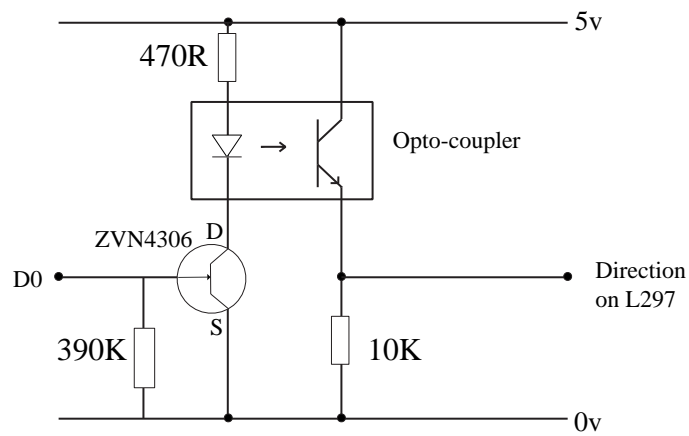


Figure 3.9: Computer connection to stepper motor circuit



alternately with one coil on, then two, then one, etc, so that the motor moves in half step increments. This produces smoother motion, though at the cost of less torque. The procedure to control the stepper motor circuit is described below.

```
REM User port set up
REM 4 O/P lines (F) and 4 I/P lines (0)
REM &62 = Data direction register
SYS"OS_Byte",151,&62,&0F
```

On the A3020, the user port has to first be set up so that it has four outputs and four inputs (though only two of the inputs are used). This is done with the code shown above, where the byte 0F is sent to the DDR (Data direction register). The byte 0F can be written in binary as 00001111, where the ones on the lowest four bits turn the user port's lowest four bits into outputs, and the zeroes on the highest four bits turn the user port's highest four bits into inputs.

```
DEFPROCUserPortSend(A%)
REM &60 = Input/Output register B
SYS"OS_Byte",151,&60,A%
ENDPROC
```

The outputs are controlled by the procedure PROCUserPortSend, as shown above. This assigns the value of the byte A% to the user port, though since only the lowest four bytes are configured as outputs, only the lowest four bytes of A% are effective. This can be seen in e.g. FNPowerOn below. If the EnableFlag% is zero, then this function sends the value 8 to the output port, i.e. it makes D3 high; D3 is connected to the Power input of the L297, so this switches the power to the stepper motor on.

```
DEF FNPowerOn
PowerFlag%=1
```

```

tot%=EnableFlag%*2
tot%+=PowerFlag%*8
PROCUserPortSend(tot%)
="OK"

```

```

DEFFNEnableStepperMotorOn
LOCAL tot%
EnableFlag%=1
tot%=EnableFlag%*2
tot%+=PowerFlag%*8
PROCUserPortSend(tot%)
="OK"

```

If this is followed by FNEnableStepperMotorOn, the value sent to the user port is now 10, i.e. 8 plus 2, meaning that D3 and D1 are set high, so that the L297's Enable input is set high, *and* the power to the stepper motor is on.

The state of the micro-switches which detect the limits of rotation of the power supply rheostat (See Figure B), are detected using FNUserPortReceive shown below. Since only bits D4 and D5 are used as inputs, the value read from the user port is masked with 48, i.e. 32 plus 16; the state of the outputs would otherwise be added to the inputs. If the result of this function is 32, then D5 is high and the lower limit switch has been activated, whilst if the result is 16, then D4 is high and the upper limit switch is on. In both of these cases the stepper motor should be stopped with immediate effect.

```

DEFFNUserPortReceive
REM Read from user port
REM &60 = Input/Output register B
SYS"OS_Byte",150,&60 TO ,b%
b%=b% AND 48
=b%

```

The above functions may be seen used in combination in the function FNPSIncrease, (i.e. Increase the current from the Power Supply) as shown below. This function has a parameter which gives the number of turns through which the stepper motor should be turned, e.g. “PSI96” would turn the stepper motor through 96 turns. After setting the Enable input of the L297 high in line 190, two values are calculated in lines 200 and 210. The value lo\_val% is set to 11 i.e. 8 plus 2 plus 1, meaning that the PWR, ENB and DIR outputs are high, but the CLK is low. The value hi\_val% is set to 15 i.e. 8 plus 4 plus 2 plus 1, meaning that the PWR, CLK, ENB and DIR outputs are all high.

In the lines 250 to 330 these two values are sent to the user port outputs in turn, meaning that the CLK input of the L297 is switched alternately low and high - this makes the stepper motor turn. Since the DIR input is also high, the motor turns clockwise, which increases the current from the power supply. (The direction of rotation is as seen from *behind* the stepper motor.) After each step, the state of the limit micro-switches is examined in line 310; if a value of 16 is detected, the upper limit switch has been closed. This causes the loop to terminate, and the function returns a string consisting of “PIL”, indicating that the (L)imit switch is on, and the value of t%, which is the number of steps not used. Should the switch not be closed, the function returns the string “PIN0”, indicating than (N)o switch was closed, and that the function used all the turns allocated to it. Finally in line 390, the Enable input of the L297 is set low again.

```

100 DEFFNPSIncrease(i$)
110 REM Increase Current from power supply by i% steps
120 REM where i%=MID$(i$,4)
130 REM Return with "PI"+switch$(N or L)+steps% not used
140 reply$="OK"
150 steps$=MID$(i$,4)
160 steps%=VAL(steps$)
170 IF steps%>0 THEN

```

```

180  REM Enable stepper motor
190  ok$=FNEnableStepperMotorOn
200  lo_val%=1+(EnableFlag%*2)+(PowerFlag%*8)
210  hi_val%=1+(EnableFlag%*2)+4+(PowerFlag%*8)
220  PROCUserPortSend(lo_val%)
230  m%=0
240  t%=steps%
250  REPEAT
260    m%+=1
270    t%-=1
280    PROCUserPortSend(lo_val%)
290    tt%=TIME:REPEAT:UNTIL TIME>=tt%+ttg%
300    PROCUserPortSend(hi_val%)
310    a%=FNUserPortReceive :REM Switches
320    a$=STR$(a%)
330  UNTIL m%>=steps% OR a%=16
340  @%="+G10.5"
350  reply$="PIN"+STR$(t%)
360  IF a%=16 reply$="PIL"+STR$(t%)
370  REM Enable OFF after 2 seconds (ok$)
380  tm%=TIME:REPEAT:UNTIL TIME>=tm%+200
390  ok$=FNEnableStepperMotorOff
400 ENDIF
410 =reply$

```

FNPSDecrease is similar to FNPSIncrease, but with the DIR output set low, this reverses the direction of rotation. Detection of the micro-switches' state indicates whether the lower limit switch has been closed, and returns with "PDZ" and the number of steps not used. ("Z" indicating zero current.)

### 3.2.12 RiscPC to A3020

The temperature sensor, relative humidity probe and power supply stepper motor are connected to the A3020 computer. But the main program controlling the other equipment is on the RiscPC. A method has to be devised therefore for the RiscPC to access the devices connected to the A3020. The method used is to connect the serial ports of both computers together, with the RiscPC being the master controller, and using the A3020 simply as a slave device. Procedures are therefore included to enable (a) the RiscPC to send commands to the A3020, and (b) for the A3020 to respond to those commands. The first task is achieved by the procedures in the GenLib library, and the second by the Worker program running on the A3020.

#### 3.2.12.1 The GenLib library

The serial port is first initialized in the following procedure. Note that, although the purpose of this procedure is the same as PROCMMInitialize\_Serial\_Port(MMport%) in Section 3.2.7, this procedure is initializing the *ordinary* serial port, and therefore does not use the procedures in the BasicLib.Serial library - the difference in the commands is obvious.

```
DEFPROCInitialize_Serial_Port
  REM 5 = Baud Receive Baud rate (4=1200)
  SYS"OS_SerialOp",5,4
  REM 6 = Baud Transmit Baud rate (4=1200)
  SYS"OS_SerialOp",6,4
  REM 1 = Initilise Serial Port 7 data 1 Stop odd Parity 1200 Baud
  SYS"OS_SerialOp",1,9
  REM 0 = Read/Write Serial status
  SYS"OS_SerialOp",0,&6,&FF00
  REM flow control = Hardware handshaking using CTS
```

```

    REM (ignoring both DCD and DSR) and RTS
ENDPROC

```

The serial port is set up with data format 7 data bits, 1 stop bit and Odd parity, with 1200 Baud being the speed for both receiving and transmitting. In this case CTS (Clear to send) handshaking is used. Note that the A3020 serial port is set up to use exactly the same format and handshaking.

Basic send and receive procedures are listed below. The outlines of these procedures can be seen to be similar to PROCMMSend and FNMMReceive in Section 3.2.7, but several changes are necessary because SYS“OS\_SerialOp” commands are now used in place of those in the BasicLib.Serial library. As with PROCMMSend, PROCSend transmits the byte A%, and repeats the action until the flag F1 is cleared.

```

DEFPROCsend(A%)
LOCAL F1
REPEAT
SYS"OS_SerialOp",3,A% TO ;F1
UNTIL (F1 AND &2 )=0
ENDPROC

```

```

DEFNReceive
LOCAL k%
rec$=" "
REM 2 = Enable Input from serial port
SYS"OS_Byte",2,2
REM 4 = Get a byte from the Serial buffer
REPEAT
SYS"OS_SerialOp",4 TO ,B% ;C%
C%=C% AND &2
UNTIL C%<>0
REPEAT
    SYS"OS_SerialOp",4,256 TO ,B% ;C%

```

```

C%=C% AND &2
IF C%=0 THEN rec$+=CHR$(B%)
UNTIL B%=13 OR B%=10
k%=LEN(rec$)-1
rec$=LEFT$(rec$,k%)
REM rec$ is a string
=rec$

```

In FNReceive, note that SYS “OS\_SerialOp” is used for different purposes depending on the first parameter i.e. the variable which is placed in register R0. If this is 2, then the serial port is enabled for input. If it is 4, then a byte is read from the serial buffer. It can be seen that the same SYS command is used in PROCsend with variable 3 in R0; in this case it transmits the byte in register R1.

PROCsend is then used in PROCStringTransmit to transmit a string of characters as their ASCII codes to the A3020 ending in ASCII 13 (Carriage Return), as shown below.

```

DEFPROCStringTransmit(a$)
LOCAL n%,ln%,pa%,pa$
REM Transmit characters in string
REM 2 = Enable Input from serial port
SYS"OS_Byte",2,2
ln%=LEN(a$)
n%=0
REPEAT
  n%+=1
  pa$=MID$(a$,n%,1)
  pa%=ASC(pa$)
  IF pa%>=0 AND pa%<=255 THEN
    PROCsend(pa%)
  ENDIF
UNTIL n%>=ln%

```

```
PROCsend(13)
ENDPROC
```

The above procedure is combined with FNReceive in FNTransmit, which sends a string representing a command to the A3020, then waits until the reply is received, this usually being either the value of the quantity the A3020 is being commanded to measure, or a string representing confirmation that an action has been carried out. The received string is padded with spaces which need to be deleted with FNStripSpaces, as shown below:

```
DEFFNTransmit(tr$)
REM transmit a string to worker
REM Get back a string which is
REM an appropriate reply.
PROCStringTransmit(tr$)
r$=FNReceive
r$=FNStripSpaces(r$)
=r$
```

As an example the temperature can be read using e.g. `this.temp = FNTransmit("TV")`. On receipt of the string "TV", the Worker program running on the A3020 switches to a procedure which measures the temperature via the analogue port. The Worker program constructs a string containing "TV" and the value of the temperature measured, and sends this back to the RiscPC. The function FNGetTemp in GenLib shown below transmits "TV", waits for the reply, confirms that the left two characters of the returned string are "TV", strips these away, leaving just the value of the temperature as its result.

```
DEFFNGetTemp
LOCAL tv$,tp$,TVFlag%
```



```
REPEAT
  TVFlag%=0
  tv$=FNTransmit("TV")
  IF LEFT$(tv$,2)="TV" THEN
    TVFlag%=1
    @%="+F10.1"
    tp$=MID$(tv$,3)
    REM read string tv$ from 3rd character to end.
    tp=VAL (tp$)
  ELSE
    TVFlag%=0
  ENDIF
UNTIL TVFlag%=1
=tp
```

Similarly, FNGetRH in GenLib sends the string "RH" to the A3020, and receives back the value of the relative humidity.

Other procedures in PSLib (running on the RiscPC) use FNTransmit to control the stepper motor connected to the power supply via the A3020 e.g.

- PROCPowerOn uses FNTransmit("PN")
- PROCPowerOff uses FNTransmit("PF")
- PROCEnableOn uses FNTransmit("EN")
- PROCEnableOff uses FNTransmit("EF")
- FNPSIncrease uses FNTransmit("PSI" +steps)
- FNPSDecrease uses FNTransmit("PSD" +steps)
- FNMoveToZero uses FNTransmit("MZ")

### 3.2.12.2 The Worker program

The Worker program, running on the A3020, is the program which receives the above commands from the RiscPC via the serial port link. Having received the command string transmitted as above, it then passes that string to FNProcess. This function then chooses the action to take, i.e. which function to run on the A3020, depending on the content of the string. This is shown below, where for instance, if the string received is “PN”, then control is passed to the function FNPowerOn, as described in Section 3.2.11.

```

DEF FNProcess(p$)
IF p$="RH" THEN =FNGetARH
IF p$="TV" THEN =FNGetATemp
IF p$="PN" THEN =FNPowerOn
IF p$="PF" THEN =FNPowerOff
IF p$="EN" THEN =FNEnableStepperMotorOn
IF p$="EF" THEN =FNEnableStepperMotorOff
IF LEFT$(p$,3)="PSI" THEN =FNPSIncrease(p$)
IF LEFT$(p$,3)="PSD" THEN =FNPSDecrease(p$)
IF p$="MZ" THEN =FNMoveToZero
="UNKNOWN"

```

The Worker program then transmits a reply to the main program running on the RiscPC, indicating either successful completion of the task, or the value of a measurement required.

### 3.2.13 Example program

A typical program which uses the procedures and functions described above is used in the experiment outlined in Section 3.5.3. In this experiment, the target current

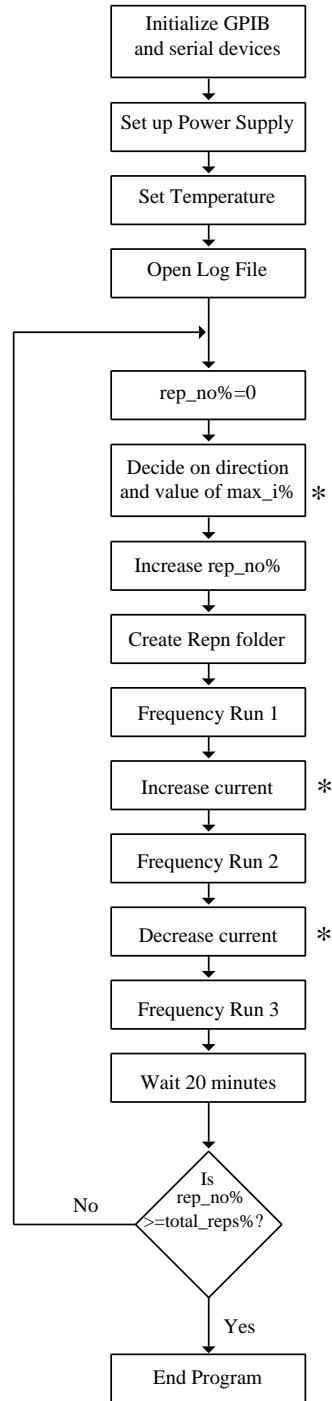


Figure 3.10: Example program

supplied to the electromagnet by the power supply (and hence the magnetic field generated) is increased in stages from 0.1 Amp to 1.1 Amp, and then decreased similarly back to 0.1 Amp. At each value of target current, three frequency scans are carried out - the first at zero current, the second at the target current, and the third at zero current. This cycle may be repeated for as long as necessary for increasing and then decreasing values of target current.

The program listed in Appendix H is a simplified version of the type of program used. It does however illustrate the main structure of a typical program, and the self-correcting assignment of the target current. In practice, the program is modified to take into account the different aim of each experiment.

The main parts of the program are illustrated as a flow chart in Figure 3.10, in which the boxes labelled with an asterisk represent sections of the program which are illustrated more fully in their own flow charts. The main sections of the program are described below.

### **3.2.13.1 PROCCheckList**

PROCChecklist is called first. It controls the procedures to:

- initialize the GPIB port to link to the Wayne-Kerr component analyser, and to set the voltage used and the speed of the scans;
- initialize the GPIB port to link to the Keithley electrometer and to set it up to read voltage;
- initialize the serial port to link to the Multimeter;
- initialize the serial port to link to Eurotherm;

- initialize the serial port to link to the A3020;

### 3.2.13.2 PROCPSSetUp

The rheostat controlling the power supply is not linear in operation i.e. for any given change in current, it turns through a larger angle at low currents than it does for large currents. Therefore the steps through which the stepper motor must turn will also be greater at low currents. PROCPSSetUp reads in values for the array  $spha(n\%)$  for  $n\%$  from 1 to 11 i.e. the steps per change of 0.01 Amps, where  $10 \times spha(n\%)$  increases the current from  $(0.1 \times (n\%-1))$  Amp to  $(0.1 \times n\%)$  Amp. e.g.  $spha(4) = 13$  means that the stepper motor is commanded to step 130 times in order to increase the current from 0.3 Amp to 0.4 Amp. (the acronym *spha* stands for “steps per hundredth amps”). Similarly, values of *sphad* are allocated for use when the current is being *decreased*. The *Target\_Current(n%)* array is also set up, where *Target\_Current(n%)* is set to a value of  $0.1 \times n\%$ ; this means that the value of any current can be called by reference to its index ( $max.i\%$ ).

### 3.2.13.3 Set temperature

The command PROCESendNewValue(“SL25.0”) is sent with the required temperature as parameter, to command the Eurotherm to maintain the temperature of the apparatus at that value. Obviously in experiments such as that described in Section 3.5.6, this command could be used to vary the temperature.

#### 3.2.13.4 Create log file

The command `u%=OPENOUT("logfile")` creates and opens for input a log file in which the values of the environmental variables measured can be stored. The parameter `u%` is the file handle which is used to address the file.

#### 3.2.13.5 Setting variables to initial values

Before starting the program's main loop, the values of the following variables are set up:

- `rep_no%=0` :This variable is used to name folders (Rep1, Rep2, etc.) each of which holds three files, each file containing the results of a frequency scan;
- `max_i%=0` :This variable is the index of the Target current array for this loop; it is also of course the *maximum* index value in the loop - `max_i%` stands for *maximum index*.
- `max_i_direction%=1` :This variable represents the direction that the target current is moving; 1 for increasing and  $-1$  for decreasing.

#### 3.2.13.6 Beginning the main loop

This is the first part of the program's main loop; this section of code (shown below) determines whether `max_i%` should continue in its present direction, i.e. either increasing or decreasing. It does this by assigning a value for `max_i_direction%`, depending on what value `max_i%` has reached. It is also illustrated as a flow chart in Figure 3.11.

```

IF max_i_direction%=1 THEN
    max_i%+=1
    IF max_i%>=11 Max_i_Flag%=-1 ELSE Max_i_Flag%=1
ENDIF

IF max_i_direction%=-1 THEN
    max_i%-=1
    IF max_i%<=1 Max_i_Flag%=1 ELSE Max_i_Flag%=-1
ENDIF

max_i_direction%=Max_i_Flag%

```

### 3.2.13.7 Create a folder for the data

In this section of the program, the value of `rep_no%` is increased by one, and this value is used to name a folder, which is created with the “`cdir`” command. In practice, the folders are stored in Data directories, each of which holds 50 Rep folders. (In RiscOS there is a limit of 70 files which can be stored in any one directory; 50 was chosen to stay well below this limit.)

```

rep_no%+=1
rep_name$="Rep"+STR$(rep_no%)
REM rep_name$ = Rep1, Rep2, Rep3, etc

REM Create directory
OSCLI("cdir "+rep_name$)

```

### 3.2.13.8 The first frequency run

`PROCSingleFrequencyRun(rep_name, "s01")` is called to measure the conductance and capacitance of the sample at the 42 frequencies produced by the Wayne-Kerr.

The temperature of the cabinet, the temperature of the sample, the relative humidity and the value of the current are also measured by this procedure, and stored in the log file. In this case, the current has not yet been switched on - the first frequency scan is always at zero current. The results of the frequency sweep are stored in the folder rep\_name in the file s01.

### 3.2.13.9 Increase current to Target\_Current(max\_i%)

After switching the power to the stepper motor on, the next section of the program increases the current from zero up to the current referenced by the value of max\_i%. It does this in a loop which increases the current in stages approximately 0.1 Amp at a time. This is illustrated in the flow-chart shown in Figure 3.12. It can be seen that the number of steps through which the stepper motor should turn is calculated from the difference between the present current (ThisI) and the next target current; this is shown in this code segment:

```
Diff_current=Target_current(n%)-ThisI
Change_factor=100*Diff_current
steps%=Change_factor*spha(n%)
```

Ideally, this should be 0.1 amp, but in practice it is found that there is some slippage in the gear system, which leads to a smaller increase in current than would be expected. Making the calculation of the number of steps dependent on the actual current change needed ensures that this is corrected at each stage.

When the current referenced by max\_i% has theoretically been reached in the main loop, a few extra lines are added to check that the current has actually been achieved (See below). This simply measures the actual current, and if some extra steps of the stepper motor are needed, then these are calculated in a similar way to that in the



loop. In practice, this section is only found to be occasionally used for maximum currents less than 0.4 amp. For larger currents, the number of steps the motor moves by is decreased, thereby leading to a decrease in the chance for slippage to occur. Also the self-correcting mechanism described above has already been activated at lower currents inside the loop.

```
Diff_current=Target_Current(max_i%)-ThisI
IF Diff_current>0.01 THEN
  Change_factor=100*Diff_current
  steps%=Change_factor*spha(n%)
  reply=FNPSIncrease(steps%)
ENDIF
```

#### 3.2.13.10 The second frequency run

PROCSingleFrequencyRun(rep\_name, "s02") is then called to measure the conductance and capacitance of the sample in exactly the same way as described in Section 3.2.13.8. In this case, the current has increased to the value referenced by max\_i%, and the file name is s02.

#### 3.2.13.11 Decrease current to zero

The next section of the program decreases the current to zero in stages, in a similar way to the procedure used to increase the current in Section 3.2.13.9. The procedure is illustrated in the form of a flow chart in Figure 3.13. In this case, of course, the variable n% which is the index inside the loop referencing the current, is decreased at each stage. The primary difference to the procedure for increasing the current is the final stage, where n% is equal to zero, i.e. the stage where the current is being decreased from 0.1 amp to zero. This time the function FNMoveToZero is called -

this steps the motor, not for a calculated number of steps, but until the closure of the zero position micro-switch is detected. The power to the stepper motor is then switched off.

#### **3.2.13.12 The third frequency run**

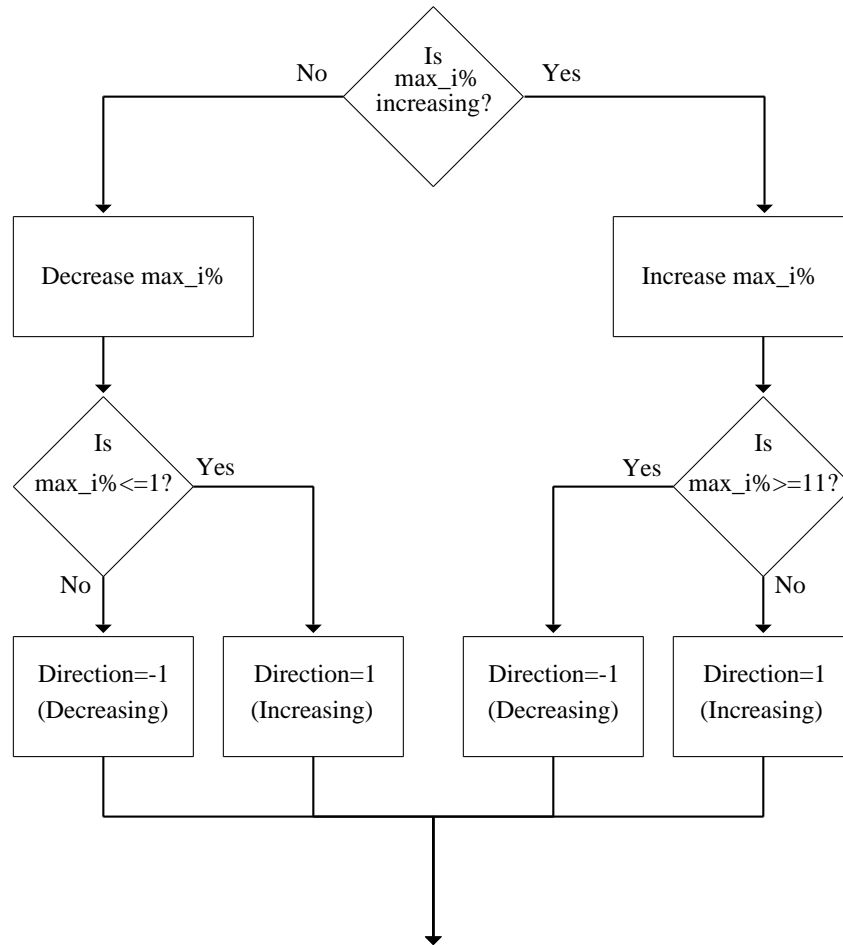
PROCSingleFrequencyRun(rep\_name, "s03") is then called to measure the conductance and capacitance of the sample in exactly the same way as described previously in Sections 3.2.13.8 and 3.2.13.10. In this case, the current has decreased to zero, and the file name is s03.

#### **3.2.13.13 Wait for sample to stabilize**

In this section of the program, the sample is allowed to stabilize for 20 minutes. Once every minute, the procedure PROCStoreValues is called - this measures the temperature of the cabinet, the temperature of the sample, the relative humidity and the value of the current, and the data is stored in the log file.

#### **3.2.13.14 Repeating the program**

The final part of the program loops back to Section 3.2.13.6, to check on the direction of max\_i%, increase rep\_no% and create the next folder. However, if rep\_no% has reached its required limit (total\_reps%), the program is terminated. A GPIB command is broadcast relinquishing computer control, and returning both devices to local control.

Figure 3.11: Direction of  $\max_i$

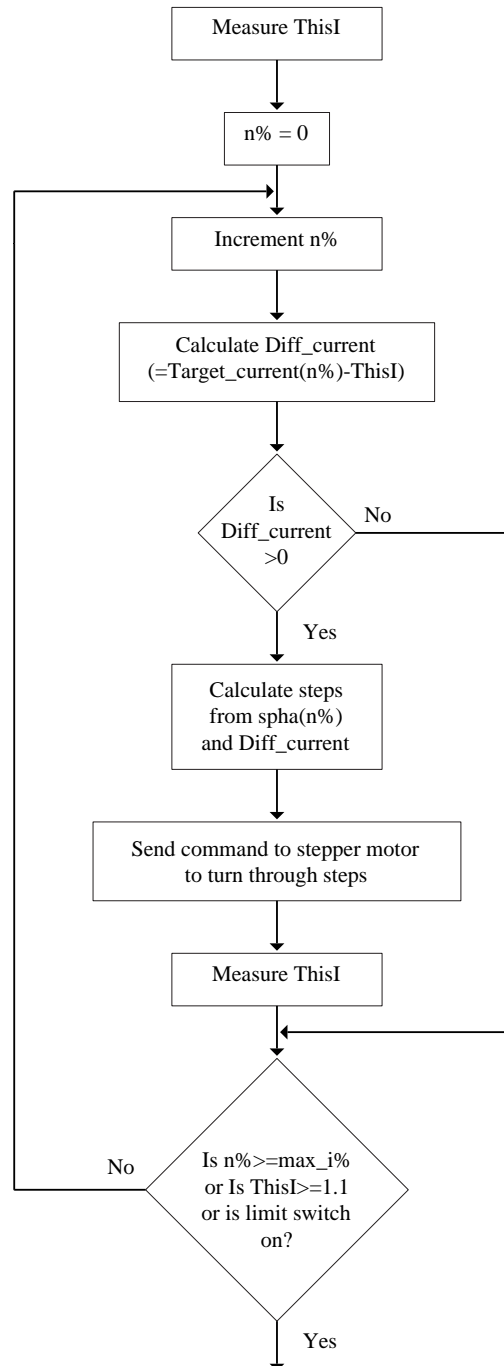


Figure 3.12: Procedure to increase current

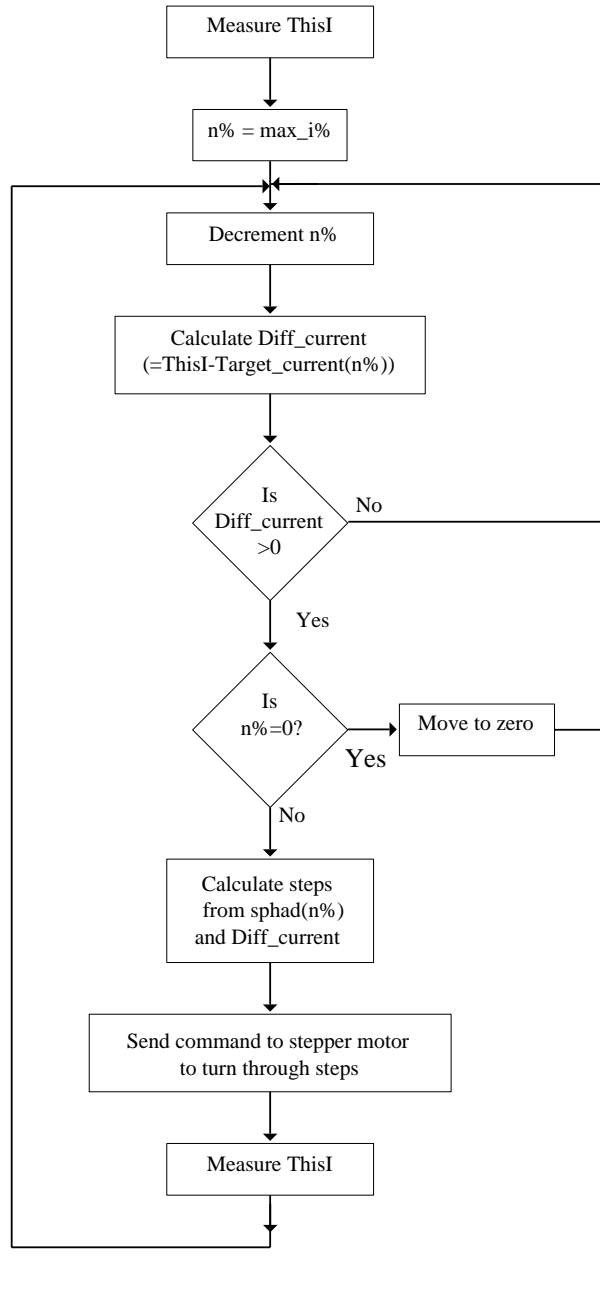


Figure 3.13: Procedure to decrease current

### 3.3 Calibration of Electromagnet

The current passing through the coils of the electromagnet is measured by the multimeter which is in series with the coils and the power supply. However, the experiments in the present work are concerned with the effect of the *magnetic field* on the samples containing DNA. It is necessary therefore to determine the relationship between the current and the magnetic field between the poles of the electromagnet. To simplify this process, the separation of the poles, which obviously also has an effect on the magnitude of the magnetic field, is standardized. The value chosen is the thickness of the planar electrode cell, as shown in Figure 3.18. The magnetic field is measured using a Hall-probe which is placed with its sensor parallel to the pole-faces, half-way between the poles and as close as possible to the centre-line.

It is found that there is a small amount of hysteresis present, so that the magnetic field as the current is increasing is slightly different to that found when the current is decreasing. The relationship for current increasing is shown in Figure 3.14, whilst that for current decreasing is shown in Figure 3.15. The data was fitted to  $m^{\text{th}}$  degree polynomials by the method of least-squares, where  $1 \leq m \leq 5$ . In both cases, the most accurate fit to the data was found for  $m = 3$  with the coefficient values shown on the graphs.

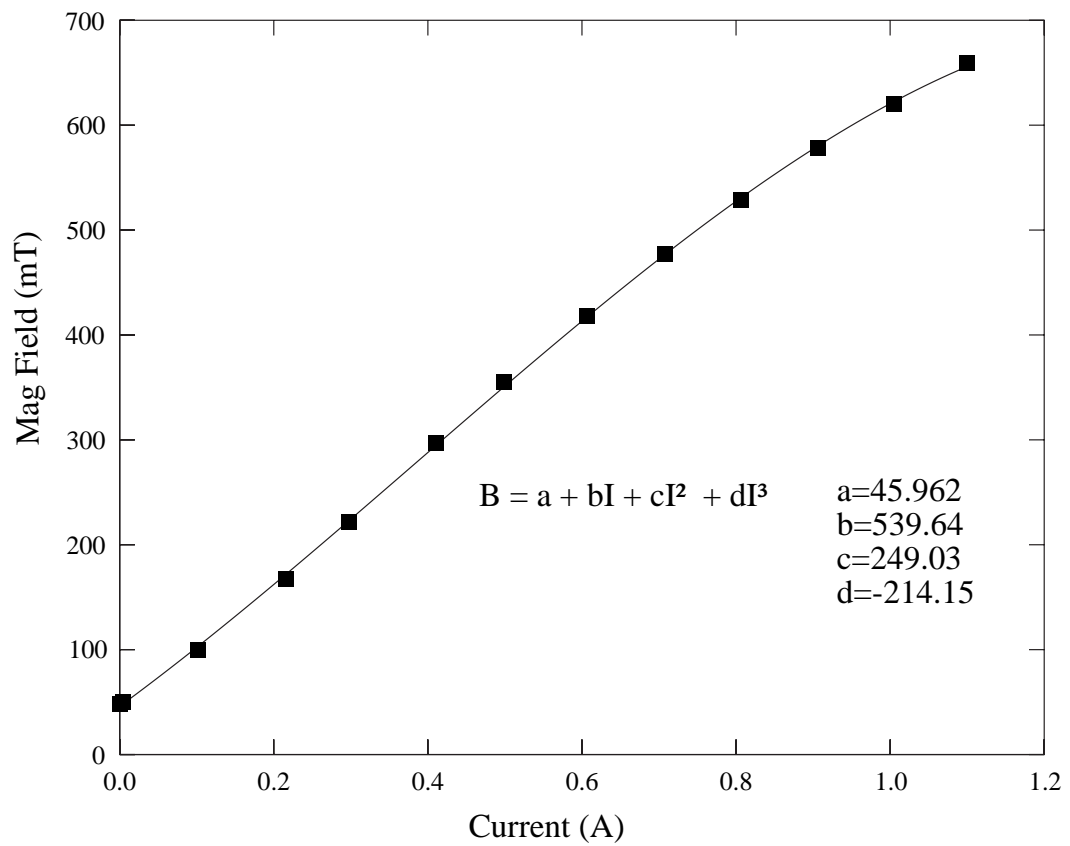


Figure 3.14: Calibration of electromagnet - current increasing

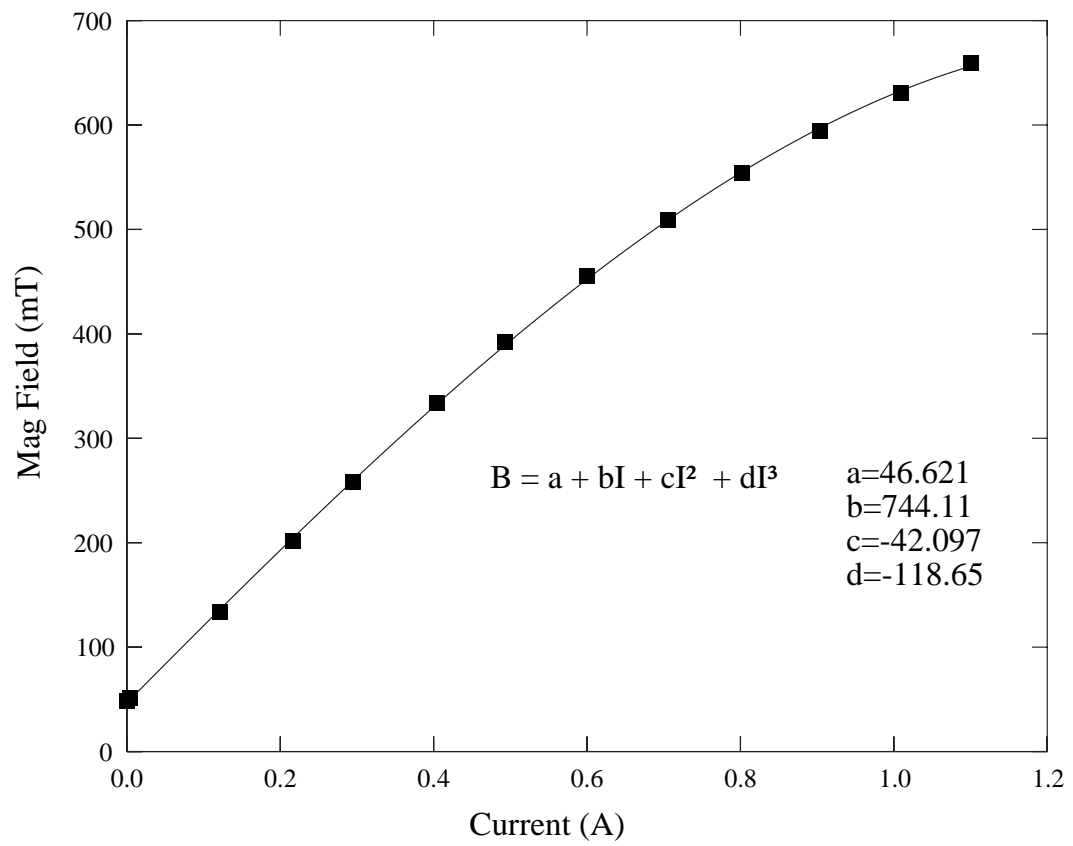


Figure 3.15: Calibration of electromagnet - current decreasing



## 3.4 Effect of low magnetic fields on high concentration DNA solutions using interdigitated electrodes

### 3.4.1 Introduction

The objective of this section is to describe the methods used to investigate the effect of low magnetic fields ( $< 0.7$  Tesla) on high concentration DNA solutions ( $> 150$  mg/ml) by allowing DNA solutions of low initial concentration to evaporate on an interdigitated gold electrode between the poles of an electromagnet. As the DNA solution becomes more concentrated, the intention is that it will pass through the cholesteric phase, and that the dielectric measurements will respond to changes in magnetic field.

As described in the Literature Review, DNA fragments in aqueous ionic solution form a variety of liquid crystal phases ((Strzelecka et al., 1988)). One such phase is called the cholesteric phase, which occurs at a concentration of between 100 – 160 mg/ml. Van Winkle and associates (Van Winkle et al., 1997) have shown that the cholesteric phase of liquid crystal DNA when exposed to moderately high magnetic fields (3.5 and 6.4 Tesla), exhibits field-stabilized birefringent stripes when observed in a polarizing microscope. When the magnetic field is removed, these stripes anneal away over a period of several days.

The aim of the experiments in this section was to identify corresponding reversible changes in the *dielectric* properties of DNA when exposed to magnetic fields of lower intensity. The following tests were carried out using interdigitated gold electrodes, as shown in Figure 3.16. A small volume of a solution of DNA in deionized water was placed on the electrode as shown in Figure 3.17. The magnetic field was

applied perpendicular to the face of the interdigitated electrode, and was therefore perpendicular to the electric field used to measure the dielectric properties of the solution. The task was to investigate the response to changes in the magnetic field of a sample of DNA with concentration in the range previous workers had identified with the cholesteric phase. Interdigitated electrodes were used in order to ensure that the solution evaporated readily, and would reach concentrations corresponding to the cholesteric phase in a reasonable time.

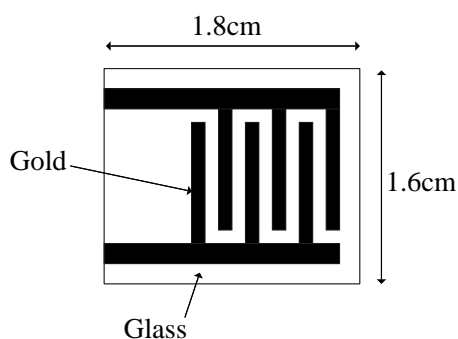


Figure 3.16: Interdigitated electrode design

The DNA used was obtained from Sigma and was described as “D6898 Deoxyribonucleic acid, sodium salt from herring testes Type XIV”. It should be noted that, although the description of this product remained constant during the period of this work, the appearance and properties of the DNA seemed to vary considerably. i.e. some samples were fibrous in nature whilst others were powdery; some dissolved easily in water, others dissolved with considerably more difficulty. Enquiries with the company led to the statement that “We do not assay for the molecular weight of this material”, but that no complaints had been received from other customers. The different samples used may explain some of the variation in dielectric measurements from experiment to experiment.

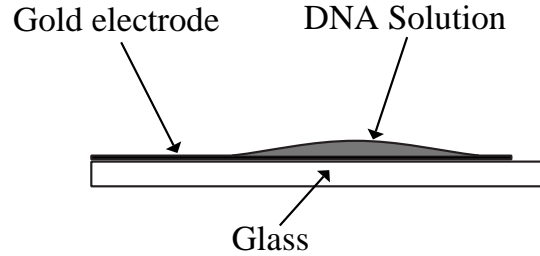


Figure 3.17: DNA solution on interdigitated electrode

Normally dielectric loss is calculated from the following equation:

$$\varepsilon'' = \frac{Gd}{2\pi f \varepsilon_0 A} \quad (3.1)$$

where  $G$  is the conductivity,  $d$  is the separation of the electrodes,  $f$  is the frequency,  $\varepsilon_0$  is the permittivity of free space and  $A$  is the area of the electrodes exposed to the DNA solution. For an interdigitated electrode however, the terms  $d$  and  $A$  have no direct meaning, and the constant  $\frac{d}{A}$  will vary with the volume of solution used and the area of the electrode over which it spreads.

Since for the purposes of the experiments in this current section, it is not necessary to calculate the absolute value of the dielectric loss, the values quoted will actually be simply  $\frac{G}{f}$ . Since all the other quantities in the equation are constant for a particular sample at a particular time, the changes in this quantity will mirror changes in the dielectric loss. The quantity  $\frac{G}{f}$  will therefore be referred to as “Gof” (G over f) in the diagrams in this chapter and the corresponding results, whilst in the text, the term “Dielectric Loss” will continue to be used.

### 3.4.2 Constant concentration

An initial study was first carried out to see whether the dielectric loss of a DNA solution of *constant* concentration changed when the magnetic field surrounding it was first increased and then decreased. Ideally the solution would be prepared with a concentration in the cholesteric phase range i.e. between 100 – 160 mg/ml, but the viscosity of solutions of the DNA (D6898, Type XIV) in this range meant that dissolving all the solid proved to be impossible.

A small sample of DNA solution was therefore prepared with a concentration of 70mg/ml. In this experiment, in order for the sample to remain in as constant a state as possible, it was decided to surround the sample with an O-ring, and cover it with a small cover-glass. The electrode and sample were placed between the poles of the electromagnet, and the current increased in steps of approximately 0.1 Amp up to 1.1 Amp, then decreased similarly to zero. The magnetic field intensity at each current can readily be calculated using the data in Section 3.3. At each value of current, a complete frequency sweep was carried out, and the dielectric data saved to a file on each occasion.

The results of this experiment are shown in Section 4.2.

### 3.4.3 Effect of magnetic field on DNA solution as it evaporates to higher concentrations

Since it had proved impossible to directly produce samples of DNA with concentration in the required range, it was decided that another approach was needed. The intention was to allow the DNA solution to evaporate slowly in order that the concentration would increase through the region where the DNA adopted the

cholesteric phase, and hopefully therefore to respond to the magnetic field.

When samples of DNA solution are left to evaporate in *air*, the dielectric loss spectrum slowly decreases in height over many hours, and the dielectric loss and permittivity values gradually reduce to zero for all frequencies in the measured range after a sufficiently long period. The spectrum also slowly moves to lower frequencies as the sample evaporates. There would therefore be no obvious way of knowing at what point the sample was at a concentration in the cholesteric phase range.

Attempts were made to see whether the rate at which the sample evaporated could be modified so that the possible conformational change on the onset of the cholesteric phase would be reflected in the dielectric loss spectrum. The response of the sample to changing magnetic field could then be tested at that point.

It was known from previous work that if the DNA solution were surrounded by dishes of saturated Sodium Chloride solution under a bell jar, the local conditions of relative humidity would affect the evaporation of the solution. A sample of DNA of initial concentration 50mg/ml was therefore placed on an interdigitated electrode as shown in Figure 3.17. The electrode was placed under a bell jar, and surrounded by several dishes containing saturated solutions of Sodium Chloride. Frequency sweeps were carried out at hourly intervals over several days, in order to detect onset of the cholesteric phase.

The results of this experiment are shown in Section 4.3

#### **3.4.4 Evaporation of DNA solution in controlled conditions**

The experiment described above was repeated over a longer time period using the brass enclosure described in Section 3.2.1. A sample of DNA of concentration

50mg/ml was placed on the interdigitated electrode and inserted into Port 2, whilst Port1 was connected to the vacuum system. The relative humidity sensor which normally would also be connected to part of the vacuum system (See Section 3.2.10), was connected instead to Port3 and placed as close as possible to the sample inside the enclosure.

A flask containing a saturated solution of Sodium Chloride was also connected to the vacuum system. All the ports were sealed, and electrical connections made through PET sockets, as described in Section 3.2.1. The brass enclosure was first isolated from the vacuum system, as was the saturated Sodium Chloride solution. The system was then evacuated, and the valve connecting the flask containing the saturated sodium chloride solution opened slowly, in order to evacuate the space above the saturated solution. After turning off the vacuum pump, the connection to the brass enclosure was opened, exposing the sample to the environment created by the saturated sodium chloride solution.

Once every hour the magnetic field was changed by first *increasing* the current through the electromagnet in increments of 0.1 Amp up to a maximum of 1.1 Amp, and then *decreasing* it in similar steps down to zero. In this way, the magnetic field was cycled through 23 values, and at each value a frequency sweep was carried out. The properties of the dielectric spectra used to monitor any changes were the peak or maximum value of the dielectric loss, and the frequency at which it occurred.

In addition, when the computer detected that the dielectric loss was changing more quickly than previously seen, the cycle of increasing then decreasing the magnetic field and performing frequency sweeps was initiated immediately.

The results of this experiment are shown in Section 4.4.

### 3.4.5 Monitoring the temperature

It would have been useful in the previous experiment to monitor the *temperature* close to the sample. Unfortunately, the brass enclosure only had three ports, one of which was used by the sample and a second by the connection to the vacuum system. It was thus impossible to fit both a relative humidity sensor and a temperature sensor to the third port at the same time.

It was decided therefore to replace the humidity sensor used in the experiment in Section 3.4.4 with a temperature sensor, as described in Section 3.2.9. It was placed as close as possible to the sample inside the brass enclosure. A new sample of DNA with concentration 50mg/ml was prepared, and the experiment repeated.

The results of this experiment are shown in Section 4.6.

## 3.5 Effect of low magnetic fields on DNA solutions of lower concentrations using planar electrodes

### 3.5.1 Preparation

In the experiments investigating the cholesteric phase, interdigitated electrodes were used, which meant that the electric field direction was at right angles to the direction of the magnetic field. It was decided to change to planar electrodes in order that the electric and magnetic fields could be parallel, as shown in Figure 3.18a. A cell was constructed by separating the electrodes by an O-ring with a single slot in one side (See Figure 3.18b and c). The DNA (bought from Sigma, and described

as “sodium salt from herring testes Type XIV D6898”) was dissolved in deionized water to a concentration of 50mg/ml, and magnetically stirred for approximately one hour. It was then allowed to stand for the same period, in order for bubbles which formed during the stirring process to migrate to the surface. The solution was then injected into the cell through the slot in the O-ring (See Figure 3.18d), and the opening closed using the point of the syringe. The electrode cell was inserted into the brass apparatus described previously, and the poles adjusted until they were just in contact with the cell.

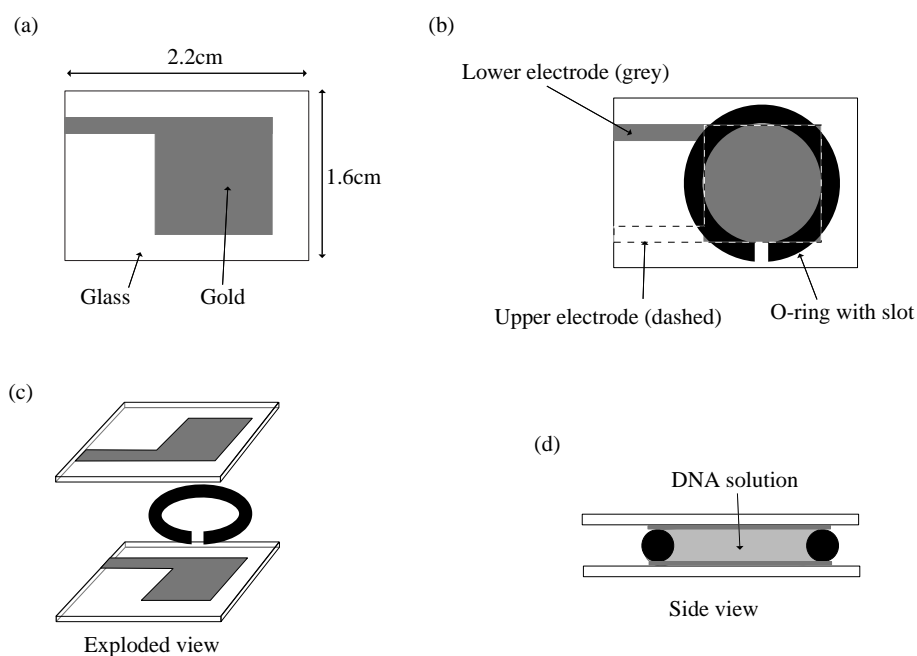


Figure 3.18: Planar electrodes



### 3.5.2 Preliminary study

The preliminary study was carried out in order to determine whether the dielectric loss of the DNA sample changed when exposed to a magnetic field. The current supplied to the electromagnet was increased in increments of 0.1A from 0.0A to 1.1A, and then decreased in the same way down to zero. The current was then kept at zero for approximately one minute, and the procedure repeated. At each value of current, the conductance was measured using the Wayne-Kerr component analyser at two different frequencies (500Hz and 5000Hz), and the Loss was then calculated from the following equation:

$$\varepsilon'' = \frac{Gd}{2\pi f \varepsilon_0 A} \quad (3.2)$$

where G is the conductance, d is the separation of the electrodes, f is the frequency,  $\varepsilon_0$  is the permittivity of free space and A is the area of the electrodes exposed to the DNA solution. (This preliminary study was also a useful way of checking that the cell and its contents had been successfully connected to the measuring apparatus.) The results of this experiment are shown in Section 5.2.

### 3.5.3 Full experiment

The Wayne-Kerr component analyser measures the dielectric properties of samples at 42 frequencies, varying from 20Hz to 300kHz. A comprehensive experiment should measure the effect of applying increasing and then decreasing values of magnetic field on the dielectric loss values at all these frequencies. It might be assumed therefore that the easiest way to carry this out would be to repeat the Initial test above, but, at every current value, to measure the dielectric loss at all 42 frequencies

instead of at only 2 frequencies. Unfortunately, taking readings at 42 frequencies would add over a minute to the time at which the electromagnet was carrying each current value. The cumulative effect of perhaps 10 or more minutes with high values of current being carried through the windings of the electromagnet would mean that the temperature would increase substantially.

The apparatus was enclosed in a temperature-controlled cabinet, which had been thought sufficient to negate the heating effects of the current passing through the coils of the electromagnet. Unfortunately, it was found that localized changes in temperature close to the sample were larger than expected. It was impractical to add water cooling to the brass enclosure, and additional air-cooling was found to be ineffective.

It was therefore decided that the following procedure should be used: A frequency scan (i.e. measuring loss over all 42 frequencies) should be carried out at zero current; the current should then be increased to a target current when another frequency scan should be run; the current should be decreased to zero and a further frequency scan should be run. Time should then be allowed for the temperature to stabilize - a period of twenty minutes was chosen. The procedure should be repeated for target currents increasing from 0.1A to 1.1A in 0.1A increments, and then decreasing in the same way to 0.1A. i.e. for every current, there would be three frequency scans - (1) with zero current (2) at the target current and (3) at zero current.

If we use the abbreviation FS for “frequency scan”, and W20 for “wait twenty minutes”, INC TO xA for “increase current to x Amp”, and DEC TO xA for “decrease current to x Amp”, the procedure could be summarised as follows:

```
FS, INC TO 0.1A, FS, DEC TO 0.0A, FS, W20  
FS, INC TO 0.2A, FS, DEC TO 0.0A, FS, W20
```

FS, INC TO 0.3A, FS, DEC TO 0.0A, FS, W20  
...  
FS, INC TO 1.0A, FS, DEC TO 0.0A, FS, W20  
FS, INC TO 1.1A, FS, DEC TO 0.0A, FS, W20  
FS, INC TO 1.0A, FS, DEC TO 0.0A, FS, W20  
...  
FS, INC TO 0.3A, FS, DEC TO 0.0A, FS, W20  
FS, INC TO 0.2A, FS, DEC TO 0.0A, FS, W20  
FS, INC TO 0.1A, FS, DEC TO 0.0A, FS, W20

This procedure could be repeated for as long as necessary, and would minimize the time for which large currents were passed through the electromagnet. Using this procedure, it was found that the temperature close to the sample varied by less than 1°C during the experiments. One complete cycle as described above would take approximately 12 hours.

The procedure was carried out for a solution of DNA (D6898) with concentration 50mg/ml, prepared as described in Section 3.5.1. The results are shown in Section 5.3.

### 3.5.4 Control Experiments

It was necessary to determine if the changes in dielectric loss with changing magnetic field were caused by the presence of the DNA in the sample cell, or whether there were other factors which could have been responsible for the observed response.

- In order to assess the effects of the apparatus, the clips connecting the Wayne-

Kerr component analyser to the electrode cell were reversed, and the experiment repeated.

- The experiment was repeated with an empty cell.
- The experiment was repeated with the DNA solution replaced by deionized water.
- The experiment was repeated with the DNA solution replaced by a solution of Sodium Chloride with the same concentration of sodium ions as found in DNA (D6898) with a concentration of 50mg/ml. This was determined to be 8mg/ml.
- The experiment was repeated with DNA solution in the cell, but with the electrical connections to the upper coil of the electromagnet reversed. The net magnetic field in the area of the cell was therefore negligible (confirmed with a Hall probe), but the heating effect of the current passing through the electromagnet coils was the same.

The results are shown in Section 5.4

### **3.5.5 Varying the concentration of DNA**

In order to determine how the response to changing magnetic field was affected by the concentration of the DNA, the full experiment was repeated for three other concentrations from 30mg/ml to 96mg/ml, and the results combined with those for 50mg/ml.

The results are shown in Section 5.5.

### 3.5.6 Variation of Temperature

In order to determine how the response to changing magnetic field was affected by temperature, frequency scans before and after application of the maximum magnetic field (0.66T) were carried out at seven temperatures between 23.5 °C and 44.1 °C for a sample of DNA at a fixed concentration of 50mg/ml.

The results are shown in Section 5.6.5.

### 3.5.7 Variation of added Sodium Chloride

Frequency scans before and after application of the maximum magnetic field (0.66T) were carried out on samples of DNA at a concentration of 50mg/ml with varying proportions of added Sodium Chloride. The DNA as purchased from Sigma is the sodium salt, with a sodium content calculated as follows:

On average a nucleotide pair has a mass of 660 Daltons, including the two sodium ions associated with that part of the DNA structure. The proportion of the mass represented by the sodium ions is therefore  $\frac{46}{660}$ , or 6.97%.

In order to calculate the mass of NaCl to add in order to multiply the proportion of NaCl in the DNA by a factor  $X$ , the following procedure was followed:

The normal procedure is to prepare a sample of 1.4ml of the DNA solution in deionized water. The concentration of DNA required is 50mg/ml, i.e. the mass of DNA used is 70mg, which contains  $0.0697 \times 70\text{mg}$  i.e. 4.88mg of sodium. 58.5mg of NaCl contains 23mg of Na; therefore 4.88mg of Na is the equivalent of  $\frac{4.88 \times 58.5}{23}$  or 12.41mg of NaCl.

i.e. 12.41mg of NaCl is in a sample of 1.4ml of 50mg/ml DNA solution. This is

equivalent to 8.86mg of NaCl in 1ml of solution. To multiply the proportion of NaCl in the DNA solution by a factor  $X$ , the deionized water should first have NaCl added to make the NaCl concentration equal to  $(X - 1) \times 8.86\text{mg/ml}$ . e.g. if  $X = 2$  44.3mg of NaCl is dissolved in 5ml of water. 1.4ml of this solution is taken, and 70mg of DNA is dissolved in it in the usual way. (See Section 3.5.1)

In addition to the DNA as purchased (D6898) (i.e. where multiple of DNA equals 1), three other samples of DNA were prepared with multiples of NaCl of 1.33, 1.65 and 1.97.

The results are shown in Section 5.6.6.

### 3.5.8 Variation of Voltage used

The Wayne-Kerr Component Analyser used for these experiments applies a variable frequency alternating potential difference across the plates of the sample holder; each frequency scan in these experiments varies the frequency of that potential difference from 20Hz to 300000Hz. There is however another property of the signal supplied by the apparatus which is adjustable - the "A.C. Drive Level", or the *magnitude* of the alternating potential difference applied to the sample. All the above experiments were carried out using a voltage of 0.4 volts a.c.

In order to determine the effect of varying that "drive level", it was decided to examine the Difference Signal for a sample of DNA with a concentration of 50mg/ml at voltages from 0.1v to 0.6v in increments of 0.1v. Two frequency scans were run at each of these voltages, one with zero magnetic field and one with maximum magnetic field. From these a Difference Signal was obtained for each voltage.

The results are shown in Section 5.6.7.

### 3.5.9 Dialysis of DNA with other salts

The DNA used in the above experiments is the Sodium salt as bought from Sigma. In order to determine the effect of changing the cation, the DNA was dialyzed with the chlorides of Lithium, Sodium, Potassium, Rubidium and Calcium. Four different concentrations of each sample were then used in the experiment, varying from approximately 25mg/ml to 100mg/ml.

The dialysis process was carried out as follows; 500mg of the DNA was dissolved in 150ml of deionized water and placed in several lengths of dialysis tubing, each closed at one end. The tubes were then suspended in a large beaker containing a 0.2M solution of the appropriate chloride. The salt solutions were magnetically stirred and the process allowed to continue for 48 hours at a temperature of 4 °C. This replaced the sodium ions in the original DNA with the cations from the chloride solution used. The DNA solutions were then dialyzed against deionized water for one week, changing the water every two days, still at the same temperature. This process resulted in the removal of excess metal ions, leaving only those bound to the DNA. The final DNA solutions were freeze-dried and stored at 4 °C.

The results are shown in Section 5.8.

# Chapter 4

## Effect of low magnetic fields on high concentration DNA solutions using interdigitated electrodes - Results

### 4.1 Introduction

This chapter examines the results of investigations into the effect of low magnetic fields on high concentration DNA solutions using interdigitated electrodes, with magnetic field applied perpendicular to the electric field, as described in Sections 3.4.1 to 3.4.5; i.e. experiments which attempt to identify the effect of magnetic fields on the cholesteric phase of DNA, which previous workers had associated with susceptibility to magnetic fields.

As described in detail in Section 3.4, in the experiments using *interdigitated* elec-



trodes, the diagrams show the quantity  $\frac{G}{f}$ , referred to as “Gof” (G over f), changes to which will reflect changes to dielectric loss. Graphs of Gof against LOG(Frequency) will be referred to as “Gof spectra”, since they will be similar in form to dielectric loss spectra. Similarly, some figures will also show dGof, i.e. the difference in Gof values found *with* a magnetic field, as compared to Gof values *without* a magnetic field; dGof plots will be of the same form as dLoss plots. In discussion of the results however, the terms dLoss and dielectric loss will be used where appropriate. (A full description of the advantages of dLoss plots, and therefore dGof plots, is given in Section 2.5.)

## 4.2 Constant concentration

This section shows the results of the experiment described in Section 3.4.2. A sample of DNA solution (D6898 from herring testes Type XIV) with a concentration of 70 mg/ml was placed on an electrode, surrounded by an O-ring, and covered with a small cover-glass. The magnetic field was increased in steps from 0.05 Tesla to 0.66 Tesla, then decreased similarly to 0.05 Tesla. The value of magnetic field for each step is shown in the key. At each value of magnetic field, a complete frequency sweep was carried out.

Each plot in Figure 4.1 shows  $dGof$  at a given value of magnetic field plotted against LOG(Frequency). The reference value for dGof calculations is taken to be the loss spectrum obtained by the first frequency sweep at a magnetic field of 0.05 Tesla. Although the magnetic field is increasing for the first 12 sweeps, and then decreasing for the next 12, it is obvious that the change in the dielectric loss is continuing to increase throughout. The Figure 4.2 shows the dGof value at 500 Hz for each plot against time in minutes. This corresponds to the approximate frequency of the maximum value for the plots in Figure 4.1. It can be seen that whilst the trend is to

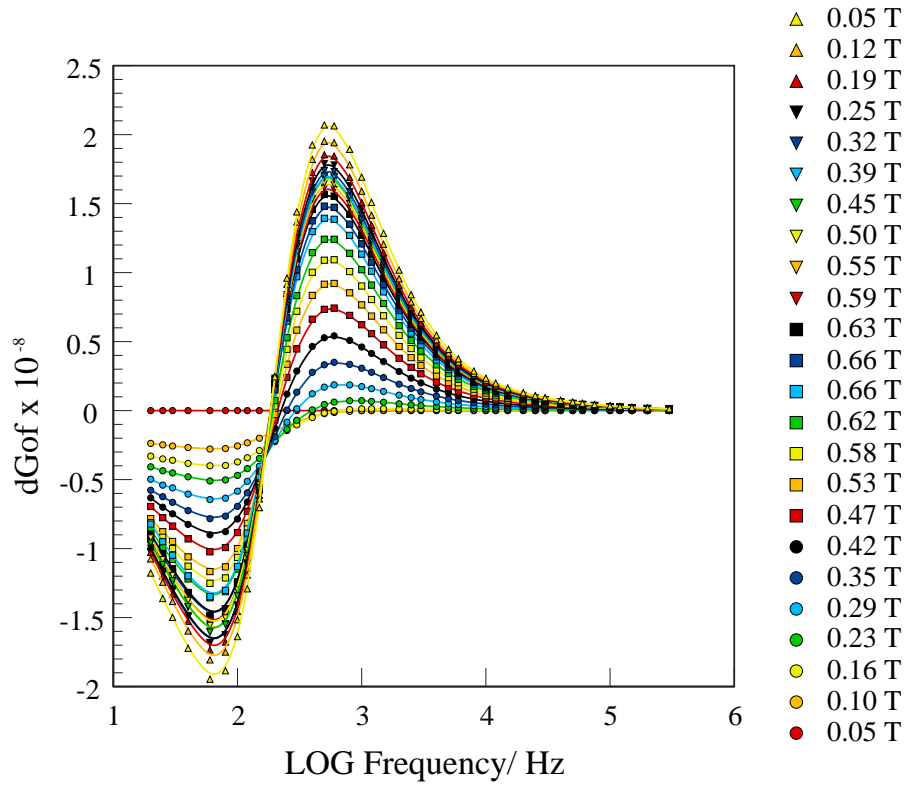


Figure 4.1: Change in dGof with change in magnetic field

increase throughout, the rate of increase is lower as the magnetic field is decreasing.

Since the change in dielectric loss is all in one direction, whilst the magnetic field is first increasing and then decreasing, it can be surmised that, whatever is causing the dielectric loss to change, it is unlikely to be simply the magnetic field. The electrode and sample were located on the face of the lower pole-piece of the electromagnet, whilst a temperature sensor was placed as close as possible, though not on the face of the electromagnet itself. The electromagnet coils were carrying quite large currents (up to 1.1 Amp) for parts of the experiment, and the heat generated caused the pole-pieces to become quite warm. Thus, although the sensor detected an increase

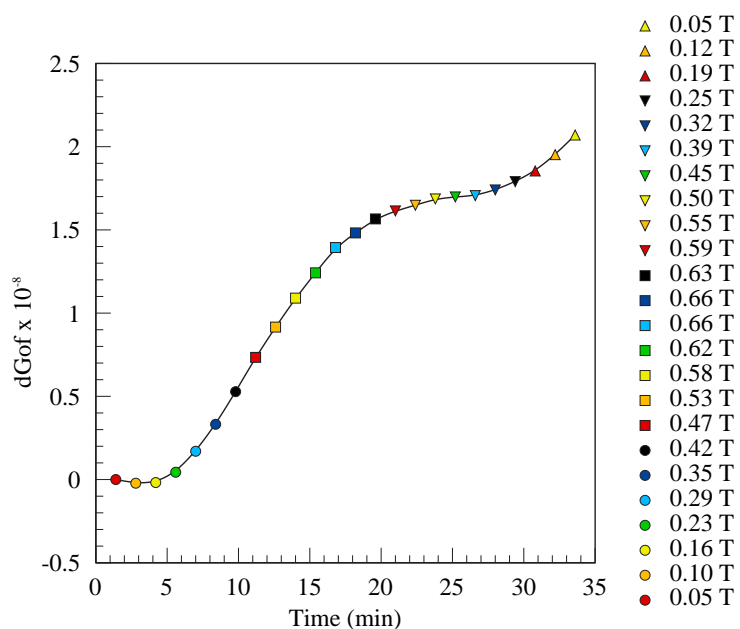


Figure 4.2: dGof at 500 Hz vs time (min), magnetic field increasing and then decreasing

of approximately  $2.0^{\circ}\text{C}$  during the experiment, it seems likely that the sample itself would have experienced a larger increase in temperature. The increase in the dGof values could be caused by a combination of the effects of heat and magnetic field on the DNA solution. The fact that the rate of increase of the maximum dGof for each plot is decreasing in the second half of the experiment could indicate either that the dGof values are reflecting the decreased magnetic field, or simply the relative decrease in heating effect as the electromagnet current was lowered.

It cannot definitely be concluded from this experiment that DNA solution at low concentrations experiences reversible changes in dielectric properties by the application of magnetic field perpendicular to the electric field. The possibility cannot

be entirely ruled out however.

### 4.3 Effect of magnetic field on DNA solution as it evaporates to higher concentrations

This section shows the results of the experiment described in Section 3.4.3, tracing the change in the dielectric loss spectrum of DNA solution of initial concentration 50mg/ml as it evaporated in the presence of saturated NaCl solution under a bell jar. Frequency sweeps were carried out at hourly intervals over several days as the DNA solution evaporated, became more concentrated, and hopefully adopted the cholesteric liquid crystal structure.

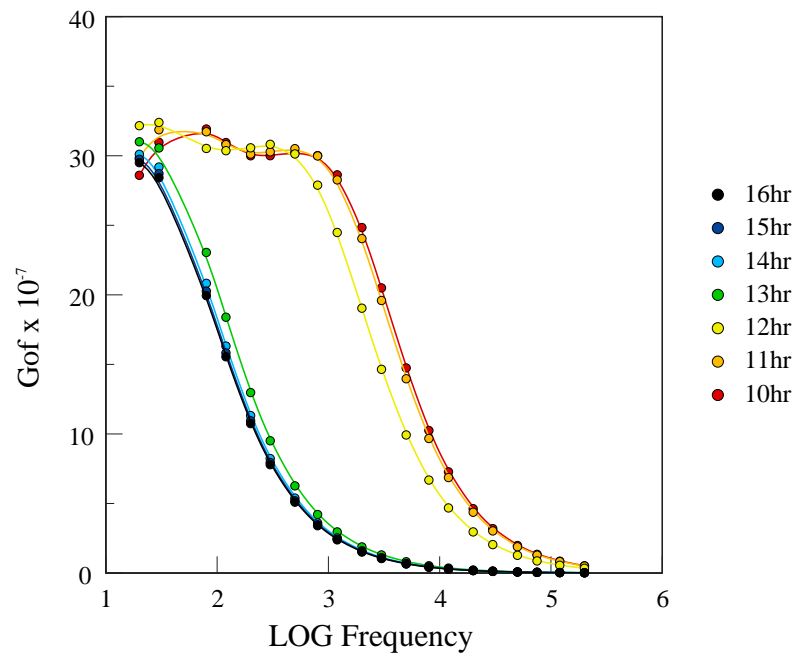


Figure 4.3: DNA Gof spectrum between 10-16 hours

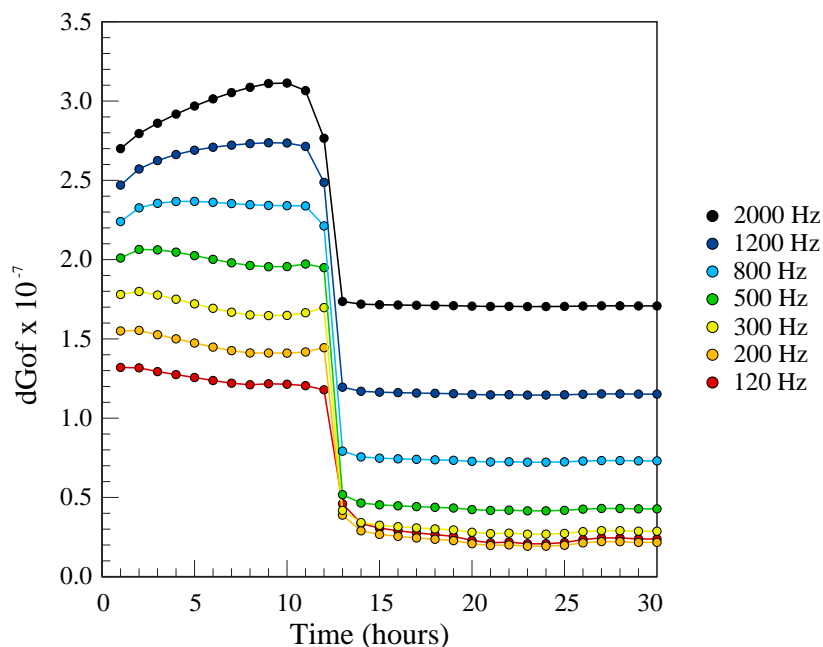


Figure 4.4: Change in single frequency Gof for first 30 hours

Figure 4.3 shows the Gof spectrum between 10 and 16 hours after evaporation started. The change in the first 10 hours was minor, but it can be seen that between 12 and 13 hours, there was a rapid change in dielectric properties to an almost steady state. The DNA film still appeared to be viscous during this period i.e. it had not completely dried out.

Figure 4.4 shows the *change* in Gof values for frequencies between 120 and 2000 Hz, for the first 30 hours. For every frequency, the values shown represent the change from the loss value for that frequency at the start of the experiment. Those initial values were normalized so that they were equally distributed on the vertical axis. Again, the change in values between 12 and 13 hours was obvious.

In order to determine the approximate concentration of the DNA on the electrode

at the end of the experiment, the slide was removed and weighed. It was evacuated in order to drive off all the remaining water and reweighed, hence giving the mass of water present. The remaining DNA was then washed off, the slide thoroughly dried, and weighed again, hence giving the mass of the DNA. Calculations then gave an approximate concentration of 170mg/ml for the DNA solution.

At this stage, it was thought that this rapid change in Gof values indicated either a conformational change in the DNA, or a change in the arrangement of DNA in the solution. The determination that the concentration of the DNA at the end of the experiment was 170mg/ml could perhaps have indicated the DNA had changed to the cholesteric phase. It was in order to further investigate this rapid change that the brass cell described in an earlier chapter was designed and constructed. The cell would enclose the sample in a closed environment, in which the relative humidity could be controlled and carefully measured, whilst still enabling the application of a magnetic field.

Further experiments therefore tracked the dielectric loss (Gof), and used the sudden change detected in this experiment as an indication that the concentration could be in the cholesteric phase concentration range.

## **4.4 Evaporation of DNA solution in controlled conditions**

This section shows the results of the experiment described in Section 3.4.4, and examines the response of a sample of DNA of initial concentration 50mg/ml as it evaporates in the presence of a saturated solution of sodium chloride between the poles of an electromagnet inside the sealed brass enclosure. Once every hour, the current through the electromagnet is increased and then decreased in steps, whilst

at each step, a frequency sweep is performed.

Figure 4.5 shows the maximum or peak value of Gof as the sample evaporates and increases its concentration. Figure 4.6 shows the variation of the LOG of the frequency of that peak value with time. As can be seen in the key in the Figure, the start of the *increase* in magnetic field, and the start of the *decrease* in magnetic field are shown each time.

The peak Gof is seen initially to decrease gradually with time, whilst its frequency slightly increases. However, at approximately 22 hours, the frequency of the peak is seen to decrease rapidly to the minimum frequency measurable by the Wayne-Kerr i.e. 20Hz. At the same time, the value of the peak Gof seems to show a very small increase as the magnetic field is increased, and an equally small decrease as the field is decreased. Unfortunately, when the peak moves to frequencies below 20Hz, neither its frequency nor its magnitude can be determined. This is indicated on the graphs by the points being coloured white; neither the frequency nor Gof values shown in white are therefore valid as direct measures of the maximum Gof. The program generating the graphs simply finds the maximum Gof value in the data, and so the peak Gof values shown in white are in reality the Gof value at 20Hz. This value seems to remain fairly constant after 25 hours, and may indicate that the peak has stopped moving to lower frequencies, and has maintained its value.

Figure 4.7 shows the relative humidity measured close to the sample. The presence of the saturated solution of sodium chloride usually provides an environment in which the relative humidity is constant at 75%. However, the initial relative humidity can be seen to be approximately 90%, and when the dispersion moves rapidly to lower frequencies, the relative humidity also decreases equally rapidly to between 40% and 50%. Note that, in contrast to the points coloured white in Figures 4.5 and 4.6, the equivalent points in Figure 4.7 *do* show the true humidity readings near the sample. The interpretation of the relative humidity measurements will be discussed

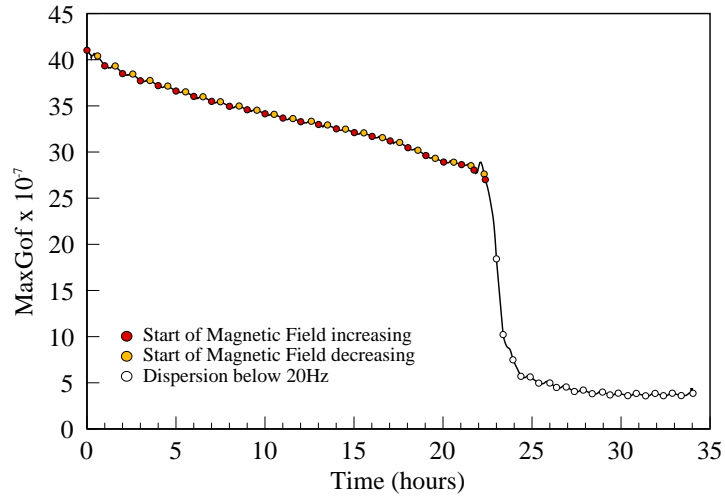


Figure 4.5: Maximum Gof versus Time

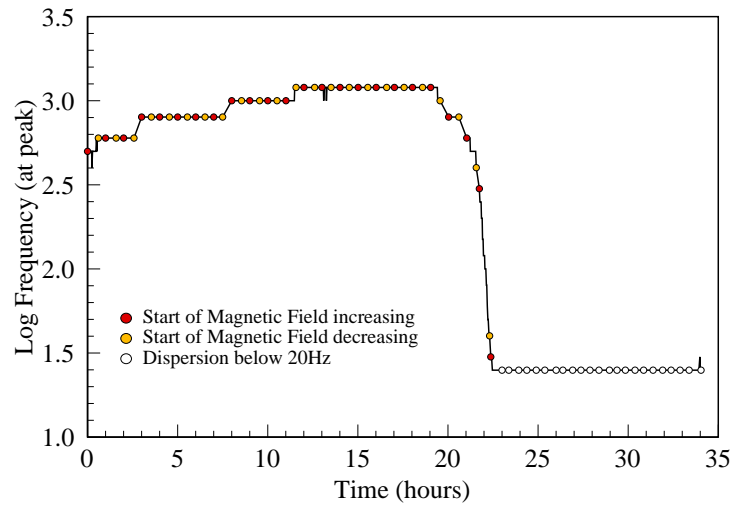


Figure 4.6: Frequency of Maximum Gof versus Time



more fully in Section 4.5.

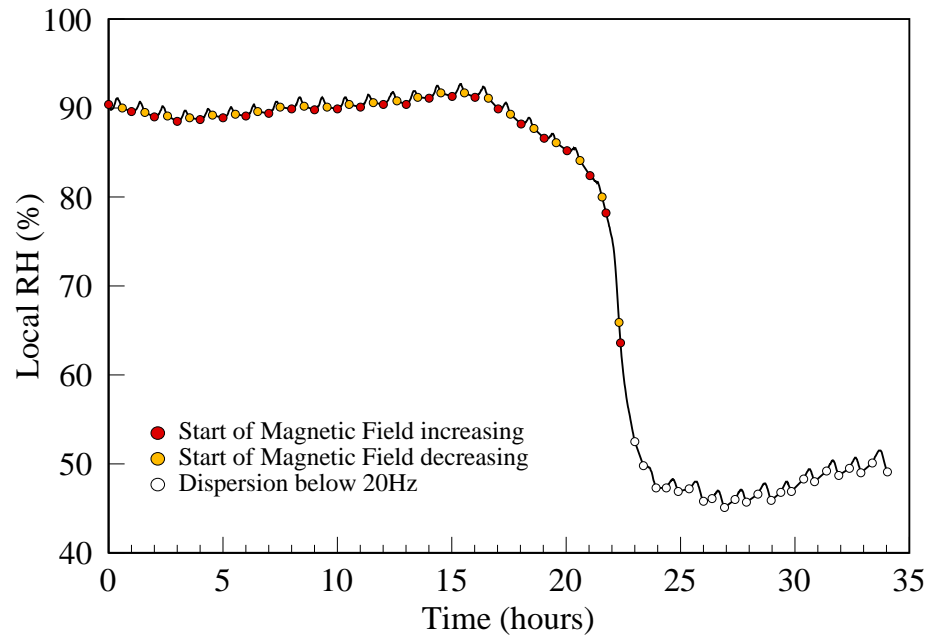


Figure 4.7: Relative Humidity versus Time

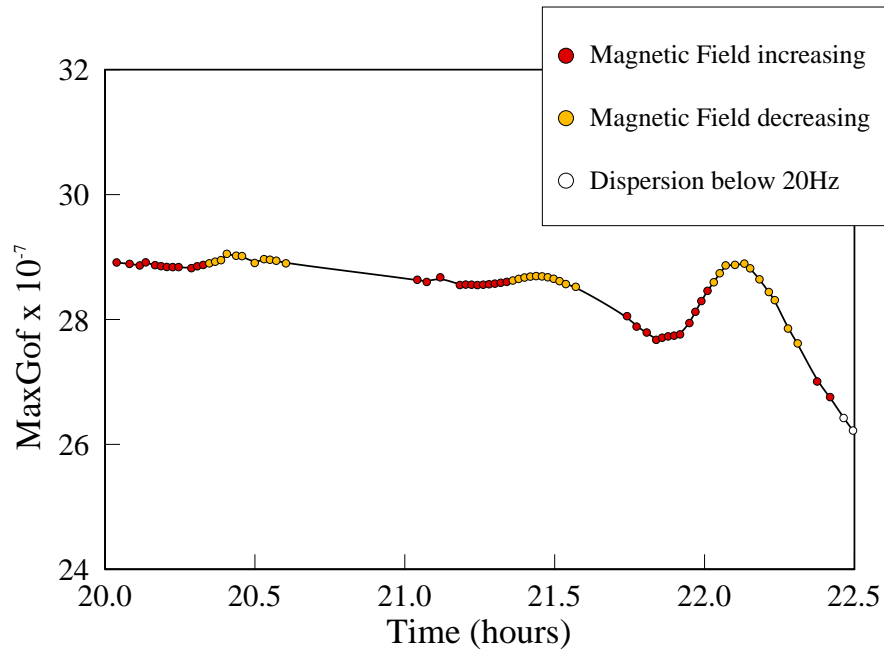


Figure 4.8: Maximum Gof versus Time: Close-up

In order to examine more closely what happens at approximately 22 hours, the Figures referred to above have been redrawn at a larger scale by showing only the time between 20 and 22.5 hours after the start of the experiment. The change in peak value of Gof is shown in Figure 4.8, whilst the change in the frequency of that peak is shown in Figure 4.9. In both these figures, the key indicates where the readings are shown for *every* step in the increasing magnetic field cycle, and every step in the decreasing magnetic field cycles. (The previous graphs only show the *start* of each cycle.)

The aim of this experiment is to determine if there is a *reversible* change in a dielectric variable as the magnetic field is increased and then decreased. In Figure 4.8, between approximately 21.7 and 22.3 hours, there may be such a change. The

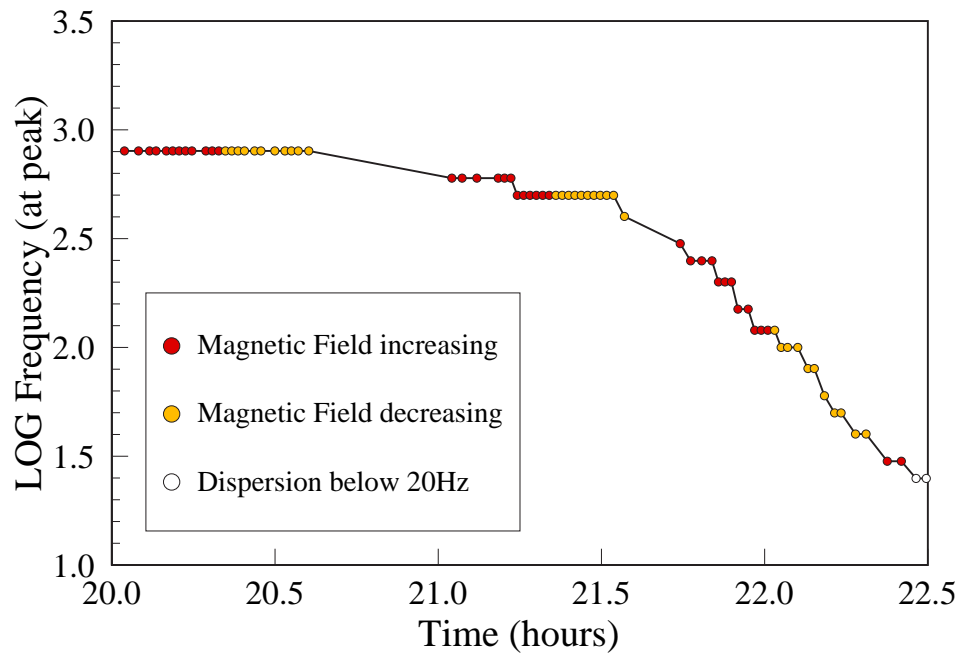


Figure 4.9: Frequency of Maximum Gof versus Time: Close-up

peak value can be seen to start to decrease, then increase as the magnetic field is increased. It continues to increase slightly, even though the magnetic field has started to decrease. It then begins to decrease also, i.e. it reflects the change in magnetic field, albeit with a slight delay. This change can be seen to occur *before* the frequency of the peak value reaches the minimum frequency barrier, and so is in the range where both the peak value and its frequency can be determined with confidence.

Figure 4.10 shows the change in the relative humidity over a slightly longer time range. The relative humidity sensor seems to react to local conditions i.e. near the sample, much more than it does to the influence of the saturated sodium chloride solution. This is seen both at the start of the experiment, when the relative humid-

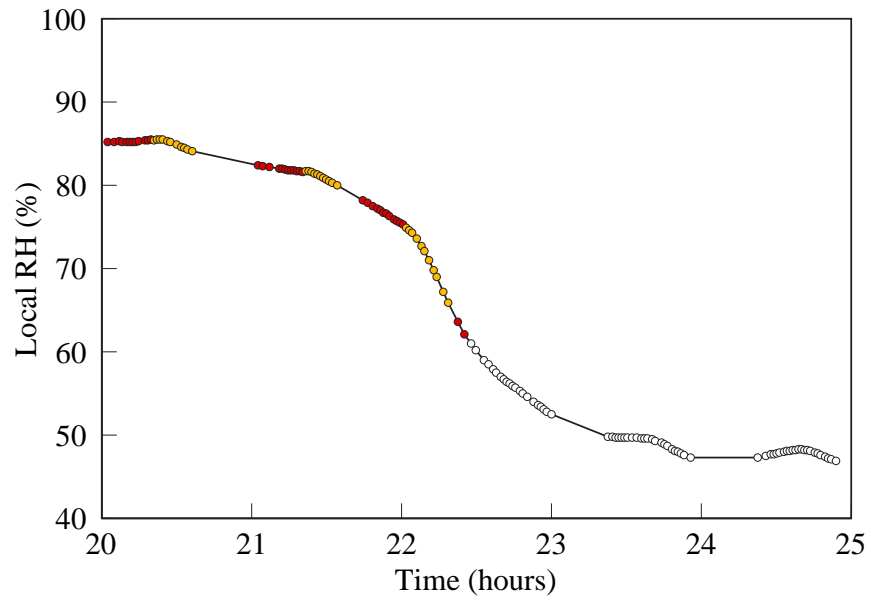


Figure 4.10: Relative Humidity versus Time: Close-up

ity due to the NaCl should be approximately 75%, and after the rapid change in dielectric readings, where it falls below 50%.

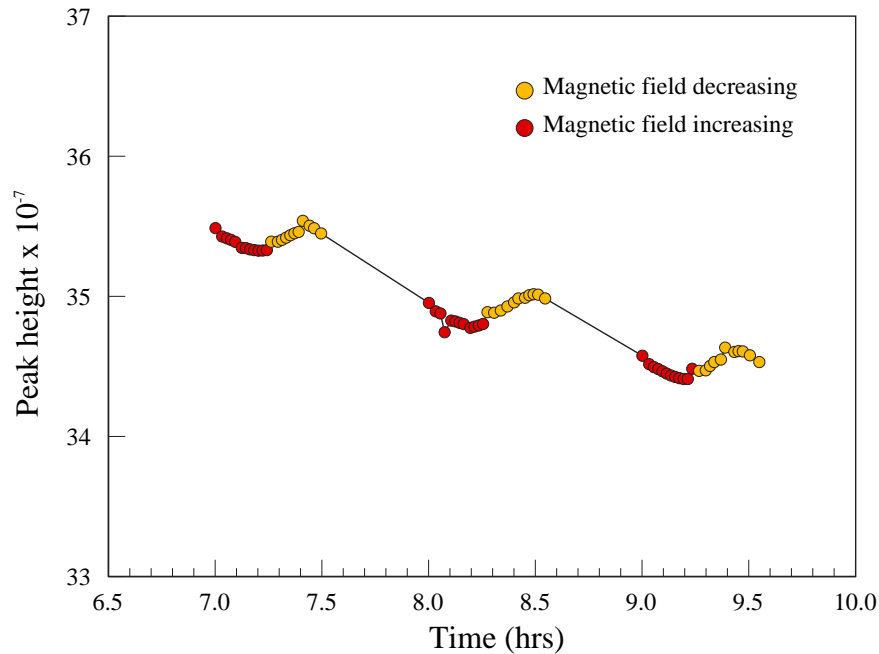


Figure 4.11: Maximum Gof versus Time: Close-up 2

In order to show the changes happening *before* the rapid change in peak height referred to above, the data between 7 and 10 hours after the start of the experiment is examined. Figure 4.11 shows a close-up of the change in peak height in this period. As can be seen, there is a gradual drift downwards in the values of the peak height. But superimposed on that drift, there seems to be some response to the changing magnetic field. This appears to show a slowing down of the downward trend when the magnetic field is increasing i.e. a tendency to increase the peak height. This increase continues even after the magnetic field starts to decrease, but then it decreases. As discussed above, this may be a delayed response to the changing magnetic field.

The frequency at which the peak occurs is slowly increasing in this period from

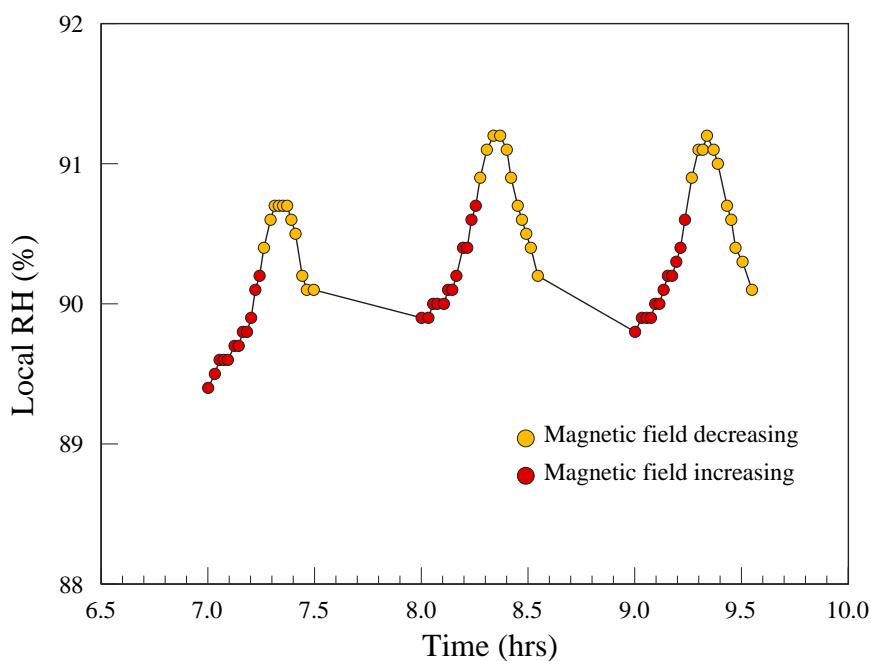


Figure 4.12: Relative Humidity versus Time: Close-up 2

approximately 800Hz to 1000Hz (See Figure 4.6). However, the frequency shows *no* response to the changing magnetic field.

Figure 4.12 shows a close-up of the change in local relative humidity for the same period. Again there seems to be some response to the changing magnetic field. The increase in the sensor response while the magnetic field is increasing continues for a short time even though the field has started to decrease. After a short time, the decrease in sensor response begins to appear. In order to discount the direct effect of the magnetic field on the relative humidity sensor itself, tests were carried out with no sample present. The sensor showed *no* response to changing magnetic field. The humidity sensor therefore seems to be reacting to the presence of the sample and the effect that the changing magnetic field is having on the sample. (See Section 4.5)

## 4.5 Interpretation of Relative Humidity Graphs

The results of the experiment described in Section 3.4.4, where the response of a sample of DNA of initial concentration 50mg/ml is examined as it evaporates in the presence of a saturated solution of sodium chloride solution between the poles of the electromagnet inside the sealed brass enclosure, are described in Section 4.4. In this section, Figure 4.7 shows the relative humidity readings during the experiment. The relative humidity readings are seen to be approximately 90% for the first 16 hours, decreasing slowly to approximately 80% over the next 5 hours, and then decreasing rapidly in less than an hour to less than 50%.

Since the humidity sensor is exposed to saturated sodium chloride solution, the relative humidity above such a solution should be 75% (Greenspan, 1977). Inside the brass enclosure however, the humidity sensor is placed very close to the evaporating DNA solution, whilst the saturated sodium chloride solution is within the attached vacuum system, and relatively distant from the sensor. During the first part of the experiment, the high humidity reading is likely to reflect the fact that the nearby DNA solution is fairly dilute, and is presumably evaporating freely. As the peak  $G_{of}$  (See Section 4.1 for explanation of this term) moves towards lower frequencies, indicating that the DNA changes to a more gel-like condition as it becomes more concentrated, the decrease in the relative humidity readings could indicate a decrease in the rate of evaporation of the DNA solution. i.e. the relative humidity sensor is reading the changing humidity in the localised environment around the DNA solution, and not the relatively static effect of the distant saturated sodium chloride solution. The saturated sodium chloride solution however has a more long-term effect on the DNA sample, since the relatively rapid transition seen in the peak  $G_{of}$  frequency is only seen when the sample is in the presence of the saturated NaCl solution. In the absence of the DNA sample, the relative humidity reading is, as would be expected, close to 75%.

Figure 4.12 shows a close-up of the relative humidity during the period from 7 to 10 hours after the start of the experiment, i.e. well before the peak Gof started moving to lower frequencies. The relative humidity readings are shown as the magnetic field surrounding the DNA is increased in stages up to its maximum and then decreased back to zero. The relative humidity reacts to the changing magnetic field by increasing as the field increases; it then continues to increase for a short while even though the field has begun to decrease. Finally, the relative humidity readings also decrease, and continue to do so until the magnetic field reaches zero. There is therefore a response in the relative humidity readings which mirrors the increase and subsequent decrease in the magnetic field, but with a consistent short delay. In the absence of the DNA sample however, the humidity sensor shows *no* response to the changing magnetic field. As the current in the electromagnet is increased, there is a small amount of localised heating in the area between the poles where the DNA sample is situated (See Section 4.6 and 4.7). The increase in temperature (of approximately 2°C) could conceivably increase the rate of evaporation of the DNA solution for a short time, thus increasing the humidity in the area of the sample. The relative humidity sensor is thus measuring the conditions in this small area around the DNA sample.

It may be concluded that the graphs of relative humidity against time shown in Figures 4.7 and 4.12 reflect only the changing environment in the immediate area close to the DNA sample. Since in the absence of DNA the humidity sensor shows *no* response to the changing magnetic field, it may also be surmised that the graphs also give information on the changes happening to the DNA solution itself.



## 4.6 Monitoring the temperature

This section shows the results of the experiment described in Section 3.4.5, and repeats the experiment whose results are described in Section 3.4.4, except that the temperature close to the sample was measured instead of the relative humidity. A new sample of DNA of initial concentration 50mg/ml on an interdigitated electrode was monitored as it evaporated in the presence of a saturated solution of sodium chloride between the poles of an electromagnet inside the sealed brass enclosure. Once every hour, the current through the electromagnet was increased and then decreased in steps, whilst at each step, a frequency sweep was performed.

Since the sample of DNA solution was different, the peak Gof values in Figures 4.13 and 4.14 are slightly different to those described in Section 4.4.

Figure 4.13 shows the peak Gof values (lower graph) and local temperature (upper graph) for a period between 5 and 7 hours after the start of the experiment; i.e. more than 10 hours before the rapid decrease in peak dielectric loss values. The lower graph shows changes in the peak Gof values which are similar to those seen in Figure 4.11 and described in Section 4.4. It is included here in order that the temperature changes seen in the upper graph may be related to the changes happening to the peak Gof. Vertical lines have been drawn on both graphs to show the beginning and end of the frequency sweeps. The keys also give an indication of when the magnetic field is increasing and decreasing and when it is off.

Figure 4.14 shows the peak Gof values (lower graph) and local temperature (upper graph) for a period between 18 and 21 hours after the start of the experiment; i.e. when the rapid decrease in peak dielectric loss values occurs for this sample. The lower graph shows changes in the peak Gof values which are similar to those seen in Figure 4.8 and described in Section 4.4. The area of interest in Figure 4.14 is

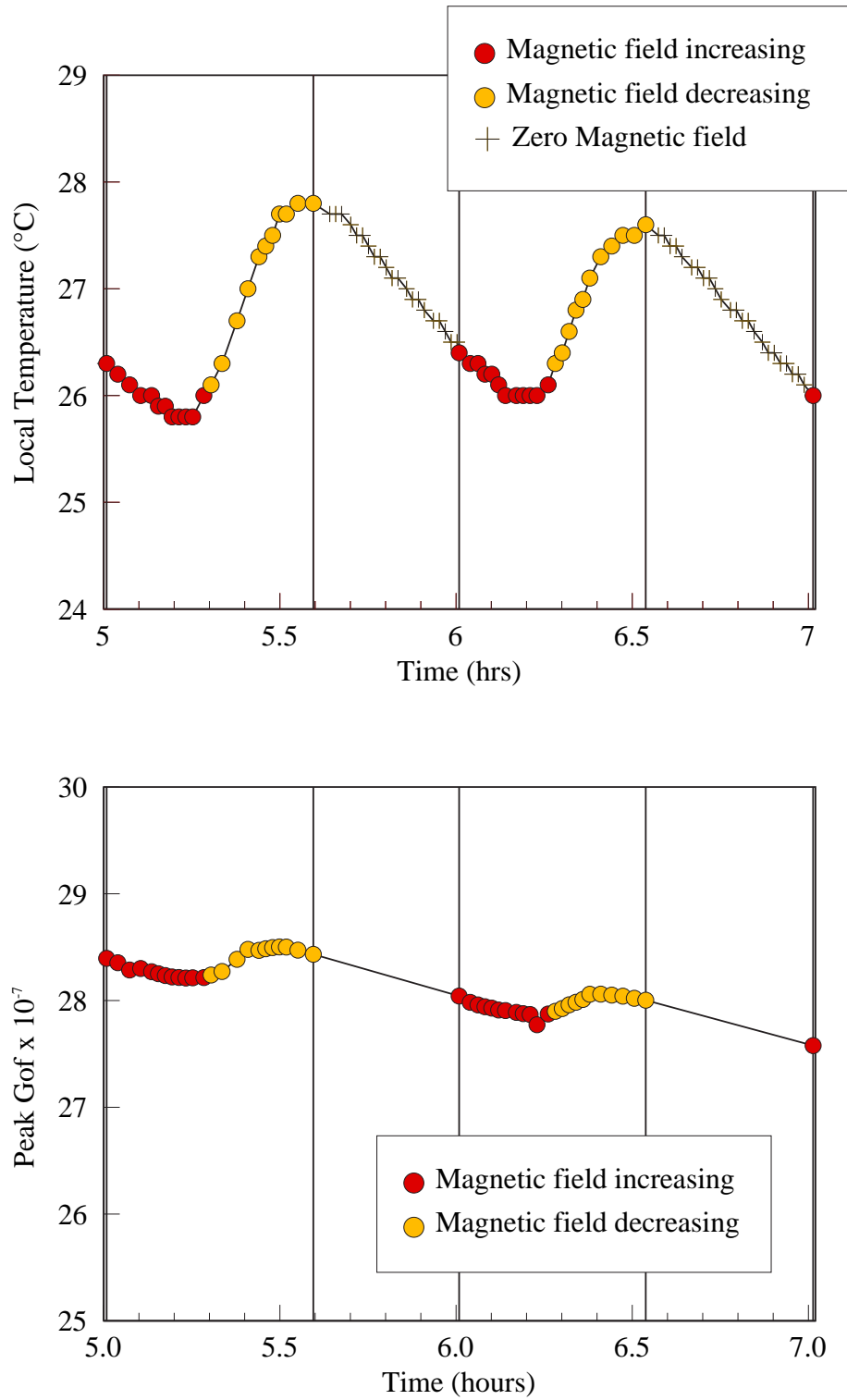


Figure 4.13: Local Temperature versus time (top) and Maximum Gof versus Time (bottom)

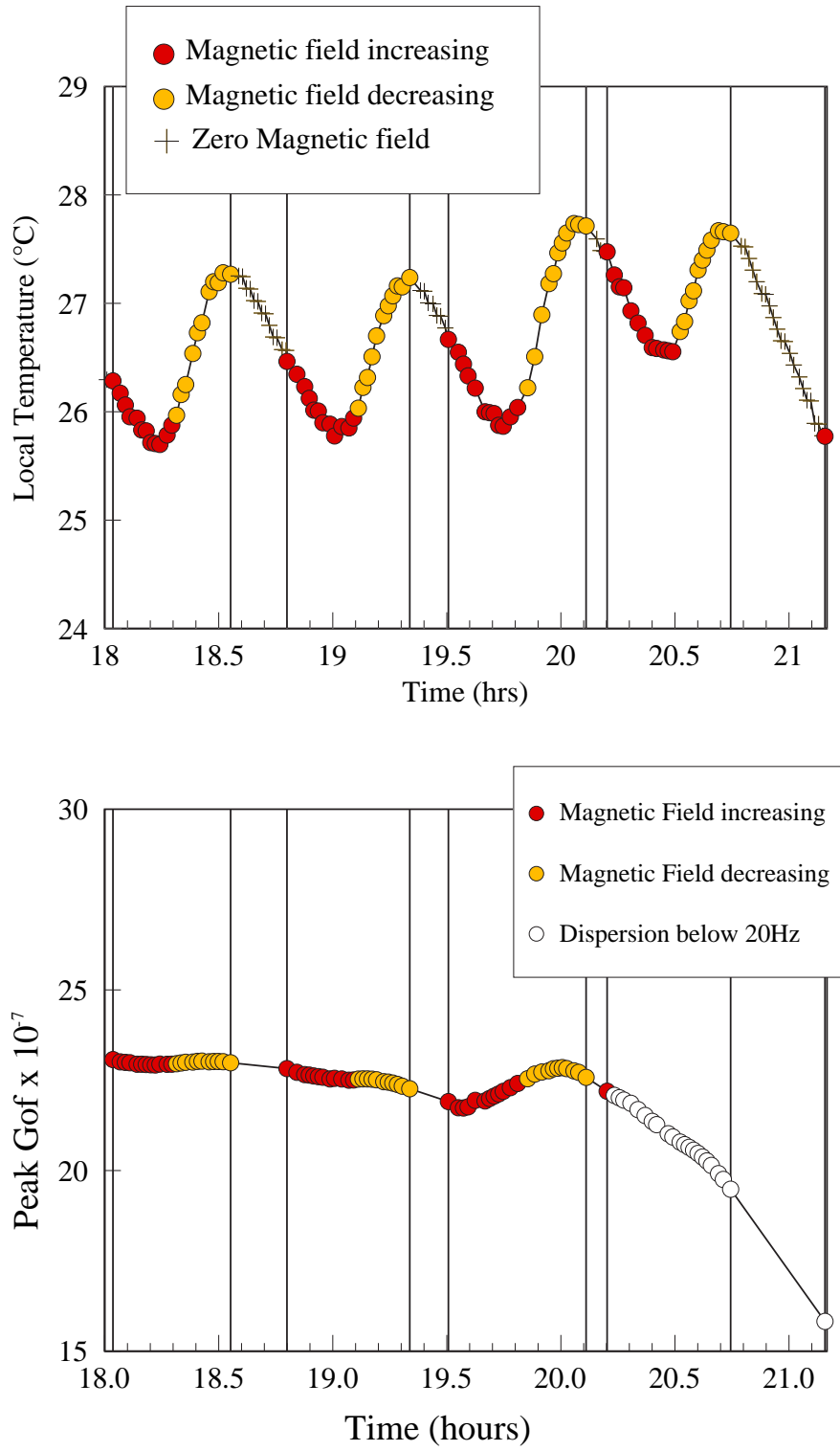


Figure 4.14: Local Temperature versus time (top) and Maximum Gof versus Time (bottom)

between approximately 19.5 and 20.1 hours, when the peak Gof value is seen to increase and then decrease as the magnetic field also increases and decreases.

## 4.7 Significance of Peak Gof changes

In Section 4.6 the results of the experiment described in Section 3.4.5 are reported. In this experiment the dielectric properties of a DNA solution and the local temperature (rather than the relative humidity) are measured as the DNA evaporates in the presence of saturated sodium chloride solution. The changes in peak Gof are similar to those reported in Section 4.4

Figure 4.13 shows the peak Gof values (lower graph) and local temperature (upper graph) for the period between 5 and 7 hours after the start of the experiment. The time scales of both graphs are identical and vertical lines have been included to indicate the start of the increase in the magnetic field, and the eventual return of the magnetic field to zero. The keys accompanying the graphs show when the magnetic field is increasing, when it is decreasing and when it is zero. Figure 4.14 shows similar graphs of peak Gof and local temperature for the period between 18.0 and 21.5 hours after the start of the experiment, i.e. in the period when peak Gof values decrease rapidly, and the corresponding frequency of that peak value moves to low frequency. (See Figure 4.11)

In the upper graphs in both Figure 4.13 and 4.14 it can be seen that when the magnetic field is off, the temperature decreases. The magnetic field then starts to increase, but it takes several minutes for the temperature to react, and to increase as well. When the magnetic field starts to decrease, its value is still close to its maximum, and the temperature continues to increase. As the magnetic field approaches zero (at the end of its decrease phase), the temperature increase starts to slow, and

finally decreases as the magnetic field is switched off.

This is consistent with the current passing through the electromagnet heating the coils, and the heat being transmitted from the coils to the part of the brass enclosure between the poles. When the magnetic field is at high values, the current is also high, and the heating effect is also greater. But it takes time for the heat developed in the coils to travel to the area in which the temperature sensor is placed. Similarly, when the magnetic field is decreasing towards zero, and the heating effect is diminished in the coils, the heat near the temperature sensor takes time to dissipate.

The main area of interest is in Figure 4.14, between approximately 19.5 and 20.1 hours, when the peak Gof value is seen to increase and then decrease at the same approximate time as the magnetic field also increases and decreases. The issue to be considered is whether the reversible change in peak Gof was caused by the corresponding change in magnetic field, or whether the change in temperature alone was responsible. In this time period, the temperature seems to increase and then decrease in a similar way to the previous time period (i.e. between 5 and 7 hours) The maximum temperature is slightly higher than before, though this happens towards the end of the period of interest. The next minimum of temperature is slightly higher than normal, probably because the computer has detected that the peak dielectric loss value has started to decrease, and has initiated the next frequency sweep sooner than would be expected.

In order to assess whether the change in temperature alone could have caused the reversible change in peak Gof, it is instructive to compare the relative changes in temperature and peak Gof in the period of interest between 19.5 and 20.1 hours, with the corresponding changes between 18.0 and 18.6 hours. The graphs in Figure 4.14 have been redrawn at slightly larger scales and are shown in Figure 4.15. It will be noted that the magnitudes of the changes in temperature and peak Gof are shown on the graphs as  $\Delta T$  and  $\Delta Gof$ , with the suffix 1 for the period between 18.0 and

18.6 hours, and the suffix 2 for the period between 19.5 and 20.1 hours. It can be seen that for the earlier period a change in peak Gof of  $0.107 \times 10^{-7}$  is accompanied by a change in temperature of  $1.55^\circ\text{C}$ , whilst for the period of interest a change in peak Gof of  $1.118 \times 10^{-7}$  is accompanied by a temperature change of  $1.85^\circ\text{C}$ . If the change in peak Gof for the earlier period were to be adjusted for the greater change in temperature experienced between 19.5 and 20.1 hours (i.e.  $1.85^\circ\text{C}$  rather than  $1.55^\circ\text{C}$ ), then the expected response for the magnetic field increasing and then decreasing is shown in Figure 4.16. On the same graph is shown the *actual* response, which can be seen to be considerably larger.

It may therefore be concluded that change in temperature alone is not likely to be responsible for the change in peak Gof. It is to be noted that the concentration of the DNA on the slide at the end of the experiment was approximately 170 mg/ml (See Section 4.3), which is within the concentration region normally considered to be cholesteric liquid crystalline. Previous workers have shown that cholesteric DNA shows reversible changes with changing magnetic field (See Section 1.5). It could therefore be surmised that this experiment has detected the presence of cholesteric DNA, and that reversible changes in its dielectric properties accompanied, and were caused by, corresponding changes in magnetic field when the magnetic field was perpendicular to the electric field.

Reversible changes in dielectric measurements seen at times prior to 19 hours after the beginning of these investigation, could be accounted for by changes in temperature which accompanied changes in magnetic field intensity. Since the concentration of the DNA solution would be expected to be lower at those times, it can be concluded that low concentration DNA shows no reversible response to magnetic fields when magnetic field is applied perpendicular to the electric field.

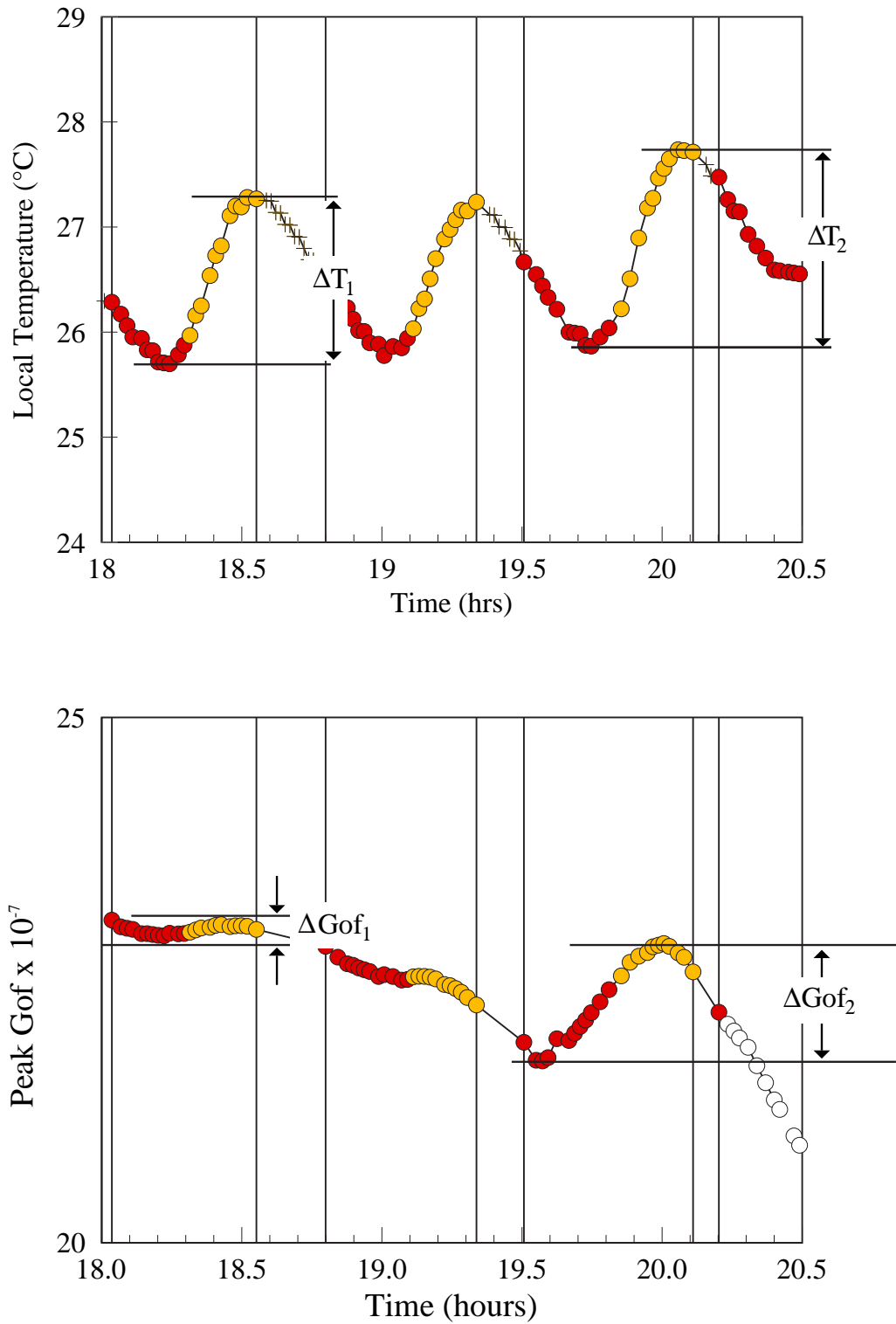
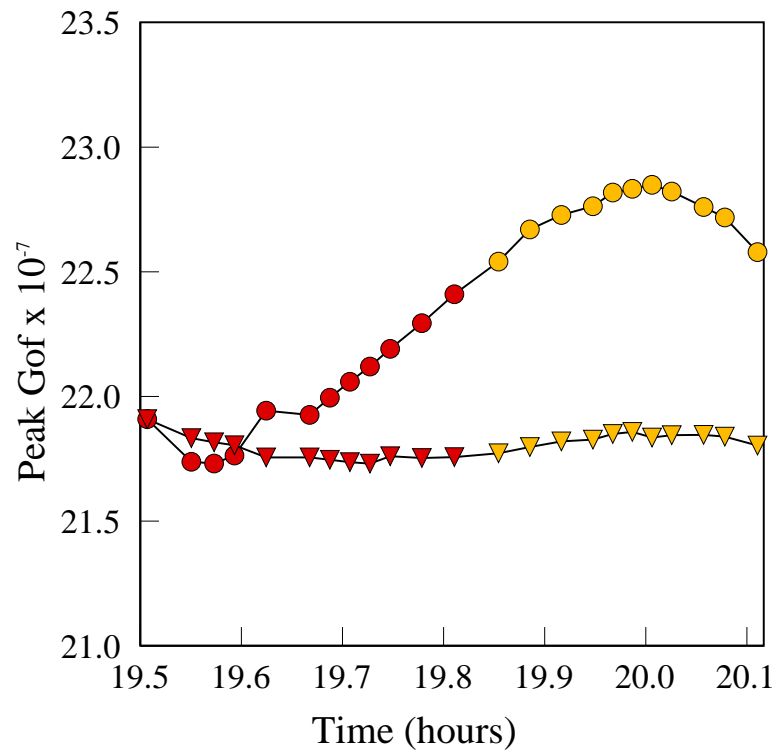


Figure 4.15: Local Temperature versus time (top) and Maximum Gof versus Time (bottom)



- Magnetic field increasing - true response
- Magnetic field decreasing - true response
- ▼ Magnetic field increasing - expected response
- ▼ Magnetic field decreasing - expected response

Figure 4.16: True and Expected responses to Magnetic Field



# Chapter 5

## Effect of low magnetic fields on DNA solutions of lower concentrations using planar electrodes - Results

### 5.1 Introduction

This chapter examines the results of the experiments described in Sections 3.5.2 to 3.5.9; i.e. experiments which examine the effect of magnetic fields on DNA of lower concentration (25 – 100 mg/ml) using planar electrodes where the magnetic field is applied parallel to the electric field.

In the experiments in this section, planar electrodes were used as shown in Figure 3.18). A cell was constructed by separating the electrodes by an O-ring with a single slot in one side. The DNA solution (D6898 Type XIV) was injected into the

cell through the slot in the O-ring, and the opening closed using the point of the syringe. The electrode cell was inserted into the brass apparatus described previously, and the poles adjusted until they were just in contact with the cell.

Since a planar electrode was used, all the quantities needed to calculate dielectric loss are available, and rather than Gof and dGof as in the previous chapter, all the text and Figures will now refer to dielectric loss and dLoss.

## 5.2 Preliminary study

The preliminary study was carried out to determine how the dielectric loss of a solution of DNA (D6898) of concentration 50mg/ml was changed when the magnetic field surrounding the solution was first increased and then decreased. In this investigation, the dielectric loss was measured at two different frequencies (5000Hz and 500Hz)

Figure 5.1 shows the percentage change in the dielectric loss value as the current through the electromagnet is varied for a frequency of 5000Hz, and Figure 5.2 shows the corresponding change for a frequency of 500Hz. The percentage loss change is shown by the red dots - its value is given by the scale on the left of the graph. The current through the electromagnet is shown by the green dots, and its value is given by the scale on the right of the graph; an increased current indicates obviously an increased magnetic field.

It is apparent that the Loss value at 5000Hz increases as the magnetic field increases, and decreases as the field decreases. For the Loss at 500Hz the opposite is true, i.e. the Loss *decreases* as the magnetic field increases, and *increases* again as the field decreases. It should also be noted that there is a gradual trend upwards in both

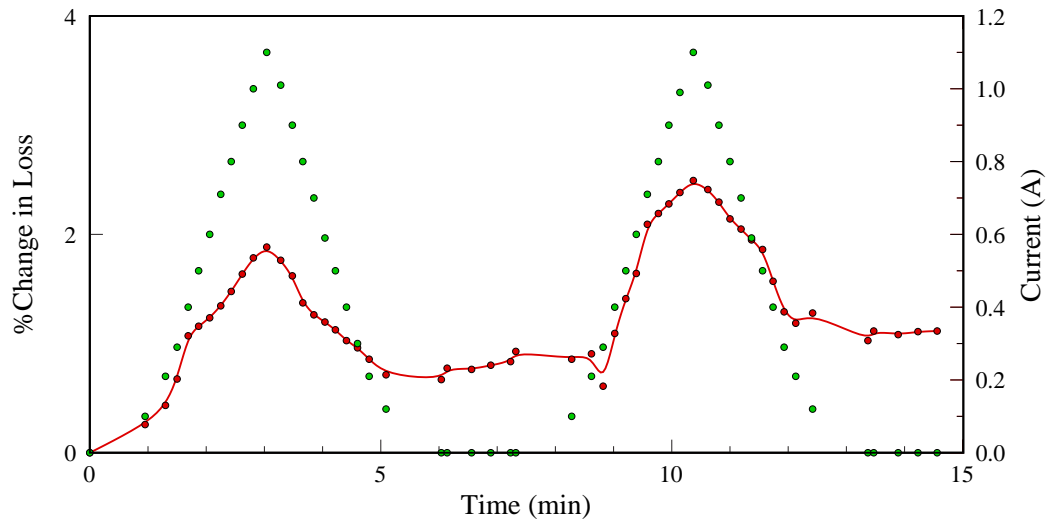


Figure 5.1: Percentage change in Loss as electromagnet current is varied.

- =Percentage change in Dielectric Loss at 5kHz (Left scale);
- =Current through Electromagnet in Amp. (Right scale)

sets of readings. This was greatest when the sample had just been placed in the cell. Tests showed that a period of 10 to 12 hours was required for the sample to stabilize sufficiently for the effect to become negligible.

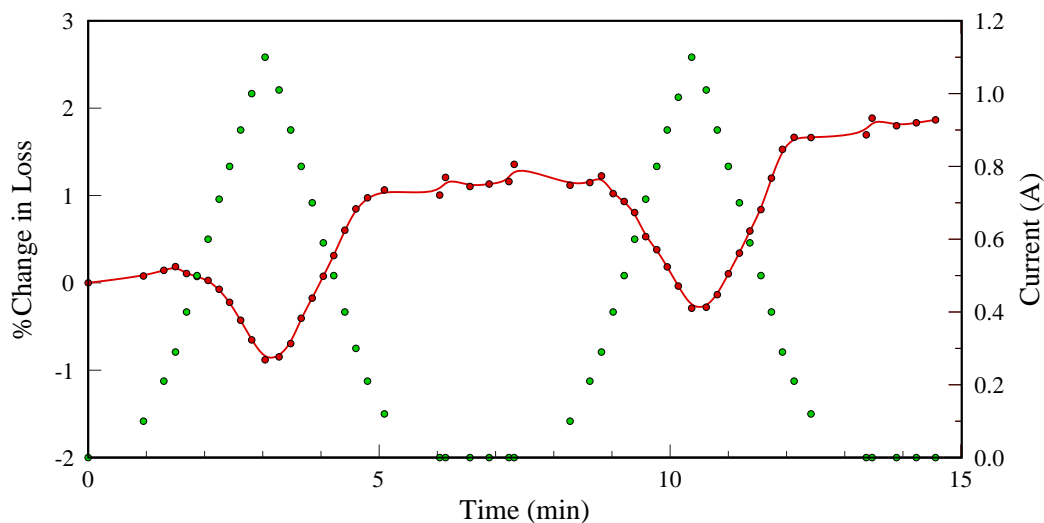


Figure 5.2: Percentage change in Loss as electromagnet current is varied.

- =Percentage change in Dielectric Loss at 500Hz (Left scale);
- =Current through Electromagnet in Amp. (Right scale)

### 5.3 Full experiment

The procedure described in Section 3.5.3 determined the effect of varying the magnetic field on the dielectric loss values at 42 frequencies. It was carried out on a solution of DNA (D6898) with a concentration of 50mg/ml.

As described in Section 2.5, it is more useful to show the *difference* between the dielectric loss values before and after applying the magnetic field, than the actual Loss values themselves, since the change is almost impossible to see in the latter. The plot of this difference (dLoss) against LOG Frequency will be referred to as the *Difference Signal* (DS). When repeated for every target current, the graphs shown in Figures 5.3 and 5.4 are the result.

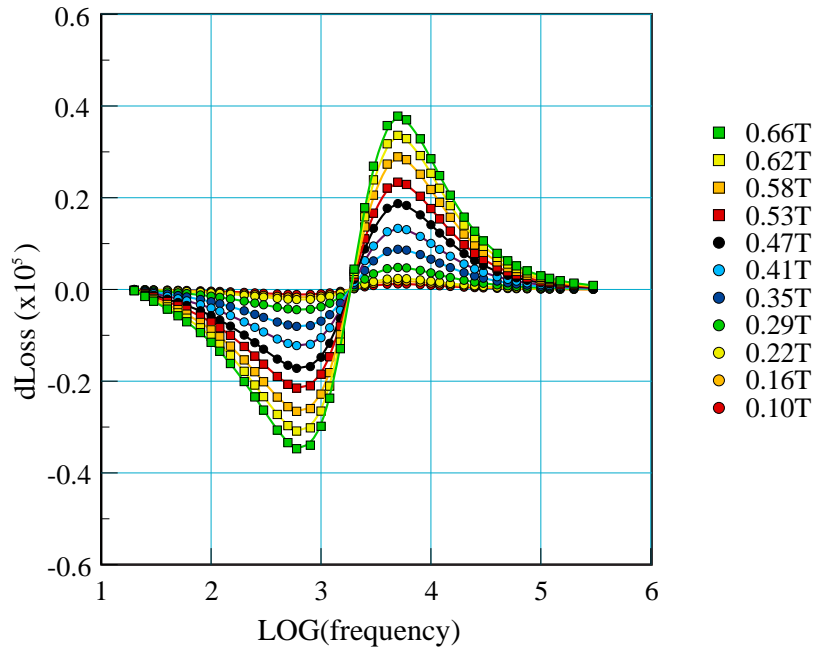


Figure 5.3: Change in Loss due to Magnetic field

Figure 5.3 shows the Difference Signal as the magnetic field is increased from to 0.66 Tesla. Figure 5.4 shows the difference signal as the target current is decreased from 1.1A to 0.1A. It would be difficult to show both sets of plots on the same graph, since they would obviously overlap. Note that a key by the side of the graphs shows the values of magnetic field corresponding to each target current value. These were obtained from the calibration of the electromagnet as seen in Figure 3.14. Note that the calibration shown in Figure 3.15, with the current decreasing is not used here, since the current is always increased from zero.

Each plot shows that at low frequencies,  $dLoss$  is negative, indicating that the dielectric loss values at these frequencies *decrease* as the magnetic field is increased. This negative Difference Signal reaches a minimum value of  $-0.35 \times 10^5$  at 600Hz for

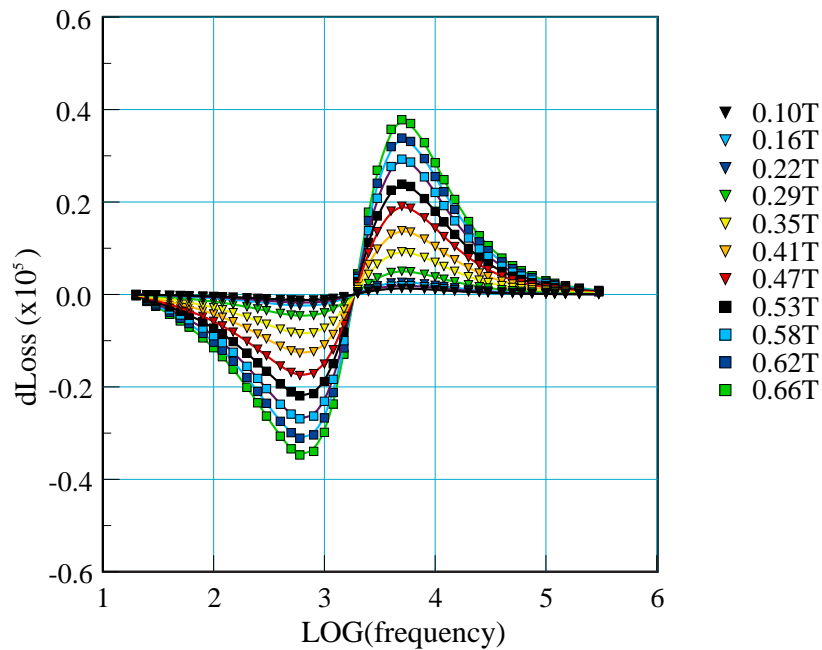


Figure 5.4: Change in Loss due to Magnetic field

maximum magnetic field. At high frequencies,  $dLoss$  is positive, showing that the dielectric loss values *increase* as the magnetic field increases. The positive Difference Signal reaches a maximum of  $0.38 \times 10^5$  at 5000Hz for maximum magnetic field. At a frequency of between 1500Hz and 2000Hz, the Difference Signal is close to zero, indicating that the magnetic field has no effect at this frequency. One interesting aspect is that the frequency of this "zero point" seems to be equal for all target currents.

Figure 5.5 shows  $dLoss$  as the target current/magnetic field increases and then decreases, but only for frequencies of 5000Hz and 600Hz. The x-axis in this case is simply the file-number, indicating the order in which the values were obtained. The change in  $dLoss$  for these frequencies plotted against the magnitude of the magnetic

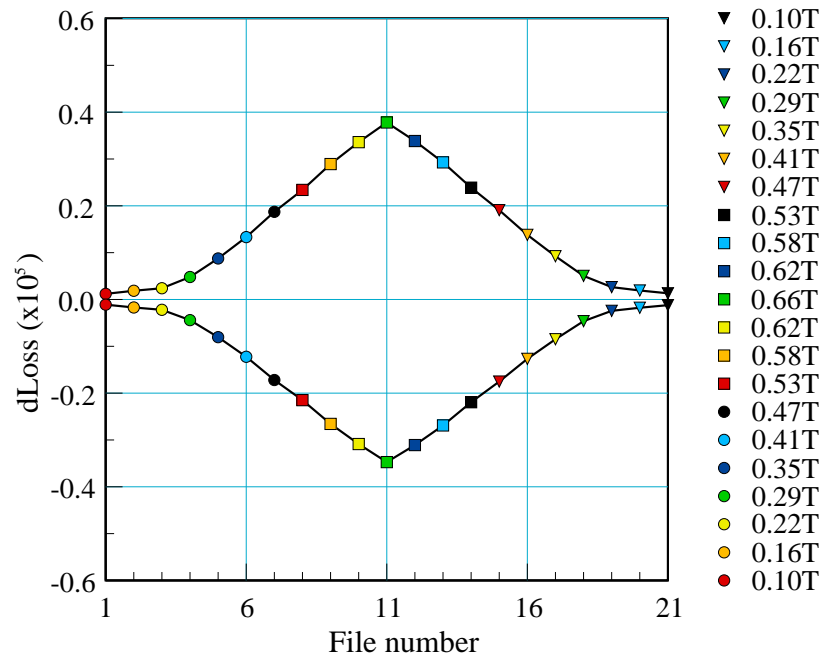


Figure 5.5: Change in Loss for 5000Hz (upper) and 600Hz (lower)

field can be seen in Figure 5.6 for 5000Hz, and Figure 5.7 for 600Hz. The dLoss values as the magnetic field is increasing and those when the field is decreasing are equal within the limits of experimental error.

For each current/magnetic field used in these experiments, three frequency scans were carried out - the first at zero current, the second at the selected current, and the third at zero current again. Because the dielectric loss readings took 10 to 12 hours to stabilize, during the first complete cycle of the full experiment, there was some indication that the drift in dielectric loss values shown in Section 5.2 was still present. The third scan was therefore slightly different from the first scan. For the remaining cycles of the experiment, the third scan was, within the limits of experimental error, indistinguishable from the first scan, indicating that the changes

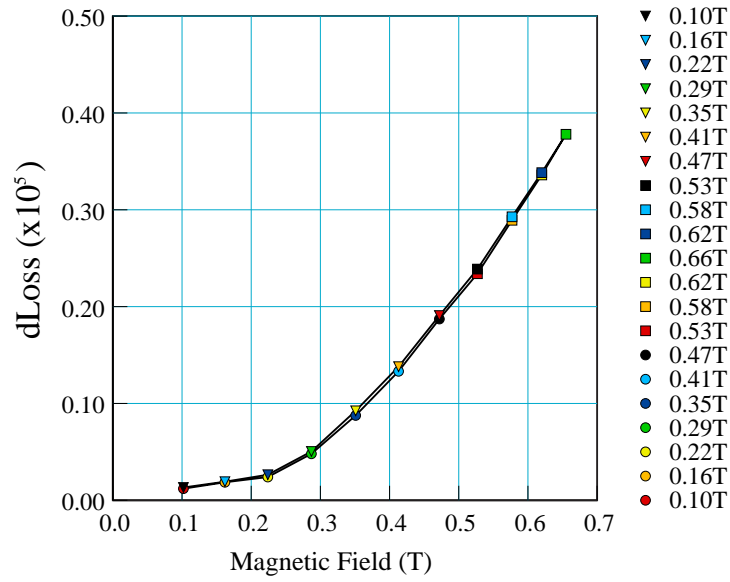


Figure 5.6: Change in Loss vs. Magnetic field at 5000Hz

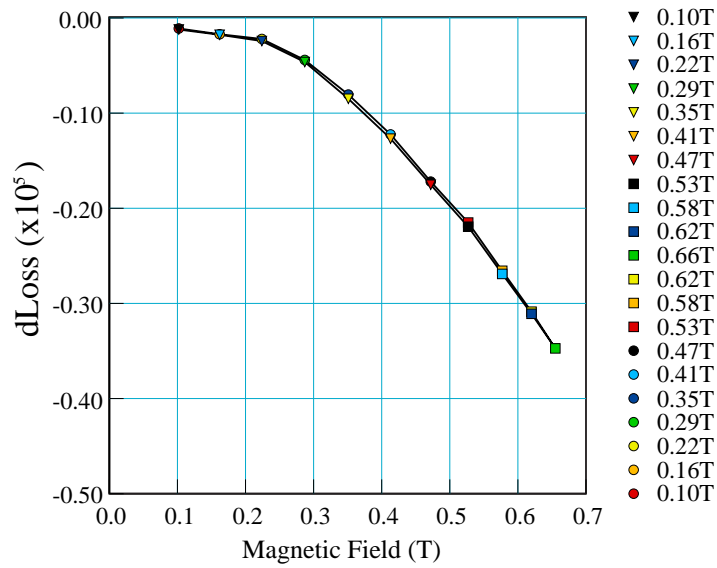


Figure 5.7: Change in Loss vs. Magnetic field at 600Hz



caused by the magnetic field were reversible in the time period used. Because of this, the results from the first complete cycle were discarded. The results above (and the results of all the experiments following) show the Difference Signal between the first and second scans. The Difference Signal between the third and second scans will of course be almost exactly the same.

## 5.4 Control Experiments

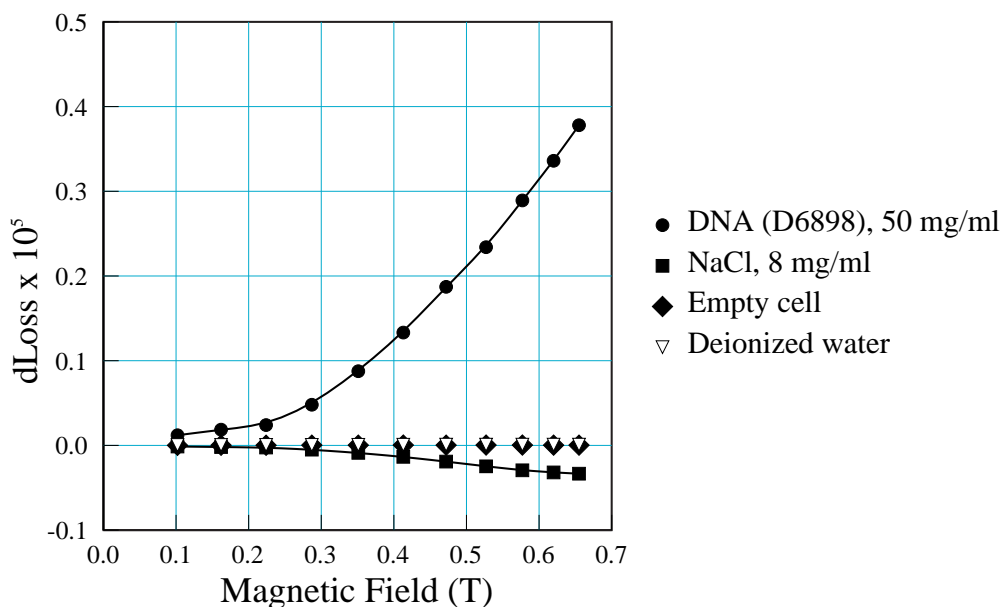


Figure 5.8: Change in Loss vs. Magnetic field at 5000Hz

The full experiment was repeated with the connections to the Wayne-Kerr component analyser reversed. As expected, no change was seen in the results, since the Wayne-Kerr applies an alternating voltage to the sample.

The results of the other control experiments are shown in Figures 5.8 and 5.9, where dLoss at 5000Hz and 600Hz respectively is plotted against the magnitude of the magnetic field for an empty cell, deionized water, Sodium Chloride solution

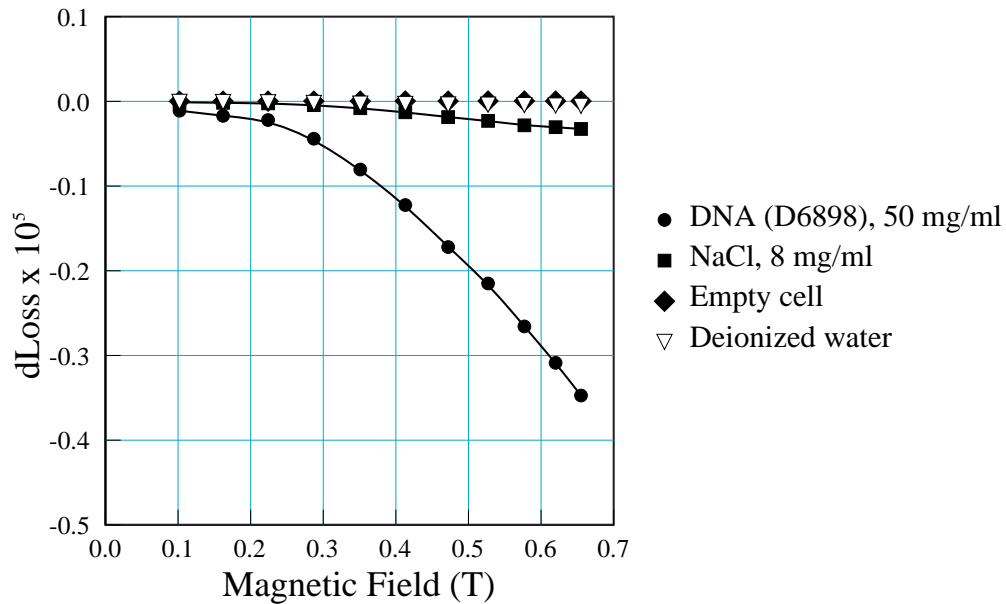


Figure 5.9: Change in Loss vs. Magnetic field at 600Hz

(8mg/ml), and compared with the response of DNA solution (D6898, 50mg/ml) from Section 5.3.

As can be seen in the Figures, the responses of the empty cell and deionized water to magnetic field are negligible. There is some response from the Sodium Chloride solution, but it is much smaller than that from the DNA solution, and for the higher frequency plot, the direction of the response is reversed. It may be concluded therefore that neither the construction of the cell, the presence of water nor sodium or chloride ions on their own, are responsible for the magnitude of the response to magnetic field seen in Section 5.3. The only remaining constituent is the presence of DNA in solution.

When the experiment was repeated with the electrical connections to the upper coil of the electromagnet reversed i.e. with negligible magnetic field in the area of the cell, no response was detected i.e. the difference between the dielectric loss spectrum

with and without current in the electromagnet was negligible. This showed that it was the change in magnetic field rather than any increase in local temperature which had caused the Difference Signal.

## 5.5 Varying the concentration of DNA

The experiment was repeated for three other concentrations of DNA from 30mg/ml to 96mg/ml, and the results combined with those for 50mg/ml. The Difference Signal in each case was of exactly the same form as seen in Figures 5.3 and 5.4, but with the minimum and maximum of the Difference Signal at different frequencies and of varying magnitudes. The variation of the magnitude of the positive maximum peak with concentration can be seen in Figure 5.10, and the variation of its frequency in Figure 5.11. As the concentration of the DNA is increased, the magnitude of the maximum positive signal increases, as does its frequency.

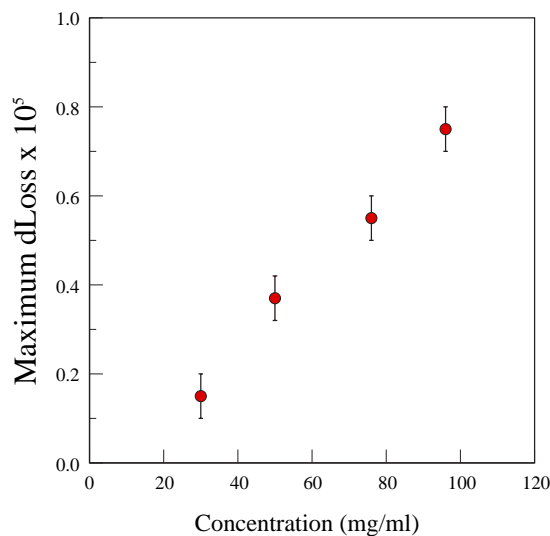


Figure 5.10: DNA : Magnitude of Maximum of DS vs. Concentration

Similarly with the minimum of the Difference Signal - the variation of its magnitude can be seen in Figure 5.12, and the variation of its frequency in Figure 5.13. As with the maximum peak, both the magnitude and frequency of the minimum increase with increase in DNA concentration.

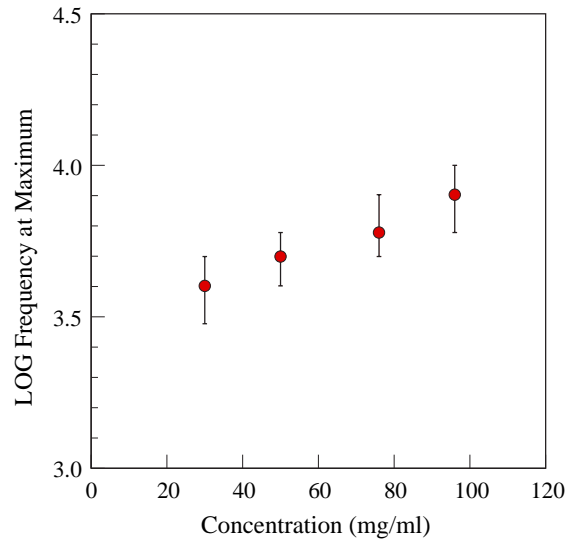


Figure 5.11: DNA : Frequency of Maximum of DS vs. Concentration

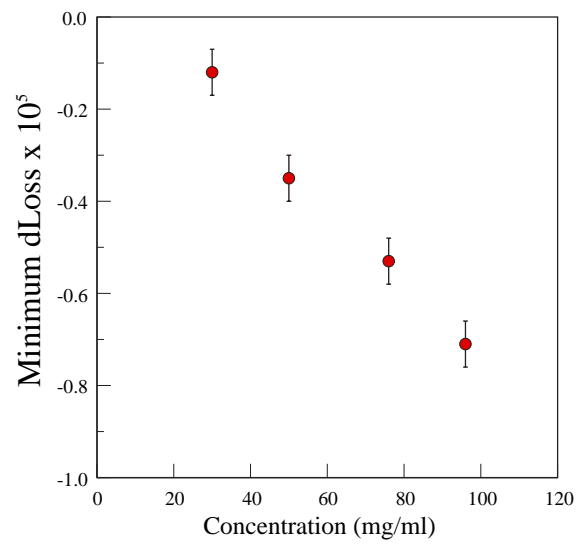


Figure 5.12: DNA : Magnitude of Minimum of Difference Signal vs. Concentration

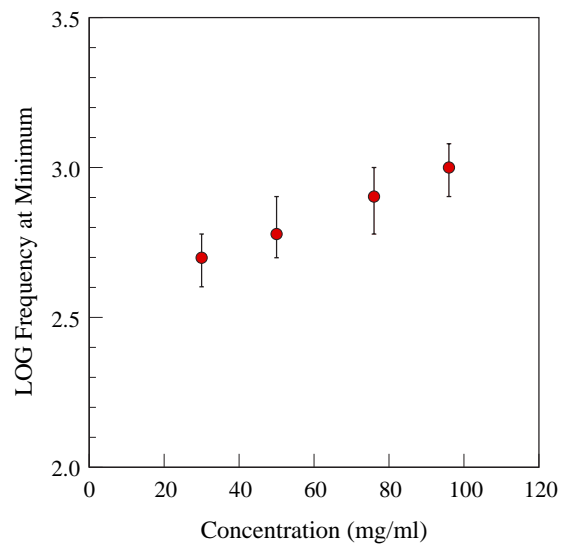


Figure 5.13: DNA : Frequency of Minimum of Difference Signal vs. Concentration

## 5.6 Analysis of data using Matlab

### 5.6.1 Analysis of Dielectric Loss

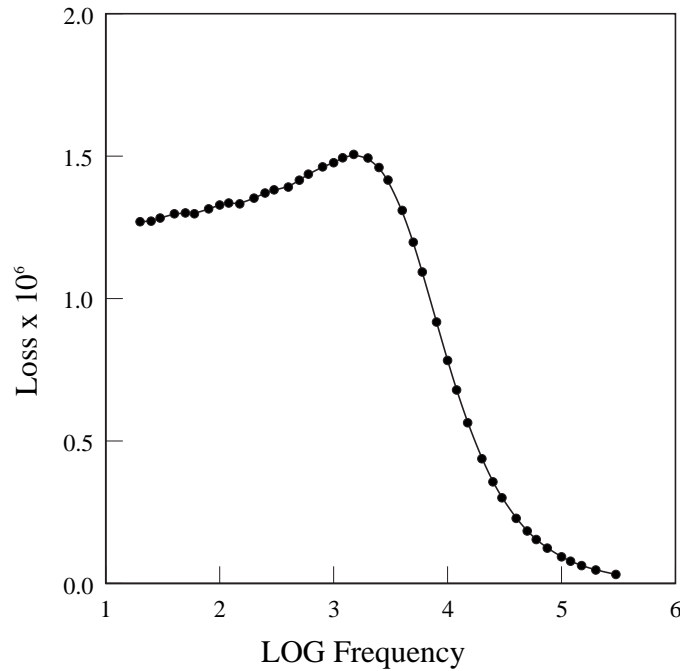


Figure 5.14: Loss vs. LOG Frequency for DNA (50mg/ml)

Figure 5.14 shows the Dielectric Loss against LOG Frequency for the DNA solution described in Section 5.3, i.e. DNA D6898 at a concentration of 50mg/ml, with no magnetic field. Attempts were made to analyse this plot with a Matlab program using a Genetic Algorithm toolbox (See Appendix J and Section 2.6). The intention was to determine the parameters of the dispersions present in the Dielectric Loss data obtained without magnetic field, and then to repeat the analysis on equivalent data after applying the maximum magnetic field. In this way, it was hoped to be able to detect the properties of the dispersion(s) affected by the field. The parameters used were: Number of games = 50, Population = 500<sup>2</sup>, Generations = 400000. It

was attempted to fit the data to one, two and three dispersions, both with and without a contribution from D.C. conductivity.

The results were inconclusive, with a large variation in the values of the variables characterising the dispersions, especially when the minimum and maximum frequencies for every dispersion in the program reflected the breadth of the frequencies in the data. When attempts were made to confine each dispersion to a more restricted range of frequencies, the results were highly dependent on the values chosen for those limits. This difficulty was probably because the dielectric loss data was quite noisy, especially at low frequencies. It was eventually decided that no useful results could be found using this method.

### 5.6.2 Analysis of Difference Signal

An alternative was to analyse the Difference Signal, as shown in Figure 5.15, which is the *maximum* response as referred to previously in Figure 5.3, i.e. the difference between the dielectric loss with zero magnetic field and that with maximum magnetic field (0.66T) for a 50mg/ml solution of DNA (D6898).

A method was developed to analyse the Difference Signal using the Matlab Genetic Algorithm Toolbox together with the programs in Appendix K. The analysis was based on the proposition that the form of the Difference Signal indicated that *one* dispersion in the Dielectric Loss spectrum was affected by the magnetic field, and that some or all the parameters defining that dispersion would therefore be changed by the magnetic field. This proposition is consistent with the theoretical difference signals shown in Section 2.5. The general shape of the Difference Signal found in these results is indicative of an increase in the frequency of the dispersion with increased magnetic field, not precluding simultaneous changes in the other parameters. Changes in two or more dispersions would have given more complicated



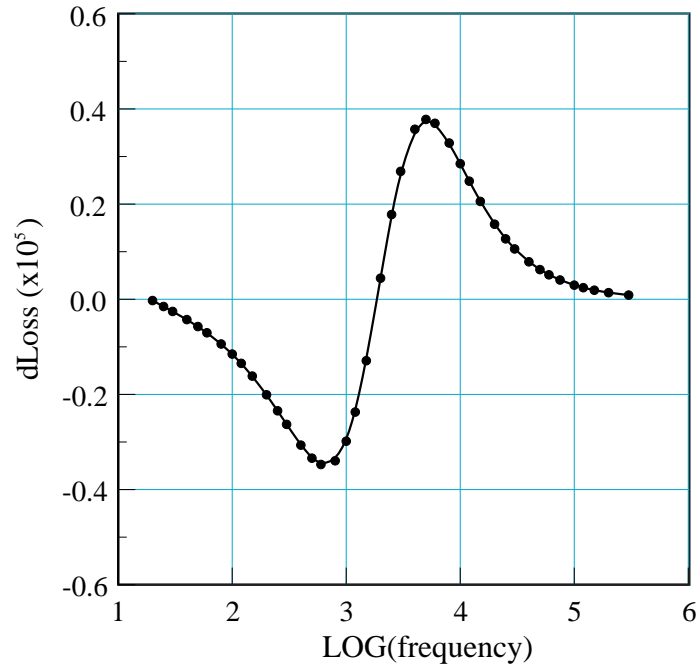


Figure 5.15: Difference Signal for DNA (50mg/ml)

difference signals.

In this case the results obtained from the program were the eight parameters defining the dispersion before and after applying the magnetic field, with the suffix "1" denoting the parameter *before* applying the field, and the suffix "2" denoting the parameters *after* applying the field. The results of the analysis were:

For the dielectric decrement:  $d\varepsilon'_1 = 5.70 \times 10^5 (\pm 0.60 \times 10^5)$ ,  $d\varepsilon'_2 = 5.66 \times 10^5 (\pm 0.60 \times 10^5)$ .

Although the magnitude of the decrements obtained from the 50 games is seen to vary considerably by approximately 10%, the ratio  $d\varepsilon'_2 : d\varepsilon'_1$  was constant at  $0.993 (\pm 0.003)$ .

For the frequency of the dispersion:  $f_1 = 1860\text{Hz} (\pm 23\text{Hz})$ ,  $f_2 = 2563\text{Hz} (\pm 25\text{Hz})$ .

The mean frequency of the dispersion was seen to increase by a factor of approximately 1.38.

For the spreading parameter:  $h_1 = 0.0900(\pm 0.0022)$ ,  $h_2 = 0.0600(\pm 0.0022)$ . In this case,  $h$  was reduced to 0.67 of its original value.

For the d.c. conductivity:  $\sigma_1 = 3.28 \times 10^{-9}(\pm 1.28 \times 10^{-9})$ ,  $\sigma_2 = 3.27 \times 10^{-6}(\pm 3.06 \times 10^{-6})$ . In this case, the mean d.c. conductivity increased by a factor of approximately 1000, although there was considerable variability in the actual magnitudes found.

### 5.6.3 Analysis of Change of DS with magnetic field

It was decided to extend the Genetic Algorithm analysis of the Difference Signal to those found with values of magnetic field lower than the maximum. As can be seen in Figure 5.3 and in Figure 5.5, the magnitude of the Difference Signals found for currents of 0.4A and lower is relatively small. It was therefore decided to analyse the signals produced by the magnetic fields generated by the seven currents between 0.5A and 1.1A, each of which is significantly different from the previous signal.

Figure 5.16 shows the change in dielectric decrement for the difference signals referred to above. As can be seen, the mean of  $d\varepsilon'_1$  is fairly constant, as would be expected, since it represents the decrement before applying the field. The magnitude of  $d\varepsilon'_2$  is very close in value to  $d\varepsilon'_1$ , and it is difficult to see whether there is any pattern in their relative magnitudes. Examination of the results of the Genetic Algorithm analysis shows however that in every game  $d\varepsilon'_1$  is always slightly greater than  $d\varepsilon'_2$ .

Figure 5.17 shows the frequencies obtained from the Genetic Algorithm analysis of the Difference Signals for increasing magnetic field. The results for  $f_1$ , the frequency

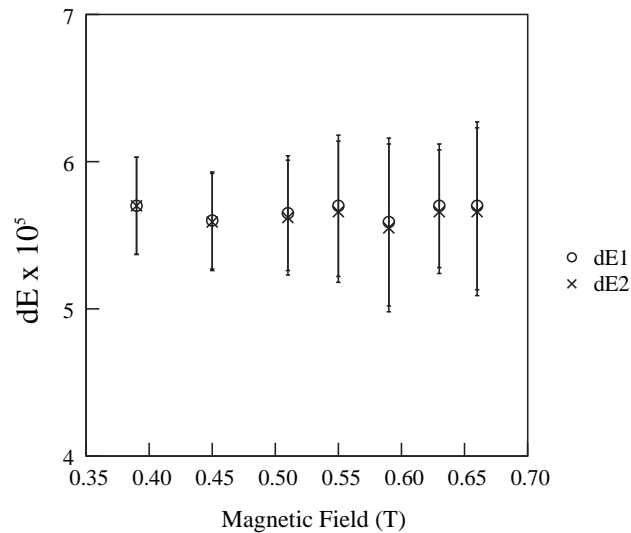


Figure 5.16: Dielectric decrement vs. magnetic field for DNA (50mg/ml)

of the dispersion before application of the magnetic field, are as would be expected, fairly constant. The increase in  $f_2$ , the frequency of the dispersion *after* applying the magnetic field, shows that as the magnetic field is increased, the dispersion moves to higher frequencies.

Figure 5.18 shows the spreading parameters obtained from the Genetic Algorithm analysis of the Difference Signals for increasing magnetic field. As would be expected, the results of the analysis show that  $h_1$ , the spreading parameter in the absence of magnetic field, is fairly constant. The spreading parameter *after* application of the magnetic field  $h_2$ , decreases as the magnetic field increases, indicating that the magnetic field causes the dispersion to have a narrower spread of relaxation frequencies.

Figure 5.19 shows the d.c. conductivity results obtained from the Genetic Algorithm analysis. The d.c. conductivity values in the absence of magnetic field  $\sigma_1$  are, as

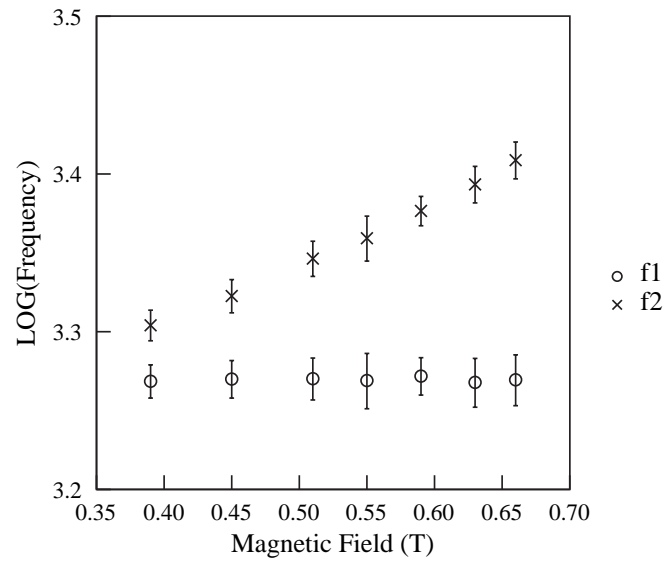


Figure 5.17: LOG Dispersion frequency vs. magnetic field for DNA (50mg/ml)

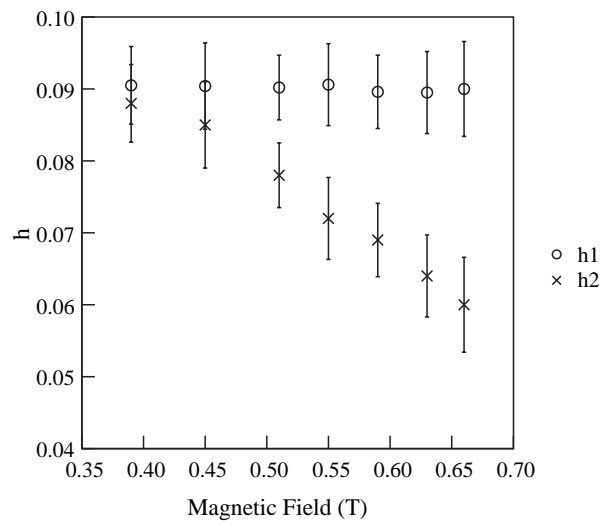


Figure 5.18: Spreading parameter vs. magnetic field for DNA (50mg/ml)

expected, fairly constant. The change in the magnitude of  $\sigma_2$  is so great that a LOG scale has to be used. Increase in the magnetic field causes an increase in the d.c. conductivity even though, as can be seen, there is considerable variation in its magnitude.

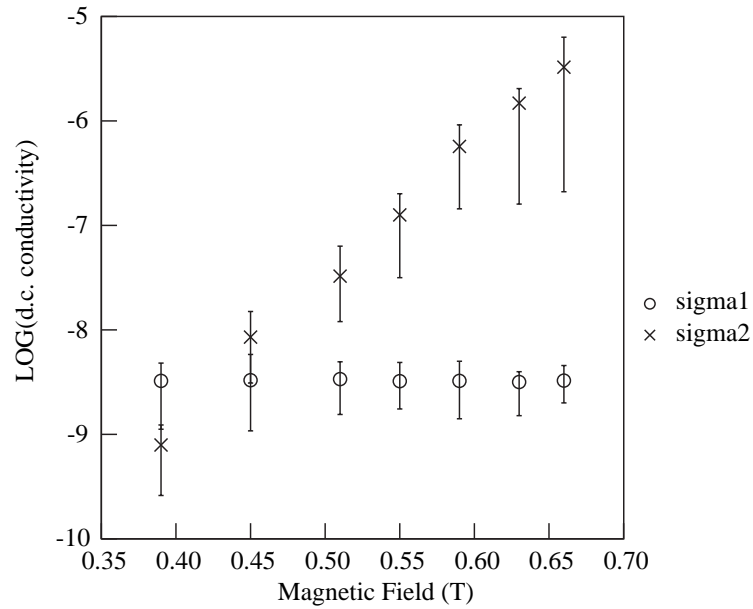
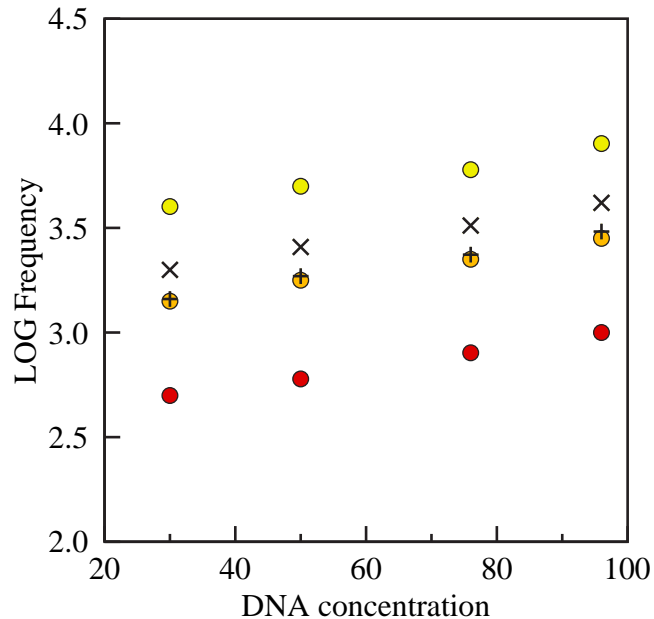


Figure 5.19: d.c. conductivity vs. magnetic field for DNA (50mg/ml)

### 5.6.4 Analysis of change in DS with concentration

Genetic Algorithm analysis was also carried out on the Difference Signal at maximum magnetic field for four concentrations of DNA, i.e. on the results in Section 5.5.



- Frequencies from Difference Signal (DS)
- f\_min - Frequency at which DS is at its minimum value
  - f\_zero - Frequency where DS is zero
  - f\_max - Frequency at which DS is at its maximum value
- Results from Genetic Algorithm (GA) Analysis of DS
- + f1 - Frequency of dispersion with zero magnetic field
  - × f2 - Frequency of dispersion with maximum magnetic field

Figure 5.20: LOG Frequency vs. concentration for DNA

Figure 5.20 shows the frequencies obtained from the Genetic Algorithm analysis of the Difference Signals for the four concentrations. Superimposed on these values are the frequencies of three notable points in the original Difference Signals, i.e. the frequencies where the Difference Signals are at their minimum, maximum and zero values. As the concentration is increased, both the frequency before application of the magnetic field  $f_1$ , and that after application of the magnetic field  $f_2$ , both

increase. In each case, the frequency *before* application of the magnetic field  $f_1$ , is seen to be only slightly higher than the frequency of the zero point of the Difference Signal. It is interesting to note that the frequency of the dispersion *after* application of the magnetic field,  $f_2$ , is larger than  $f_1$  by a constant factor ( $1.38 \pm 0.01$ ).

The spreading parameter  $h_1$  (i.e. before applying magnetic field) is constant at 0.090 for all concentrations, and its equivalent after application of magnetic field  $h_2$ , is also constant at 0.060.

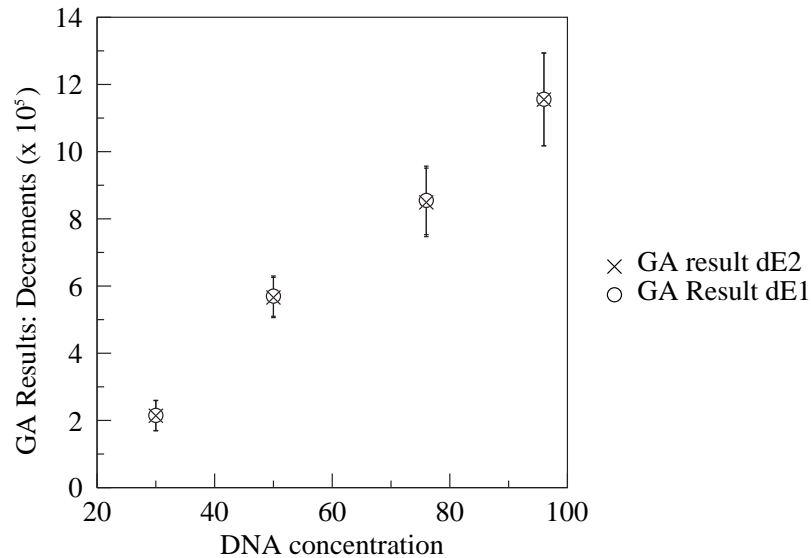


Figure 5.21: Dielectric decrements vs. concentration for DNA

The dielectric decrement before ( $d\varepsilon'_1$ ) and after ( $d\varepsilon'_2$ ) applying the field are shown in Figure 5.21, and increase with DNA concentration,  $d\varepsilon'_1$  being only slightly larger than  $d\varepsilon'_2$ . Examination of the relative magnitudes of the dielectric decrement  $d\varepsilon'_1$  and the positive maximum in the Difference Signal (DSmax), reveals that the ratio  $d\varepsilon'_1$ :DSmax is almost constant for the four concentrations, at a value of  $14.9 \pm 0.6$ .

The D.C. conductivity values obtained from the analysis are shown in Figure 5.22.  $\sigma_1$  seems to remain constant, whilst  $\sigma_2$  is seen to increase with increased concentra-

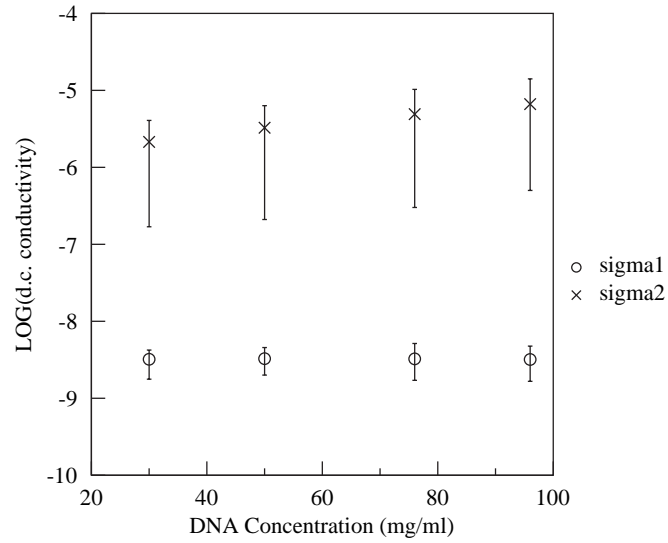


Figure 5.22: d.c. conductivity vs. concentration for DNA

tion, although the LOG scale tends to conceal its extent. There is a large variation in the D.C. conductivity values, which the LOG scale again tends to make less obvious.



### 5.6.5 Variation of Temperature

Frequency scans before and after application of the maximum magnetic field were carried out at seven temperatures. The outline form of the Difference Signal obtained at each temperature was the same as seen in Section 5.6. The change in the parameters of the dispersion susceptible to magnetic field with temperature were obtained as before by analysing the Difference Signals using the Matlab programs in Appendix K.

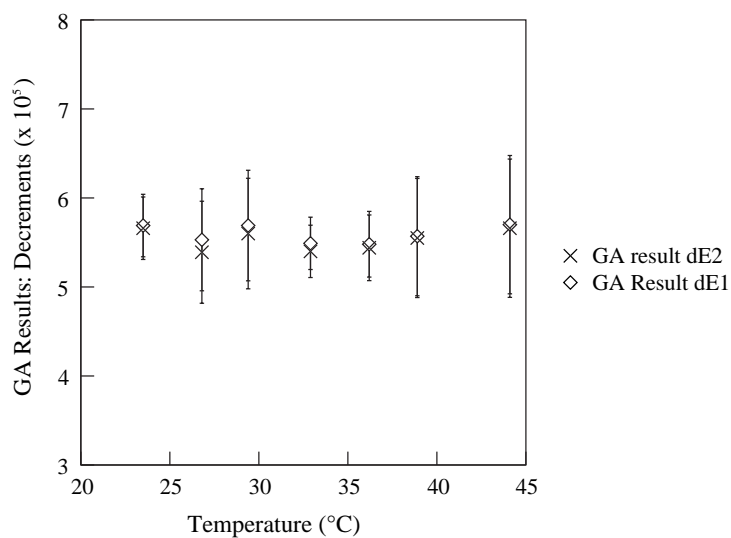


Figure 5.23: GA:Dielectric Decrements vs. Temperature

As can be seen in Figure 5.23, the dielectric decrements found from the analysis do not seem to be dependent on temperature. The only consistent facet seems to be that throughout the range,  $d\epsilon'_1$  is always slightly larger than  $d\epsilon'_2$ . The temperature independence of the dielectric decrements is an indication that the process causing the dispersion is due to interfacial polarisation, of which fluctuations in the counterions in the condensed phase close to the DNA chain is an example.

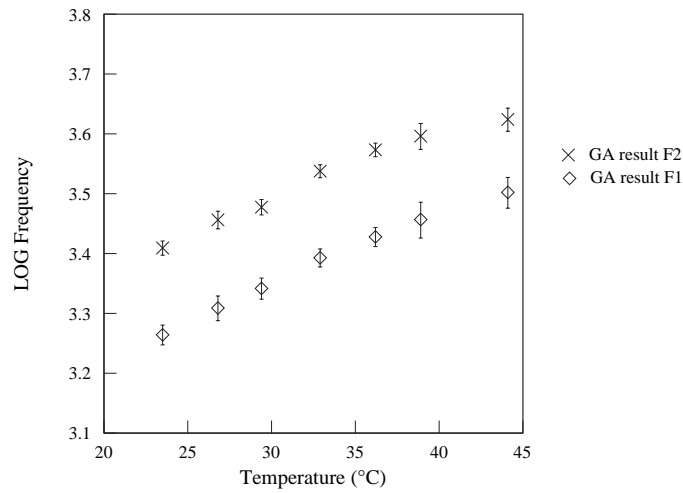


Figure 5.24: GA: LOG Frequency vs. Temperature

From Figure 5.24, it can be seen that both  $f_1$  and  $f_2$  increase almost linearly with temperature, although at above 40 °C, there may be an indication that the plot is decreasing in its gradient.

The effect of temperature on the magnetic response is discussed in more detail in Section 5.6.5.1.

In Figure 5.25 it can be seen that  $h_1$  (the spreading parameter before application of the magnetic field) and its equivalent after applying the field,  $h_2$ , are both increasing almost linearly with temperature. i.e. as the temperature increases, the dispersion displays an *increase* in the spread of relaxation times around a mean value. The ratio  $h_2 : h_1$  may be showing a slight increase as the temperature increases. (0.67 to 0.70).

Figure 5.26 shows that the D.C. conductivity values seem to show no change as the temperature increases. The ratio of D.C. conductivity before and after application

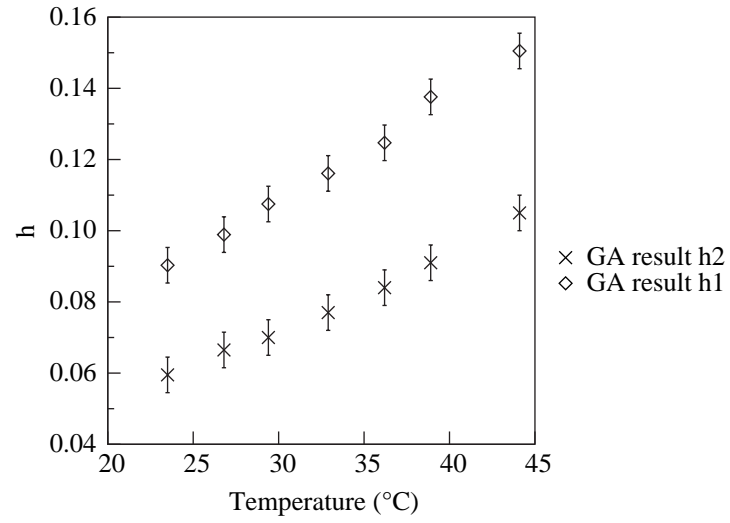


Figure 5.25: GA: Spreading parameter vs. Temperature

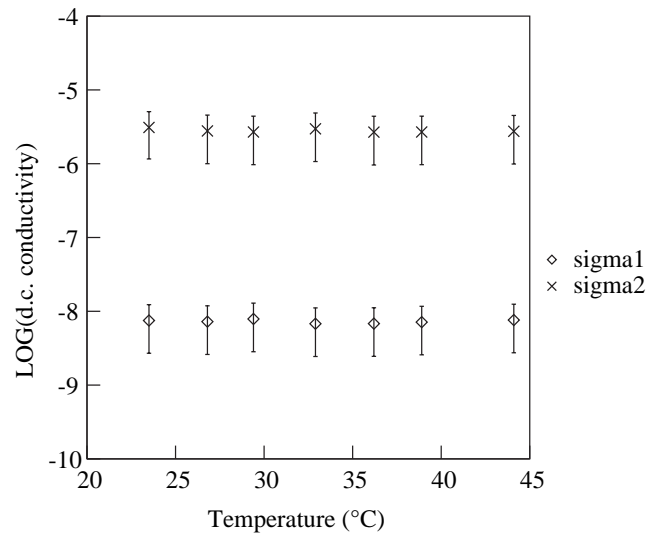


Figure 5.26: GA: LOG(D.C. conductivity) vs. Temperature

of the magnetic field seems to remain almost constant, although there is a large variation in the values determined from the Genetic Algorithm analysis.

### 5.6.5.1 Discussion of effect of temperature

The effect of temperature on the response of DNA to magnetic field was described in Section 5.6.5. Genetic Algorithm analysis of the Difference Signal concluded that the frequency of the dispersion before ( $f_1$ ) and after application of the magnetic field ( $f_2$ ) increased almost linearly with temperature, as shown in Figure 5.24

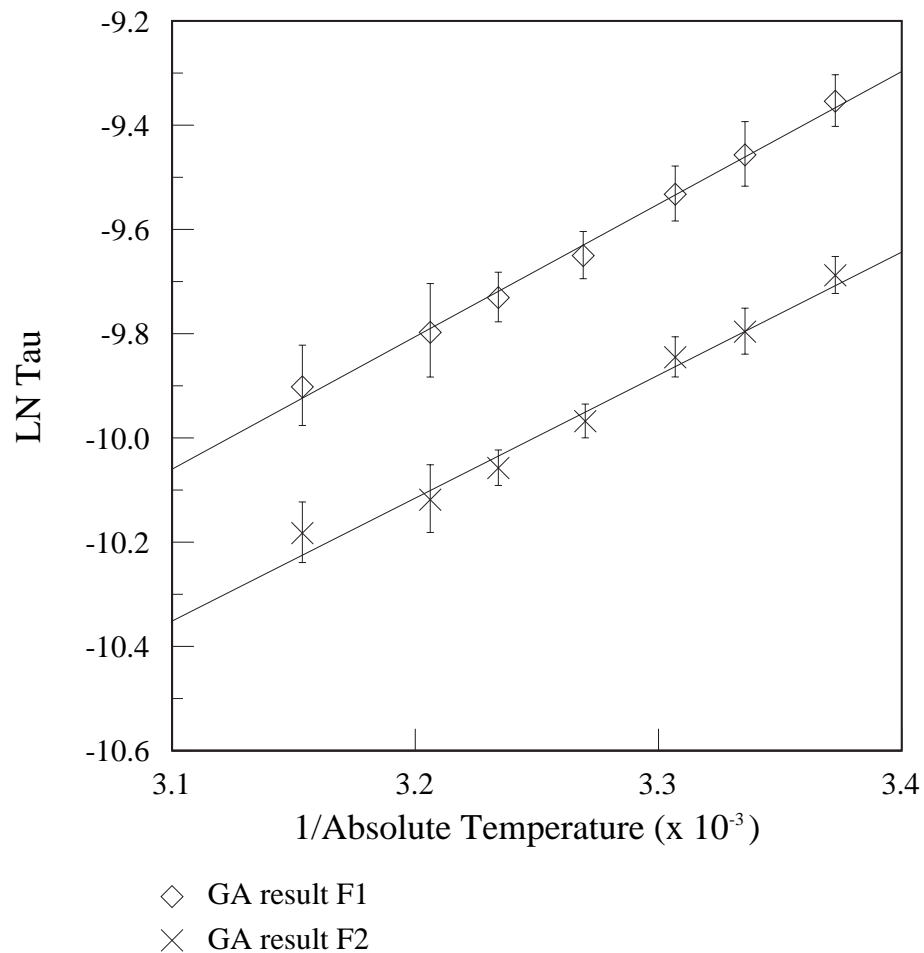


Figure 5.27: GA: LOG Tau vs. 1/Absolute Temperature

The Arrhenius equation relates the relaxation time of a dispersion  $\tau$  to the temperature as shown in the following equation:

$$\tau = \tau_0 e^{\frac{E_A}{RT}} \quad (5.1)$$

where  $E_A$  is the activation energy,  $R$  is the molar gas constant,  $T$  is the absolute temperature, and  $\tau_0$  is called the pre-exponential factor, which is assumed to be temperature-independent. It follows that:

$$\ln(\tau) = \frac{E_A}{R} \left( \frac{1}{T} \right) + \ln(\tau_0) \quad (5.2)$$

Therefore determination of the gradient of the graph of  $\ln(\tau)$  against the reciprocal of the absolute temperature enables calculation of the Activation energy. Figure 5.27 shows the  $\ln(\tau)$  against  $\frac{1}{T}$  plot determined from the Genetic Algorithm results for  $f_1$ , which gives a gradient of  $2.543 \times 10^3$ . Hence the Activation energy can be calculated to be  $21.1 \text{ kJ mol}^{-1}$  or  $5.06 \pm 0.09 \text{ kcal mol}^{-1}$ . Similarly, the Activation energy for  $f_2$  results may be calculated to be  $4.69 \pm 0.09 \text{ kcal mol}^{-1}$ .

It is interesting to compare these values with activation energies for hydrogen bonds found by other workers. Yanson (Yanson et al., 1979) found that the energy of the hydrogen bond in the Guanine-Cytosine base-pair in DNA was  $21 \text{ kcal mol}^{-1}$ , and the equivalent in the Adenine-Thymine base-pair was  $13 \text{ kcal mol}^{-1}$ . Guerra (Guerra et al., 2000) quotes values of  $21.0 \text{ kcal mol}^{-1}$  and  $12.1 \text{ kcal mol}^{-1}$  respectively. Thrane (Thrane et al., 1995) quotes  $5.0 \text{ kcal mol}^{-1}$  for the energy of the hydrogen bond in liquid water. Hasted (Hasted, 1973) notes that the dielectric properties of bound water are "not known in detail", but are presumed to lie "somewhere between those of ice and those of liquid water"; he states that the activation energy

of the hydrogen bond in liquid water is  $4.5 \text{ kcal mol}^{-1}$ , whereas that in ice crystals, the activation energy is  $13 \text{ kcal mol}^{-1}$ .

It can thus be concluded that the dispersion which is thought susceptible to change by the application of magnetic field, is caused by a process which has an activation energy of the same order of magnitude as the energy of the hydrogen bond in liquid water.

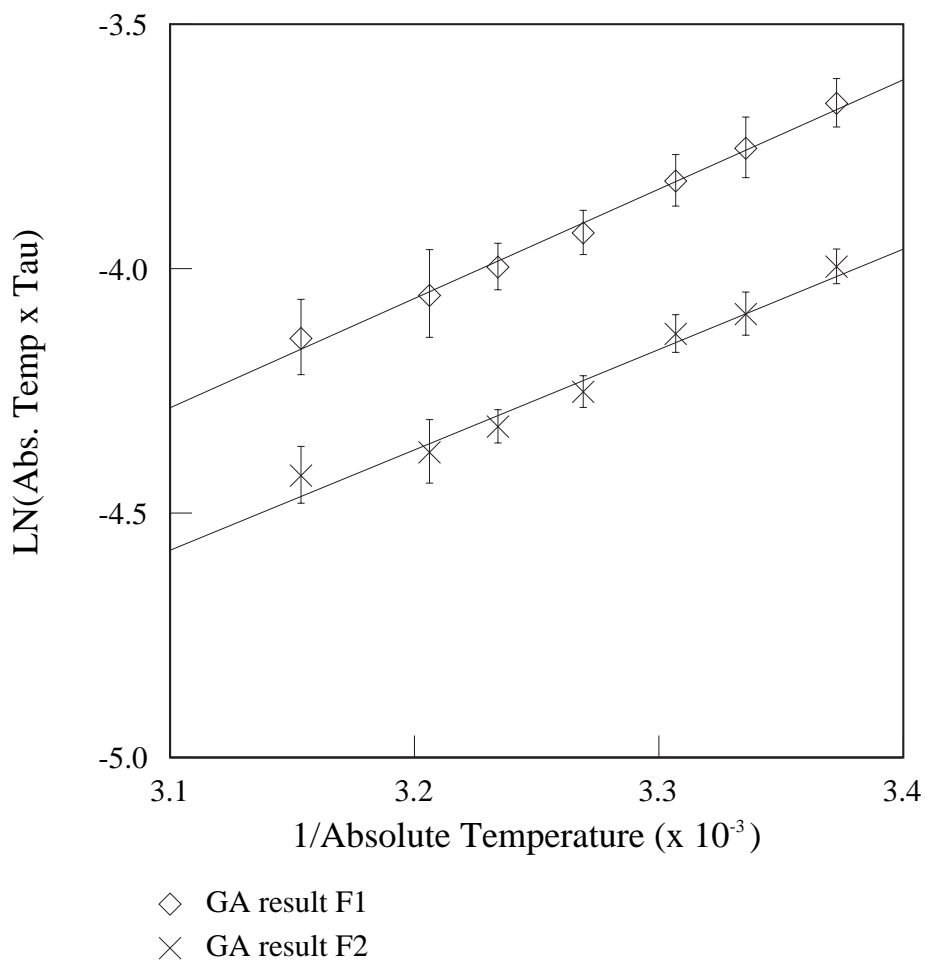


Figure 5.28: GA: LOG (Absolute temperature x Tau) vs. 1/Absolute Temperature

The values for entropy  $\Delta S$  for dielectric relaxations can also be calculated using the variation of the relaxation time  $\tau$  with temperature. The calculation uses Eyring's equation (Glasstone et al., 1941), following Starkweather (Starkweather, 1990):

$$\omega = \left(\frac{kT}{h}\right) \exp\left(\frac{-\Delta H}{RT}\right) \exp\left(\frac{\Delta S}{R}\right) \quad (5.3)$$

where  $\omega$  is the inverse of the relaxation time,  $k$  is Boltzmann's constant,  $h$  is Planck's constant,  $\Delta H$  and  $\Delta S$  are the activation enthalpy and entropy respectively,  $R$  is the molar gas constant, and  $T$  is the absolute temperature.

$$\tau = \left(\frac{h}{kT}\right) \exp\left(\frac{\Delta H}{RT}\right) \exp\left(\frac{-\Delta S}{R}\right) \quad (5.4)$$

$$T\tau = \left(\frac{h}{k}\right) \exp\left(\frac{\Delta H}{RT}\right) \exp\left(\frac{-\Delta S}{R}\right) \quad (5.5)$$

$$\ln(T\tau) = \ln\left(\frac{h}{k}\right) + \frac{\Delta H}{RT} - \frac{\Delta S}{R} \quad (5.6)$$

$$\ln(T\tau) = \left(\frac{\Delta H}{R}\right) \left(\frac{1}{T}\right) + \ln\left(\frac{h}{k}\right) - \frac{\Delta S}{R} \quad (5.7)$$

Thus a graph of  $\ln(T\tau)$  versus  $\frac{1}{T}$  enables the entropy to be calculated from the intercept on the  $\ln(T\tau)$  axis. Figure 5.28 shows the  $\ln(T\tau)$  against  $\frac{1}{T}$  plot for data determined from the Genetic Algorithm results for  $f_1$ , from which the entropy  $\Delta S$  is found to be  $-24.9 \pm 0.3 \text{ cal mol}^{-1} \text{ K}^{-1}$ . Similarly for  $f_2$ , the entropy is  $-25.5 \pm 0.3 \text{ cal mol}^{-1} \text{ K}^{-1}$ .



The enthalpy  $\Delta H$  may also be calculated from the gradient of the graph. The data for  $f_1$  gives  $\Delta H = 4.45 \pm 0.08 \text{ kcal mol}^{-1}$ , and for  $f_2$ ,  $\Delta H = 4.08 \pm 0.08 \text{ kcal mol}^{-1}$ .

### 5.6.6 Variation of added Sodium Chloride

Frequency scans before and after application of the maximum magnetic field (0.66T) were carried out on samples of DNA at a concentration of 50mg/ml with varying proportions of added Sodium Chloride.

The outline form of the Difference Signal obtained for each sample was the same as seen in Section 5.6. The change in the parameters of the dispersion susceptible to magnetic field with multiple of NaCl were obtained as before by analysing the Difference Signals using the Matlab programs in Appendix K.

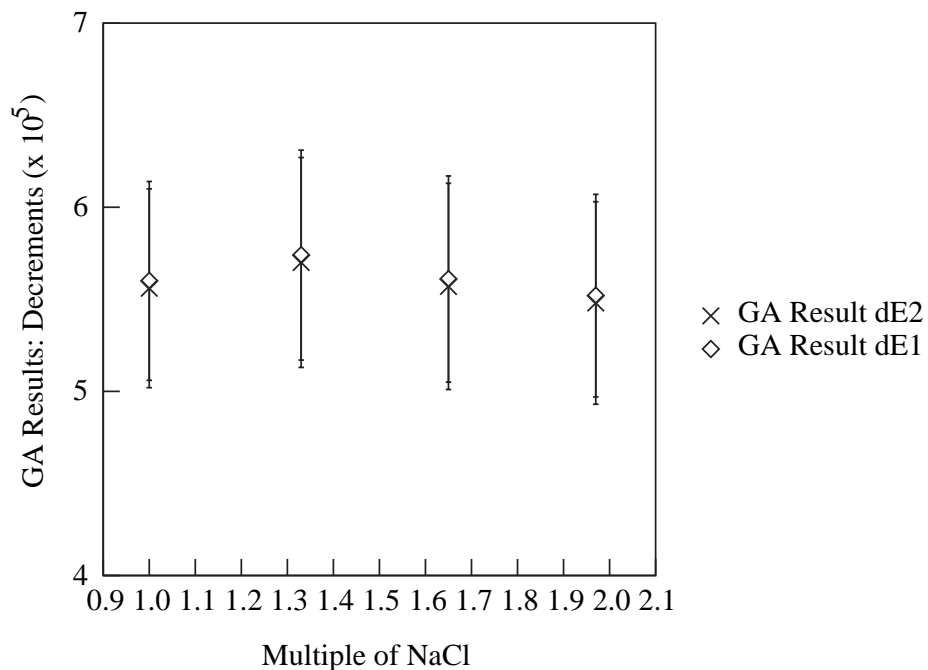


Figure 5.29: GA: Dielectric decrements vs. Added NaCl

Figure 5.29 shows the variation in the derived dielectric decrements with and without magnetic field. The dielectric decrements found from the analysis do not seem to be dependent on amount of added NaCl. The only consistent fact seems to be that

throughout the range,  $d\varepsilon'_1$  is always slightly larger than  $d\varepsilon'_2$ .

The spreading parameter  $h_1$  (i.e. before applying magnetic field) is constant at 0.09 for all samples, and its equivalent after application of magnetic field  $h_2$ , is also constant at 0.06.

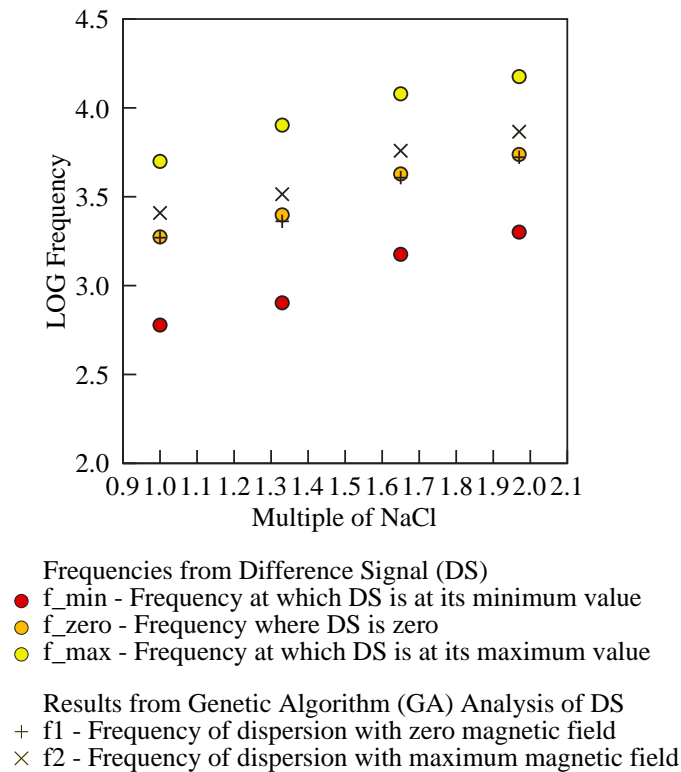


Figure 5.30: GA: LOG(Frequencies) vs. Added NaCl

Figure 5.30 shows the frequency of the dispersion before and after application of the magnetic field together with frequencies from the Difference Signal for the four samples.  $f_1$  is seen to be either equal to or slightly lower than the frequency of the zero point of the Difference Signal.  $f_2$  is larger than  $f_1$  by a constant factor ( $1.38 \pm 0.01$ ). As the amount of added Sodium Chloride is increased, both  $f_1$  and

$f_2$  increase.

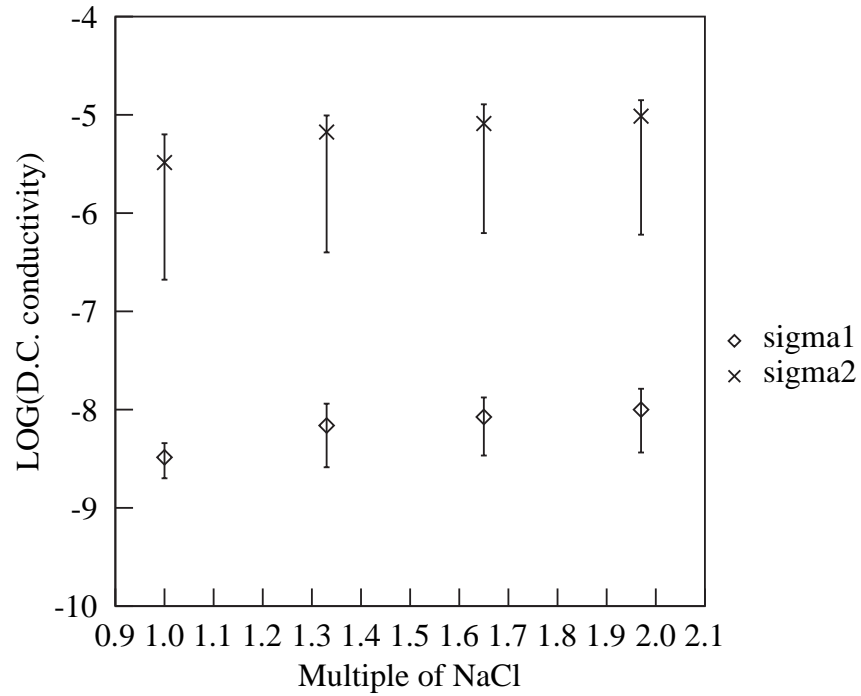


Figure 5.31: GA: LOG(D.C. conductivity) vs. Added NaCl

The D.C. conductivity values obtained from the analysis are shown in Figure 5.31, and are seen to increase with addition of NaCl, although as before, the LOG scale tends to conceal its extent.

### 5.6.7 Variation of Voltage used

This experiment examined the effect on the Difference Signal of varying the magnitude of the a.c. voltage used from 0.1v to 0.6v in increments of 0.1v. (See Section 3.5.8)

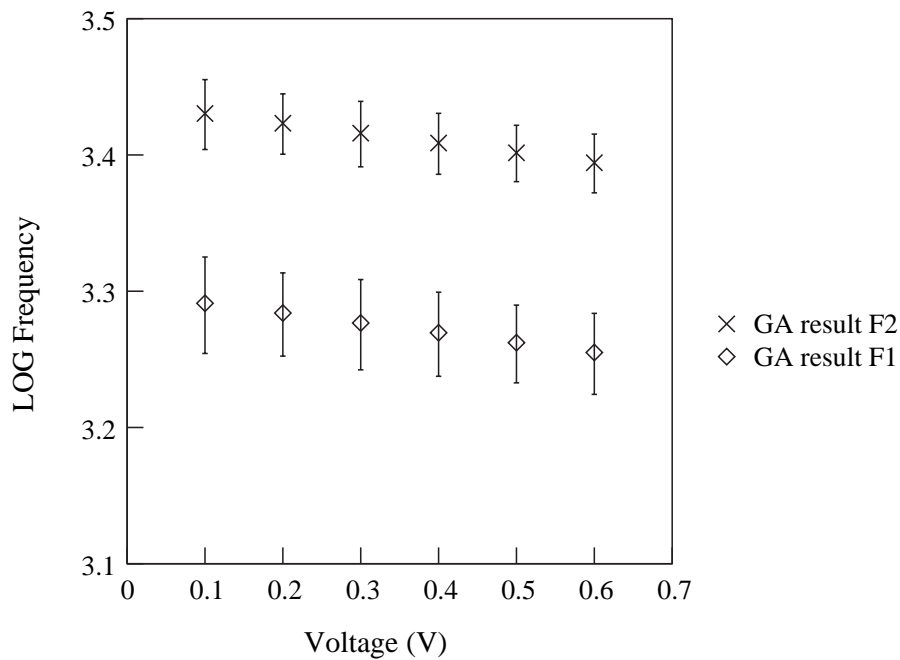


Figure 5.32: GA: LOG Frequency vs. Voltage

Figure 5.32 shows the frequencies of the dispersion with ( $f_2$ ) and without ( $f_1$ ) magnetic field as the voltage is varied. There is a slight decrease in  $f_1$  and  $f_2$  with increased voltage; the variation over the voltage range used represents a change of less than 10% in the frequency. This could be contrasted for instance, with an increase of approximately 100% in the frequency of the Difference Signal when the concentration of the DNA is increased from approximately 30mg/ml to 96mg/ml. (See Section 5.6.4 )

The spreading parameter  $h_1$  (i.e. before applying magnetic field) is constant at 0.090 for all voltages, and its equivalent after application of the magnetic field  $h_2$ , is also constant at 0.060.

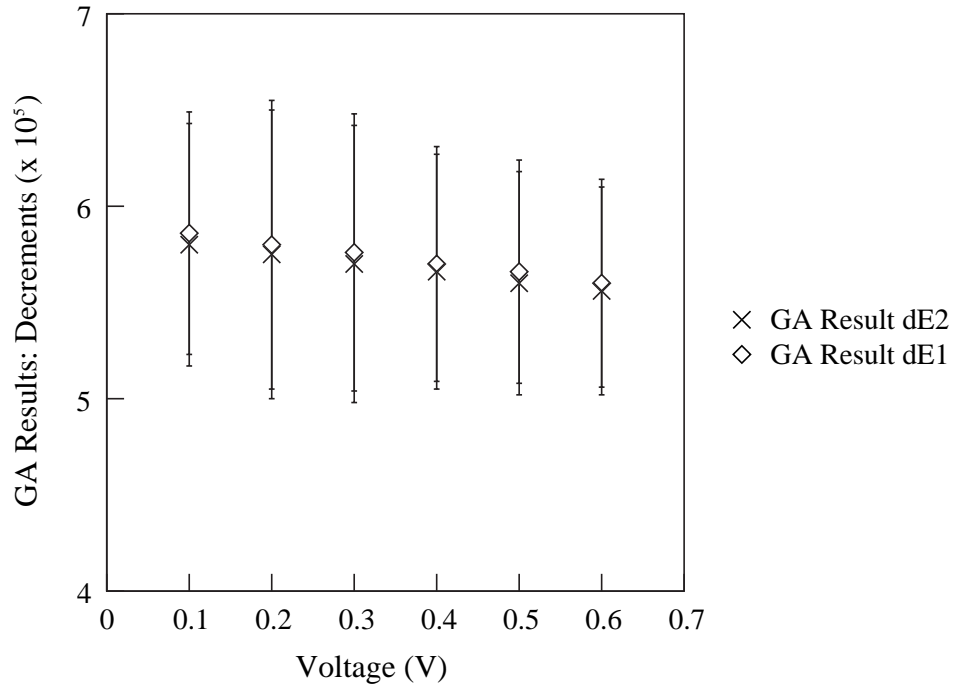


Figure 5.33: GA:Dielectric Decrements vs. Voltage

Figure 5.33 shows the derived dielectric decrements of the dispersion with ( $d\varepsilon'_2$ ) and without ( $d\varepsilon'_1$ ) magnetic field as the voltage is varied. There is a small decrease of approximately 5% in both  $d\varepsilon'_1$  and  $d\varepsilon'_2$  as the voltage is increased over the range, with the ratio  $d\varepsilon'_2:d\varepsilon'_1$  remaining at  $0.993 \pm 0.003$  throughout. Despite the constancy of the *ratio*, the analysis shows that there is quite a wide variation in the actual values of the derived decrements at each voltage.

Figure 5.34 shows the derived D.C. conductivities with ( $\sigma_2$ ) and without ( $\sigma_1$ ) magnetic field as the voltage is varied. There is an increase in both  $\sigma_1$  and  $\sigma_2$  as the

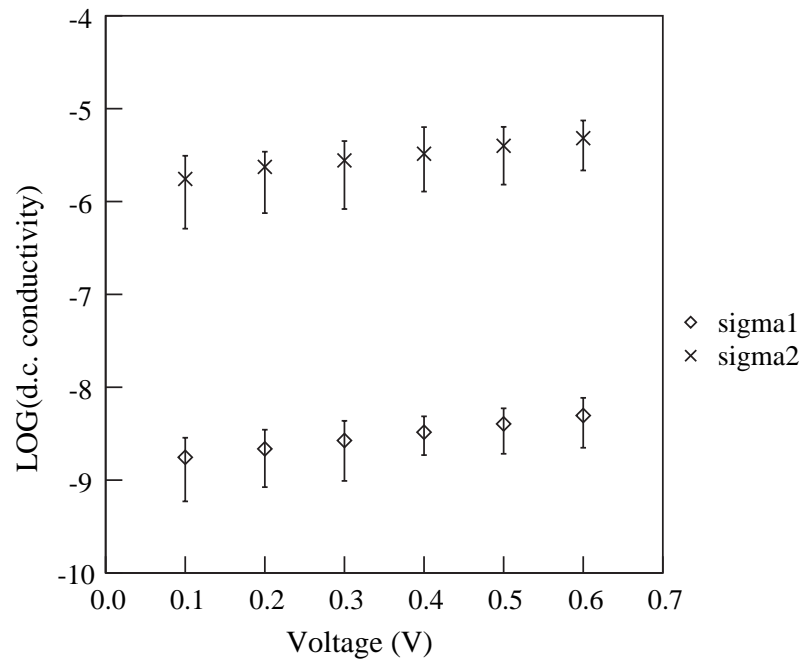


Figure 5.34: GA: LOG(D.C. conductivity) vs. Voltage

voltage is increased, with an approximate trebling of the values over this range.

## 5.7 Summary of factors affecting dispersion

It is proposed that the results obtained can be explained by the presence of a dispersion in the dielectric spectrum of DNA solution which changes significantly on application of a magnetic field of intensity 0.66 Tesla. In this section is a summary of how additional factors, such as increasing the concentration of the DNA solution, affect the changes to the parameters of that dispersion. The summary enables direct comparison to be made of the magnitude of the changes caused by the different factors. The summary lists the changes caused by the following investigations:

- The magnetic field is increased from 0.38 Tesla to 0.66 Tesla as shown in Section 5.6.3;
- The concentration of the DNA solution is increased from approximately 30mg/ml to 95mg/ml as shown in Section 5.6.4;
- The temperature of the DNA solution is increased from approximately 23 °C to 44 °C as shown in Section 5.6.5;
- The amount of Sodium Chloride added to the DNA solution is increased to approximately twice the amount in DNA as bought (See Section 5.6.6);
- The a.c. voltage applied to the DNA solution is increased from approximately 0.1 volts to 0.6 volts (See Section 5.6.7):

The following symbols are used, as in previous sections, for the results of Genetic Algorithm analysis of the relevant Difference Signals.

Before application of the magnetic field:  $d\varepsilon'_1$  is the dielectric decrement,  $f_1$  is the frequency of the dispersion,  $h_1$  is the Cole-Cole spreading parameter and  $\sigma_1$  is the d.c.conductivity,



Similarly, after application of the magnetic field:  $d\epsilon'_2$  is the dielectric decrement,  $f_2$  is the frequency of the dispersion,  $h_2$  is the Cole-Cole spreading parameter and  $\sigma_2$  is the d.c.conductivity.

The summary is shown in three ways, as an aid to comparison:

- As a table in Figure 5.35;
- By investigation, i.e. as a list of how each parameter is changed, considered one investigation at a time e.g. how each of the parameters is changed by increasing temperature;
- By parameter, i.e. as a list of how each parameter is changed, considered one parameter at a time e.g. how  $f_2$  is changed by every investigation.

## 5.7.1 By investigation

### 5.7.1.1 Magnetic field

Genetic Algorithm analysis shows that as the magnetic field is increased from approximately 0.38 Tesla to 0.66 Tesla, as shown in Section 5.6.3:

- $d\epsilon'_2$  decreases very slightly (by 1%)
- $f_2$  increases from 2014 Hz to 2563 Hz,
- $h_2$  decreases from 0.088 to 0.060 i.e. the magnetic field causes the dispersion to have a narrower spread of relaxation frequencies,
- $\sigma_2$  increases by a factor of approximately  $10^3$  from  $7.9 \times 10^{-10}$  to  $3.27 \times 10^{-6}$ ; though at the lowest magnetic field examined (0.38 Tesla), application of the

	Increase Magnetic Field	Increase Concentration	Increase Temperature	Increase Added NaCl	Increase a.c. voltage
$f_1$	0	Increased 1446 to 3038Hz	Increased 1837 to 3178Hz	Increased 1860 to 5277Hz	Decreased 1955 to 1799Hz
$f_2$	Increased 2014 to 2563Hz	Increased 1993 to 4166Hz	Increased 2566 to 4208Hz	Increased 2563 to 7345Hz	Decreased 2694 to 2479Hz
$d\epsilon_1$	0	Increased 2.15E5 to 11.56E5	0	0	Decreased 5.86E5 to 5.60E5
$d\epsilon_2$	Decreased 5.70E5 to 5.66E5	Increased 2.14E5 to 11.55E5	0	0	Decreased 5.80E5 to 5.56E5
$h_1$	0	0	Increased 0.090 to 0.150	0	0
$h_2$	Decreased 0.088 to 0.060	0	Increased 0.059 to 0.105	0	0
$\sigma_1$	0	0	0	Increased 3.28E-9 to 1.00E-8	Increased 1.76E-9 to 4.96E-9
$\sigma_2$	Increased 7.9E-10 to 3.27E-6	Increased 2.14E-6 to 6.63E-6	0	Increased 3.27E-6 to 9.70E-6	Increased 1.75E-6 to 4.81E-6

Figure 5.35: Summary of the effects of changing various conditions on the parameters of the proposed dispersion in the dielectric spectrum of DNA (Results of Genetic Algorithm Analysis). The effects are (i) Increasing the magnetic field from 0.38 Tesla to 0.66 Tesla; (ii) Increasing the concentration of the DNA solution from 30mg/ml to 95mg/ml; (iii) Increasing the temperature from 23 °C to 44 °C; (iv) Increasing the amount of added NaCl from approximately 6% to 12%; (v) Increasing the a.c. voltage applied to the DNA solution from 0.1 volts to 0.6 volts

magnetic field causes an apparent *decrease* in the d.c.conductivity from its value before application of the field.

### 5.7.1.2 Concentration

Genetic Algorithm analysis shows that as concentration of DNA is increased from approximately 30mg/ml to 95mg/ml as shown in Section 5.6.4

- $d\varepsilon'_1$  and  $d\varepsilon'_2$  both increase by a factor of over 5,  $d\varepsilon'_1$  remaining slightly larger than  $d\varepsilon'_2$ . The increase is larger than would be expected for a concentration change of just over 3 times. However, the change in specific dielectric decrement (See Figure 5.36 in Section 5.7.2.1) shows that above 50 mg/ml, the decrement increases at the same rate as the concentration.
- $f_1$  increases from 1446 Hz to 3038 Hz,  $f_2$  increases from 1993 Hz to 4166 Hz, the ratio  $\frac{f_2}{f_1}$  remains constant at 1.38,
- $h_1$  is constant,  $h_2$  is constant,
- $\sigma_1$  is constant and  $\sigma_2$  increases by a factor of approximately 3, with  $\sigma_2$  being larger than  $\sigma_1$  by a factor in the order of  $10^3$ .

### 5.7.1.3 Temperature

Genetic Algorithm analysis shows that as temperature of DNA is increased from approximately 23 °C to 44 °C, as shown in Section 5.6.5

- $d\varepsilon'_1$  is constant,  $d\varepsilon'_2$  is constant,  $d\varepsilon'_1$  remaining slightly larger than  $d\varepsilon'_2$
- $f_1$  increases from 1837 Hz to 3178 Hz,  $f_2$  increases from 2566 Hz to 4208 Hz,

- $h_1$  increases from 0.090 to 0.150,  $h_2$  increases from 0.059 to 0.105 - the spread of frequencies present in the dispersion is increased,
- $\sigma_1$  and  $\sigma_2$  both remain constant, with  $\sigma_2$  being larger than  $\sigma_1$  by a factor in the order of  $10^3$ .

#### 5.7.1.4 Added Sodium Chloride

Genetic Algorithm analysis shows that as the amount of Sodium Chloride added to DNA solution is increased to approximately twice the amount in DNA as bought (See Section 5.6.6):

- $d\varepsilon'_1$  is constant,  $d\varepsilon'_2$  is constant,  $d\varepsilon'_1$  remaining slightly larger than  $d\varepsilon'_2$
- $f_1$  increases by from 1860 Hz to 5277 Hz,  $f_2$  increases from 2563 Hz to 7345 Hz,
- $h_1$  is constant,  $h_2$  is constant,
- $\sigma_1$  and  $\sigma_2$  both increase by a factor of approximately 3, with  $\sigma_2$  being larger than  $\sigma_1$  by a factor in the order of  $10^3$ .

#### 5.7.1.5 Voltage

Genetic Algorithm analysis shows that as the a.c. voltage applied to the DNA solution is increased from approximately 0.1 volts to 0.6 volts (See Section 5.6.7):

- $d\varepsilon'_1$  and  $d\varepsilon'_2$  both decrease slightly by less than 5%,  $d\varepsilon'_1$  remaining slightly larger than  $d\varepsilon'_2$

- $f_1$  decreases from 1955 Hz to 1799 Hz and  $f_2$  decreases from 2694 Hz to 2479 Hz,
- $h_1$  is constant,  $h_2$  is constant,
- $\sigma_1$  and  $\sigma_2$  both increase by a factor of approximately 3, with  $\sigma_2$  being larger than  $\sigma_1$  by a factor in the order of  $10^3$ .

## 5.7.2 By parameter

### 5.7.2.1 Dielectric decrement

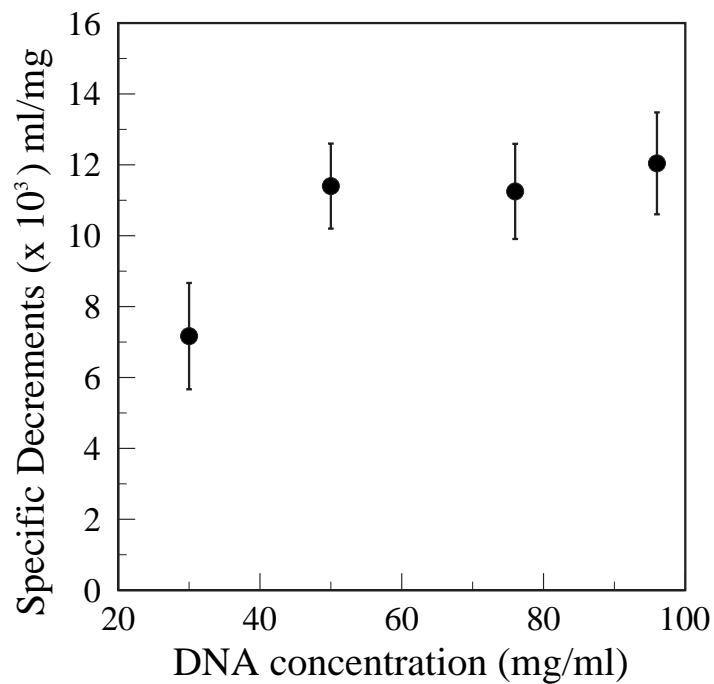


Figure 5.36: Variation of Specific Dielectric Decrement with concentration for DNA (D6898 from herring testes Type XIV)

The dielectric decrement of the dispersion decreases very slightly by 1% as the magnetic field intensity is increased. As the concentration of the DNA solution

is increased, the decrement increases by a factor of over 5; this is true both with and without magnetic field. The variation of the *specific* dielectric decrement (i.e.  $d\epsilon'_1$  divided by concentration) with concentration can be seen in Figure 5.36. Its value increases as the concentration increases from 30 mg/ml to 50 mg/ml, but then seems to be constant for higher concentrations. Sakamoto (Sakamoto et al., 1979) found that for salmon testes DNA, the specific dielectric decrement was constant for concentrations less than 0.2 mg/ml, but then increased rapidly for higher concentrations up to 2 mg/ml. Values of specific decrement at the higher concentrations used in the present work do not seem to have been reported previously.

Added Sodium Chloride seems to have no effect on the dielectric decrement of the dispersion. Increasing the a.c. voltage applied to the DNA solution cause the decrements with and without magnetic field to decrease slightly by less than 5%.

The fact that the magnitude of the dielectric decrement is independent of temperature indicates that the dispersion is caused by a form of interfacial polarisation of which the fluctuations of counter-ions in the condensed phase close to the DNA chain is an example. This is strong evidence for the source of the dispersion.

### 5.7.2.2 Frequency

The frequency of the dispersion increases by 38% as the magnetic field intensity is increased. Both the frequency with and without magnetic field increase with increased concentration of DNA (by 110%), with increased temperature (by 70%) and with added sodium chloride (by 180%). Increasing the a.c. voltage causes the frequencies with and without magnetic field to decrease by less than 10%.

### 5.7.2.3 Cole-Cole spreading parameter

As the magnetic field is increased  $h$  decreases by 33% i.e. the magnetic field causes the dispersion to have a narrower spread of relaxation frequencies. Increasing the temperature causes an increase in the value of  $h$  both with and without magnetic field,  $h_1$  by 67% and  $h_2$  by 76% i.e. the spread of relaxation frequencies becomes wider. Neither increasing the concentration, the added sodium chloride nor the applied a.c. voltage seems to have any effect on the spreading parameter.

### 5.7.2.4 D.C. Conductivity

Increasing the magnetic field intensity from approximately 0.38 Tesla to 0.66 Tesla causes the d.c. conductivity to increase by a factor of the order of  $10^3$ . Increasing the temperature seems to have little effect on the d.c. conductivity. Increasing the concentration of the DNA causes the d.c. conductivity with magnetic field to increase by a factor of 3, whilst having no effect on the d.c. conductivity without magnetic field. The d.c. conductivity both without and with magnetic field increase with added sodium chloride (by a factor of 3) and with increased a.c. voltage (by a factor of slightly less than 3). The reliability of these determinations of d.c. conductivity changes by Genetic Algorithm analysis may however be variable, as discussed in Section 2.7

## 5.8 Dialysis of DNA with other salts

This section shows the results of changing the cation associated with the DNA, as described experimentally in Section 3.5.9.

In every case, the form of the Difference Signal (DS) was found to be consistent with that in the original experiment in Section 5.5, varying only in the magnitude and frequency of the peaks. The results below show therefore, for *all* the cations used:

- The variation of the *magnitudes* of the positive maxima with concentration;
- The variation of the *frequencies* of the positive maxima with concentration;
- The variation of the *magnitudes* of the negative minima with concentration;
- The variation of the *frequencies* of the negative minima with concentration;

The results for the DNA as bought from Sigma, and described in Section 5.5, are also included here.

The detailed graphs for each individual cation are shown in Appendix N.

Figure 5.37 shows the magnitudes of the *positive* peaks against concentration. As can be seen, the results indicate that while the magnitude increases with concentration, changing the counter ion associated with the DNA seems to have little effect within the limits of experimental error. Figure 5.38 shows variation of the frequencies of the positive maxima with concentration. For each salt, the frequency increases with concentration, but in this case the type of counter ion also has a large effect. The DNA dialyzed against Calcium chloride gives positive peaks with the lowest frequencies, and the DNA dialyzed against Rubidium the highest.



Figure 5.39 shows the magnitude of the *negative* peaks of the difference signal for all salts. As with the positive maxima, the magnitude increases with concentration, but the type of counter ion seems to have little effect. Figure 5.40 shows the matching frequencies of the minima, and again the frequencies increase with concentration. Changing the counter ions associate with the DNA can be seen to affect the frequencies of the minima in ways which reflect the changes in the frequencies of the maxima; i.e. the whole Difference Signal is moved along the frequency axis.

The results for the DNA dialized against Sodium Chloride are, as would be expected, similar to those for the DNA as purchased directly from Sigma, since this is produced as the *sodium* salt (The description is “D6898 Deoxyribonucleic acid, sodium salt from herring testes, Type XIV”)

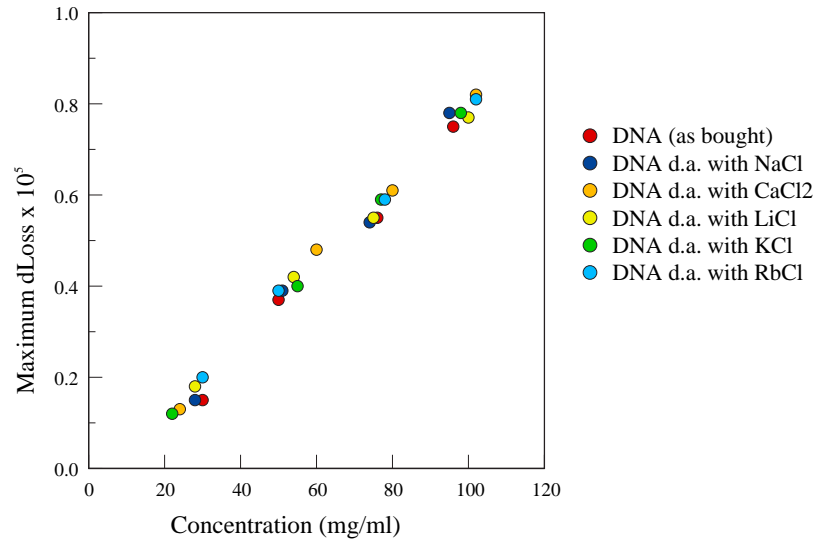


Figure 5.37: All salts: Magnitude of Maximum of DS vs. Concentration

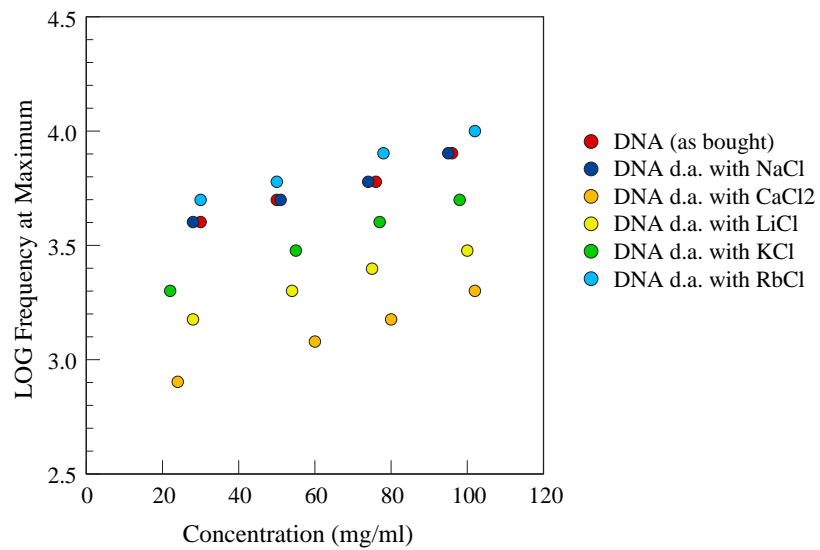


Figure 5.38: All salts: Frequency of Maximum of DS vs. Concentration

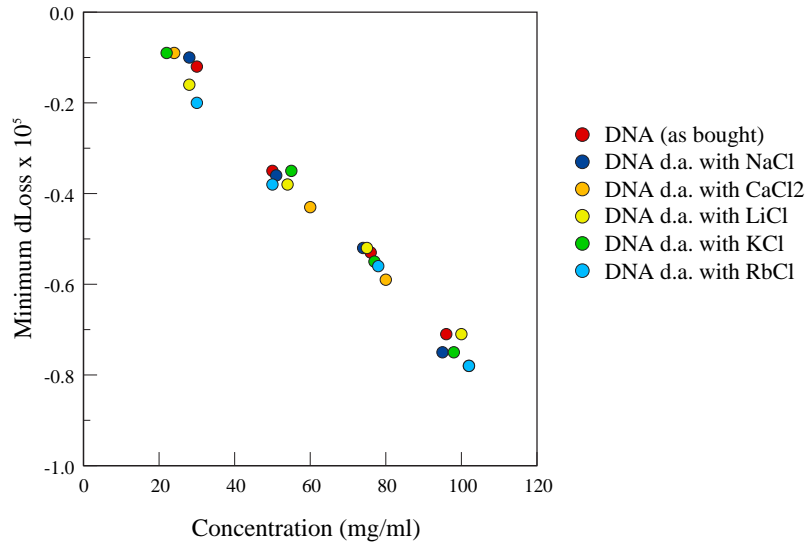


Figure 5.39: All salts: Magnitude of Minimum of DS vs. Concentration

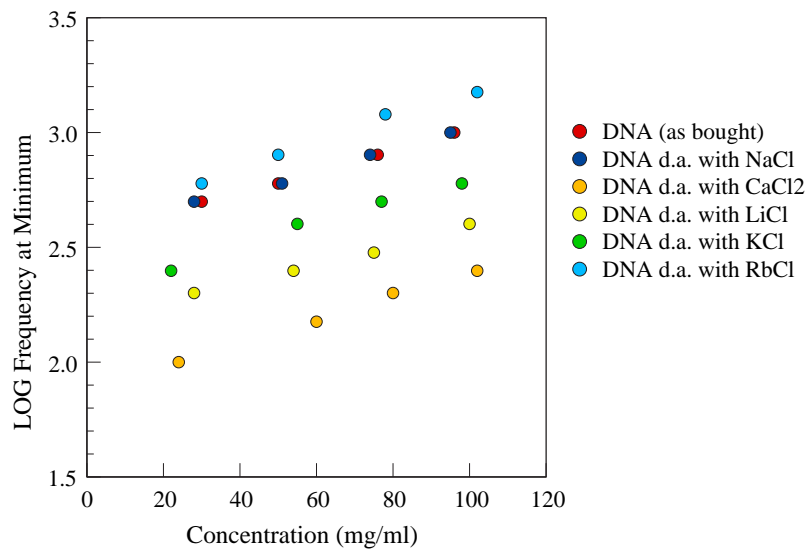


Figure 5.40: All salts: Frequency of Minimum of DS vs. Concentration

## 5.9 Discussion of dialysis of DNA with other salts

The results presented in Section 5.8 show the properties of the Difference Signal for DNA dialyzed against several salts, thereby replacing the sodium in the DNA as bought from Sigma with the relevant cation from the salt. The cations used were calcium, lithium, potassium and rubidium; sodium was also used to confirm that this would not change the properties of the solution of the DNA as bought. In all cases the Difference Signal (DS) was found to be consistent with that in the original experiment in Section 5.5, varying only in the magnitude and frequency of the peaks. It was found that, whilst changing the counter-ion associated with the DNA seemed to have little effect on the *magnitudes* of the Difference Signals, the frequencies of the peaks in the Difference Signals were affected by the cation; i.e. changing the cation simply moved the whole Difference Signal along the frequency axis.

In this section, various properties of the cations will be examined in order to explain the trend shown in the frequency of the Difference Signal as the cation is changed. The frequency of the maximum peak in the Difference Signal will be used as a measure of the position of the relevant Difference Signal on the LOG Frequency axis. (The frequency of the minimum peak or that of the zero value of the Difference Signal could equally validly have been used.) Since the frequency also varied with the concentration of the DNA solution, the frequency of the positive maximum in the Difference Signal for DNA with a concentration of 50mg/ml will be used. Where the exact value is not found in Figure 5.38, the value for the 50mg/ml is found by extrapolation.

In all the graphs in the following sections the y-axis is the same, and represents the LOG of the frequency of the maximum peak of the Difference Signal for DNA of concentration 50mg/ml dialyzed against the relevant cation, denoted  $LOG f_{max}$ , and

referred to as the Difference Signal Frequency parameter.

### 5.9.1 Diamagnetism

Figure 5.41 shows three graphs which show how the Difference Signal Frequency parameter varies with Pascal's constants, the dielectric susceptibility and the mass susceptibility for the cations.

The magnetic susceptibility of a compound is found by the addition of the contribution from the paramagnetic susceptibility and the diamagnetic susceptibility. Because the former is much larger than the latter, the diamagnetic susceptibility may be ignored in most cases. Where more accurate calculations are needed however, both the paramagnetic and diamagnetic contributions from each component part of the molecule must be added together. The diamagnetic contribution of a given element or ion to the susceptibility of the whole molecule is given by Pascal's constants. The Diamagnetic susceptibility has been defined in Section 2.4, and the Mass susceptibility is calculated by dividing the (volume) diamagnetic susceptibility by the density of the element. Pascal's constants and the susceptibility values were obtained from Bain (Bain and Berry, 2008).

No obvious correlation can be seen between the three diamagnetic parameters and the relevant  $LOGf_{max}$  for the given cations.

### 5.9.2 Radii

Figure 5.42 shows three graphs which show how the vary with the Difference Signal Frequency parameter varies with the Covalent radius, Van der Waals radius and Ionic radius in solution for the cations.

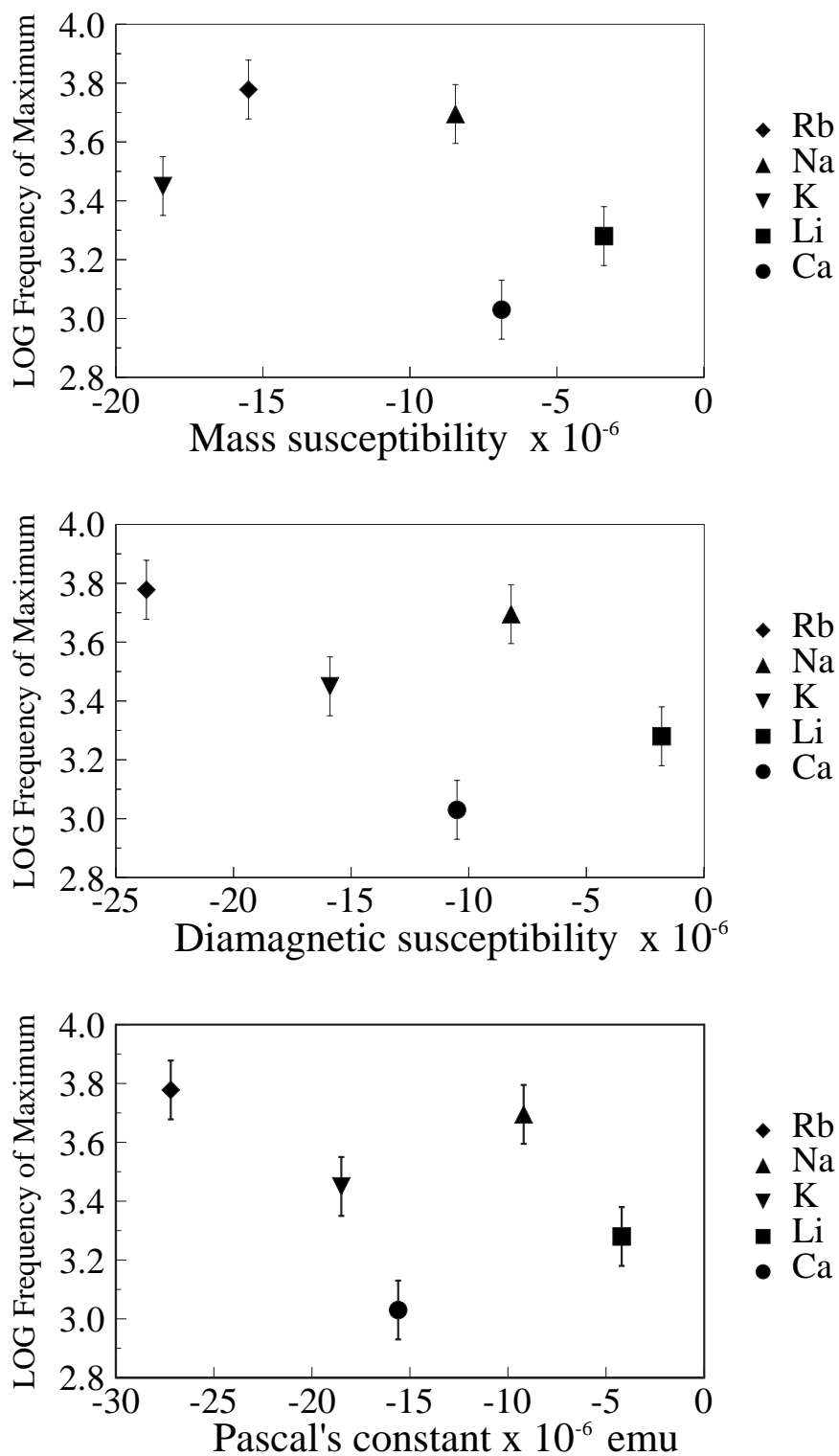


Figure 5.41: Variation of Difference Signal Frequency parameter with Pascal's constants (lower), Diamagnetic susceptibility (middle), and mass susceptibility (top).

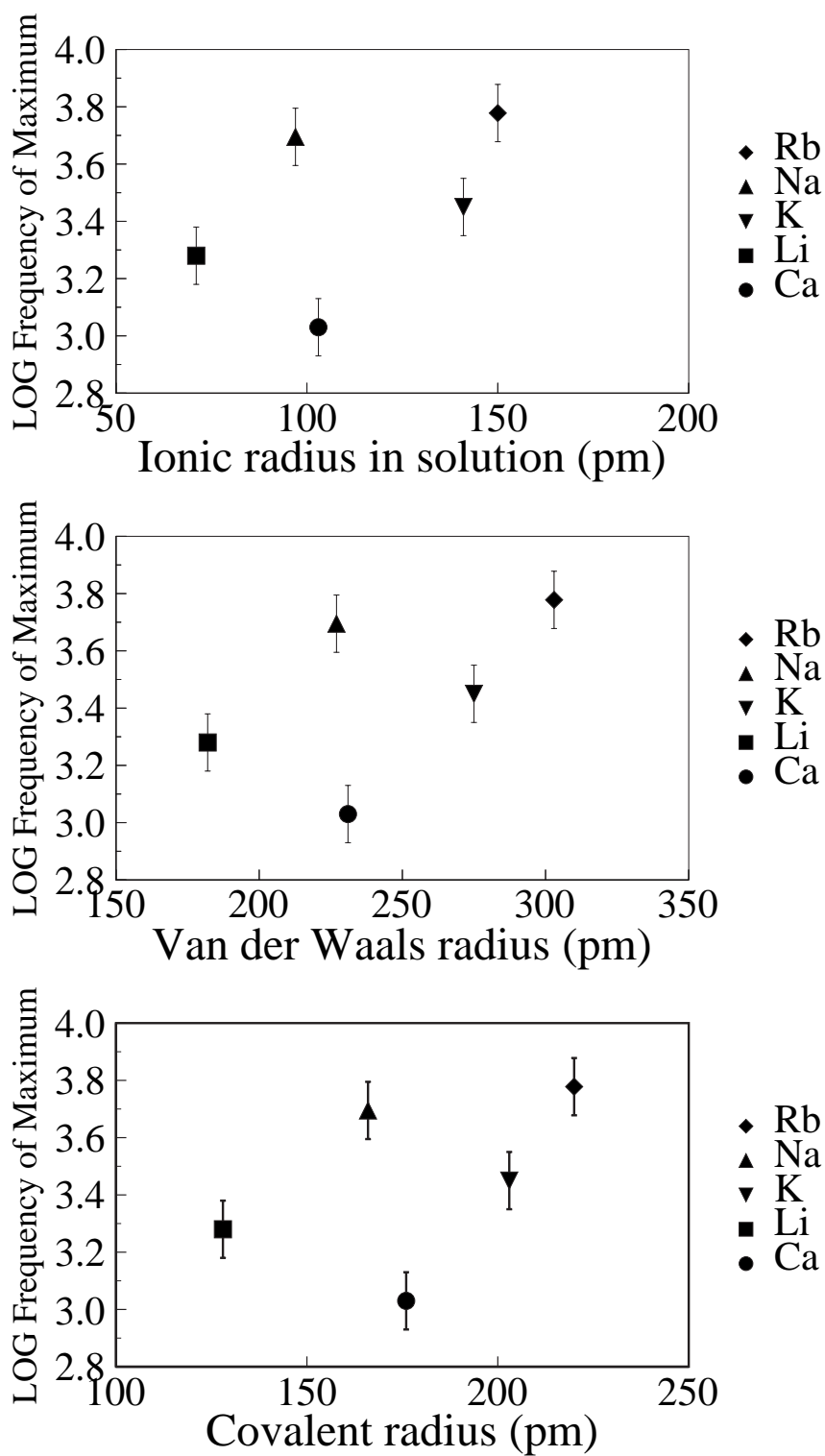


Figure 5.42: Variation of Difference Signal Frequency parameter with Covalent radius (lower), Van der Waals radius (middle) and Ionic radius in solution (top).

The covalent radius of an atom refers to the magnitude of an atom forming a covalent bond with another atom. In theory this should be directly related to the covalent bond length, but in practice, the chemical environment also modifies the bond length. The Van der Waals radius is equal to one half the distance between two atoms that are not bonded when there is no net electrostatic force between them. The van der Waals radius of an atom may be thought of as the radius of a sphere used to model a particular type of atom. The covalent radii and Van der Waals radii were obtained from Bondi (Bondi, 1964) and the Ionic radii in solution from Marcus (Marcus, 1988).

No obvious correlation can be seen between the three radius parameters and the relevant  $LOGf_{max}$  for the given cations.

### 5.9.3 Diffusion

Figure 5.43 shows two graphs which show how the Difference Signal Frequency parameter varies with the Diffusion Coefficient and the Ionic Mobility for the cations.

The Diffusion coefficient for an ion in aqueous solution is the proportionality constant relating the diffusive flux (the rate of diffusion of an ion per unit area per unit time) to the concentration gradient. An ion's mobility is its drift velocity per unit electric field intensity applied, and is directly proportional to its diffusion coefficient. Graphs involving the two parameters should therefore show the same trends. The values were obtained from Koneshan (Koneshan et al., 1998).

As the mobility and Diffusion coefficient increase, there is a tendency for the relevant Difference Signal Frequency parameter to also increase. The DNA dialyzed with sodium chloride is an obvious exception to this; its DS Frequency parameter would be expected to be close to that of Lithium, if the mobility or diffusion coefficients



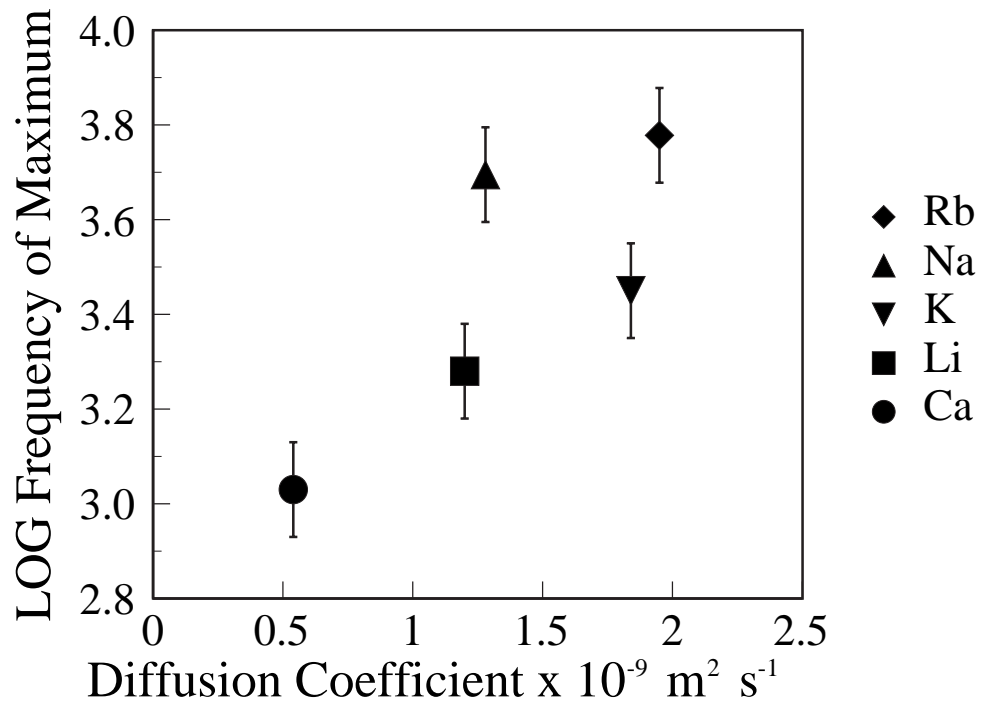
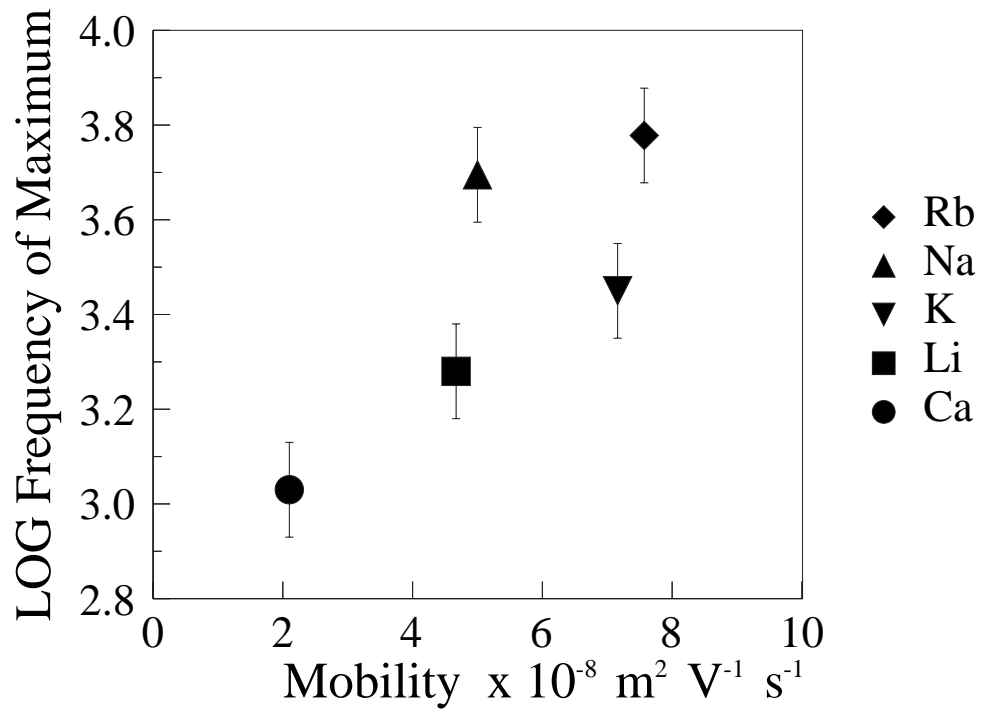


Figure 5.43: Variation of Difference Signal Frequency parameter with Diffusion Coefficient (lower) and Ion Mobility (upper).

alone were responsible for the difference signal frequency. With the exception of the DNA dialized with sodium chloride, the Difference Signal Frequency parameter could be proportional to the Mobility (and therefore to the Diffusion Coefficient).

#### 5.9.4 Hydration

Figure 5.44 shows two graphs which show how the the Difference Signal Frequency parameter varies with the Ion-size parameters and the Hydration numbers for the cations.

The effective Hydration number of the cation in aqueous solution is the mean number of water molecules associated with the cation. The ion-size parameter is the nearest distance to which the centre of an anion can approach the centre of the hydrated cation. It may be interpreted as an idealized radius for a hydrated cation surrounded by the hydration number of water molecules. There is an obvious relationship between the two parameters, since the larger the hydration number, the larger the ion-size parameter will be. Graphs involving these two parameters should show similar trends. Values were obtained from Stokes (Stokes and Robinson, 1948) and Bates (Bates et al., 1970).

There is a tendency for the Difference Signal Frequency parameter to be inversely proportional to both the hydration number and ion-size parameter. However, neither the D.S. frequency parameter for the DNA dialized with Sodium chloride nor potassium chloride fit exactly into the inverse relationship.

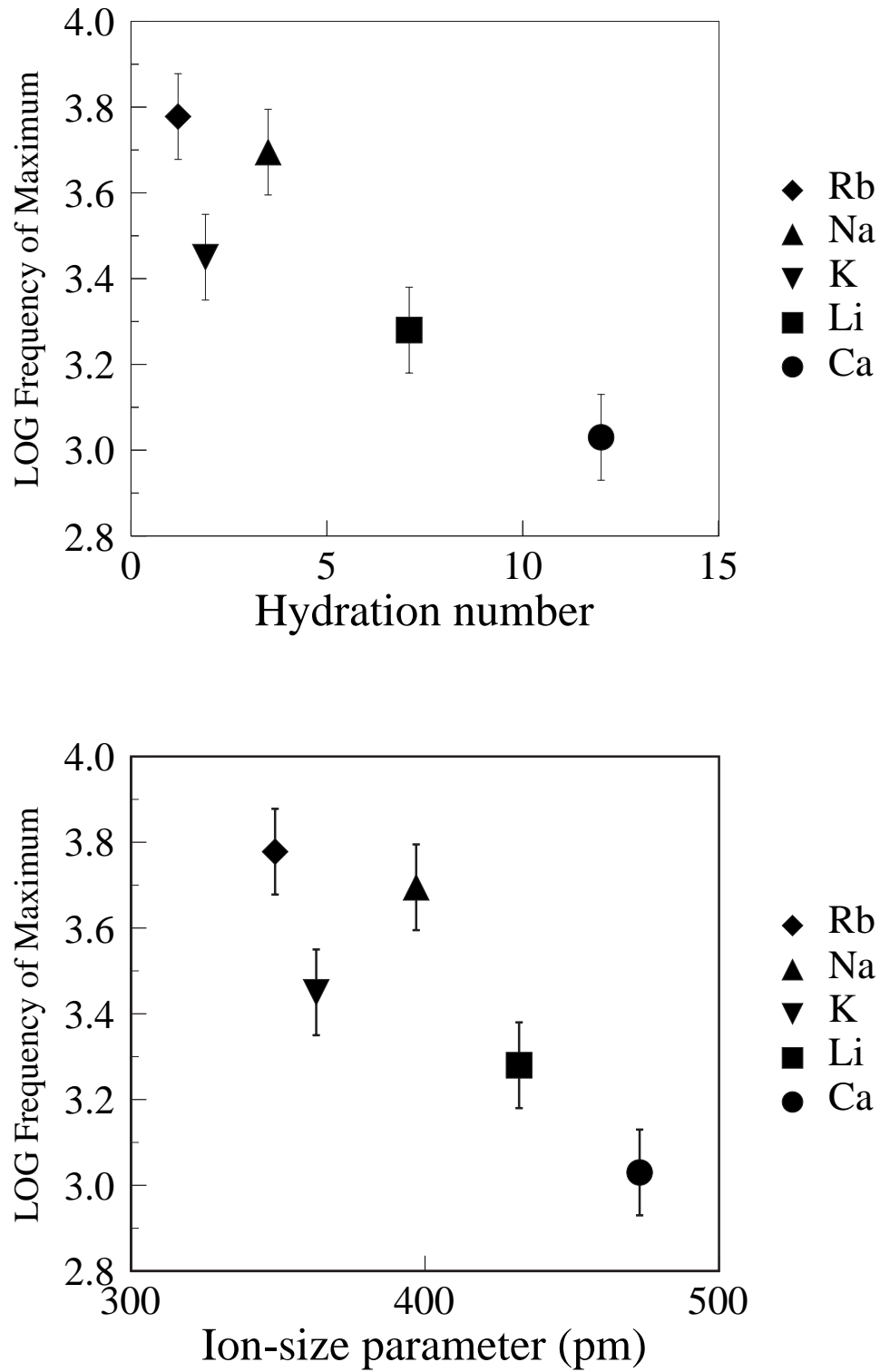


Figure 5.44: Variation of the Difference Signal Frequency parameter with Ion-size parameter (lower) and the Hydration number (upper).

### 5.9.5 General properties

Figure 5.45 shows three graphs which show how the Difference Signal Frequency parameter varies with the Atomic number, Atomic Mass and Density for the cations.

No obvious correlation can be seen between the Atomic number or Atomic mass and the relevant  $LOG f_{max}$  for the given cations. In the density graph (top graph in Figure 5.45), if only the monovalent cations lithium, potassium, sodium and Rubidium are considered, there seems to be some correlation between density of the element and Difference Signal Frequency parameter. The frequency of the point associated with the sodium cation seems slightly too high.

### 5.9.6 Conclusions

No obvious explanation has been found for the change in the frequency of the Difference Signal as the cation is changed. In section 5.9.4, it could be argued that as the mobility of the ion increases, so does the frequency of the Difference Signal. The discrepancy in the value for the DNA dialized with sodium chloride is obviously a problem with this explanation. This is especially true since the frequency of the Difference Signal obtained with the DNA as bought from Sigma, which of course is the sodium salt, confirms the findings found for the DNA dialized against sodium chloride (See Section 5.8)

Similarly, in Section 5.9.5, the correlation between the density of the element and the Difference Signal Frequency parameter for the monovalent cations could be significant. However, it is difficult to see why the density of the solid element should have an effect on the movement of the counter-ions surrounding the DNA chain.

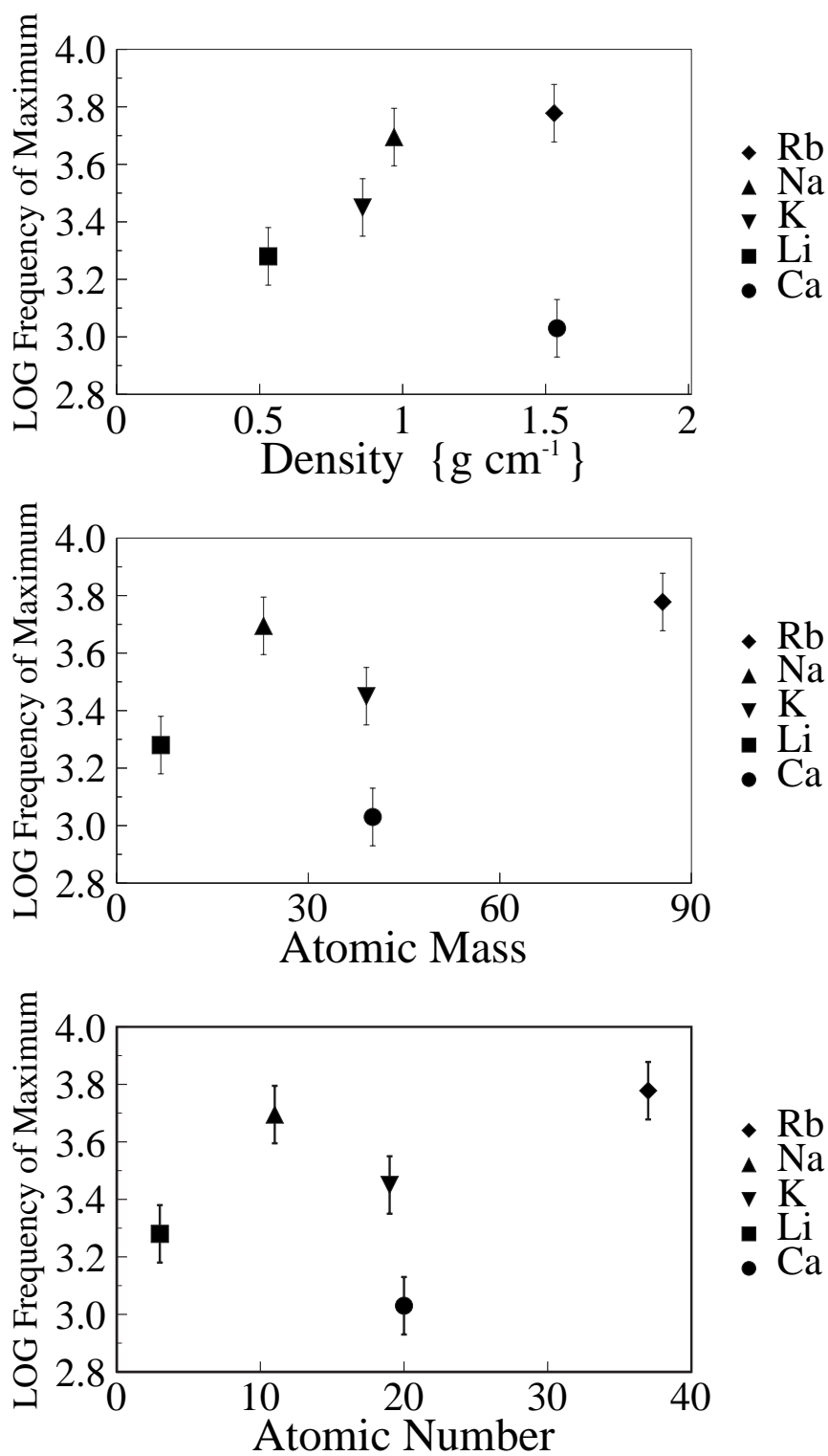


Figure 5.45: Variation of the Difference Signal Frequency parameter with Atomic number (lower), Atomic Mass (middle) and Density (upper).

The obvious differences in the samples of DNA bought from Sigma, as explained in Section 3.4.1, could perhaps be responsible for the lack of convincing correlation between any property of the cations and the associated Difference Signal Frequency parameter. Since all the Difference Signals obtained for different concentrations with one cation were found for a dialized sample produced with one sample of DNA, they would be consistent across concentration. Since different DNA samples were used to dialize with different cations, conceivably this could have affected the results.

## 5.10 Cause of dispersion

In searching for the cause of the proposed dispersion which is susceptible to changing magnetic field in the present work, it is of interest to examine the properties of low frequency dispersions found by other workers in the dielectric spectrum of DNA, and to compare them to those reported in Sections 5.3 to 5.8.

Takashima (Takashima, 1963) investigated the dielectric properties of DNA with a range of molecular weights. The frequency of the dispersion he found was 1700 Hz for the highest molecular weight samples, a frequency which is similar to that found in the present work. At the maximum concentration of 2 mg/ml, the dielectric decrement was found to be approximately 1000, increasing a little as the concentration was decreased. Since the lowest concentration used in the present work is approximately 25 mg/ml, it is difficult to compare the dielectric decrements directly. However, the trend shown in Figure 5.21 is not inconsistent with Takashima's result. A major discrepancy is that in the concentration range used in the present work (approximately 25 – 95 mg/ml), the dielectric decrement increases with increasing concentration, whilst Takashima showed the decrement decreasing with increased concentration at very low concentrations, then levelling off at concentrations above 0.4 mg/ml. He also found that the spreading or Cole-Cole parameter for native DNA was 0.39, indicating a much wider spread of relaxation times than found in the present work.

Bonincontro (Bonincontro et al., 1984) found the dielectric decrement of low molecular weight DNA to be approximately 110 at a concentration of 5 mg/ml. This value seems to be much lower than those values found in the present work (See Figure 5.21), but when the relative concentrations and molecular weights are taken into account, the value does not rule out the dispersion found in the present work being caused by similar mechanisms to those proposed by Bonincontro. At first sight, the

frequency of the low frequency dispersion found by Bonincontro would seem to be too high for it to be considered as being similar to that found in the present work. However, the frequency of the dispersion is known to be inversely proportional to the square of the molecular weight of the DNA. The molecular weight of the DNA used in the present work is not known, (See Section 3.4.1), but is likely to be much larger than the sonicated DNA used by Bonincontro. Since the lowest frequency found by Bonincontro is only a factor of approximately 5 times higher than a typical frequency found in the present work, the disparity in the frequencies is not critical, and the dispersions could be caused by the same process.

It is of interest to compare the properties found by Sun (Sun et al., 2005) for the dispersion he found at low kHz frequencies i.e. the dispersion he denoted HFP (Higher frequency process) with those of the proposed dispersion which is susceptible to change by magnetic field in the present work. The value of the dielectric decrement for the HFP dispersion may appear to be substantially lower than that found in the present work (e.g. 110 at 203K for a concentration of 5 mg/ml, compared to approximately  $2 \times 10^5$  at 298K for a concentration of 30 mg/ml). However, two factors have to be taken into consideration. Firstly, the magnitude of the HFP dielectric decrement was found to be increasing with increased temperature, and could be much larger at the temperatures used in the present work. Secondly, examination of the variation of dielectric decrement with concentration in Figure 5.21, suggests that extrapolation of the trend towards lower concentrations would give values of dielectric decrement of the same order as those found by Sun. Sun found that an Arrhenius plot between 183 to 263K was a straight line with an activation energy of  $27 \text{ kJ mole}^{-1}$  or  $6.7 \text{ kcal mol}^{-1}$ , compared with  $5.06 \text{ kcal mol}^{-1}$  found for the dispersion in the present work.

Sun found that the relaxation times and therefore frequencies were independent of concentration. In the present work however, the frequency of the proposed disper-



sion was found to increase with concentration. (See Figure 5.20) The concentration range used by Sun however is substantially lower than that used in the present work (less than 5 mg/ml compared to a range of 30 to 90 mg/ml). Odijk (Odijk, 1979) has theorized that varying the concentration of DNA can change quite markedly the intermolecular interactions between neighbouring DNA chains. At very low concentrations, the DNA chains lie in an ordered parallel state, whereas at higher concentration, there are multiple cross-over interactions between neighbouring chains. In the low concentration region, counter-ion fluctuations reflect the local conformation of the DNA, whilst at higher concentrations, intermolecular effects predominate. Thus it is conceivable that the responses of the dielectric parameters of a dispersion to changing concentration could vary considerably in differing regions of concentration.

# Chapter 6

## Conclusion

### 6.1 General Conclusions

It seems likely that the dispersion found in the present work is due to fluctuations in the counter-ion sheath surrounding the DNA chain. The response of the hydrated cations in the counter-ion cloud to the sinusoidal electric field produced by the Wayne-Kerr component analyser would be to move parallel to the length of the DNA chain. Manning (Manning, 1978) noted that NMR relaxation measurements demonstrated that *all* the hydrated  $\text{Na}^+$  and  $\text{Rb}^+$  ions condensed onto DNA at low concentrations have almost unrestricted movement, with no evidence of dehydrated localized binding to the DNA. Thus the DNA would acquire an induced polarization along its longitudinal axis.

The frequency of the dispersion suggests that it is associated with a relaxation process involving redistribution of counter-ions along lengths of the same order of magnitude as the DNA molecule itself. The mobility of the hydrated cations would obviously affect the relaxation frequency of the dispersion, as implied in Sections 5.8

and 5.9.3. The increased frequency of the dispersion with increased concentration (Section 5.6.4) could be accounted for by an increase in the counter-ion mobility with concentration, as postulated by Bone (Bone and Small, 1995) to account for similar dependence of frequency on concentration for dispersions in DNA in the MHz range. The temperature independence of the dielectric decrement, as seen in Section 5.6.5, points to interfacial polarisation as a cause of the dispersion, which is consistent with a mechanism involving movement of the counter-ions surrounding the DNA chain.

The relaxation of the counter-ions is an activated process i.e. an energy barrier must be overcome for the cations to respond to the changing electric field. Following Kauzmann (Kauzmann, 1942), it is postulated that it is a discontinuous not a gradual process, and a quantity  $K$  may be defined as the mean number of counter-ion fluctuations per unit time. The relaxation time  $\tau$  is then the inverse of  $K$ . Movement of the hydrated cations could involve continuous making and breaking of the hydrogen bonds linking the cations to the water in their hydration shells, and could explain the close similarity between the activation energy of the process to that of hydrogen bonds in liquid water (See Section 5.6.5.1). It is more likely however, that the magnitude of the activation energy is just a reflection of the relatively weak interaction between the phosphate groups and the counter-ions.

Negative values of  $\Delta S$  for the proposed dispersion must involve a decrease in the number of degrees of freedom in the transition state. This may be explained by the assumption that the hydrated cations must be in a particular orientation for movement parallel to the longitudinal DNA axis to occur. This would obviously mean that the number of degrees of freedom of the transition complex would be reduced when compared with the “ground” state of the counter-ions, thus making  $\Delta S$  negative. It is also however conceivable that the relatively ordered transition state could be characterized simply by co-operative movement of the cations and their

hydration shells, thus decreasing the entropy of the “DNA + cations + hydration shell” system.

The fact that increasing the amount of Sodium Chloride in the solution surrounding the DNA chains has no effect on the dielectric decrement of the dispersion (See Section 5.7.1.4) may imply that the dispersion is totally dependent on the ions inside the charge cloud, and that the charge cloud is saturated with  $\text{Na}^+$  ions before adding further sodium ions. Increasing the amount of sodium chloride does however increase the frequency of the dispersion. This is in agreement with Tomic (Tomic et al., 2007), who suggested that increased numbers of free counter-ions limited the displacement of counter-ions in the condensed layer, and would therefore cause the frequency of the dispersion to increase.

The results of the present work show that changing the magnetic field intensity modifies this dispersion. As the cations move through the counter-ion cloud parallel to the DNA chain, there will be a component of the magnetic field perpendicular to the direction of this movement. The cations will therefore experience a force perpendicular both to their motion and to the direction of the magnetic field component. This fluctuation however could only produce polarization transverse to the DNA rod, and hence is unlikely to affect a dispersion caused by fluctuations in the longitudinal direction.

In Section 1.4, the effect of magnetic fields on the orientation of DNA chains was described. Maret (Maret et al., 1975) concluded that the base-pairs were responsible for the magnetic orientability of the DNA molecules, since they consist partly of aromatic rings which are diamagnetically anisotropic. The rings tend to align their planes parallel to the magnetic field. Since over substantial lengths of the DNA structure these rings will all be parallel to each other, their additive anisotropy will ensure that lengths of the DNA molecule will try to orient with the filament perpendicular to the field direction. There could also be localised effects on the

counter-ions if nearby purine and pyrimidine rings experience a re-orientation force due to application of magnetic field.

The re-orientating effect of the magnetic field on the DNA as a whole would cause the angle between the long axis of the DNA rods and the a.c.field direction to decrease, causing the longitudinal polarization also to be decreased (when the magnetic and electric fields are parallel). A simplistic analysis of the effect of this on the dispersion would lead to a decrease in the movement of the counter-ions. The dielectric decrement does decrease a small amount when the magnetic field is applied (See Section 5.6.2), but this mechanism does not explain why the frequency of the dispersion increases when magnetic field is applied.

The enthalpy calculations in Section 5.6.5.1 show that the height of the potential energy barrier to relaxation is decreased by approximately 8% when magnetic field is applied ( $\Delta H = 4.45 \pm 0.08$  kcal mol<sup>-1</sup> to  $\Delta H = 4.08 \pm 0.08$  kcal mol<sup>-1</sup>.) The relatively high concentrations used in the present work could mean that interaction between neighbouring DNA chains would cause them to be perturbed from being perfectly straight rod-like structures. The re-orientating of the whole DNA molecule due to magnetic field would then tend to slightly straighten the DNA chain. According to the model of counter-ion condensation proposed by Manning (Manning, 1978), long-range overlap of the coulomb fields due to the regularly spaced phosphate groups, produces maximum delocalization of the counter-ions for straight polymer chains. Thus, the straighter the DNA chain, then the looser the residual attraction of the phosphate groups for the counter-ions. The straightening of the DNA chain would then lower the potential barrier and make it easier for the counter-ions to move. From Eyring's equation, the lowering of the potential barrier i.e. the enthalpy of activation of the transition state, would also cause the frequency of the dispersion to increase, as is found in the present work on application of magnetic field.

There may be a small decrease in entropy of activation by approximately 2% when the magnetic field is increased to its maximum value, indicating that the transition state with magnetic field is more ordered than that without magnetic field. The decrease in the Cole-Cole spreading parameter on application of magnetic field, i.e. a decrease in the spread of relaxation times, also points to an increase in order in the system. The magnetically-induced straightening of the DNA chain discussed above could cause the counter-ions and their hydration shells to show slightly more co-operative behaviour in the transition state, and hence decreased activation entropy. This could also be due to the effects of magnetic field on the orientation of the purine and pyrimidine rings having short-range localized effects on the movement of ions in the counter-ion sheath. Because of the uncertainty in the results however, the existence of the change in entropy with magnetic field is not certain. ( $-24.9 \pm 0.3$  cal mol<sup>-1</sup> K<sup>-1</sup> to  $-25.5 \pm 0.3$  cal mol<sup>-1</sup> K<sup>-1</sup>).

Thus the present work has shown that there is a dispersion in the low kHz region of the dielectric spectrum of DNA which is susceptible to magnetic fields as low as 0.66 Tesla. This dispersion is caused by co-operative relaxation of the hydrated counter-ions in a direction parallel to the longitudinal axis of the DNA chain. This relaxation is an activated process with activation energy similar in magnitude to the energy of a hydrogen bond in liquid water. The negative activation entropy indicates that the transition state displays a greater degree of order than the equilibrium state of the molecule, with the counter-ions and their bound water molecules moving co-operatively. This process is modified when magnetic field is applied because of the short-range effect of the magnetic re-orientation of nearby aromatic rings inside the DNA structure, and the tendency of the whole DNA chain to straighten under the influence of the magnetic field.

## 6.2 Further Work

Suggestions for further work include:

- It would be of interest to repeat the main experiment as described in Section 3.5.3 with samples of DNA of known molecular weights, with concentrations confirmed by spectrophotometry. Should the relaxation time of the proposed dispersion be proportional to the square of the molecular weight, this would confirm the mechanism suggested in Section 6.1.
- The main experiment could be repeated over a wider temperature range, especially at low temperatures, where the effect of d.c.conductivity would be lowered. Direct comparison could then be made between the dispersion derived from the difference signal and the HFP dispersion found by Sun (Sun et al., 2005) (See Section 5.10).
- The results for DNA dialized with different cations could be repeated over a range of temperatures, with concentrations confirmed by spectrophotometry. The effect of changing the cation on the activation energy and entropies would throw further light on the mechanism of the dispersion. It would also be of interest to repeat the main experiment on DNA dialized with Silver Chloride, since it is known that silver ions do not form charge clouds surrounding the DNA chain, but are bound to the bases in the interior of the DNA molecule.
- DNA has dispersions at frequencies in the MHz range, as detected by Time-Domain Reflectometry e.g.see Bone (Bone and Small, 1995). These dispersions are thought to be caused by fluctuations of counter-ions along short segments of the DNA chain. It would be of interest to examine whether these dispersions too were modified by the application of magnetic field.

- In Section 5.2, an initial test was carried out to determine how the dielectric loss of a solution of DNA was changed when the magnetic field surrounding the solution was first increased and then decreased, with readings being taken at one frequency only. With the apparatus available, the maximum rate at which the magnetic field could be changed was limited by the nature of the power supply control mechanism. Power supplies are available which are directly controlled by GPIB, hence enabling variation in the rate at which the current (and hence the magnetic field) changes. With such apparatus, it would perhaps be possible to investigate the rate at which the dielectric properties of DNA respond to the changing magnetic field.



# Appendices

# Appendix A

## WKLib

These are the procedures and functions concerned with communicating with the Wayne-Kerr Component Analyser via GPIB.

```
REM >WKLib
REM All procedures in this library start with W_

REM GPIB with Wayne Kerr

REM Assign these libraries
REM LIBRARY"<IEEE488$Dir>.BASICLib.BAS488"
REM LIBRARY"<IEEE488$Dir>.BASICLib.XBAS488"
REM LIBRARY ADFS::HardDisc4.$DNA.!AllLibs.WKLib

REM Because there are two GPIB devices using different eos$
REM Wayne-Kerr: PROCeos_out_1chr(10) and PROCeos_in_1chr(10)
REM Keithley: PROCeos_out_1chr(13) and PROCeos_in_1chr(13)
REM
REM The only function which uses the Keithley (FNG_GetVoltage)
REM Changes these to 13 at the start,
```

```
REM then changes them back to 10 at the end

REM Before starting, use these PROCs
REM PROCW_Variables: the frequencies used by the Wayne-Kerr as strings
REM PROCW_SetUpTheGPIBSystem
REM PROCW_SetSpeed
REM PROCW_SetVoltage(volts)
REM PROCW_SetBias(bias)

REM Parameters n%,f% etc. are position of frequency in array
REM 1=20Hz, 8=100Hz, 18=1kHz, 28=10kHz, 38=100kHz, 42=300kHz

REM PROCW_Sweep(z%,n1%,n2%)
REM PROCW_OneFrequency(n%)
REM FNW_OneLossReading(f%) :REM N.B. "Loss"=Conductance/Freq
REM FNW_OneCapacitanceReading(f%)

REM PROCW_Sweep_and_Save(file$,n1%,n2%)

REM Finish with this PROC
REM PROCren_false
REM Return to local control, and clear local lockout

REM Example
REM PROCW_Variables
REM PROCW_Assign_Libraries
REM PROCW_SetUpTheGPIBSystem
REM PROCW_SetSpeed
REM PROCW_SetVoltage(0.4)
REM wfile$="ADFS::HardDisc4.$DNA.WKRes"
REM PRINTTAB(5,5);"Start frequency sweep"
REM PROCW_Sweep_and_Save(wfile$,1,42)
REM PRINTTAB(5,7);"End frequency sweep  "
REM PROCren_false
REM END
```

```
DEFPROCW_Sweep_and_Save(sfile$,sn1%,sn2%)
LOCAL d%
d%=OPENOUT(sfile$)
PROCW_Sweep(d%,sn1%,sn2%)
CLOSE#d%
ENDPROC
```

```
DEFPROCW_SetVoltage(volts)
@%="+F10.1"
volt$="c;g;level"+STR$(volts)+"v"
PROCadrantoutput(w_mode%,w_device_adr%,volt$)
ENDPROC
```

```
DEFPROCW_SetSpeed
PROCadrantoutput(w_mode%,w_device_adr%,"AUTO;REP;NOR")
ENDPROC
```

```
DEFPROCW_SetBias(bias)
@%="+F10.1"
IF bias=0 THEN
    bias$="BSOF;BA0"
ELSE
    bias$="BSON;BA"+STR$(bias_voltage)+"v"
ENDIF
PROCadrantoutput(w_mode%,w_device_adr%,bias$)
ENDPROC
```

```
DEFPROCW_Sweep(z%,n1%,n2%)
REM z%=File-handle
LOCAL n%,p$
REM n1%=Freq no of lower freq in range (>=1)
```

```

REM n2%=Freq no of higher freq in range (<=42)
IF n1%<1 n1%=1
IF n2%>42 n2%=42
n%=n1%-1
REPEAT
  n%+=1
  PROCW_OneFrequency(n%)
  p$=Global_freq$+" "+Global_cap$
  p$+=" "+Global_con$+" "+Global_cdbf$
  BPUT#z%,p$
UNTIL n%>=n2%
ENDPROC

```

```

DEFPROCW_OneFrequency(f%)
REM Return with Global_cap,Global_con and Global_cdbf
LOCAL freq,freq$,ft%,a$,status1%,status2%,cap$,con$
REPEAT
  freq$="FREQ"+Global_f$(f%)
  PROCadrandoutput(w_mode%,w_device_adr%,freq$)
  PROCadrandoutput(w_mode%,w_device_adr%,"TRIGGER")
  ft%=TIME:REPEAT:UNTIL TIME>=ft%+1
  a$ = FNAdrandinput(w_mode%,w_device_adr%,255)
  ft%=TIME:REPEAT:UNTIL TIME>=ft%+1
  @%="+E10.5"
  status1%=FNXadrandinput(cap$,w_mode%,w_device_adr%,255)
  status2% = FNXadrandinput(con$,w_mode%,w_device_adr%,255)
  @%="+E10.5"
  Global_freq$=Global_f$(f%)
  Global_cap$=cap$
  Global_con$=con$
  freq=VAL(Global_freq$)
  con=VAL(con$)
  Global_cdbf=con/freq
  REM cdbf=Conductivity Divided by Frequency
  Global_cdbf$=STR$(Global_cdbf)

```

```
UNTIL INSTR(con$,"E")>0 AND INSTR(cap$,"E")>0
ENDPROC
```

```
DEFFNW_OneLossReading(f%)
LOCAL freq$,ft%,a$,con,freq
REPEAT
  freq$="FREQ"+Global_f$(f%)
  PROCadrandoutput(w_mode%,w_device_adr%,freq$)
  PROCadrandoutput(w_mode%,w_device_adr%,"TRIGGER")
  ft%=TIME:REPEAT:UNTIL TIME>=ft%+1
  a$ = FNadrandinput(w_mode%,w_device_adr%,255)
  ft%=TIME:REPEAT:UNTIL TIME>=ft%+1
  status1%=FNXadrandinput(cap$,w_mode%,w_device_adr%,255)
  status2% = FNXadrandinput(con$,w_mode%,w_device_adr%,255)
  con=VAL(con$)
  freq=VAL(Global_f$(f%))
  Loss=con/freq
UNTIL INSTR(con$,"E")>0 AND INSTR(cap$,"E")>0
=Loss
```

```
DEFFNW_OneCapacitanceReading(f%)
LOCAL freq$,ft%,a$,con,freq
REPEAT
  freq$="FREQ"+Global_f$(f%)
  PROCadrandoutput(w_mode%,w_device_adr%,freq$)
  PROCadrandoutput(w_mode%,w_device_adr%,"TRIGGER")
  ft%=TIME:REPEAT:UNTIL TIME>=ft%+1
  a$ = FNadrandinput(w_mode%,w_device_adr%,255)
  ft%=TIME:REPEAT:UNTIL TIME>=ft%+1
  status1%=FNXadrandinput(cap$,w_mode%,w_device_adr%,255)
  status2% = FNXadrandinput(con$,w_mode%,w_device_adr%,255)
  cap=VAL(cap$)
UNTIL INSTR(con$,"E")>0 AND INSTR(cap$,"E")>0
=cap
```

```
DEFPROCW_SetUpTheGPIBSystem
w_device_adr% = 6
sysctrl_adr% = 0
w_mode% = 0
PROCTimeout_period(40.0)
PROCTimeout_on
PROCEscape_on
PROCinit      :REM Sends REN, IFC, ATN=false
PROCEos_out_1chr(10)
PROCEos_in_1chr(10)
ENDPROC
```

```
DEFPROCW_Variables
LOCAL n%
DIM Global_f$(43)
RESTORE+2
FOR n%=1 TO 42
READ Global_f$(n%)
NEXT
DATA 20,25,30,40,50,60,80
DATA 100,120,150,200,250,300,400,500,600,800
DATA 1000,1200,1500,2000,2500,3000,4000,5000,6000,8000
DATA 10000,12000,15000,20000,25000,30000,40000,50000,60000,75000
DATA 100000,120000,150000,200000,300000
ENDPROC
```

```
DEFNNumber_from_freq(this_freq)
REM Get number n% of Global_f$(n%) from value of this_freq
REM Call PROCW_Variables first
LOCAL k%,Flag%,freq
k%=0
Flag%=0
```

```
REPEAT
  k%+=1
  freq=VAL(Global_f$(k%))
  IF freq>=this_freq THEN
    Flag%=1
  ENDIF
UNTIL n%>=42 OR Flag%=1
IF Flag%=0 =0
=k%
```

```
DEFPROCW_Error
PROCren_false
REM Return to local control, and clear local lockout
PRINTREPORT$; " at line ";ERL
ENDPROC
```

```
DEFPROCW_Assign_Libraries
LIBRARY"<IEEE488$Dir>.BASICLib.BAS488"
LIBRARY"<IEEE488$Dir>.BASICLib.XBAS488"
ENDPROC
```



# Appendix B

## KeithleyLib

These are the procedures and functions concerned with communicating with the Keithley 617 Programmable Electrometer via GPIB.

```
REM >KeithleyLib
REM Read temperature near sample, using Keithley Electrometer
REM via GPIB
REM All procedures called from this
REM library start with "G_"

REM LIBRARY ADFS::HardDisc4.$GPIB.II_Disc.Module.!IEEE488.
                                     BASICLib.BAS488
REM LIBRARY ADFS::HardDisc4.$GPIB.II_Disc.Module.!IEEE488.
                                     BASICLib.XBAS488
REM LIBRARY ADFS::HardDisc4.$DNA.!AllLibs.KeithleyLib

REM PROCG_SetUpTheGPIBSystem : Set up electrometer correctly
REM FNG_GetVoltage           : Read from electrometer
REM FNG_ChangeFormat(d$)    : Change from exponential format string
REM PROCG_Error
```

```
REM Because there are two GPIB devices using different eos$
REM Wayne-Kerr: PROCeos_out_1chr(10) and PROCeos_in_1chr(10)
REM Keithley: PROCeos_out_1chr(13) and PROCeos_in_1chr(13)
REM
REM The only function which uses the Keithley (FNG_GetVoltage)
REM changes these to 13 at the start, then changes them back
REM to 10 at the end.
```

```
DEFFNG_GetVoltage
LOCAL data$,voltage$
PROCeos_out_1chr(13)
PROCeos_in_1chr(13)
data$ = FNadrainput(g_mode%,g_device_adr%,255)
voltage$=FNG_ChangeFormat(data$)
PROCeos_out_1chr(10)
PROCeos_in_1chr(10)
voltage=VAL(voltage$)
=voltage
```

```
DEFFNG_ChangeFormat(d$)
LOCAL k,m,e,m$,e$,k$
m$=LEFT$(d$,8)
m=VAL(m$)
e$=MID$(d$,10,3)
e=VAL(e$)
k=m*(10^e)
@%="+F10.3"
k$=STR$(k)
=k$
```

```
DEFPROCG_SetUpTheGPIBSystem
g_device_adr% = 27
sysctrl_adr% = 0
```

```

g_mode% = 0
PROCtimeout_period(40.0)
PROCtimeout_on
PROCescape_on
PROCinit      :REM Sends REN, IFC, ATN=false
PROCadrandoutput(g_mode%,g_device_adr%,"FOX")
REM F0=Volts
PROCadrandoutput(g_mode%,g_device_adr%,"G1X")
REM G1=No prefix
PROCadrandoutput(g_mode%,g_device_adr%,"R3X")
REM R0=Auto R3=20volts
PROCadrandoutput(g_mode%,g_device_adr%,"C1XZ1XC0X")
REM Zero meter
PROCadrandoutput(g_mode%,g_device_adr%,"BOX")
REM Electrometer
PROCadrandoutput(g_mode%,g_device_adr%,"DOX")
REM Electrometer display
ENDPROC

```

```

DEFPROCG_Error
PROCren_false
REM Return to local control, and clear local lockout
text%=REPORT$+ "("+STR$(ERL)+)"
PROCG_CentreReprint(text$,640,300,7)
text%="Press any key"
PROCG_CentreReprint(text$,640,200,7)
gt=GET
text%=" The program has finished - Press SPACE twice "
PROCG_CentreReprint(text$,640,600,7)
gt=GET
PROCG_CentreReprint("",640,200,7)
END
ENDPROC

```

# Appendix C

## PSLib

These are the procedures and functions controlling the Power Supply via the RiscPC serial port to A3020 serial port link.

```
REM Main prog should start with:
REM LIBRARY "ADFS::HardDisc4.$.Comms.!IIDual.BASICLib.Serial"
REM and ...
REM LIBRARY "ADFS::HardDisc4.$.DNA.!AllLibs.PSLib"

REM These are the procedures in this library:

REM Switch Power supply ON
REM PROCPowerOn

REM Switch Power supply OFF
REM PROCPowerOff

REM Increase current by steps% (i.e. pulses to stepper motor)
REM reply$=FNPSIncrease(steps%)
```

```

REM Analyse result in this way:
REM IF LEFT$(reply$,2)="PI" THEN
REM   switch$=MID$(reply$,3,1)      :N=Normal, L=Limit
REM   steps_left$=MID$(reply$,4)    :Number of steps NOT
REM                                   used if limit reached

REM Decrease current by steps% (i.e. pulses to stepper motor)
REM reply$=FNPSDecrease(steps%)
REM Analyse result in this way:
REM   IF LEFT$(reply$,2)="PD" THEN
REM       switch$=MID$(reply$,3,1)  :N=Normal, Z=Zero
REM       steps_left$=MID$(reply$,4):Number of steps NOT
REM                                   used if zero reached

REM Decrease current until zero point reached
REM   ns$=FNMovetoZero
REM   MID$(ns$,4) gives total number of steps used

REM *****

REM Procedures and functions

REM *****

DEFPROCPSSetup
LOCAL n%
DIM Target_Current(12)
FOR n%=0 TO 12
Target_Current(n%)=n%/10
NEXT

DIM spha(11)
REM steps per hundredth Amp (increasing)
REM To get to Target_Current(n%) use spha(n%)
RESTORE +1
FOR n%=1 TO 11

```

```
    READ spha(n%)
NEXT
REM 230 = to get to 0.1, 60 = to get to 0.2
DATA 230,60
DATA 20,13,13,14,14,14,14,14,14

DIM sphad(11)
REM steps per hundredth Amp (decreasing)
REM To get to Target_Current(n%) use sphad(n%)
FOR n%=10 TO 0 STEP -1
    READ sphad(n%)
NEXT
REM 27 = to get to 1.0, 14 = to get to 0.9
DATA 27,14
REM Then
DATA 14,14,14,14,13,13,20,40,230
ENDPROC

DEFPROCPowerOn
LOCAL PSFlag%,sf$,sc$
REM Switch Power supply ON
REPEAT
    PSFlag%=0
    ps$=FNTransmit("PN")
    IF ps$="OK" THEN
        PSFlag%=1
    ELSE
        PSFlag%=0
    ENDIF
UNTIL PSFlag%=1
ENDPROC

DEFPROCPowerOff
```

```
LOCAL PSFlag%,sf$,sc$
REM Switch Power supply OFF
REPEAT
  PSFlag%=0
  ps$=FNTransmit("PF")
  IF ps$="OK" THEN
    PSFlag%=1
  ELSE
    PSFlag%=0
  ENDIF
UNTIL PSFlag%=1
ENDPROC
```

```
DEFPROCEnableOn
LOCAL ENFlag%,en$,ec$
REM Stepper Motor Enable ON
REM Increasing or decreasing current
REM enables ON before starting, and
REM enables OFF 2 seconds after stopping
REM Enabling is done in Worker program
REM so these procedures aren't needed.
REPEAT
  ENFlag%=0
  en$=FNTransmit("EN")
  IF en$="OK" THEN
    ENFlag%=1
  ELSE
    ENFlag%=0
  ENDIF
UNTIL ENFlag%=1
ENDPROC
```

```
DEFPROCEnableOff
LOCAL EFFlag%,ef$,ec$
```

```
REM Stepper Motor Enable OFF
REM Increasing or decreasing current
REM enables ON before starting, and
REM enables OFF 2 seconds after stopping
REM Enabling is done in Worker program
REM so these procedures aren't needed.
REPEAT
  EFFlag%=0
  ef$=FNTransmit("EF")
  IF ef$="OK" THEN
    EFFlag%=1
  ELSE
    EFFlag%=0
  ENDIF
UNTIL EFFlag%=1
ENDPROC

DEFFNPSIncrease(st%)
LOCAL PIFlag%,st$,si$
REM Increase current from power supply by st% steps
REM reply$
@%="+G10.5"
st$=STR$(st%)
REPEAT
  PIFlag%=0
  si$=FNTransmit("PSI"+st$)
  IF LEFT$(si$,2)="PI" THEN
    PIFlag%=1
  ELSE
    PIFlag%=0
  ENDIF
UNTIL PIFlag%=1
reply$=si$
=reply$
```



```
DEFFNPSDecrease(sd%)
LOCAL PDFlag%,sd$,si$
REM Decrease current from power supply by sd% steps
REM reply$
@%="+G10.5"
sd$=STR$(sd%)
REPEAT
  PDFlag%=0
  si$=FNTransmit("PSD"+sd$)
  IF LEFT$(si$,2)="PD" THEN
    PDFlag%=1
  ELSE
    PDFlag%=0
  ENDIF
UNTIL PDFlag%=1
reply$=si$
=reply$
```

```
DEFFNMoveToZero
LOCAL PZFlag%,sz$,si$
REM Decrease current from power supply until
REM Zero switch detected
REM Reply is MZZxxxx, where xxxx=No of steps used
REPEAT
  PZFlag%=0
  si$=FNTransmit("MZ")
  IF LEFT$(si$,3)="MZZ" THEN
    PZFlag%=1
  ELSE
    PZFlag%=0
  ENDIF
UNTIL PZFlag%=1
reply$=si$
=reply$
```

# Appendix D

## EuroLib

These are the procedures and functions concerned with communicating with the Eurotherm temperature controller using serial port protocols.

```
REM *****  
  
REM   - Library of procedures concerned with Eurotherm  
  
REM *****  
  
REM  PROCPrepare  
REM  FNEsendEnquiry(m$)  
REM  PROCESendNewValue(v$)  
REM  FNEReceive  
REM  PROCESend(A%)  
REM  PROCInitialize_Serial_Port  
REM  FNEReplyReceived  
REM  PROCInitialize  
REM  PROCESendAndConfirmSetPoint(Set_Point)  
REM  FNEReadTemp  
REM  FNEFindSetPoint
```

```

REM *****
REM PROCPrepare must be run at start of program
REM *****

```

```

DEFPROCPrepare
PROCInitialize
PROCInitialize_Serial_Port
ENDPROC

```

```

DEFNESendEnquiry(m$)
REM m$= 2 character mnemonic e.g. "SP"

```

```

    mnem1$=LEFT$(mnem$,1)
    mnem2$=MID$(mnem$,2,1)
    mnem_asc_1%=ASC(mnem1$)
    mnem_asc_2%=ASC(mnem2$)

```

```

    PROCesend(&4)           :REM EOT
    PROCesend(&30)          :REM GID
    PROCesend(&30)          :REM GID
    PROCesend(&30)          :REM UID
    PROCesend(&30)          :REM UID
    PROCesend(mnem_asc_1%)
    PROCesend(mnem_asc_2%)
    PROCesend(&5)           :REM ENQ

```

```

REM Monitor Serial port until
REM received string <> "0"
j%=0
REPEAT
    j%+=1
    IF j%>1 PROCesend(&15)

```

```

    r$=FNERReplyReceived
    UNTIL j%>=20 OR r$<>"0"

    REM IF rb%(4)=4 i.e. EOT, mnemonic has not been recognised
    IF rb%(4)=4 THEN
        ="0"
    ENDIF

    IF r$<>"0" AND bcc%=0 THEN
        tr$=""
        FOR n%=1 TO LEN(r$)-1 STEP 2
            a$=(MID$(r$,n%,2))
            IF a$="" a$="11"
            a%=EVAL("&"+a$)
            IF a%>&20 THEN
                c$=CHR$(a%)
                tr$+=c$
            ENDIF
        NEXT
        ltr%=LEN(tr$)
        ntr$=MID$(tr$,3,ltr%)
        ntr=VAL(ntr$)
        @%="+G10.5"
    ENDIF
=ntr

DEFPROCSEndNewValue(t$)
    REM t$ = "SL18" i.e. mnemonic and value
    L%=LEN(t$)
    bcc%=0
    FOR C%=1 TO L%
        B%=ASC(MID$(t$,C%,1))
        bcc%=bcc% EOR B%
    NEXT
    bcc%=bcc% EOR 3

```

```

REPEAT
    SYS"IIDual_SendBreak",Eport%,2
    PROCESend(4) :REM EOT - End of Transmission
    PROCESend(&30) :REM GID - Group address Identifier
    PROCESend(&30) :REM GID - Group address Identifier - repeated
    PROCESend(&30) :REM UID - Unit address Identifier
    PROCESend(&30) :REM UID - Unit address Identifier - repeated
    PROCESend(2) :REM STX - Start of Text
    FOR C%=1 TO L%
        B%=ASC(MID$(t$,C%,1))
        PROCESend(B%)
    NEXT
    PROCESend(3) :REM ETX - End of Text
    PROCESend(bcc%) :REM - verification digit
    reply%=FNEReceive
UNTIL reply%=6
ENDPROC

```

```

DEFFNEReceive
SYS"IIDual_SendBreak",Eport%,2
REM 4 = Get a byte from the Serial buffer
REPEAT
    SYS"IIDual_GetByte",Eport% TO ,B% ;C%
    C%=C% AND &2
UNTIL C%<>0
rt%=TIME
REM Get more bytes from the Serial buffer
REPEAT
    SYS"IIDual_GetByte",Eport% TO ,B% ;C%
    C%=C% AND &2
UNTIL (C%=0 AND (B%=6 OR B%=15)) OR TIME>rt%+200
REM Return value of return byte
=B%

```

```

DEFPROCsend(A%)
LOCAL F1
REPEAT
SYS"IIDual_SendByte",Eport%,A% TO ;F1
UNTIL (F1 AND &2 )=0
ENDPROC

```

```

DEFPROCInitialize_Serial_Port
REM 0 = Read/Write Serial status
SYS"IIDual_ReadWriteSerialStatus",Eport%,&B6,&FFFFFF00
REM 1 = Initilise Serial Port 9600 Baud 7 data 1 start
REM      1 Stop Even Parity
SYS"IIDual_ReadWriteDataFormat",Eport%,&19
REM 5 = Baud Receive Baud rate (0=9600)
SYS"IIDual_ReadWriteRxBaudRate",Eport%,0
REM 6 = Baud Transmit Baud rate (0=9600)
SYS"IIDual_ReadWriteTxBaudRate",Eport%,0
ENDPROC

```

```

DEFFNEReplyReceived
rec$=""
SYS"IIDual_SendBreak",Eport%,2
REM 4 = Get a byte from the Serial buffer
REPEAT
  SYS"IIDual_GetByte",Eport% TO ,B% ;C%
  C%=C% AND &2
UNTIL C%<>0
REM Include this byte in rb%
REM rec$+=STR$~(B%)
rb%(0)=B%
REM Initialize variables to zero
rt%=TIME
nrb%=0

```

```

bcc%=0

REM Get more bytes from the Serial buffer
REM calculating bcc% verification digit after STX (2)
REPEAT
  SYS"IIDual_GetByte",Eport% TO ,B% ;C%
  C%=C% AND &2
  IF C%=0 THEN
    nrb%+=1
    b$=STR$~(B%)
    IF LEN(b$)=1 b$="0"+b$
    rec$+=b$
    rb%(nrb%)=B%
    IF nrb%>1 bcc%=bcc% EOR B%
  ENDIF
UNTIL B%=6 OR B%=15 OR TIME>rt%+200
REM tnrb%= Total number of bytes obtained
tnrb%=nrb%
REM Return list of captured ASCII values as string rec$
REM and as values in rb%(n%), n%=0 TO tnrb%
REM bcc% should be 0
REM If mnemonic not recognised rb%(4)=4
=rec$

DEFPROCInitialize
DIM rb%(100)
DIM sb%(100)
DIM Set_Temp$(100)
DIM Set_Temp(100)
ENDPROC

DEFPROCSendAndConfirmSetPoint(Set_Point)
LOCAL Set_Point$,Check_set_point
REM Send set point command to Eurotherm, and check it

```

```
@%="+G10.3"  
Set_Point$="SL"+STR$(Set_Point)  
REPEAT  
    PROCESendNewValue(Set_Point$)  
    Check_set_point=FNESendEnquiry("SP")  
UNTIL Check_set_point=Set_Point  
ENDPROC
```

```
DEFFNReadTemp  
Actual_temp=0  
REPEAT  
    Actual_temp=FNESendEnquiry("PV")  
UNTIL Actual_temp<>0  
=Actual_temp
```

```
DEFFNEFindSetPoint  
=FNESendEnquiry("SP")
```



# Appendix E

## MMLib

These are the procedures and functions for reading the current being measured by the multimeter using serial port protocols.

```
REM Main prog should contain the next line
REM LIBRARY "ADFS::HardDisc4.$Comms.!IIDual.BASICLib.Serial"
REM ... and
REM LIBRARY "ADFS::HardDisc4.$DNA.!AllLibs.MMLib"
```

```
REM Start with:
REM PROCMMInitialize_Serial_Port(1)
```

```
REM Get current with:
b=FNMMGetCurrent(1)
```

```
DEFNMMGetCurrent(MMport%)
LOCAL Flag%,a$
Flag%=0
REPEAT
  PROCMMSend(ASC("P"),MMport%)
```

```

a$=FNMMReceive(MMport%)
IF LEFT$(a$,2)="DC" AND RIGHT$(a$,1)="A" Flag%=1
UNTIL Flag%=1
=FNMMValueOfCurrent(a$)

```

```

DEFNMMValueOfCurrent(c$)
LOCAL mult,k%,l%,n$,pn$
IF RIGHT$(c$,2)="mA" mult=1E-3 ELSE mult=1
l%=LEN(c$)
k%=0
n$=""
REPEAT
  k%+=1
  pn$=MID$(c$,k%,1)
  IF INSTR("0123456789.",pn$)>0 n$+=pn$
UNTIL k%>=l%
v=mult*(VAL(n$))
=v

```

```

DEFNMMReceive(MMport%)
LOCAL byte%,flags%,att%
REM Receive a string
data$=""
REPEAT
  REPEAT
    SYS"IIDual_GetByte",MMport% TO ,byte% ;flags%
  UNTIL (flags% AND %0010) = %0000
  IF byte%>31 data$+=CHR$(byte%)
  att%=TIME:REPEAT:UNTIL TIME>=att%+5
UNTIL FNSerial_ReadEntriesInBuf(MMport%)=0
=data$

```

```

DEFPROCMMSend(A%,MMport%)

```

```
LOCAL F1
REPEAT
REM SYS"OS_SerialOp",3,A% TO ;F1
SYS"IIDual_SendByte",MMport%,A% TO ;F1
UNTIL (F1 AND &2 )=0
ENDPROC

DEFPROCMMInitialize_Serial_Port(MMport%)
REM 0 = Read/Write Serial status
REM SYS"OS_SerialOp",0,&96,&FF00
SYS"IIDual_ReadWriteSerialStatus",MMport%,&96,&FFFFFF00

REM 1 = Initilise Serial Port 7 data 2 Stop No Parity
REM SYS"OS_SerialOp",1,5
SYS"IIDual_ReadWriteDataFormat",MMport%,&5

REM 5 = Baud Receive Baud rate (12=600)
REM SYS"OS_SerialOp",5,12
SYS"IIDual_ReadWriteRxBaudRate",MMport%,12

REM 6 = Baud Transmit Baud rate (12=600)
REM SYS"OS_SerialOp",6,12
SYS"IIDual_ReadWriteTxBaudRate",MMport%,12

REM PROCSerial_FlushInBuf(MMport%)
WHILE FNSerial_ReadEntriesInBuf(MMport%)>0
b$=FNMMReceive(MMport%)
ENDWHILE

ENDPROC
```

# Appendix F

## GenLib

This is a General Library of procedures used by the RiscPC to communicate with the A3020 over the serial port to serial port link.

```
REM Main prog should contain:
```

```
REM LIBRARY "ADFS::HardDisc4.$DNA.!AllLibs.GenLib"
```

```
REM List of procedures:
```

```
REM Initialise Ordinary serial port
```

```
REM PROCInitialize_Serial_Port
```

```
REM Quit both Master and Worker programmes
```

```
REM PROCQuit
```

```
REM Read RH (in main part of vacuum system)
```

```
REM RH_val=FNGetRH
```

```
REM Read Temperature
```

```
REM Temp_val=FNGetTemp
```

```
REM Wait t seconds, showing time at upper
REM right of screen
REM PROCWait(t,"sec")

REM Wait t seconds, without display
REM PROCSimpleWait(t,"sec")

REM Get the first part of the string, up
REM to the first space
REM String then becomes the rest of the original string
REM FNStripString(a$)

REM Similar to StripString, but convert to number
REM FNStripNumber(a$)

REM *****

REM The procedures above use the following
REM functions and procedures:

REM *****

REM Function to transmit a string to worker
REM Get back a string which is related to t$
REM rec$=FNTransmit(tr$)

REM Procedure which does the transmitting
REM PROCStringTransmit(tr$)

REM Procedure to send ASCII digit
REM PROCsend(A%)

REM Receive a string back from the A3020
REM r$=FNReceive

REM Strip spaces from a string
```

```
REM used to clear up string returned from A3020
REM FNStripSpaces(p$)
```

```
DEFPROCQuit
LOCAL QUFlag%,qu$
REPEAT
  QUFlag%=0
  qu$=FNTransmit("QU")
  IF qu$="OK" THEN
    QUFlag%=1
  ELSE
    QUFlag%=0
  ENDIF
UNTIL QUFlag%=1
ENDPROC
```

```
DEFNGetTemp
LOCAL tv$,tp$,TVFlag%
REPEAT
  TVFlag%=0
  tv$=FNTransmit("TV")
  IF LEFT$(tv$,2)="TV" THEN
    TVFlag%=1
    @="+F10.1"
    tp$=MID$(tv$,3)
    tp=VAL (tp$)
  ELSE
    TVFlag%=0
  ENDIF
UNTIL TVFlag%=1
=tp
```

```
DEFNGetRH
```

```

LOCAL hv$,rh$,RHFlag%
REPEAT
  RHFlag%=0
  hv$=FNTransmit("RH")
  IF LEFT$(hv$,2)="RH" THEN
    RHFlag%=1
    @%="+F10.1"
    rh$=MID$(hv$,3)
    rh=VAL (rh$)
  ELSE
    RHFlag%=0
  ENDIF
UNTIL RHFlag%=1
=rh

```

```

DEFNTransmit(tr$)
LOCAL
REM transmit a string to worker
REM Get back a string which is related to t$
PROCStringTransmit(tr$)
r$=FNReceive
r$=FNStripSpaces(r$)
=r$

```

```

DEFNStripSpaces(p$)
LOCAL k%,OK$,np$,pp$,l%
REM Strip p$ of all chars except A-Z,0-9, and .
OK$="ABCDEFGHIJKLMNOPQRSTUVWXYZ0123456789."
k%=0
l%=LEN(p$)
np$=""
REPEAT
  k%+=1
  pp$=MID$(p$,k%,1)

```

```

    IF INSTR(OK$,pp$)>0 THEN
        np$+=pp$
    ENDIF
UNTIL k%>=1%
=np$

DEFPROCStringTransmit(a$)
LOCAL n%,ln%,pa%,pa$
REM Transmit characters in a$
REM 2 = Enable Input from serial port
SYS"OS_Byte",2,2
ln%=LEN(a$)
n%=0
REPEAT
    n%+=1
    pa$=MID$(a$,n%,1)
    pa%=ASC(pa$)
    IF pa%>=0 AND pa%<=255 THEN
        PROCsend(pa%)
    ENDIF
UNTIL n%>=ln%
PROCsend(13)
REM tm%=TIME:REPEAT:UNTIL TIME>tm%+20
ENDPROC

```

```

DEFPROCsend(A%)
LOCAL F1
REPEAT
SYS"OS_SerialOp",3,A% TO ;F1
UNTIL (F1 AND &2 )=0
ENDPROC

```

```

DEFFNReceive

```



```

LOCAL k%
rec$=" "
REM 2 = Enable Input from serial port
SYS"OS_Byte",2,2
REM 4 = Get a byte from the Serial buffer
REPEAT
SYS"OS_SerialOp",4 TO ,B% ;C%
C%=C% AND &2
UNTIL C%<>0
REPEAT
    SYS"OS_SerialOp",4,256 TO ,B% ;C%
    C%=C% AND &2
    IF C%=0 THEN rec$+=CHR$(B%)
UNTIL B%=13 OR B%=10
k%=LEN(rec$)-1
rec$=LEFT$(rec$,k%)
=rec$

DEFPROCInitialize_Serial_Port
    REM 5 = Baud Receive Baud rate (4=1200)
    SYS"OS_SerialOp",5,4
    REM 6 = Baud Transmit Baud rate (4=1200)
    SYS"OS_SerialOp",6,4
    REM 1 = Initilise Serial Port 7 data 1 Stop odd Parity 1200 Baud
    SYS"OS_SerialOp",1,9
    REM 0 = Read/Write Serial status
    SYS"OS_SerialOp",0,&6,&FF00
    REM flow control = Hardware handshaking using CTS
    REM (ignoring both DCD and DSR) and RTS
ENDPROC

DEFPROCWait(t,unit$)
LOCAL nt%,t%,gt5$,ag%,eag%,peag%,message$,d_o_Flag$
REM Wait t seconds

```

```

nt%=INT(t)
gt5$="n"
ag%=TIME
t%=TIME+t*100
peag%=0
REPEAT
  eag%=INT((TIME-ag%)/100)
  message$=""
  IF eag%<>peag% THEN
    @%="+G10.5"
    message$+="Wait "+STR$(eag%)+"/"+STR$(nt%)
    PROCcentreReprint(message$,1250,1100,0)
    peag%=eag%
  ENDIF
  gt5$=INKEY$(2)
  gt5$=LEFT$(gt5$,1)
  IF INSTR("Qq",gt5$)>0 AND gt5$<>"" THEN PROCError
UNTIL TIME>=t%
ENDPROC

```

```

DEFPROCsimpleWait(t,unit$)
LOCAL t%
REM Wait t seconds
t%=TIME+t*100
REPEAT
UNTIL TIME>=t%
ENDPROC

```

```

DEFNStripString(RETURN sa$)
nsa$=""
REM Get rid of leading spaces
WHILE LEFT$(sa$,1)=" "
  sa$=MID$(sa$,2)
ENDWHILE

```

```
REM Read until first double space
s_pos%=INSTR(sa$," ")
string$=MID$(sa$,1,s_pos%-1)
REM Return remainder of string as sa$
sa$=MID$(sa$,s_pos%+1)
REM Result of function is first part of string
=string$

DEFFNStripNumber(RETURN sa$)
REM Get rid of leading spaces
WHILE LEFT$(sa$,1)=" "
  sa$=MID$(sa$,2)
ENDWHILE
REM Read until first double space
s_pos%=INSTR(sa$," ")
REM Result of function is first part of string
quan$=MID$(sa$,1,s_pos%-1)
REM Return remainder of string as sa$
sa$=MID$(sa$,s_pos%+1)

REM Check that result of function only contains numbers
new_quan$=""
FOR sn%=1 TO LEN(quan$)
  a$=MID$(quan$,sn%,1)
  IF INSTR("+-0123456789E",a$)>0 new_quan$+=a$
NEXT

=VAL(new_quan$)
```

# Appendix G

## ShowLib

These are the procedures and functions concerned with:

- Controlling the initialization of the GPIB and serial connections;
- Printing on the screen of the RiscPC.

```
REM >ShowLib
```

```
REM Display checks before main program starts
```

```
REM PROCCheckSwitches
```

```
REM PROCChecklist
```

```
REM Printing procedures
```

```
REM PROClrp(text$,xfrac,yfrac,c%)
```

```
REM PROCcrc(text$,yfrac,c%)
```

```
REM PROCPrint(text$,x%,y%,c%)
```

```
REM PROCcentrePrint(text$,x%,y%,c%)
```

```
REM PROCleftReprint(text$,x%,y%,c%)
```

```
REM PROCcentreReprint(text$,x%,y%,c%)
```

```
REM PROCrightReprint(text$,x%,y%,c%)
```

```
REM PROCclearScreen
```

```
DEFPROCCheckSwitches
```

```
PROCclearScreen
```

```
REM Make sure switch boxes are at B
```

```
text$="Both Switch-boxes to position B,"
```

```
PROCcrc(text$,0.8,0)
```

```
text$="Adjust Next slot to maximum,"
```

```
PROCcrc(text$,0.7,0)
```

```
REM text$="Switch Wayne-Kerr and Keithley ON."
```

```
text$="Switch Wayne-Kerr ON."
```

```
PROCcrc(text$,0.6,0)
```

```
text$="Press any key when these are correct"
```

```
PROCcrc(text$,0.4,0)
```

```
text$="Otherwise quit with ALT-Break"
```

```
PROCcrc(text$,0.2,11)
```

```
gt$=GET$
```

```
ENDPROC
```

```
DEFPROCChecklist
```

```
PROCclearScreen
```

```
REM Set up GPIB for Wayne-Kerr
```

```
text$="Checklist of Setup procedures"
```

```
PROCcrc(text$,0.85,0)
```

```
PROCW_Variables
```

```
text$="Wayne-Kerr set up variables OK"
```

```
PROCcrc(text$,0.75,11)
```

```
PROCW_SetUpTheGPIBSystem
```

```
text$="Wayne-Kerr Set up GPIB OK"
```

```
PROCcrc(text$,0.7,11)
```

```
PROCW_SetSpeed
```

```
text$="Wayne-Kerr Set Speed OK"
```

```
PROCcrc(text$,0.65,11)
```

```
PROCW_SetVoltage(0.4)
```

```
text$="Wayne-Kerr Voltage set to 0.4v OK"
```

```

PROCcrc(text$,0.60,11)
REM Set up GPIB for Keithley Electrometer
PROCG_SetUpTheGPIBSystem
text$="Keithley setup OK"
PROCcrc(text$,0.55,11)
REM Initialize link with A3020
PROCInitialize_Serial_Port
text$="Link with A3020 initialised"
PROCcrc(text$,0.50,11)
REM Initialize link with Multimeter
PROCMMInitialize_Serial_Port(1)
text$="Link with multimeter initialised"
PROCcrc(text$,0.45,11)
text$="Press any key"
PROCcrc(text$,0.35,11)
text$="Otherwise quit with ALT-Break"
PROCcrc(text$,0.2,11)
gt$=GET$
PROCClearScreen
text$="Press key when Worker program is ready"
PROCcrc(text$,0.3,0)
text$="Otherwise quit with ALT-Break"
PROCcrc(text$,0.2,11)
gt$=GET$
ENDPROC

```

```

DEFPROCPrint(text$,x%,y%,c%)
IF c%=0 GCOL0,0,0,0
IF c%=7 GCOL0,255,255,255
IF c%=11 GCOL0,255,0,0
VDU5
MOVE x%,y%
PRINTtext$;
ENDPROC

```

```

DEFPROCCentrePrint(text$,x%,y%,c%)

```

```

LOCAL l%
l%=8*LEN(text$)
x%=x%-l%-10
PROCPrint(text$,x%,y%,c%)
ENDPROC

```

```

DEFPROCSetGlobalOverlap(xgo%,ygo%)
Global_x_Overlap%=xgo%
Global_y_Overlap%=ygo%
ENDPROC

```

```

DEFPROCLeftReprint(text$,x%,y%,c%)
LOCAL l%,xoverlap%,yoverlap%,w%,h%
xoverlap%=Global_x_Overlap%
yoverlap%=Global_y_Overlap%
l%=16*LEN(text$)
rx%=x%-xoverlap%
ry%=y%-2*yoverlap%
rw%=(2*xoverlap%)+l%
rh%=(2*yoverlap%)+10
REM GCOL0,2
GCOL0,255,255,255
RECTANGLE FILL rx%,ry%,rw%,rh%
PROCPrint(text$,x%,y%,c%)
ENDPROC

```

```

DEFPROCllrp(text$,xfrac,yfrac,c%)
PROCLeftReprint(text$,Global_xs*xfrac,Global_ys*yfrac,c%)
ENDPROC

```

```

DEFPROCcrc(text$,yfrac,c%)
REM Centre Reprint(text$,Global_midx,Global_ys*yfrac,c%)
PROCCentreReprint(text$,Global_midx,Global_ys*yfrac,c%)
ENDPROC

```

```

DEFPROCCentreReprint(text$,x%,y%,c%)

```

```

LOCAL l%,xoverlap%,yoverlap%,w%,h%
xoverlap%=Global_x_Overlap%
yoverlap%=Global_y_Overlap%
l%=16*LEN(text$)
rx%=x%-l%/2-xoverlap%
ry%=y%-2*yoverlap%
rw%=2*xoverlap%+l%
rh%=2*yoverlap%+10
GCOLOR,255,255,255
RECTANGLE FILL rx%,ry%,rw%,rh%
PROCCentrePrint(text$,x%,y%,c%)
ENDPROC

```

```

DEFPROCRightReprint(text$,x%,y%,c%)
LOCAL l%,xoverlap%,yoverlap%,w%,h%
xoverlap%=Global_x_Overlap%
yoverlap%=Global_y_Overlap%
l%=16*LEN(text$)
rx%=x%-l%-xoverlap%
ry%=y%-2*yoverlap%
rw%=(2*xoverlap%)+l%
rh%=(2*yoverlap%)+10
GCOLOR,255,255,255
RECTANGLE FILL rx%,ry%,rw%,rh%
PROCPrint(text$,x%-l%,y%,c%)
ENDPROC

```

```

DEFPROCClearScreen
LOCAL width,height,wh_low_margin,bl_left_overlap
LOCAL bl_base_overlap,wh_x_lo,wh_y_lo,bl_x_lo
LOCAL bl_y_lo
  Global_xs=1600
  Global_ys=1200
  Global_midx=0.5*Global_xs
  REM Clear Screen to grey
  GCOLOR,160,160,160

```



```
RECTANGLE FILL 0,0,Global_xs,Global_ys
REM Do white window with black shadow
width=0.9*Global_xs
height=0.9*Global_ys
wh_low_margin=80
bl_left_overlap=30
bl_base_overlap=30
wh_x_lo=(Global_xs-width)/2
wh_y_lo=wh_low_margin
bl_x_lo=wh_x_lo-bl_left_overlap
bl_y_lo=wh_y_lo-bl_base_overlap
REM Black?
GCOL0,0,0,0
RECTANGLE FILL bl_x_lo,bl_y_lo,width,height
REM White
GCOL0,255,255,255
RECTANGLE FILL wh_x_lo,wh_y_lo,width,height
GCOL0,0,0,0
RECTANGLE wh_x_lo,wh_y_lo,width,height
Global_x_Overlap%=40
Global_y_Overlap%=40
ENDPROC
```

# Appendix H

## Main Program

This is the listing of the main program as described in Section 3.2.13.

```
PROCChecklist
```

```
PROCPSSetUp
```

```
REM Set up Power supply
```

```
PROCESendNewValue("SL25.0")
```

```
REM Set up the temperature of the experiment
```

```
u%=OPENOUT("logfile")
```

```
total_reps%=221
```

```
rep_no%=0
```

```
max_i%=0
```

```
max_i_direction%=1
```

```
REPEAT
```

```
Time1%=TIME
```

```
IF max_i_direction%=1 THEN
    max_i%+=1
    IF max_i%>=11 Max_i_Flag%=-1 ELSE Max_i_Flag%=1
ENDIF

IF max_i_direction%=-1 THEN
    max_i%-=1
    IF max_i%<=1 Max_i_Flag%=1 ELSE Max_i_Flag%=-1
ENDIF

max_i_direction%=Max_i_Flag%

REM Get directory in which 3 scan files are to be saved
rep_no%+=1
rep_name$="Rep"+STR$(rep_no%)

REM Create directory
OSCLI("cdir "+rep_name$)

REM Inside Reprn, the first file is for zero current (s01)
REM and the next file are for maximum current (s02)
REM and the last for zero current (s03)

PROCSingleFrequencyRun(rep_name$,"s01")

REM Now increase the current/mag field to max_i%

PROCPowerOn

ThisI=FNMMGetCurrent(1)

n%=0
switch$="N"

REPEAT
```

```
n%+=1

Next_current=Target_Current(n%)
REM This is the next target

Diff_current=Next_current-ThisI

IF Diff_current>0 THEN

    Change_factor=100*Diff_current
    steps%=Change_factor*spha(n%)

    reply$=FNPSIncrease(steps%)
    switch$=MID$(reply$,3,1)

    ThisI=FNMMGetCurrent(1)

ELSE
    REM Miss out next current value

ENDIF

UNTIL n%>=max_i% OR ThisI>=1.1 OR switch$="L"

REM Check that current has reached Target_Current(max_i%)

Diff_current=Target_Current(max_i%)-ThisI

IF Diff_current>0.01 THEN

    Change_factor=100*Diff_current
    steps%=Change_factor*spha(n%)
    reply$=FNPSIncrease(steps%)

ENDIF

ENDIF
```

```
REM Now do frequency sweep
PROCSingleFrequencyRun(rep_name$, "s02")

REM Now decrease maximum current
n%=max_i%

ThisI=FNMMGetCurrent(1)

REPEAT

    n%-=1

    Next_current=Target_Current(n%)
    REM This is the next target

    Diff_current=ThisI-Next_current

    IF Diff_current>0 THEN

        Change_factor=100*Diff_current

        steps%=Change_factor*sphad(n%)

        IF n%>0 THEN
            reply$=FNPSDecrease(steps%)
            switch$=MID$(reply$,3,1)
        ELSE
            REM This is when n%=0
            ns$=FNMoveToZero
            switch$=MID$(reply$,3,1)
        ENDIF

        ThisI=FNMMGetCurrent(1)
```

```
ELSE
    REM Miss out next current value

ENDIF

UNTIL n%<=0 OR ThisI<=0.07 OR switch$="Z"

PROCPowerOff

PROCSingleFrequencyRun(rep_name$, "s03")

REM Wait 20 minutes
REM store RH, temp etc every minute
C_Flag%=0
Time1%=TIME
LTP_Time%=TIME
Prev_Change_Time%=0
REPEAT

    Time2%=TIME
    Change_Time%=(Time2%-Time1%) DIV 100
    REM in seconds

    REM store RH, temp etc every minute
    LTP_now%=TIME
    LTP_change%=(LTP_now%-LTP_Time%)/100 :REM In seconds
    IF LTP_change%>=60 THEN
        LTP_Time%=TIME
        PROCStoreValues :REM store in log file
    ENDIF

    IF Change_Time%>=20*60 THEN
        C_Flag%=1
    ELSE
```

```
        C_Flag%=0
    ENDIF

UNTIL C_Flag%=1

UNTIL rep_no%>=total_reps%

PROCren_false :REM Restore local control to GPIB equipment

END

DEFPROCSingleFrequencyRun(folder$,file$)

REM folder$=Repn
REM file$=s01, s02 or s03

filename$=folder$+"."+file$

REM Get time from start
this_time=TIME-Time1%
this_time$=STR$(this_time)

REM Get temperature of cabinet
tmp=FNGetTemp
tmp$=STR$(tmp)

REM Get Local RH via ADC
lrh=FNGetRH
lrh$=STR$(lrh)

REM Used for local temperature
REM via Keithley
ltp=FNG_GetVoltage
```

```
ltp$=STR$(ltp)

REM Get current
cur_I=FNMMGetCurrent(1)
cur_I$=STR$(cur_I)

p$=this_time$+" "
p$+=folder$+" "
p$+=file$+" "
p$+=tmp$+" "
p$+=lrh$+" "
p$+=ltp$+" "
p$+=cur_I$

REM store all values in logfile
BPUT#u%,p$

REM Open file to store data
w%=OPENOUT(filename$)
n%=0
REPEAT
  n%+=1
  PROCW_OneFrequency(n%)
  res$=Global_freq$+" "+Global_cap$
  res$+=" "+Global_con$+" "+Global_cdbf$
  BPUT#w%,res$
UNTIL n%>=42
CLOSE#w%

ENDPROC
```



# Appendix I

## Worker Program

This is the listing of the Worker program running on the A3020 as described in Section 3.2.12.2.

```
ON ERROR:PROCError:END
REM Worker program on A3020
REM to obey commands from Master program on RiscPC
REM via serial cable

REM *****
REM On both programs
REM *****
PROCInitialize_Serial_Port
PROCClearScreen

REM User port set up
REM 4 O/P lines (F) and 4 I/P lines (0)
REM &62 = Data direction register
SYS"OS_Byte",151,&62,&0F
PROCUserPortSend(0)
```

```

PowerFlag%=0
EnableFlag%=0

REM time to wait between clock
REM cycles to stepper motor
ttg%=1

REM *****
REM Only on Worker
REM *****
RH_Gradient=1
RH_Offset=0
text$="Press key when ready to receive"
PROCCentreReprint(text$,600,800,7)
gt$=GET$
text$="Ready"
PROCCentreReprint(text$,600,800,7)

EndFlag%=0
REPEAT
  r$=FNReceive
  r$=FNStripSpaces(r$)
  REM PRINTTAB(5,5);r$;"
  text$="          From RiscPC = "+r$+"
  PROCCentreReprint(text$,600,800,7)
  rep$=FNProcess(r$)
  IF rep$="Quit" THEN
    rep$="OK"
    EndFlag%=1
  ENDIF
  PROCStringTransmit(rep$)
  text$="          From procedure = "+rep$+"
  PROCCentreReprint(text$,600,700,7)
UNTIL EndFlag%=1
END

```

```

DEFNProcess(p$)
IF p$="RH" THEN =FNGetARH
IF p$="HU" THEN =FNGetHumilab
IF p$="TV" THEN =FNGetATemp
IF p$="PN" THEN =FNPowerOn
IF p$="PF" THEN =FNPowerOff
IF p$="EN" THEN =FNEnableStepperMotorOn
IF p$="EF" THEN =FNEnableStepperMotorOff
IF LEFT$(p$,3)="PSI" THEN =FNPSIncrease(p$)
IF LEFT$(p$,3)="PSD" THEN =FNPSDecrease(p$)
IF p$="MZ" THEN =FNMoveToZero
IF p$="QU" THEN ="Quit"
="UNKNOWN"

```

REM User Port procedures

```

DEFNUserPortReceive
REM Read from user port
REM &60 = Input/Output register B
SYS"OS_Byte",150,&60 TO ,,b%
b%=b% AND 48
=b%

```

```

DEFPROCUserPortSend(A%)
REM &60 = Input/Output register B
SYS"OS_Byte",151,&60,A%
ENDPROC

```

```

DEFNPowerOn
LOCAL tot%
text$="          Power On          "
PROCCentreReprint(text$,600,600,7)
PowerFlag%=1
tot%=EnableFlag%*2

```

```
tot%+=PowerFlag%*8
PROCUserPortSend(tot%)
="OK"
```

```
DEFFNPowerOff
LOCAL tot%
text$="          Power Off          "
PROCCentreReprint(text$,600,600,7)
PowerFlag%=0
tot%=EnableFlag%*2
tot%+=PowerFlag%*8
PROCUserPortSend(tot%)
="OK"
```

```
DEFFNEnableStepperMotorOn
LOCAL tot%
EnableFlag%=1
tot%=EnableFlag%*2
tot%+=PowerFlag%*8
PROCUserPortSend(tot%)
="OK"
```

```
DEFFNEnableStepperMotorOff
LOCAL tot%
EnableFlag%=0
tot%=EnableFlag%*2
tot%+=PowerFlag%*8
PROCUserPortSend(tot%)
="OK"
```

```
DEFFNPSIncrease(i$)
LOCAL steps$,steps%,tm%,m%,t%,hi_val%,lo_val%
LOCAL tt%,ok$,a%,a$
REM Increase Current from power supply by i% steps
REM i%=MID$(i$,4)
REM Return with "PI"+switch$(N or L)+steps% not used
```

```

text$="          Increase Current          "
PROCCentreReprint(text$,600,600,7)
reply$="OK"
steps$=MID$(i$,4)
steps%=VAL(steps$)
IF steps%>0 THEN
  REM Enable stepper motor
  ok$=FNEnableStepperMotorOn
  lo_val%=1+(EnableFlag%*2)+(PowerFlag%*8)
  hi_val%=1+(EnableFlag%*2)+4+(PowerFlag%*8)
  PROCUserPortSend(lo_val%)
  m%=0
  t%=steps%
  REPEAT
    m%+=1
    t%-=1
    PROCUserPortSend(lo_val%)
    text$="Clock pulses = "+STR$(m%)
    PROCCentreReprint(text$,600,500,11)
    tt%=TIME:REPEAT:UNTIL TIME>=tt%+ttg%
    PROCUserPortSend(hi_val%)
    a%=FNUserPortReceive :REM Switches
    a$=STR$(a%)
    text$="Input = "+a$
    PROCCentreReprint(text$,600,400,11)
  UNTIL m%>=steps% OR a%=16
  @%="+G10.5"
  reply$="PIN"+STR$(t%)
  IF a%=32 reply$="PIZ"+STR$(t%)
  IF a%=16 reply$="PIL"+STR$(t%)
  REM Enable OFF after 2 seconds
  tm%=TIME:REPEAT:UNTIL TIME>=tm%+200
  ok$=FNEnableStepperMotorOff
ENDIF
=reply$

```

```

DEFNPSDecrease(d$)
LOCAL steps$,steps%,tm%,m%,t%,hi_val%,lo_val%
LOCAL tt%,ok$,a%,a$
REM Decrease Current from power supply by i% steps
REM i%=MID$(i$,4)
REM Return with "PD"+switch$(N or Z)+steps% not used
reply$="NoSteps"
steps%=MID$(d$,4)
text$="Decrease Current "+d$+" (" +steps$+" ) "
PROCCentreReprint(text$,600,600,7)
steps%=VAL(steps$)
IF steps%>0 THEN
  REM Enable stepper motor
  ok$=FEnableStepperMotorOn
  lo_val%=0+(EnableFlag%*2)+(PowerFlag%*8)
  hi_val%=0+(EnableFlag%*2)+4+(PowerFlag%*8)
  PROCUserPortSend(lo_val%)
  m%=0
  t%=steps%
  REPEAT
    m%+=1
    t%-=1
    PROCUserPortSend(lo_val%)
    text$="Clock pulses = "+STR$(m%)
    PROCCentreReprint(text$,600,500,11)
    tt%=TIME:REPEAT:UNTIL TIME>=tt%+ttg%
    PROCUserPortSend(hi_val%)
    a%=FNUserPortReceive :REM Switches
    a$=STR$(a%)
    text$="Input = "+a$
    PROCCentreReprint(text$,600,400,11)
  UNTIL m%>=steps% OR a%=32
  @%="+G10.5"
  reply$="PDN"+STR$(t%)
  IF a%=32 reply$="PDZ"+STR$(t%)
  IF a%=16 reply$="PDL"+STR$(t%)

```

```

    REM Enable OFF after 2 seconds
    tm%=TIME:REPEAT:UNTIL TIME>=tm%+200
    ok%=FNEnableStepperMotorOff
ENDIF
=reply$

DEFNMovetoZero
LOCAL steps$,steps%,tm%,m%,t%,hi_val%,lo_val%
LOCAL tt%,ok$,a%,a$
REM Decrease Current from power supply
REM until zero switch detected
REM return with no of stps used
text$="          Current to Zero          "
PROCCentreReprint(text$,600,600,7)
reply$="NoSteps"
REM Enable stepper motor
ok%=FNEnableStepperMotorOn
lo_val%=0+(EnableFlag%*2)+(PowerFlag%*8)
hi_val%=0+(EnableFlag%*2)+4+(PowerFlag%*8)
PROCUserPortSend(lo_val%)
m%=0
REPEAT
    m%+=1
    PROCUserPortSend(lo_val%)
    text$="Clock pulses = "+STR$(m%)
    PROCCentreReprint(text$,600,500,11)
    tt%=TIME:REPEAT:UNTIL TIME>=tt%+ttg%
    PROCUserPortSend(hi_val%)
    a%=FNUserPortReceive :REM Switches
    a%=STR$(a%)
    text$="Input = "+a$
    PROCCentreReprint(text$,600,400,11)
UNTIL a%=32
@%="+G10.5"
reply$="MZZ"+STR$(m%)

```

```
REM Enable OFF after 2 seconds
tm%=TIME:REPEAT:UNTIL TIME>=tm%+200
ok$=FNEnableStepperMotorOff
=reply$
```

```
DEFFNGetATemp
LOCAL tp
text$="          Get temperature          "
PROCCentreReprint(text$,600,600,7)
@%="+F10.1"
tp=FNTemperature(1000)
IF tp>=0 THEN
    tv$="TV"+STR$(tp)
ELSE
    tv$="UNKNOWN"
ENDIF
=tv$
```

```
DEFFNGetARH
LOCAL rh
text$="          Get RH          "
PROCCentreReprint(text$,600,600,7)
@%="+F10.2"
rh=FNReal_RH(5000)
IF rh>=0 THEN
    rh$="RH"+STR$(rh)
ELSE
    rh$="UNKNOWN"
ENDIF
=rh$
```

```
DEFFNGetHumilab
LOCAL hv
@%="+F10.2"
hv=FNHumilab_reading(3000)
hr$="HU"+STR$(hv)
```



```

=hr$

DEFNStripSpaces(p$)
LOCAL k%,OK$,np$,pp$,l%
REM Strip p$ of all chars except A-Z,0-9, and .
OK$="ABCDEFGHIJKLMNOPQRSTUVWXYZ0123456789."
k%=0
l%=LEN(p$)
np$=""
REPEAT
  k%+=1
  pp$=MID$(p$,k%,1)
  IF INSTR(OK$,pp$)>0 THEN
    np$+=pp$
  ENDIF
UNTIL k%>=l%
=np$

DEFPROCStringTransmit(a$)
LOCAL n%,ln%,pa%,pa$
REM Transmit characters in a$
REM 2 = Enable Input from serial port
SYS"OS_Byte",2,2
ln%=LEN(a$)
n%=0
REPEAT
  n%+=1
  pa$=MID$(a$,n%,1)
  pa%=ASC(pa$)
  IF pa%>=0 AND pa%<=255 THEN
    PROCsend(pa%)
  ENDIF
UNTIL n%>=ln%
PROCsend(13)
REM tm%=TIME:REPEAT:UNTIL TIME>tm%+20
ENDPROC

```

```

DEFPROCsend(A%)
LOCAL F1
REPEAT
SYS"OS_SerialOp",3,A% TO ;F1
UNTIL (F1 AND &2 )=0
ENDPROC

DEFNReceive
LOCAL k%,ams%,hyd_ams%,Flag%
FSFlag%=0
rec$=" "
REM 2 = Enable Input from serial port
SYS"OS_Byte",2,2
REM 4 = Get a byte from the Serial buffer
REPEAT
SYS"OS_SerialOp",4 TO ,B% ;C%
C%=C% AND &2
UNTIL C%<>0
text$="Waiting for serial buffer data      "
ams%=TIME
PROCCentreReprint(text$,600,200,7)
REPEAT
  SYS"OS_SerialOp",4,256 TO ,B% ;C%
  C%=C% AND &2
  IF C%=0 THEN rec$+=CHR$(B%)
  IF PowerFlag%=1 THEN
    hyd_ams%=(TIME-ams%)/(100*60)
    IF hyd_ams%>=15 FSFlag%=1
  ENDIF
UNTIL B%=13 OR B%=10 OR FSFlag%=1
k%=LEN(rec$)-1
rec$=LEFT$(rec$,k%)
IF FSFlag%=1 THEN
  rec$="FS"
  text$="      *** Failsafe condition ***      "

```

```

ELSE
    text$=rec$+" detected on serial buffer      "
ENDIF
PROCcentreReprint(text$,600,200,7)
=rec$

DEFPROCInitialize_Serial_Port
    REM 5 = Baud Receive Baud rate (4=1200)
    SYS"OS_SerialOp",5,4
    REM 6 = Baud Transmit Baud rate (4=1200)
    SYS"OS_SerialOp",6,4
    REM 1 = Initilise Serial Port 7 data 1 Stop odd Parity 1200 Baud
    SYS"OS_SerialOp",1,9
    REM 0 = Read/Write Serial status
    SYS"OS_SerialOp",0,&6,&FF00
    REM flow control = Hardware handshaking using CTS
    REM (ignoring both DCD and DSR) and RTS
ENDPROC

DEFPROCError
PRINTTAB(5,5);REPORT$;" at line ";ERL
END
ENDPROC

DEFPROCPrint(text$,x%,y%,c%)
GCOL0,c%
VDU5
MOVE x%,y%
PRINTtext$;
ENDPROC

DEFPROCReprint(text$,x%,y%,c%)
LOCAL l%,overlap%,w%,h%
overlap%=20
l%=16*LEN(text$)
rx%=x%-overlap%

```

```

ry%=y%-2*overlap%
rw%=2*overlap%+1%
rh%=2*overlap%+10
GCOLOR,0
RECTANGLE FILL rx%,ry%,rw%,rh%
PROCPrint(text$,x%,y%,c%)
ENDPROC

DEFPROCcentrePrint(text$,x%,y%,c%)
LOCAL l%
l%=8*LEN(text$)
x%=x%-l%-10
PROCPrint(text$,x%,y%,c%)
ENDPROC

DEFPROCcentreReprint(text$,x%,y%,c%)
LOCAL l%,overlap%,w%,h%
overlap%=20
l%=16*LEN(text$)
rx%=x%-l%/2-overlap%
ry%=y%-2*overlap%
rw%=2*overlap%+1%
rh%=2*overlap%+10
GCOLOR,0
RECTANGLE FILL rx%,ry%,rw%,rh%
PROCcentrePrint(text$,x%,y%,c%)
ENDPROC

DEFPROCrightReprint(text$,x%,y%,c%)
LOCAL l%,overlap%,w%,h%
overlap%=20
l%=16*LEN(text$)
rx%=x%-l%-overlap%
ry%=y%-2*overlap%
rw%=2*overlap%+1%
rh%=2*overlap%+10

```

```
GCOL0,0
RECTANGLE FILL rx%,ry%,rw%,rh%
PROCPrint(text$,x%,y%,c%)
ENDPROC

DEFPROCclearScreen
LOCAL width,height,wh_low_margin,bl_left_overlap
LOCAL bl_base_overlap,wh_x_lo,wh_y_lo,bl_x_lo
LOCAL bl_y_lo
    REM Clear Screen to grey
    GCOL0,2
    RECTANGLE FILL 0,0,1279,960
    REM Do white window with black shadow
    width=1100
    height=800
    wh_low_margin=100
    bl_left_overlap=20
    bl_base_overlap=20
    wh_x_lo=(1280-width)/2
    wh_y_lo=wh_low_margin
    bl_x_lo=wh_x_lo-bl_left_overlap
    bl_y_lo=wh_y_lo-bl_base_overlap
    GCOL0,7
    RECTANGLE FILL bl_x_lo,bl_y_lo,width,height
    GCOL0,0
    RECTANGLE FILL wh_x_lo,wh_y_lo,width,height
    GCOL0,7
    RECTANGLE wh_x_lo,wh_y_lo,width,height
ENDPROC

DEFFNTemperature(tttotal%)
LOCAL ch%,t
ch%=3
t=FNVoltage(ch%,tttotal%)
t=t*100
=t
```

```

DEFNReal_RH(rhtotal%)
LOCAL Hum_rh
Hum_rh=FNHumilab_reading(rhtotal%)
Real_RH=(RH_Gradient*Hum_rh) + (RH_Offset)
=Real_RH

DEFNHumilab_reading(rttotal%)
LOCAL ch%,v
ch%=1
v=FNVoltage(ch%,rttotal%)
v=v*100
=v

DEFNVoltage(vch%,vttotal%)
LOCAL VRef,Reading,Ref_Reading,m,c
REM Reads average voltage on channel vch%
REM over vttotal% readings with reference
REM to the external voltage on CH2
VRef=1.227
m=1+1.771E-3
c=-1.367E-3
Reading=FNReadAdval(vch%,vttotal%)
Ref_Reading=FNReadAdval(2,vttotal%)
voltage=Reading*VRef/Ref_Reading
voltage=m*voltage+c
=voltage

DEFNReadAdval(ch%,total%)
REM Gives Average of total% readings on channel ch%
REM with maximum 4096
LOCAL n%,t
t=0
n%=0
REPEAT
  n%+=1

```

```

    t+=ADVAL(ch%)/16
UNTIL n%>=total%
Global_adc=t/n%
=Global_adc

DEFPROCWait(t,unit$)
LOCAL nt%,t%,gt5$,ag%,eag%,peag%,message$,d_o_Flag$
REM Wait t seconds
nt%=INT(t)
gt5$="n"
ag%=TIME
t%=TIME+t*100
peag%=0
REPEAT
    eag%=INT((TIME-ag%)/100)
    message$=""
    IF eag%<>peag% THEN
        @%="+G10.5"
        message$+="Wait "+STR$(eag%)+"/"+STR$(nt%)
        PROCCentreReprint(message$,1050,850,7)
        peag%=eag%
    ENDIF
    gt5$=INKEY$(2)
    gt5$=LEFT$(gt5$,1)
    IF INSTR("Qq",gt5$)>0 AND gt5$<>" THEN PROCError
UNTIL TIME>=t%
ENDPROC

DEFPROCSimpleWait(t,unit$)
LOCAL t%
REM Wait t seconds
t%=TIME+t*100
REPEAT
UNTIL TIME>=t%
ENDPROC

```

```

DEFNStripString(RETURN sa$)
nsa$=""
REM Get rid of leading spaces
WHILE LEFT$(sa$,1)=" "
  sa$=MID$(sa$,2)
ENDWHILE
REM Read until first double space
s_pos%=INSTR(sa$," ")
string$=MID$(sa$,1,s_pos%-1)
REM Return remainder of string as sa$
sa$=MID$(sa$,s_pos%+1)
REM Result of function is first part of string
=string$

DEFNStripNumber(RETURN sa$)
REM Get rid of leading spaces
WHILE LEFT$(sa$,1)=" "
  sa$=MID$(sa$,2)
ENDWHILE
REM Read until first double space
s_pos%=INSTR(sa$," ")
REM Result of function is first part of string
quan$=MID$(sa$,1,s_pos%-1)
REM Return remainder of string as sa$
sa$=MID$(sa$,s_pos%+1)

REM Check that result of function only contains numbers
new_quan$=""
FOR sn%=1 TO LEN(quan$)
  a$=MID$(quan$,sn%,1)
  IF INSTR(" +-.0123456789E",a$)>0 new_quan$+=a$
NEXT

=VAL(new_quan$)

```



# Appendix J

## MATLAB programs - analysis of Dielectric data

These are the MATLAB programs which use the Genetic Algorithm toolbox to analyse the dielectric spectrum into three dispersions with d.c. conductivity. They are:

- WGA3\_LF.m
- WCC3\_LF.m
- W\_Get\_data(A)

### J.1 WGA3\_LF.m

```
clc
clear
name_file='diel_a.txt';
```

```
W_Get_data(name_file);

gen=400000;
pop=500^2;
games=50;

%base = results files will be called baseXX.txt
base='a_';
res='cd Results1';
home='cd ..';

global f_pts
global exp_permit
global exp_loss
global mod_permit
global mod_loss
global time
global options

%set up x vector (fill with random data)
for z = 1:11
    x(z) = rand;
end

%set the limits for mutation
%dE and alpha
dE_min(1) = 0;
dE_max(1) = 9e6;
a_min(1) = 0.00;
a_max(1) = 0.25;

dE_min(2) = 0;
dE_max(2) = 9e6;
a_min(2) = 0;
a_max(2) = 0.25;
```

```

dE_min(3) = 0;
dE_max(3) = 9e6;
a_min(3) = 0;
a_max(3) = 0.25;

%Ensures f1<f2 and f2<f3
f_mult_min(1) = 0.001;
f_min(2) = 100;
f_mult_min(3) = 1.01;

f_mult_max(1) = 0.99;
f_max(2) = 2000;
f_mult_max(3) = 100;

Ei_min = 0;
Ei_max = 3500;

Sigma_min = 1e-9;
Sigma_max = 1e-5;

tic;
startP2=clock;

mutation_limits = [dE_min(1) f_mult_min(1) a_min(1) ...
                  dE_min(2) f_min(2) a_min(2)...
                  dE_min(3) f_mult_min(3) a_min(3)...
                  Ei_min Sigma_min; ...
                  dE_max(1) f_mult_max(1) a_max(1) ...
                  dE_max(2) f_max(2) a_max(2)...
                  dE_max(3) f_mult_max(3) a_max(3) ...
                  Ei_max Sigma_max];
options = gaoptimset('PopInitRange', mutation_limits);

%set the GA options
options = gaoptimset(options, 'Generations', gen, ...
                    'TimeLimit', inf, 'StallGenLimit', 5, ...

```

```

        'StallTimeLimit', inf);
options = gaoptimset(options, 'tolfun', 10^-7);
options = gaoptimset(options, 'PopulationSize', pop);
options = gaoptimset(options, 'CrossoverFraction', 0.8);
options = gaoptimset(options, 'MutationFcn', {@mutationuniform, 1});
options = gaoptimset(options, 'EliteCount', 4);

for game = 1:games
    t_game=int2str(game);
    start_tm_this_game=clock;
    [GA_x_values(game,:) fit_error(game,:)] = ga(@WCC3_LF,11,options);
    disp(['fit_error = ', num2str(fit_error(game,:))]);
    end_tm_this_game=clock;
    diff_tm_this_game=etime(end_tm_this_game,start_tm_this_game);
    textt1=sprintf('%-.0f',round(diff_tm_this_game));
    disp(['Time this game = ',textt1,' seconds']);
    diff_tm_this_part=etime(end_tm_this_game,startP2);
    textt2=sprintf('%-.0f',round(diff_tm_this_part));
    disp(['Time this Part = ',textt2,' seconds']);
    disp(' ');

    if game>=1
        eval([res]);
        if length(t_game)==1
            t_game=['0',t_game];
        end
        text_file=[base,t_game,'.txt'];
        tfid=fopen(text_file,'wt');

        endP2=clock;
        diffP2=etime(endP2,startP2);

        texta=sprintf('%-.0f \n',diffP2);
        textb=sprintf('%-.0f ',game);
        textc=sprintf('%-.0f ',sqrt(pop));
        textc=[textc,'^2'];
    end
end

```

```

textd=sprintf('%.0f \n',gen);
w_text=['Time' = ',texta,' Num games = ',...
        textb,' Pop = ',textc,' Gen = ',textd];
fprintf(tfid,w_text);
disp(w_text);
text=['      '];
fprintf(tfid,' %s \n',text);

%take mean and stdev of xvalues and fit error
%for saving as the result for those games
final_x_values_mean = mean(GA_x_values,1);
%mean(vals,1)=mean of columns, mean(vals,2)=mean of rows
final_x_values_stdev = std(GA_x_values,0,1);
%0=ordinary formula, 1=std of column values
final_x_values_pc=100*(final_x_values_stdev./final_x_values_mean);
final_fit_error_mean = mean(fit_error);
final_fit_error_stdev = std(fit_error);

%Values from this game only
textb=sprintf('%.0f ',game);
text=['For this game ',textb];
fprintf(tfid,text);
text='      ';
fprintf(tfid,' %s \n',text);

%Size of dispersion
text=['dE1', ' = '];
fprintf(tfid,' %s ',text);
fprintf(tfid,'% -8.3f ',(GA_x_values(game,1)));
%Frequency
text=[' f1', ' = '];
fprintf(tfid,' %s ',text);
fprintf(tfid,'% -8.0f ',((GA_x_values(game,2))...
                        *(GA_x_values(game,5))));
%Cole-Cole parameter
text=[' a1', ' = '];

```

```

fprintf(tfid,' %s ',text);
fprintf(tfid,'% -8.2f ',(GA_x_values(game,3)));
text=['      '];
fprintf(tfid,' %s \n',text);

text=['dE2', ' = '];
fprintf(tfid,' %s ',text);
fprintf(tfid,'% -8.3f ',(GA_x_values(game,4)));
%Frequency
text=[' f2', ' = '];
fprintf(tfid,' %s ',text);
fprintf(tfid,'% -8.0f ',((GA_x_values(game,5))));
%Cole-Cole parameter
text=[' a2', ' = '];
fprintf(tfid,' %s ',text);
fprintf(tfid,'% -8.2f ',(GA_x_values(game,6)));
text=['      '];
fprintf(tfid,' %s \n',text);

text=['dE3', ' = '];
fprintf(tfid,' %s ',text);
fprintf(tfid,'% -8.3f ',(GA_x_values(game,7)));
%Frequency
text=[' f3', ' = '];
fprintf(tfid,' %s ',text);
fprintf(tfid,'% -8.0f ',((GA_x_values(game,8))...
*(GA_x_values(game,5))));
%Cole-Cole parameter
text=[' a3', ' = '];
fprintf(tfid,' %s ',text);
fprintf(tfid,'% -8.2f ',(GA_x_values(game,9)));

text=['      '];
fprintf(tfid,' %s \n',text);
text=['      '];
fprintf(tfid,' %s \n',text);

```

```

%Epsilon infinity
text=['Ei', ' = '];
fprintf(tfid, ' %s ', text);
fprintf(tfid, '%-8.0f ', (GA_x_values(game,10)));

%Sigma
text=['sigma', ' = '];
fprintf(tfid, ' %s ', text);
fprintf(tfid, '%-8.3f ', (GA_x_values(game,11)));

text=['      '];
fprintf(tfid, ' %s \n', text);

text=['      '];
fprintf(tfid, ' %s \n', text);

%Mean values for all games so far

for dip = 1:3
    dip_count=dip-1;

    %Size of dispersion
    text=['dE', int2str(dip), ' = '];
    fprintf(tfid, ' %s ', text);
    fprintf(tfid, '%-8.2f ', (final_x_values_mean(dip_count*3+1)));

    text=['      '];
    fprintf(tfid, ' %s ', text);
    fprintf(tfid, '%-8.2f ', (final_x_values_stdev(dip_count*3+1)));

    text=[' % = '];
    fprintf(tfid, ' %s ', text);
    fprintf(tfid, '%-8.0f \n', (final_x_values_pc(dip_count*3+1)));

%Frequency

```

```

text=['f',int2str(dip),' = '];
fprintf(tfid,' %s ',text);
fprintf(tfid,'%8.0f ',final_x_values_mean(dip_count*3+2));

text=['  '];
fprintf(tfid,' %s ',text);
fprintf(tfid,'%8.0f ',final_x_values_stdev(dip_count*3+2));

text=[' % = '];
fprintf(tfid,' %s ',text);
fprintf(tfid,'%8.0f \n',(final_x_values_pc(dip_count*3+2)));

%Cole-Cole parameter
text=['a',int2str(dip),' = '];
fprintf(tfid,' %s ',text);
fprintf(tfid,'%8.2f ',final_x_values_mean(dip_count*3+3));

text=['  '];
fprintf(tfid,' %s ',text);
fprintf(tfid,'%8.2f ',final_x_values_stdev(dip_count*3+3));

text=[' % = '];
fprintf(tfid,' %s ',text);
fprintf(tfid,'%8.0f \n',(final_x_values_pc(dip_count*3+3)));

text=['      '];
fprintf(tfid,' %s \n',text);
end

%Epsilon dash infinity
text=['Ei',' = '];
fprintf(tfid,' %s ',text);
fprintf(tfid,'%8.0f ',final_x_values_mean(10));

text=['  '];
fprintf(tfid,' %s ',text);

```



```

fprintf(tfid,'%8.0f ',final_x_values_stdev(10));

text=[' % = '];
fprintf(tfid,' %s ',text);
fprintf(tfid,'%8.0f \n',final_x_values_pc(10));

%Sigma
text=['Sigma', ' = '];
fprintf(tfid,' %s ',text);
fprintf(tfid,'%8.3e ',final_x_values_mean(11));

text=['  '];
fprintf(tfid,' %s ',text);
fprintf(tfid,'%8.3e ',final_x_values_stdev(11));

text=[' % = '];
fprintf(tfid,' %s ',text);
fprintf(tfid,'%8.0f \n',final_x_values_pc(11));

text=['  '];
fprintf(tfid,' %s \n',text);

text=['mean fit_error per point for each game'];
fprintf(tfid,' %s \n',text);
fprintf(tfid,' %8.2e \n',fit_error/42);

text=['  '];
fprintf(tfid,' %s \n',text);

text=['Mean:'];
fprintf(tfid,' %s \n',text);
fprintf(tfid,'%8.5e \n',final_x_values_mean);

text=['StDev: '];
fprintf(tfid,' %s \n',text);
fprintf(tfid,'%8.5e \n',final_x_values_stdev);

```

```
text=['Error Mean: ');
fprintf(tfid,' %s \n',text);
fprintf(tfid,'%8.5e \n',final_fit_error_mean);
disp(['Error_mean = ', num2str(final_fit_error_mean)]);

text=['Error StDev: Part ',int2str(rhan)];
fprintf(tfid,' %s \n',text);
fprintf(tfid,'%8.5e \n',final_fit_error_stdev);

%Close text_file
fclose(tfid);

eval([home]);

end

end
```

## J.2 WCC3\_LF

```
function [fit_error] = WCC3_LF(x)
%based on Cole-Cole Equation
%Calculates model spectra and fit
%error between model and experimental.

global f_pts
global exp_permit
global exp_loss
global Etot
global mod_permit
global mod_loss
```

```

%Calculate Modelled data fit from starting values
%convert to angular frequency
w = 2*pi*f_pts;

% dielectric values
dE(2)= x(4);
f(2) = x(5);
a(2) = x(6);

dE(1)= x(1);
f(1)= x(2)*x(5);
a(1)= x(3);

dE(3)= x(7);
f(3)= x(8)*x(5);
a(3)= x(9);

Ei=x(10);

Sigma=x(11);

%calculate the total effective complex permittivity from
%combination of dispersions
[s,t]=(size(w));
Eind=zeros(s,3);
for k=1:3/1;          %assumes Ei dispersions plus Ei
    T(k)=1./(2*pi*f(k));
    Eind(:,k) = (dE(k))./(1+(i.*w*T(k)).^(1-a(k)));
    %calculates permittivities of each dispn for each frequency
end;

Etot=Ei+Eind(:,1)+Eind(:,2)+Eind(:,3);
%adds all contributions from each dispersion for each frequency

mod_permit = real(Etot);

```

```

%defines modelled permittivity

%modelled loss = (ac_loss + d.c.conductivity)
mod_loss = (imag(Etot)+(Sigma./(w*8.854E-12)));

diff_permit = mod_permit - exp_permit;
diff_loss = mod_loss - exp_loss;

fit_error = sum(sqrt(((diff_permit).^2)+((diff_loss).^2)));

```

### J.3 W\_Get\_data(A)

```

function []= W_Get_data(A)
%loads data file with frequency, permittivity and loss

%clear all;
global exp_permit;
global exp_loss;
global data1;
global f_pts;

%import data file from cdata directory
cd cdata;
fid=fopen(A);
data1=fscanf(fid,'%g %g %g',[3 inf]);
data1=data1';
f_pts=data1(:,3);
exp_permit=data1(:,1);
exp_loss=data1(:,2);
fclose(fid);
cd ..;

```

# Appendix K

## MATLAB programs - analysis of Difference Signal

These are the MATLAB programs which use the Genetic Algorithm toolbox to analyse the Difference Signal i.e. the difference between the dielectric spectrum obtained with and without the application of a magnetic field. They are:

- Diff\_main.m
- diff\_calc.m
- diff\_get\_data

### K.1 Diff\_main

```
clc  
clear
```

```
for part = 1:3

    pop_part2=200^2;
    gen_part2=400000;
    games=50;
    game_print=games-1;

    switch part

    case 1
        base='a_';
        name_file='data_a.txt';
        diff_get_data(name_file);
        number_disps=1;

    case 2
        base='b_';
        name_file='data_b.txt';
        diff_get_data(name_file);
        number_disps=1;

    case 3
        base='c_';
        name_file='data_c.txt';
        diff_get_data(name_file);
        number_disps=1;

    end

    % Directory where results are saved
    res='cd Results1';
    home='cd ..';

    global f_pts;
    %global exp_permit
    global exp_loss;
```

```
%global mod_permit
global mod_loss;
global diff_loss;
global time;
global options;

%set up x vector (fill with random data)
for z = 1:11
    x(z) = rand;
end

%set the limits for mutation
%dE1 and alpha and f
%Change as appropriate

dE_min(1) = 1.0e5;
dE_max(1) = 9.9e5;
f_min(1) = 1000;
f_max(1) = 3000;
a_min(1) = 0.05;
a_max(1) = 0.20;

mult_dE_min=0.5;
mult_dE_max=1.5;
% dE2>=dE1 or dE2<dE1
mult_f_min=1.0001;
mult_f_max=2.0;
% f2>f1
mult_a_min=0.1;
mult_a_max=1.5;

sigma_min(1)=1.0E-9;
sigma_max(1)=9.9E-8;
mult_sigma_min=0.1;
mult_sigma_max=10000;
```

```

% start of section to process data
t_part=int2str(part);
tic;
startP2=clock;

clear fit_error;
clear GA_x_values;

mutation_limits = [dE_min(1) f_min(1) a_min(1) ...
                  mult_dE_min mult_f_min mult_a_min ...
                  sigma_min(1) mult_sigma_min; ...
                  dE_max(1) f_max(1) a_max(1)...
                  mult_dE_max mult_f_max mult_a_max ...
                  sigma_max(1) mult_sigma_max];

options = gaoptimset('PopInitRange', mutation_limits);

%set the GA options
options = gaoptimset(options, 'Generations', gen_part2, ...
                    'TimeLimit', inf, 'StallGenLimit', ...
                    5, 'StallTimeLimit', inf);
options = gaoptimset(options, 'tolfun', 10^-7);
options = gaoptimset(options, 'PopulationSize', pop_part2);
options = gaoptimset(options, 'CrossoverFraction', 0.8);
options = gaoptimset(options, 'MutationFcn', {@mutationuniform, 1});
options = gaoptimset(options, 'EliteCount', 4);

disp(['Starting Part',t_part]);
disp(['Population Part',t_part,' = ', ...
      num2str(round(sqrt(pop_part2))),'^2']);
disp(['  ']);

for game = 1:games
    t_game=int2str(game);
    start_tm_this_game=clock;
    [GA_x_values(game,:) fit_error(game,:)] = ga(@diff_calc, 8, options);

```



```

disp(['Part = ', t_part,' game = ', int2str(game), ...
      ' Population = ',num2str(sqrt(pop_part2)),'^2']);
disp(['fit_error = ', num2str(fit_error(game,:))]);
end_tm_this_game=clock;
diff_tm_this_game=etime(end_tm_this_game,start_tm_this_game);
textt1=sprintf('%-.0f',round(diff_tm_this_game/60));
disp(['Time this game = ',textt1,' minutes']);
diff_tm_this_part=etime(end_tm_this_game,startP2);
textt2=sprintf('%-.0f',round(diff_tm_this_part/60));
disp(['Time this Part = ',textt2,' minutes']);
disp(' ');

if game>=game_print

    eval([res]);
    if length(t_part)==1
        t_part=['0',t_part];
    end
    if length(t_game)==1
        t_game=['0',t_game];
    end
    text_file=[base,t_game,'.txt'];
    tfid=fopen(text_file,'wt');

    endP2=clock;
    diffP2=etime(endP2,startP2);
    diffP2=diffP2./3600;

    texta=sprintf('%.3f ',diffP2);
    texta=[texta,' hours \n'];
    textb=sprintf('%-.0f ',game);
    textc=sprintf('%-.0f ',sqrt(pop_part2));
    textc=[textc,'^2'];
    textd=sprintf('%-.0f \n',gen_part2);

```

```

w_text=['File = ',name_file,' Time for Part',t_part,...
        ' = ',texta, 'Num games = ',textb,' Pop = ',...
        textc,' Gen = ',textd];
fprintf(tfid,w_text);
disp(w_text);

text=['      '];
fprintf(tfid,' %s \n',text);

%take mean and stdev of xvalues and fit error for
%saving as the result for those games
final_x_values_mean = mean(GA_x_values,1);

%mean(vals,1)=mean of columns, mean(vals,2)=mean of rows
final_x_values_stdev = std(GA_x_values,0,1);

final_x_values_pc=100*(final_x_values_stdev./final_x_values_mean);

final_fit_error_mean = mean(fit_error);
final_fit_error_stdev = std(fit_error);

%Mean values up to this game
text=['Mean including this game (Game',textb,')'];
fprintf(tfid,text);
text='      ';
fprintf(tfid,' %s \n',text);

%Size of dispersion
text=['dE', ' = '];
fprintf(tfid,' %s ',text);
fprintf(tfid,'%-.8.3f ',(final_x_values_mean(1)));
fprintf(tfid,'%-.8.3f ',(final_x_values_mean(1)...
                    *final_x_values_mean(4)));

text=' Mult = ';
fprintf(tfid,' %s ',text);

```

```

fprintf(tfid,'%8.3f ',final_x_values_mean(4));

text='  ';
fprintf(tfid,'%s',text);
fprintf(tfid,'%8.3f ',(final_x_values_stdev(1)));

text='  % = ';
fprintf(tfid,'%s',text);
fprintf(tfid,'%8.0f \n',(final_x_values_pc(1)));

%Frequency
text=[' f', ' = '];
fprintf(tfid,' %s ',text);
fprintf(tfid,'%8.0f ',(final_x_values_mean(2)));
fprintf(tfid,'%8.0f ',(final_x_values_mean(2)...
                *final_x_values_mean(5)));
text='  Mult = ';
fprintf(tfid,' %s ',text);
fprintf(tfid,'%8.3f ',final_x_values_mean(5));
text='  ';
fprintf(tfid,'%s',text);
fprintf(tfid,'%8.0f ',(final_x_values_stdev(2)));
text='  % = ';
fprintf(tfid,'%s',text);
fprintf(tfid,'%8.0f \n',(final_x_values_pc(2)));

%Cole-Cole parameter
text=[' a', ' = '];
fprintf(tfid,' %s ',text);
fprintf(tfid,'%8.3f ',(final_x_values_mean(3)));
fprintf(tfid,'%8.3f ',(final_x_values_mean(3)...
                *final_x_values_mean(6)));
text='  Mult = ';
fprintf(tfid,' %s ',text);
fprintf(tfid,'%8.3f ',final_x_values_mean(6));
text='  ';

```

```

fprintf(tfid,'%s',text);
fprintf(tfid,'%8.3f ',(final_x_values_stdev(3)));
text='  % = ';
fprintf(tfid,'%s',text);
fprintf(tfid,'%8.0f \n',(final_x_values_pc(3)));

%Sigma
text=[' s', ' = '];
fprintf(tfid,' %s ',text);
fprintf(tfid,'%12.3e',(final_x_values_mean(7)));
fprintf(tfid,'%12.3e ',(final_x_values_mean(7)...
                *final_x_values_mean(8)));
text='  Mult = ';
fprintf(tfid,' %s ',text);
fprintf(tfid,'%12.3f ',final_x_values_mean(8));
text='  ';
fprintf(tfid,'%s',text);
fprintf(tfid,'%8.3f ',(final_x_values_stdev(7)));
text='  % = ';
fprintf(tfid,'%s',text);
fprintf(tfid,'%8.0f \n',(final_x_values_pc(7)));

text='  ';
fprintf(tfid,' %s \n',text);
text=['  '];
fprintf(tfid,' %s \n',text);

for gem = 1:game

    %Values from this game only
    textb=sprintf('%0f ',gem);
    text=['For game ',textb];
    fprintf(tfid,text);
    text='  ';
    fprintf(tfid,' %s \n',text);

```

```

%Size of dispersion
text=['dE', ' = '];
fprintf(tfid, ' %s ', text);
fprintf(tfid, '%-8.3f ', (GA_x_values(gem,1)));
fprintf(tfid, '%-8.3f ', (GA_x_values(gem,1)...
    *GA_x_values(gem,4)));
text=' Mult = ';
fprintf(tfid, ' %s ', text);
fprintf(tfid, '%-8.3f \n', GA_x_values(gem,4));

%Frequency
text=[' f', ' = '];
fprintf(tfid, ' %s ', text);
fprintf(tfid, '%-8.0f ', (GA_x_values(gem,2)));
fprintf(tfid, '%-8.0f ', (GA_x_values(gem,2)...
    *GA_x_values(gem,5)));
text=' Mult = ';
fprintf(tfid, ' %s ', text);
fprintf(tfid, '%-8.3f \n', GA_x_values(gem,5));

%Cole-Cole parameter
text=[' a', ' = '];
fprintf(tfid, ' %s ', text);
fprintf(tfid, '%-8.3f ', (GA_x_values(gem,3)));
fprintf(tfid, '%-8.3f ', (GA_x_values(gem,3)...
    *GA_x_values(gem,6)));
text=' Mult = ';
fprintf(tfid, ' %s ', text);
fprintf(tfid, '%-8.3f \n', GA_x_values(gem,6));

%Sigma
text=[' s', ' = '];
fprintf(tfid, ' %s ', text);
fprintf(tfid, '%-12.3e', (GA_x_values(gem,7)));
fprintf(tfid, '%-12.3e ', (GA_x_values(gem,7)...

```

```

        *GA_x_values(gem,8)));
    text=' Mult = ';
    fprintf(tfid,' %s ',text);
    fprintf(tfid,'%12.0f \n',GA_x_values(gem,8));
    text='          ';
    fprintf(tfid,' %s \n',text);
    fprintf(tfid,' %s \n',text);

%end (for gem = 1:game)
end

text=['mod_loss for each game'];
fprintf(tfid,' %s \n',text);
fprintf(tfid,' %8.2e \n',mod_loss);
text='          ';
fprintf(tfid,' %s \n',text);

text='mean fit_error per point for each game';
fprintf(tfid,' %s \n',text);
fprintf(tfid,' %8.2e \n',fit_error/42);

text='          ';
fprintf(tfid,' %s \n',text);

text=['Mean: Part ',int2str(part)];
fprintf(tfid,' %s \n',text);
fprintf(tfid,'%8.5e \n',final_x_values_mean);

text=['StDev: Part ',int2str(part)];
fprintf(tfid,' %s \n',text);
fprintf(tfid,'%8.5e \n',final_x_values_stdev);

text=['Error Mean: Part ',int2str(part)];
fprintf(tfid,' %s \n',text);
fprintf(tfid,'%8.5e \n',final_fit_error_mean);
disp(['Error_mean = ', num2str(final_fit_error_mean)]);

```

```

    text=['Error StDev: Part ',int2str(part)];
    fprintf(tfid,' %s \n',text);
    fprintf(tfid,'%8.5e \n',final_fit_error_stdev);

    %Close text_file
    fclose(tfid);
    eval([home]);

    %end (if game>=1)
    end

    %end (for game = 1:games)
    end

    %end (for part = 1:3)
    end

```

## K.2 Diff\_calc

```

function [fit_error] = diff_calc(x)
global f_pts
global exp_loss
global mod_loss
%convert to angular frequency
w = 2*pi*f_pts;

dE(1)= x(1);    %decrement
f(1)= x(2);    %frequency
a(1)= x(3);    %Cole_Cole parameter
mult_dE= x(4); %mult decrement
mult_f= x(5);  %mult frequency
mult_a= x(6);  %mult Cole_Cole parameter

```

```

dE(2)=dE(1)*mult_dE;
f(2)=f(1)*mult_f;
a(2)=a(1)*mult_a;

[s,t]=(size(w));
% Eind=zeros(s,3);          %setup array for data
Eind_real=zeros(s,3);
Eind_imag=zeros(s,3);

for k=1:2/1;
    T(k)=1./(2*pi*f(k));
    sphot=sin(0.5*pi*a(k));
    cphot=cos(0.5*pi*a(k));
    omh=1-a(k);
    wtau=w.*T(k);
    wttomh=(wtau).^(omh);
    t_mbs=wttomh*sphot;
    t_add1=t_mbs+1;
    t_multdE=t_add1*dE(k);
    b_part3=(wtau).^(2*omh);
    b_part2=2*wttomh.*sphot;
    b_all=1+b_part2+b_part3;
    Eind_imag(:,k)=wttomh.*cphot.*dE(k)./b_all;
end;

%Modelled dLoss = Loss 2 - Loss 1
mod_loss=Eind_imag(:,2)-Eind_imag(:,1);
%Error = Theoretical Loss - Experimental Loss
err_loss = mod_loss - exp_loss;
fit_error = sum(sqrt(((err_loss).^2)));

```



### K.3 Diff\_get\_data

```
function []= diff_get_data(A)
%chooses data file with frequency and "difference in loss"

global exp_loss;
global data1;
global f_pts;
cd cdata;
fid=fopen(A);
data1=fscanf(fid,'%g %g',[2 inf]);
data1=data1';
f_pts=data1(:,1);
exp_loss=data1(:,2);
fclose(fid);

cd ..;
```

# Appendix L

## BASIC Serial Library

These are the procedures and functions which accompany the Intelligent Interfaces Dual High-speed Serial Card for the RiscPC.

```
REM *****
```

```
REM > Serial 0.30 (22 Apr 1997)
```

```
REM for IIDual Module
```

```
REM *****
```

```
DEF PROCSerial_Init(port%, baud%, data_format%,  
    flow_control%)
```

```
SYS"IIDual_ReadWriteRxBaudRate",port%,baud%
```

```
SYS"IIDual_ReadWriteTxBaudRate",port%,baud%
```

```
SYS"IIDual_ReadWriteDataFormat",port%,data_format%
```

```
SYS"IIDual_FlushInBuf",port%
```

```
SYS"IIDual_FlushOutBuf",port%
```

```
CASE flow_control% OF
  WHEN 0, 4, 8
    REM flow control = none
    SYS"IIDual_ReadWriteSerialStatus",port%,&00000036,
      &FFFFFFC8
  WHEN 1
    REM flow control = Hardware handshaking using DSR,
    REM CTS and RTS (default)
    SYS"IIDual_ReadWriteSerialStatus",port%,&00000000,
      &FFFFFFC8
  WHEN 2, 6, 10
    REM flow control = Software (Xon/Xoff) handshaking
    REM (ignoring DSR and CTS)
    SYS"IIDual_ReadWriteSerialStatus",port%,&00000017,
      &FFFFFFC8
  WHEN 3
    REM flow control = Both hardware and software
    REM (Xon/Xoff) handshaking using DSR and CTS
    SYS"IIDual_ReadWriteSerialStatus",port%,&00000001,
      &FFFFFFC8
  WHEN 5
    REM Acorn Cable Wiring
    REM flow control = Hardware handshaking using DSR
    REM (ignoring CTS) and RTS
    SYS"IIDual_ReadWriteSerialStatus",port%,&00000010,
      &FFFFFFC8
  WHEN 7
    REM Acorn Cable Wiring
    REM flow control = Both hardware and software
    REM (Xon/Xoff) handshaking using DSR (ignoring CTS)
    SYS"IIDual_ReadWriteSerialStatus",port%,&00000011,
      &FFFFFFC8
  WHEN 9
    REM PC Cable Wiring
    REM flow control = Hardware handshaking using CTS
```

```
    REM (ignoring DSR) and RTS
    SYS"IIDual_ReadWriteSerialStatus",port%,&00000004,
        &FFFFFFC8
    WHEN 11
    REM PC Cable Wiring
    REM flow control = Both hardware and software
    REM (Xon/Xoff) handshaking using CTS (ignoring DSR)
    SYS"IIDual_ReadWriteSerialStatus",port%,&00000005,
        &FFFFFFC8
    ENDCASE

    SYS"IIDual_ReadWriteSerialStatus",port%,&00000002,
        &FFFFFFFD

    ENDPROC

    REM *****

    DEF PROCSerial_Final(port%)

    SYS"IIDual_ReadWriteSerialStatus",port%,&00000000,
        &FFFFFFFE

    SYS"IIDual_FlushOutBuf",port%
    SYS"IIDual_FlushInBuf",port%

    REM set data format 8 data 1 stop no parity
    SYS"IIDual_ReadWriteDataFormat",port%,%00000000

    REM transmit baud rate 9600
    SYS"IIDual_ReadWriteTxBaudRate",port%,7
    REM receive baud rate 9600
    SYS"IIDual_ReadWriteRxBaudRate",port%,7

    ENDPROC
```

```
REM *****  
  
DEF FNSerial_Status(port%)  
LOCAL status%  
  
SYS"IIDual_ReadWriteSerialStatus",port%,&00000000,  
&FFFFFFFF TO ,,status%  
  
=status%  
  
REM *****  
  
DEF PROCSerial_EnableDTR(port%)  
  
SYS"IIDual_ReadWriteSerialStatus",port%,&00000000,  
    &FFFFFFFF7  
  
ENDPROC  
  
REM *****  
  
DEF PROCSerial_DisableDTR(port%)  
  
SYS"IIDual_ReadWriteSerialStatus",port%,&00000008,  
    &FFFFFFFF7  
  
ENDPROC  
  
REM *****  
  
DEF PROCSerial_EnableRTS(port%)  
  
SYS"IIDual_ReadWriteSerialStatus",port%,&00000000,  
    &FFFFFFFF7F  
  
ENDPROC
```

```
REM *****
```

```
DEF PROCSerial_DisableRTS(port%)
```

```
SYS"IIDual_ReadWriteSerialStatus",port%,&00000080,  
    &FFFFFF7F
```

```
ENDPROC
```

```
REM *****
```

```
DEF PROCSerial_SendBreak(port%, time%)
```

```
SYS"IIDual_SendBreak", port%, time%
```

```
ENDPROC
```

```
REM *****
```

```
DEF PROCSerial_EnableInput(port%)
```

```
SYS"IIDual_EnableDisableInput",port%, 1
```

```
ENDPROC
```

```
REM *****
```

```
DEF PROCSerial_DisableInput(port%)
```

```
SYS"IIDual_EnableDisableInput",port%,0
```

```
ENDPROC
```

```
REM *****
```

```
DEF PROCSerial_FlushInBuf(port%)

SYS"IIDual_FlushInBuf",port%

ENDPROC

REM *****

DEF PROCSerial_FlushOutBuf(port%)

SYS"IIDual_FlushOutBuf",port%

ENDPROC

REM *****

DEF FNSerial_ReadEntriesInBuf(port%)
LOCAL entries%, lo%, hi%

SYS"IIDual_ReadEntriesInBuf",port% TO ,entries%

=entries%

REM *****

DEF FNSerial_ReadSpaceOutBuf(port%)
LOCAL space%, lo%, hi%

SYS"IIDual_ReadSpaceOutBuf",port% TO ,space%

=space%

REM *****

DEF PROCSerial_SendByte(port%, byte%)
```

```
LOCAL flags%

REPEAT
  SYS"IIDual_SendByte",port%,byte% TO ;flags%
UNTIL (flags% AND %0010) = %0000

ENDPROC

REM *****

DEF FNSerial_GetByte(port%)
LOCAL byte%,flags%

REPEAT
  SYS"IIDual_GetByte",port% TO ,byte% ;flags%
UNTIL (flags% AND %0010) = %0000

=byte%

REM *****

DEF PROCSerial_SendString(port%,data$)
LOCAL len%, cnt%,flags%

len% = LEN(data$)
cnt% = len%

REPEAT
  SYS "IIDual_SendBlk", port%, MID$(data$, len%-cnt%+1,
    cnt%), cnt% TO ,,cnt%;flags%
UNTIL ((flags% AND &02) = &00)

ENDPROC

REM *****
```



```

DEF FNSerial_GetString(port%,match$)
  LOCAL matchcnt%, cnt%, incnt%, data$, indata$, flags%

  matchcnt% = - LEN(match$)
  cnt% = 254
  data$ = STRING$(cnt%,CHR$(0))

  REPEAT
    SYS "IIDual_ExamineBlkInBufUntilMatch", port%, data$,
      cnt%, match$, matchcnt% TO ,,incnt% ;flags%
  UNTIL (((flags% AND &02) = &00) OR (incnt% = 0))

  SYS "IIDual_GetBlk", port%, data$, - (cnt%-incnt%)
    TO ,,outdata$;flags%

= outdata$

REM *****

DEF PROCSerial_SendBlock(port%, adr%, cnt%)
  LOCAL flags%

  REPEAT
    SYS"IIDual_SendBlk", port%, adr%, cnt% TO , adr%,
      cnt%;flags%
  UNTIL (flags% AND %0010) = %0000

ENDPROC

REM *****

DEF PROCSerial_GetBlock(port%, adr%, cnt%)
  LOCAL flags%

  REPEAT
    SYS"IIDual_GetBlk", port%, adr%, cnt% TO , adr%,

```

```
        cnt%;flags%
UNTIL (flags% AND %0010) = %0000

ENDPROC
```

# Appendix M

## BASIC GPIB Libraries

These are the libraries of procedures and functions which accompany the Intelligent Interfaces GPIB card for the RiscPC. They are:

- BAS488 Library
- XBAS488 Library

### M.1 BAS488 Library

```
REM INTELLIGENT INTERFACES LTD IEEE488 PROCEDURES
REM AND FUNCTIONS LIBRARY V2.02
REM abort on error
REM Copyright Intelligent Interfaces Ltd
REM 13 Feb 1998

DEF PROCeos_out_1chr(eos1%)
SYS &40340,&00,&03,&01,eos1%
ENDPROC
```

```
DEF PROCeos_out_2chr(eos1%,eos2%)
SYS &40340,&00,&03,&02,eos1%,eos2%
ENDPROC
```

```
DEF PROCeos_in_1chr(eos1%)
SYS &40340,&00,&04,&01,eos1%
ENDPROC
```

```
DEF PROCeos_in_2chr(eos1%,eos2%)
SYS &40340,&00,&04,&02,eos1%,eos2%
ENDPROC
```

```
DEF PROCtimeout_period(period)
SYS &40340,&00,&05,INT(&00200000*(period/8))
ENDPROC
```

```
DEF PROCtimeout_on
SYS &40340,&00,&06
ENDPROC
```

```
DEF PROCtimeout_off
SYS &40340,&00,&07
ENDPROC
```

```
DEF PROCescape_on
SYS &40340,&00,&48
ENDPROC
```

```
DEF PROCescape_off
SYS &40340,&00,&49
ENDPROC
```

```
DEF PROCinit
LOCAL d0%,d1%,ma%
SYS &40340,&00,&02 TO d0%,d1%,ma%
```

```
IF (ma% AND &80) THEN
    SYS &40340,&00,&11,ma%
ELSE
    SYS &40340,&00,&10,ma%
ENDIF
ENDPROC
```

```
DEF PROCifc
SYS &40340,&00,&0D
ENDPROC
```

```
DEF PROCren_true
SYS &40340,&00,&0E
ENDPROC
```

```
DEF PROCren_false
SYS &40340,&00,&0F
ENDPROC
```

```
DEF PROCdevice(archadr%)
SYS &40340,&00,&10,archadr%
ENDPROC
```

```
DEF PROCcontroller(archadr%)
SYS &40340,&00,&11,archadr%
ENDPROC
```

```
DEF PROCatn_true
SYS &40340,&00,&12
ENDPROC
```

```
DEF PROCatn_true_sync
SYS &40340,&00,&13
ENDPROC
```

```
DEF PROCcmd(cmd%)
```

```
SYS &40340,&00,&14,&00,&00,&00,CHR$(cmd%),&01
ENDPROC
```

```
DEF PROClisten(lad%)
SYS &40340,&00,&15,&00,lad%
ENDPROC
```

```
DEF PROClistenext(lad%,sad%)
SYS &40340,&00,&16,&00,lad%,sad%
ENDPROC
```

```
DEF PROCtalk(tad%)
SYS &40340,&00,&17,&00,tad%
ENDPROC
```

```
DEF PROCtalkext(tad%,sad%)
SYS &40340,&00,&18,&00,tad%,sad%
ENDPROC
```

```
DEF PROCsecondary(sad%)
SYS &40340,&00,&19,&00,&00,sad%
ENDPROC
```

```
DEF PROCunlisten
SYS &40340,&00,&1A
ENDPROC
```

```
DEF PROCuntalk
SYS &40340,&00,&1B
ENDPROC
```

```
DEF PROCadr_to_listen(lad%)
SYS &40340,&00,&1C,&00,lad%
ENDPROC
```

```
DEF PROCadr_to_listenext(lad%,sad%)
```

```
SYS &40340,&00,&1D,&00,lad%,sad%  
ENDPROC
```

```
DEF PROCadr_to_talk(tad%)  
SYS &40340,&00,&1E,&00,tad%  
ENDPROC
```

```
DEF PROCadr_to_talkext(tad%,sad%)  
SYS &40340,&00,&1F,&00,tad%,sad%  
ENDPROC
```

```
DEF PROCgo_to_local(lad%)  
SYS &40340,&00,&20,&00,&00,&00,CHR$(lad%),&01  
ENDPROC
```

```
DEF PROCselected_device_clear(lad%)  
SYS &40340,&00,&21,&00,&00,&00,CHR$(lad%),&01  
ENDPROC
```

```
DEF PROCgroup_execute_trigger(lad%)  
SYS &40340,&00,&22,&00,&00,&00,CHR$(lad%),&01  
ENDPROC
```

```
DEF PROClocal_lockout  
SYS &40340,&00,&23  
ENDPROC
```

```
DEF PROCdevice_clear  
SYS &40340,&00,&24  
ENDPROC
```

```
DEF PROCparallel_poll_unconfigure  
SYS &40340,&00,&25  
ENDPROC
```

```
DEF PROCatn_false
```

```
SYS &40340,&00,&26
ENDPROC
```

```
DEF PROCrequest_service(stb%)
SYS &40340,&00,&29, stb%
ENDPROC
```

```
DEF FNserial_poll(tad%)
LOCAL d0%,d1%,stb%
SYS &40340,&00,&2B,&00,tad% TO d0%,d1%,stb%
=stb%
```

```
DEF PROCparallel_poll_enable(lad%,sp3p2p1%)
SYS &40340,&00,&2E,sp3p2p1%,lad%
ENDPROC
```

```
DEF PROCparallel_poll_disable(lad%)
SYS &40340,&00,&2F,&00,lad%
ENDPROC
```

```
DEF FNparallel_poll
LOCAL d0%,d1%,ppr%
SYS &40340,&00,&30 TO d0%,d1%,ppr%
=ppr%
```

```
DEF PROCpasscontrol(tad%)
SYS &40340,&00,&31,&00,tad%
ENDPROC
```

```
DEF PROCoutput(mode%,data$)
SYS &40340,&00,&08,mode%
SYS &40340,&00,&36,&00,&00,&00,data$,LEN(data$)
ENDPROC
```

```
DEF PROCadrandoutput(mode%,lad%,data$)
SYS &40340,&00,&08,mode%
```



```

SYS &40340,&00,&3C,&00,lad%,&00,data$,LEN(data$)
ENDPROC

```

```

DEF PROCadnextandoutput(mode%,lad%,sad%,data$)
SYS &40340,&00,&08,mode%
SYS &40340,&00,&3E,&00,lad%,sad%,data$,LEN(data$)
ENDPROC

```

```

DEF PROCoutputmem(mode%,memadr%,bytecnt%)
SYS &40340,&00,&08,mode%
SYS &40340,&00,&36,&00,&00,&00,memadr%,bytecnt%
ENDPROC

```

```

DEF PROCadrandoutputmem(mode%,lad%,memadr%,bytecnt%)
SYS &40340,&00,&08,mode%
SYS &40340,&00,&3C,&00,lad%,&00,memadr%,bytecnt%
ENDPROC

```

```

DEF PROCadnextandoutputmem(mode%,lad%,sad%,memadr%,bytecnt%)
SYS &40340,&00,&08,mode%
SYS &40340,&00,&3E,&00,lad%,sad%,memadr%,bytecnt%
ENDPROC

```

```

DEF FNinput(mode%,bytecnt%)
LOCALd0%,d1%,d2%,d3%,d4%,databuf$,d6%,xcnt%
IFbytecnt%>254THEN bytecnt% = 254
databuf$ = STRING$(bytecnt%," ")
SYS &40340,&00,&09,mode%
SYS &40340,&00,&37,&00,&00,&00,databuf$,bytecnt% TO
  d0%,d1%,d2%,d3%,d4%,databuf$,d6%,xcnt%
=LEFT$(databuf$,xcnt%)

```

```

DEF FNadrandinput(mode%,tad%,bytecnt%)
LOCALd0%,d1%,d2%,d3%,d4%,databuf$,d6%,xcnt%
IFbytecnt%>254THEN bytecnt% = 254
databuf$ = STRING$(bytecnt%," ")

```

```

SYS &40340,&00,&09,mode%
SYS &40340,&00,&3D,&00,tad%,&00,databuf$,bytecnt% TO
  d0%,d1%,d2%,d3%,d4%,databuf$,d6%,xcnt%
=LEFT$(databuf$,xcnt%)

DEF FNadnextandinput(mode%,tad%,sad%,bytecnt%)
LOCALd0%,d1%,d2%,d3%,d4%,databuf$,d6%,xcnt%
IFbytecnt%>254THEN bytecnt% = 254
databuf$ = STRING$(bytecnt%," ")
SYS &40340,&00,&09,mode%
SYS &40340,&00,&3F,&00,tad%,sad%,databuf$,bytecnt% TO
  d0%,d1%,d2%,d3%,d4%,databuf$,d6%,xcnt%
=LEFT$(databuf$,xcnt%)

DEF PROCinputmem(mode%,memadr%,bytecnt%)
SYS &40340,&00,&09,mode%
SYS &40340,&00,&37,&00,&00,&00,memadr%,bytecnt%
ENDPROC

DEF PROCadrandinputmem(mode%,tad%,memadr%,bytecnt%)
SYS &40340,&00,&09,mode%
SYS &40340,&00,&3D,&00,tad%,&00,memadr%,bytecnt%
ENDPROC

DEF PROCadnextandinputmem(mode%,tad%,sad%,memadr%,bytecnt%)
SYS &40340,&00,&09,mode%
SYS &40340,&00,&3F,&00,tad%,sad%,memadr%,bytecnt%
ENDPROC

DEF FNservice_requested
LOCAL d0%,d1%,d2%,d3%,bussts%,status%
SYS &40340,&00,&43 TO d0%,d1%,d2%,d3%,bussts%
IF (bussts% AND &04) = 0 THEN status%=FALSE ELSE status% = TRUE
=status%

DEF FNtalker

```

```

LOCAL d0%,d1%,d2%,d3%,d4%,addsts%,status%
SYS &40340,&00,&43 TO d0%,d1%,d2%,d3%,d4%,addsts%
IF (addsts% AND &0A) = 0 THEN status%=FALSE ELSE status% = TRUE
=status%

```

```

DEF FNlistener
LOCAL d0%,d1%,d2%,d3%,d4%,addsts%,status%
SYS &40340,&00,&43 TO d0%,d1%,d2%,d3%,d4%,addsts%
IF (addsts% AND &14) = 0 THEN status%=FALSE ELSE status% = TRUE
=status%

```

```

DEF FNattention
LOCAL d0%,d1%,d2%,d3%,bussts%,status%
SYS &40340,&00,&43 TO d0%,d1%,d2%,d3%,bussts%
IF (bussts% AND &80) = 0 THEN status%=FALSE ELSE status% = TRUE
=status%

```

```

DEF FNlocked_out
LOCAL d0%,d1%,d2%,d3%,d4%,addsts%,status%
SYS &40340,&00,&43 TO d0%,d1%,d2%,d3%,d4%,addsts%
IF (addsts% AND &40) = 0 THEN status%=FALSE ELSE status% = TRUE
=status%

```

```

DEF FNremote
LOCAL d0%,d1%,d2%,d3%,d4%,addsts%,status%
SYS &40340,&00,&43 TO d0%,d1%,d2%,d3%,d4%,addsts%
IF (addsts% AND &80) = 0 THEN status%=FALSE ELSE status% = TRUE
=status%

```

```

DEF FNdevice_cleared
LOCAL d0%,d1%,d2%,d3%,d4%,d5%,devsts%,status%
SYS &40340,&00,&44 TO d0%,d1%,d2%,d3%,d4%,d5%,devsts%
IF (devsts% AND &08) = 0 THEN status%=FALSE ELSE status% = TRUE
=status%

```

```

DEF FNtriggered

```

```

LOCAL d0%,d1%,d2%,d3%,d4%,d5%,devsts%,status%
SYS &40340,&00,&45 TO d0%,d1%,d2%,d3%,d4%,d5%,devsts%
IF (devsts% AND &80) = 0 THEN status%=FALSE ELSE status% = TRUE
=status%

DEF FNinterface_cleared
LOCAL d0%,d1%,d2%,d3%,d4%,d5%,devsts%,status%
SYS &40340,&00,&46 TO d0%,d1%,d2%,d3%,d4%,d5%,devsts%
IF (devsts% AND &0100) = 0 THEN status%=FALSE ELSE status% = TRUE
=status%

DEF FNsh_error
LOCAL d0%,d1%,d2%,d3%,d4%,d5%,devsts%,status%
SYS &40340,&00,&47 TO d0%,d1%,d2%,d3%,d4%,d5%,devsts%
IF (devsts% AND &4000) = 0 THEN status%=FALSE ELSE status% = TRUE
=status%

DEF FNcontroller_in_charge
LOCAL d0%,d1%,d2%,d3%,d4%,d5%,d6%,ctrlinchg%,status%
SYS &40340,&00,&43 TO d0%,d1%,d2%,d3%,d4%,d5%,d6%,ctrlinchg%
IF (ctrlinchg% AND &FF) = 0 THEN status%=FALSE ELSE status% = TRUE
=status%

DEF FNsystem_controller
LOCAL d0%,d1%,ma%
SYS &40340,&00,&02 TO d0%,d1%,ma%
IF (ma% AND &80) = 0 THEN status%=FALSE ELSE status% = TRUE
=status%

DEF FNinitialised
=TRUE

DEF FNaddress
LOCAL d0%,d1%,ma%
SYS &40340,&00,&02 TO d0%,d1%,ma%
=(ma% AND &1F)

```

## M.2 XBAS488 Library

```
REM INTELLIGENT INTERFACES LTD IEEE488
REM BASIC XFUNCTIONS LIBRARY V2.02
REM return error status
REM Copyright Intelligent Interfaces Ltd
REM 13 Feb 1998
```

```
DEF FNXeos_out_1chr(eos1%)
LOCAL d0%
SYS &60340,&00,&03,&01,eos1% TO d0%
IF d0% = 0 THEN
= &00
ELSE
= (!d0% AND &FF)
ENDIF
```

```
DEF FNXeos_out_2chr(eos1%,eos2%)
LOCAL d0%
SYS &60340,&00,&03,&02,eos1%,eos2% TO d0%
IF d0% = 0 THEN
= &00
ELSE
= (!d0% AND &FF)
ENDIF
```

```
DEF FNXeos_in_1chr(eos1%)
LOCAL d0%
SYS &60340,&00,&04,&01,eos1% TO d0%
IF d0% = 0 THEN
= &00
```

```
ELSE
= (!d0% AND &FF)
ENDIF
```

```
DEF FNXeos_in_2chr(eos1%,eos2%)
LOCAL d0%
SYS &60340,&00,&04,&02,eos1%,eos2% TO d0%
IF d0% = 0 THEN
= &00
ELSE
= (!d0% AND &FF)
ENDIF
```

```
DEF FNXtimeout_period(period)
LOCAL d0%
SYS &60340,&00,&05,INT(&00200000*(period/8)) TO d0%
IF d0% = 0 THEN
= &00
ELSE
= (!d0% AND &FF)
ENDIF
```

```
DEF FNXtimeout_on
LOCAL d0%
SYS &60340,&00,&06 TO d0%
IF d0% = 0 THEN
= &00
ELSE
= (!d0% AND &FF)
ENDIF
```

```
DEF FNXtimeout_off
LOCAL d0%
SYS &60340,&00,&07 TO d0%
IF d0% = 0 THEN
= &00
```

```
ELSE
= (!d0% AND &FF)
ENDIF

DEF FNXescape_on
LOCAL d0%
SYS &60340,&00,&48 TO d0%
IF d0% = 0 THEN
= &00
ELSE
= (!d0% AND &FF)
ENDIF

DEF FNXescape_off
LOCAL d0%
SYS &60340,&00,&49 TO d0%
IF d0% = 0 THEN
= &00
ELSE
= (!d0% AND &FF)
ENDIF

DEF FNXinit
LOCAL d0%,d1%,ma%
SYS &60340,&00,&02 TO d0%,d1%,ma%
IF d0% = 0 THEN
  IF (ma% AND &80) THEN
    SYS &60340,&00,&11,ma% TO d0%
  ELSE
    SYS &60340,&00,&10,ma% TO d0%
  ENDIF
ENDIF
ENDIF
IF d0% = 0 THEN
= &00
ELSE
= (!d0% AND &FF)
```

```
ENDIF
```

```
DEF FNXifc
LOCAL d0%
SYS &60340,&00,&0D TO d0%
IF d0% = 0 THEN
= &00
ELSE
= (!d0% AND &FF)
ENDIF
```

```
DEF FNXren_true
LOCAL d0%
SYS &60340,&00,&0E TO d0%
IF d0% = 0 THEN
= &00
ELSE
= (!d0% AND &FF)
ENDIF
```

```
DEF FNXren_false
LOCAL d0%
SYS &60340,&00,&0F TO d0%
IF d0% = 0 THEN
= &00
ELSE
= (!d0% AND &FF)
ENDIF
```

```
DEF FNXdevice(archadr%)
LOCAL d0%
SYS &60340,&00,&10,archadr% TO d0%
IF d0% = 0 THEN
= &00
ELSE
= (!d0% AND &FF)
```



ENDIF

```
DEF FNxcontroller(archadr%)
LOCAL d0%
SYS &60340,&00,&11,archadr% TO d0%
IF d0% = 0 THEN
= &00
ELSE
= (!d0% AND &FF)
ENDIF
```

```
DEF FNxatn_true
LOCAL d0%
SYS &60340,&00,&12 TO d0%
IF d0% = 0 THEN
= &00
ELSE
= (!d0% AND &FF)
ENDIF
```

```
DEF FNxatn_true_sync
LOCAL d0%
SYS &60340,&00,&13 TO d0%
IF d0% = 0 THEN
= &00
ELSE
= (!d0% AND &FF)
ENDIF
```

```
DEF FNxcmd(cmd%)
LOCAL d0%
SYS &60340,&00,&14,&00,&00,&00,CHR$(cmd%),&01 TO d0%
IF d0% = 0 THEN
= &00
ELSE
= (!d0% AND &FF)
```

ENDIF

```
DEF FNXlisten(lad%)
LOCAL d0%
SYS &60340,&00,&15,&00,lad% TO d0%
IF d0% = 0 THEN
= &00
ELSE
= (!d0% AND &FF)
ENDIF
```

```
DEF FNXlistenext(lad%,sad%)
LOCAL d0%
SYS &60340,&00,&16,&00,lad%,sad% TO d0%
IF d0% = 0 THEN
= &00
ELSE
= (!d0% AND &FF)
ENDIF
```

```
DEF FNXtalk(tad%)
LOCAL d0%
SYS &60340,&00,&17,&00,tad% TO d0%
IF d0% = 0 THEN
= &00
ELSE
= (!d0% AND &FF)
ENDIF
```

```
DEF FNXtalkext(tad%,sad%)
LOCAL d0%
SYS &60340,&00,&18,&00,tad%,sad% TO d0%
IF d0% = 0 THEN
= &00
ELSE
= (!d0% AND &FF)
```

```
ENDIF
```

```
DEF FNsecondary(sad%)  
LOCAL d0%  
SYS &60340,&00,&19,&00,&00,sad% TO d0%  
IF d0% = 0 THEN  
= &00  
ELSE  
= (!d0% AND &FF)  
ENDIF
```

```
DEF FNunlisten  
LOCAL d0%  
SYS &60340,&00,&1A TO d0%  
IF d0% = 0 THEN  
= &00  
ELSE  
= (!d0% AND &FF)  
ENDIF
```

```
DEF FNuntalk  
LOCAL d0%  
SYS &60340,&00,&1B TO d0%  
IF d0% = 0 THEN  
= &00  
ELSE  
= (!d0% AND &FF)  
ENDIF
```

```
DEF FNadr_to_listen(lad%)  
LOCAL d0%  
SYS &60340,&00,&1C,&00,lad% TO d0%  
IF d0% = 0 THEN  
= &00  
ELSE  
= (!d0% AND &FF)
```

ENDIF

```
DEF FNAdr_to_listenext(lad%,sad%)
LOCAL d0%
SYS &60340,&00,&1D,&00,lad%,sad% TO d0%
IF d0% = 0 THEN
= &00
ELSE
= (!d0% AND &FF)
ENDIF
```

```
DEF FNAdr_to_talk(tad%)
LOCAL d0%
SYS &60340,&00,&1E,&00,tad% TO d0%
IF d0% = 0 THEN
= &00
ELSE
= (!d0% AND &FF)
ENDIF
```

```
DEF FNAdr_to_talkext(tad%,sad%)
LOCAL d0%
SYS &60340,&00,&1F,&00,tad%,sad% TO d0%
IF d0% = 0 THEN
= &00
ELSE
= (!d0% AND &FF)
ENDIF
```

```
DEF FNgo_to_local(lad%)
LOCAL d0%
SYS &60340,&00,&20,&00,&00,&00,CHR$(lad%),&01 TO d0%
IF d0% = 0 THEN
= &00
ELSE
= (!d0% AND &FF)
```

ENDIF

```
DEF FNselected_device_clear(lad%)
LOCAL d0%
SYS &60340,&00,&21,&00,&00,&00,CHR$(lad%),&01 TO d0%
IF d0% = 0 THEN
= &00
ELSE
= (!d0% AND &FF)
ENDIF
```

```
DEF FNgroup_execute_trigger(lad%)
LOCAL d0%
SYS &60340,&00,&22,&00,&00,&00,CHR$(lad%),&01 TO d0%
IF d0% = 0 THEN
= &00
ELSE
= (!d0% AND &FF)
ENDIF
```

```
DEF FNlocal_lockout
LOCAL d0%
SYS &60340,&00,&23 TO d0%
IF d0% = 0 THEN
= &00
ELSE
= (!d0% AND &FF)
ENDIF
```

```
DEF FNdevice_clear
LOCAL d0%
SYS &60340,&00,&24 TO d0%
IF d0% = 0 THEN
= &00
ELSE
= (!d0% AND &FF)
```

```
ENDIF
```

```
DEF FNXparallel_poll_unconfigure
LOCAL d0%
SYS &60340,&00,&25 TO d0%
IF d0% = 0 THEN
= &00
ELSE
= (!d0% AND &FF)
ENDIF
```

```
DEF FNXatn_false
LOCAL d0%
SYS &60340,&00,&26 TO d0%
IF d0% = 0 THEN
= &00
ELSE
= (!d0% AND &FF)
ENDIF
```

```
DEF FNXrequest_service(stb%)
LOCAL d0%
SYS &60340,&00,&29,stb% TO d0%
IF d0% = 0 THEN
= &00
ELSE
= (!d0% AND &FF)
ENDIF
```

```
DEF FNXserial_poll(RETURN stb%,tad%)
LOCAL d0%,d1%
SYS &60340,&00,&2B,&00,tad% TO d0%,d1%,stb%
IF d0% = 0 THEN
= &00
ELSE
= (!d0% AND &FF)
```

```
ENDIF
```

```
DEF FNparallel_poll_enable(lad%,sp3p2p1%)
LOCAL d0%
SYS &60340,&00,&2E,sp3p2p1%,lad% TO d0%
IF d0% = 0 THEN
= &00
ELSE
= (!d0% AND &FF)
ENDIF
```

```
DEF FNparallel_poll_disable(lad%)
LOCAL d0%
SYS &60340,&00,&2F,&00,lad% TO d0%
IF d0% = 0 THEN
= &00
ELSE
= (!d0% AND &FF)
ENDIF
```

```
DEF FNparallel_poll(RETURN ppr%)
LOCAL d0%,d1%
SYS &60340,&00,&30 TO d0%,d1%,ppr%
IF d0% = 0 THEN
= &00
ELSE
= (!d0% AND &FF)
ENDIF
```

```
DEF FNpasscontrol(tad%)
LOCAL d0%
SYS &60340,&00,&31,&00,tad% TO d0%
IF d0% = 0 THEN
= &00
ELSE
= (!d0% AND &FF)
```

```
ENDIF
```

```
DEF FNxoutput(mode%,data$)
```

```
LOCAL d0%
```

```
SYS &60340,&00,&08,mode% TO d0%
```

```
IF d0% = 0 THEN
```

```
  SYS &60340,&00,&36,&00,&00,&00,data$,LEN(data$) TO d0%
```

```
ENDIF
```

```
IF d0% = 0 THEN
```

```
= &00
```

```
ELSE
```

```
= (!d0% AND &FF)
```

```
ENDIF
```

```
DEF FNxadroutput(mode%,lad%,data$)
```

```
LOCAL d0%
```

```
SYS &60340,&00,&08,mode% TO d0%
```

```
IF d0% = 0 THEN
```

```
  SYS &60340,&00,&3C,&00,lad%,&00,data$,LEN(data$) TO d0%
```

```
ENDIF
```

```
IF d0% = 0 THEN
```

```
= &00
```

```
ELSE
```

```
= (!d0% AND &FF)
```

```
ENDIF
```

```
DEF FNxadrextandoutput(mode%,lad%,sad%,data$)
```

```
LOCAL d0%
```

```
SYS &60340,&00,&08,mode% TO d0%
```

```
IF d0% = 0 THEN
```

```
  SYS &60340,&00,&3E,&00,lad%,sad%,data$,LEN(data$) TO d0%
```

```
ENDIF
```

```
IF d0% = 0 THEN
```

```
= &00
```

```
ELSE
```

```
= (!d0% AND &FF)
```



```
ENDIF
```

```
DEF FNxoutputmem(mode%,memadr%,bytecnt%)
```

```
LOCAL d0%
```

```
SYS &60340,&00,&08,mode% TO d0%
```

```
IF d0% = 0 THEN
```

```
  SYS &60340,&00,&36,&00,&00,&00,memadr%,bytecnt% TO d0%
```

```
ENDIF
```

```
IF d0% = 0 THEN
```

```
= &00
```

```
ELSE
```

```
= (!d0% AND &FF)
```

```
ENDIF
```

```
DEF FNxadroutputmem(mode%,lad%,memadr%,bytecnt%)
```

```
LOCAL d0%
```

```
SYS &60340,&00,&08,mode% TO d0%
```

```
IF d0% = 0 THEN
```

```
  SYS &60340,&00,&3C,&00,lad%,&00,memadr%,bytecnt%
```

```
ENDIF
```

```
IF d0% = 0 THEN
```

```
= &00
```

```
ELSE
```

```
= (!d0% AND &FF)
```

```
ENDIF
```

```
DEF FNxadrextandoutputmem(mode%,lad%,sad%,memadr%,bytecnt%)
```

```
LOCAL d0%
```

```
SYS &60340,&00,&08,mode% TO d0%
```

```
IF d0% = 0 THEN
```

```
  SYS &60340,&00,&3E,&00,lad%,sad%,memadr%,bytecnt% TO d0%
```

```
ENDIF
```

```
IF d0% = 0 THEN
```

```
= &00
```

```
ELSE
```

```
= (!d0% AND &FF)
```

ENDIF

```

DEF FNxinput(RETURN data$,mode%,bytecnt%)
LOCALd0%,d1%,d2%,d3%,d4%,databuf$,d6%,xcnt%
IFbytecnt%>254THEN bytecnt%=254
databuf$ = STRING$(bytecnt%," ")
SYS &60340,&00,&09,mode% TO d0%
IF d0% = 0 THEN
  SYS &60340,&00,&37,&00,&00,&00,databuf$,bytecnt%
  d0%,d1%,d2%,d3%,d4%,databuf$,d6%,xcnt%
  data$ = LEFT$(databuf$,xcnt%)
ENDIF
IF d0% = 0 THEN
  = &00
ELSE
  data$ = ""
  = (!d0% AND &FF)
ENDIF

```

```

DEF FNxadrainput(RETURN data$,mode%,tad%,bytecnt%)
LOCALd0%,d1%,d2%,d3%,d4%,databuf$,d6%,xcnt%
IFbytecnt%>254THEN bytecnt%=254
databuf$ = STRING$(bytecnt%," ")
SYS &60340,&00,&09,mode% TO d0%
IF d0% = 0 THEN
  SYS &60340,&00,&3D,&00,tad%,&00,databuf$,bytecnt% TO
  d0%,d1%,d2%,d3%,d4%,databuf$,d6%,xcnt%
  data$ = LEFT$(databuf$,xcnt%)
ENDIF
IF d0% = 0 THEN
  = &00
ELSE
  data$ = ""
  = (!d0% AND &FF)
ENDIF

```

```

DEF FNxadrestandinput(RETURN data$,mode%,tad%,sad%,bytecnt%)
LOCAL d0%,d1%,d2%,d3%,d4%,databuf$,d6%,xcnt%
IF bytecnt%>254 THEN bytecnt%=254
databuf$ = STRING$(bytecnt%," ")
SYS &60340,&00,&09,mode% TO d0%
IF d0% = 0 THEN
  SYS &60340,&00,&3F,&00,tad%,sad%,databuf$,bytecnt% TO
  d0%,d1%,d2%,d3%,d4%,databuf$,d6%,xcnt%
  data$ = LEFT$(databuf$,xcnt%)
ENDIF
IF d0% = 0 THEN
  = &00
ELSE
  data$ = ""
  = (!d0% AND &FF)
ENDIF

DEF FNxinputmem(mode%,memadr%,bytecnt%)
LOCAL d0%
SYS &60340,&00,&09,mode% TO d0%
IF d0% = 0 THEN
  SYS &60340,&00,&37,&00,&00,&00,memadr%,bytecnt% TO d0%
ENDIF
IF d0% = 0 THEN
  = &00
ELSE
  = (!d0% AND &FF)
ENDIF

DEF FNxadrainputmem(mode%,tad%,memadr%,bytecnt%)
LOCAL d0%
SYS &60340,&00,&09,mode% TO d0%
IF d0% = 0 THEN
  SYS &60340,&00,&3D,&00,tad%,&00,memadr%,bytecnt% TO d0%
ENDIF
IF d0% = 0 THEN

```

```

= &00
ELSE
= (!d0% AND &FF)
ENDIF

DEF FNxadrextandinputmem(mode%, tad%, sad%, memadr%, bytecnt%)
LOCAL d0%
SYS &60340, &00, &09, mode% TO d0%
IF d0% = 0 THEN
SYS &60340, &00, &3F, &00, tad%, sad%, memadr%, bytecnt% TO d0%
ENDIF
IF d0% = 0 THEN
= &00
ELSE
= (!d0% AND &FF)
ENDIF

DEF FNxservice_requested(RETURN status%)
LOCAL d0%, d1%, d2%, d3%, bussts%
SYS &60340, &00, &43 TO d0%, d1%, d2%, d3%, bussts%
IF (bussts% AND &04) = 0 THEN status%=FALSE ELSE status% = TRUE
IF d0% = 0 THEN
= &00
ELSE
= (!d0% AND &FF)
ENDIF

DEF FNxtalker(RETURN status%)
LOCAL d0%, d1%, d2%, d3%, d4%, addsts%
SYS &60340, &00, &43 TO d0%, d1%, d2%, d3%, d4%, addsts%
IF (addsts% AND &0A) = 0 THEN status%=FALSE ELSE status% = TRUE
IF d0% = 0 THEN
= &00
ELSE
= (!d0% AND &FF)
ENDIF

```

```
DEF FNxlistener(RETURN status%)
LOCAL d0%,d1%,d2%,d3%,d4%,addsts%
SYS &60340,&00,&43 TO d0%,d1%,d2%,d3%,d4%,addsts%
IF (addsts% AND &14) = 0 THEN status%=FALSE ELSE status% = TRUE
IF d0% = 0 THEN
= &00
ELSE
= (!d0% AND &FF)
ENDIF
```

```
DEF FNxattention(RETURN status%)
LOCAL d0%,d1%,d2%,d3%,bussts%
SYS &60340,&00,&43 TO d0%,d1%,d2%,d3%,bussts%
IF (bussts% AND &80) = 0 THEN status%=FALSE ELSE status% = TRUE
IF d0% = 0 THEN
= &00
ELSE
= (!d0% AND &FF)
ENDIF
```

```
DEF FNxlocked_out(RETURN status%)
LOCAL d0%,d1%,d2%,d3%,d4%,addsts%
SYS &60340,&00,&43 TO d0%,d1%,d2%,d3%,d4%,addsts%
IF (addsts% AND &40) = 0 THEN status%=FALSE ELSE status% = TRUE
IF d0% = 0 THEN
= &00
ELSE
= (!d0% AND &FF)
ENDIF
```

```
DEF FNxremote(RETURN status%)
LOCAL d0%,d1%,d2%,d3%,d4%,addsts%
SYS &60340,&00,&43 TO d0%,d1%,d2%,d3%,d4%,addsts%
IF (addsts% AND &80) = 0 THEN status%=FALSE ELSE status% = TRUE
IF d0% = 0 THEN
```

```
= &00
ELSE
= (!d0% AND &FF)
ENDIF
```

```
DEF FNxdevice_cleared(RETURN status%)
LOCAL d0%,d1%,d2%,d3%,d4%,d5%,devsts%
SYS &60340,&00,&44 TO d0%,d1%,d2%,d3%,d4%,d5%,devsts%
IF (devsts% AND &08) = 0 THEN status%=FALSE ELSE status% = TRUE
IF d0% = 0 THEN
= &00
ELSE
= (!d0% AND &FF)
ENDIF
```

```
DEF FNxtriggered(RETURN status%)
LOCAL d0%,d1%,d2%,d3%,d4%,d5%,devsts%
SYS &60340,&00,&45 TO d0%,d1%,d2%,d3%,d4%,d5%,devsts%
IF (devsts% AND &80) = 0 THEN status%=FALSE ELSE status% = TRUE
IF d0% = 0 THEN
= &00
ELSE
= (!d0% AND &FF)
ENDIF
```

```
DEF FNxinterface_cleared(RETURN status%)
LOCAL d0%,d1%,d2%,d3%,d4%,d5%,devsts%
SYS &60340,&00,&46 TO d0%,d1%,d2%,d3%,d4%,d5%,devsts%
IF (devsts% AND &0100) = 0 THEN status%=FALSE ELSE status% = TRUE
IF d0% = 0 THEN
= &00
ELSE
= (!d0% AND &FF)
ENDIF
```

```
DEF FNxsh_error(RETURN status%)
```

```

LOCAL d0%,d1%,d2%,d3%,d4%,d5%,devsts%
SYS &60340,&00,&47 TO d0%,d1%,d2%,d3%,d4%,d5%,devsts%
IF (devsts% AND &4000) = 0 THEN status%=FALSE ELSE status% = TRUE
IF d0% = 0 THEN
= &00
ELSE
= (!d0% AND &FF)
ENDIF

```

```

DEF FNxcontroller_in_charge(RETURN status%)
LOCAL d0%,d1%,d2%,d3%,d4%,d5%,d6%,ctrlinchg%
SYS &60340,&00,&43 TO d0%,d1%,d2%,d3%,d4%,d5%,d6%,ctrlinchg%
IF (ctrlinchg% AND &FF) = 0 THEN status%=FALSE ELSE status% = TRUE
IF d0% = 0 THEN
= &00
ELSE
= (!d0% AND &FF)
ENDIF

```

```

DEF FNxsystem_controller(RETURN status%)
LOCAL d0%,d1%,ma%
SYS &60340,&00,&02 TO d0%,d1%,ma%
IF (ma% AND &80) = 0 THEN status%=FALSE ELSE status% = TRUE
IF d0% = 0 THEN
= &00
ELSE
= (!d0% AND &FF)
ENDIF

```

```

DEF FNxinitialised(RETURN status%)
status% = TRUE
=&00

```

```

DEF FNxaddress(RETURN ma%)
LOCAL d0%,d1%
SYS &60340,&00,&02 TO d0%,d1%,ma%

```

```
ma%=(ma% AND &1F)
IF d0% = 0 THEN
= &00
ELSE
= (!d0% AND &FF)
ENDIF
```



# Appendix N

## Dialysis of DNA with other salts

This chapter shows the results of changing the cation associated with the DNA, as described in Section 3.5.9.

In every case, the form of the Difference Signal (DS) was found to be consistent with that found in the original experiment, varying only in the magnitude and frequency of the peaks. The results below show therefore, for each *individual* cation used:

- The variation of the magnitude of the positive maximum with concentration;
- The variation of the frequency of the positive maximum with concentration;
- The variation of the magnitude of the negative minimum with concentration;
- The variation of the frequency of the negative minimum with concentration;

In each graph, error bars indicate the degree of uncertainty in the results.

A summary of these results is given in Section 5.8, where the effect of the different cations may be more easily compared.

### N.0.1 Lithium Chloride

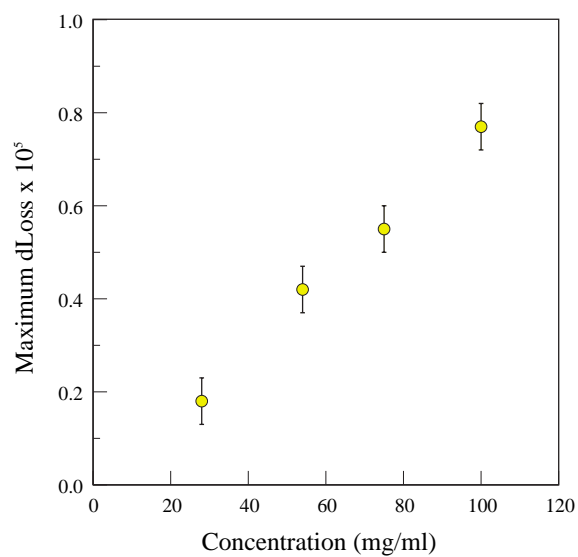


Figure N.1: DNA d.a. LiCl : Magnitude of Maximum of DS vs. Concentration

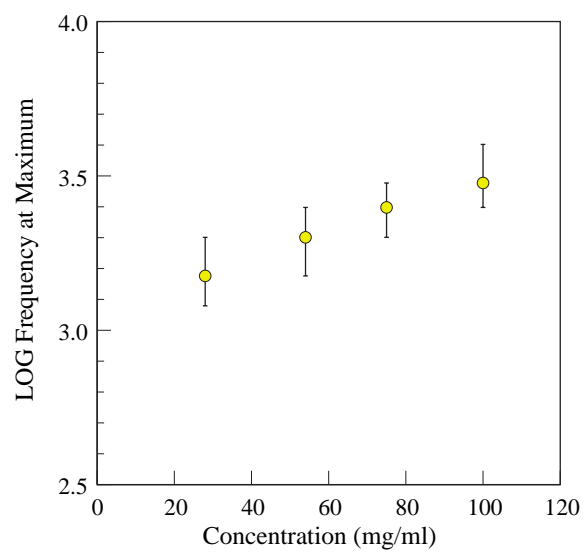


Figure N.2: DNA d.a. LiCl : Frequency of Maximum of DS vs. Concentration

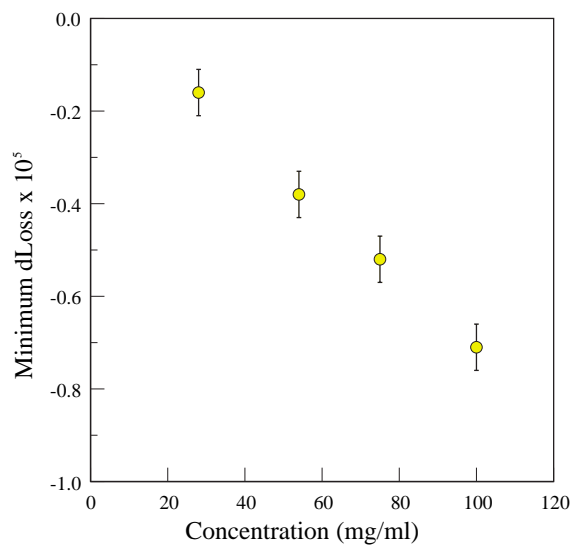


Figure N.3: DNA d.a. LiCl : Magnitude of Minimum of DS vs. Concentration

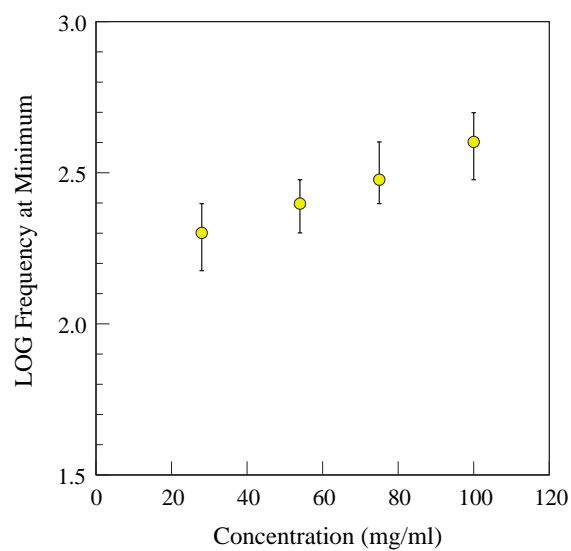


Figure N.4: DNA d.a. LiCl : Frequency of Minimum of DS vs. Concentration

## N.0.2 Sodium Chloride

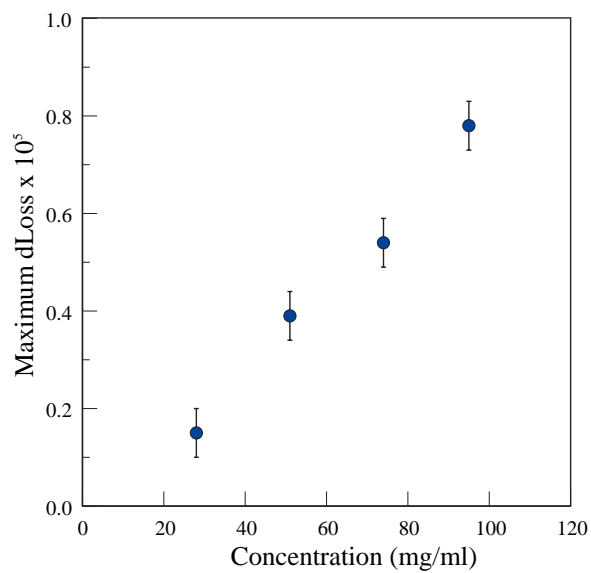


Figure N.5: DNA d.a. NaCl : Magnitude of Maximum of DS vs. Concentration

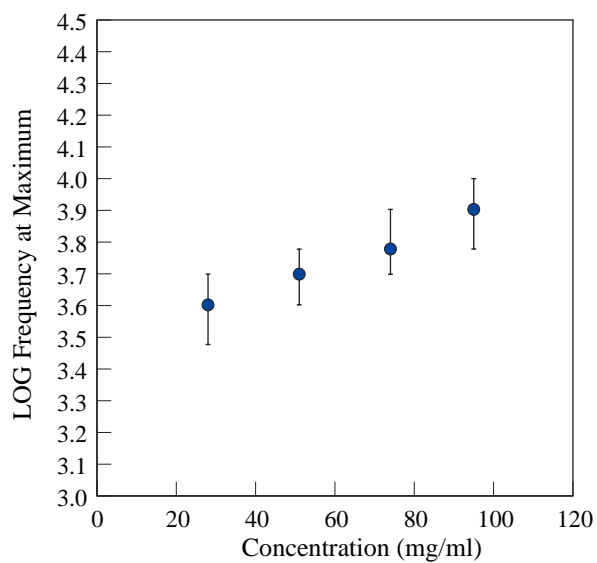


Figure N.6: DNA d.a. NaCl : Frequency of Maximum of DS vs. Concentration

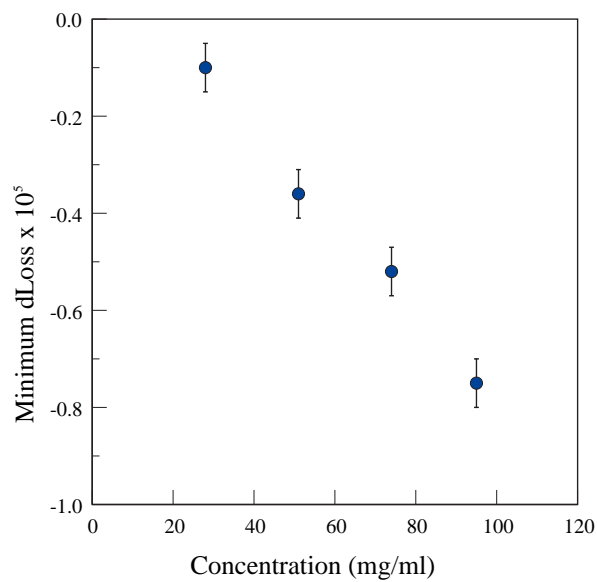


Figure N.7: DNA d.a. NaCl : Magnitude of Minimum of DS vs. Concentration

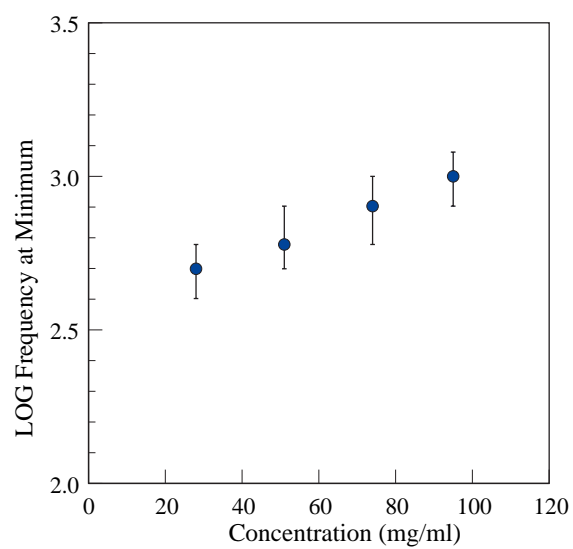


Figure N.8: DNA d.a. NaCl : Frequency of Minimum of DS vs. Concentration

### N.0.3 Potassium Chloride

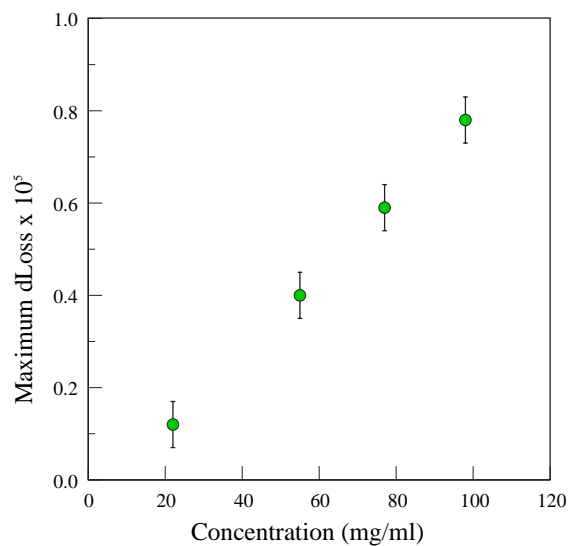


Figure N.9: DNA d.a. KCl : Magnitude of Maximum of DS vs. Concentration

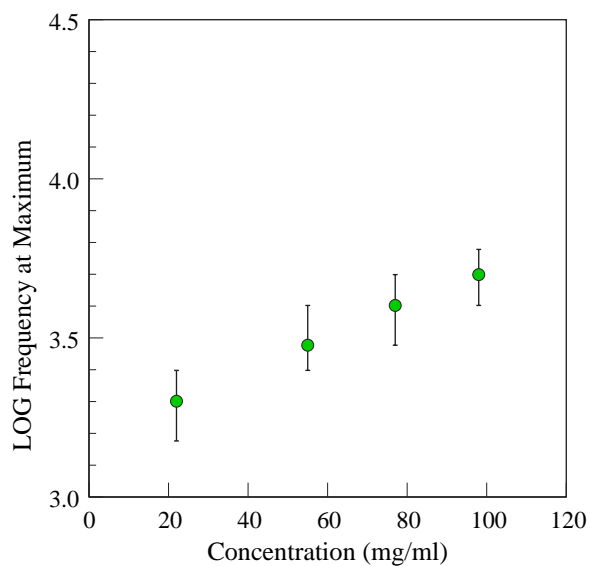


Figure N.10: DNA d.a. KCl : Frequency of Maximum of DS vs. Concentration

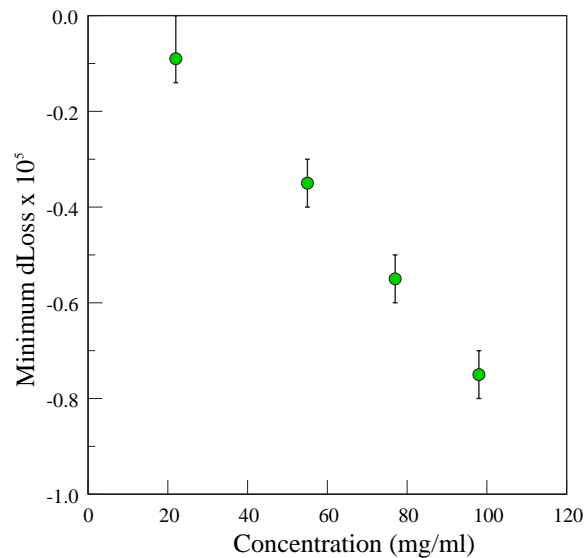


Figure N.11: DNA d.a. KCl : Magnitude of Minimum of DS vs. Concentration

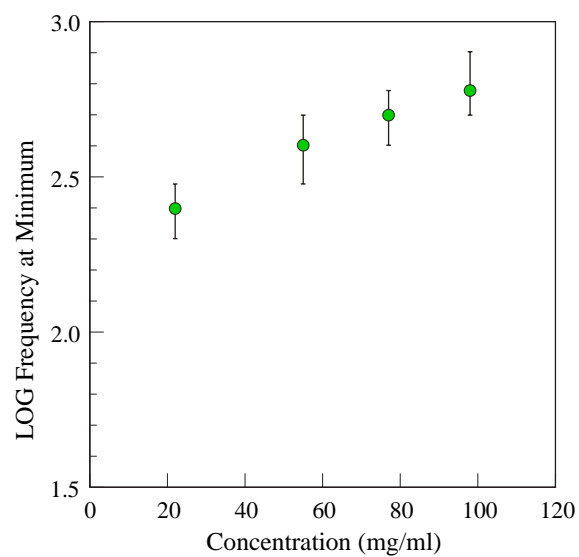


Figure N.12: DNA d.a. KCl : Frequency of Minimum of DS vs. Concentration

### N.0.4 Rubidium Chloride

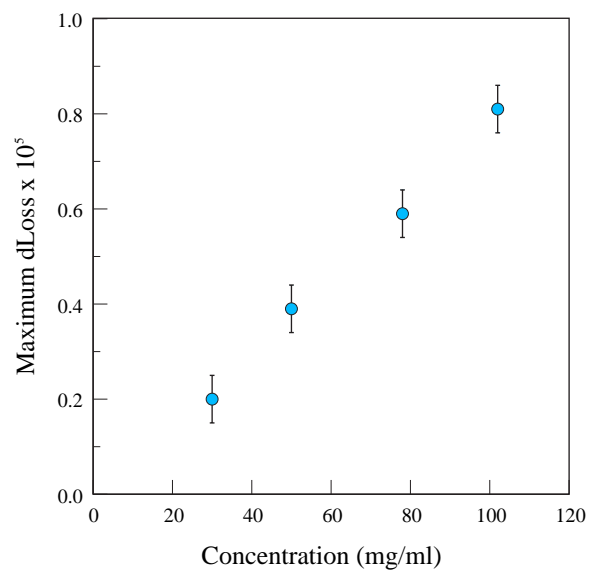


Figure N.13: DNA d.a. RbCl : Magnitude of Maximum of DS vs. Concentration

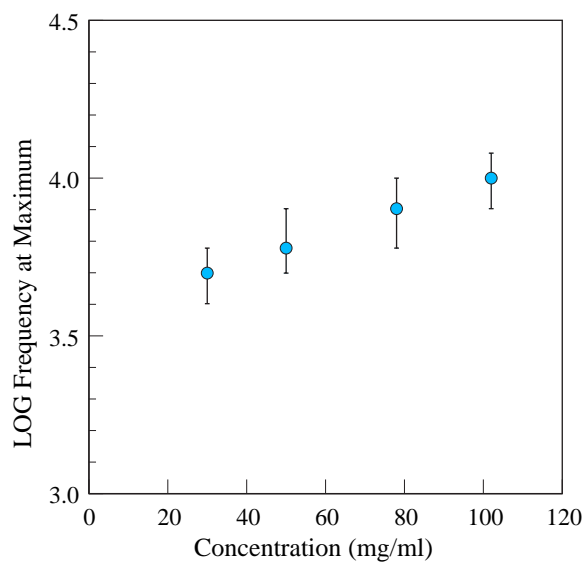


Figure N.14: DNA d.a. RbCl : Frequency of Maximum of DS vs. Concentration



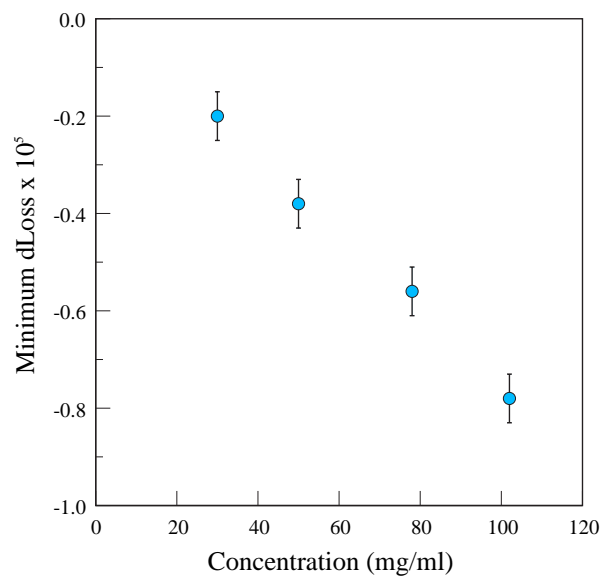


Figure N.15: DNA d.a. RbCl : Magnitude of Minimum of DS vs. Concentration

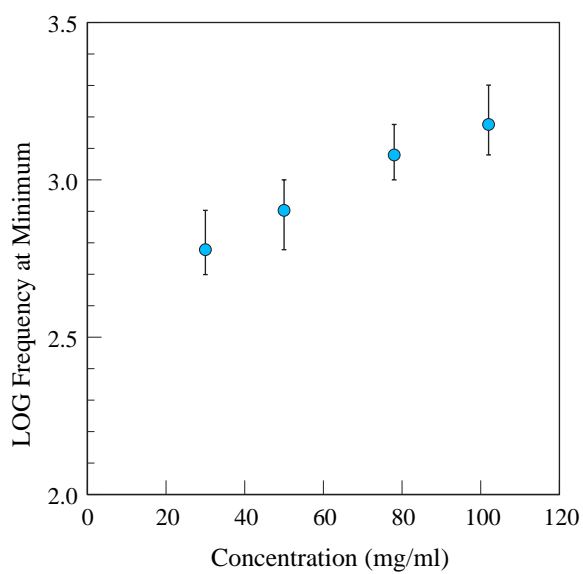


Figure N.16: DNA d.a. RbCl : Frequency of Minimum of DS vs. Concentration

### N.0.5 Calcium Chloride

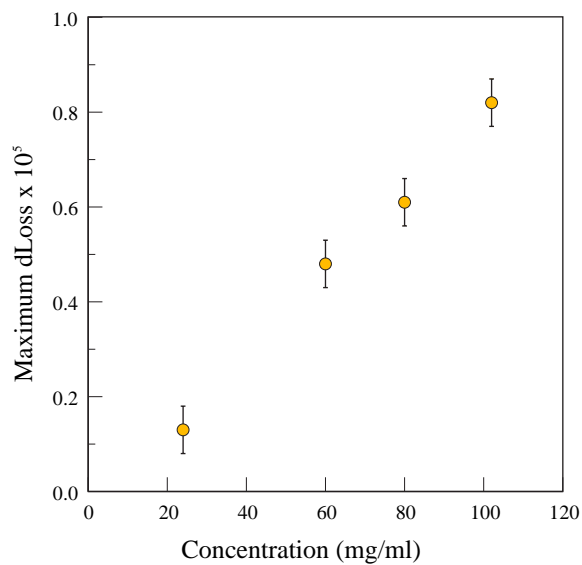


Figure N.17: DNA d.a. CaCl<sub>2</sub> : Magnitude of Maximum of DS vs. Concentration

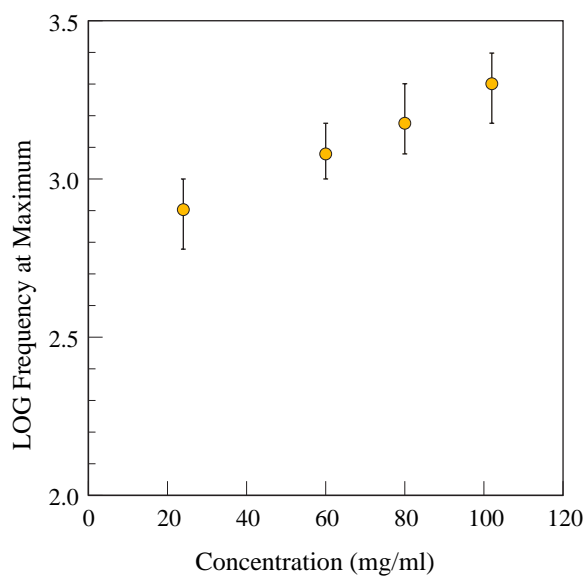
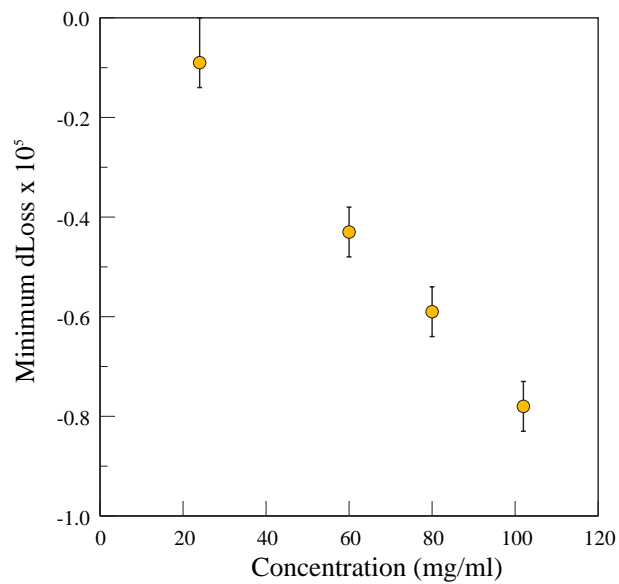
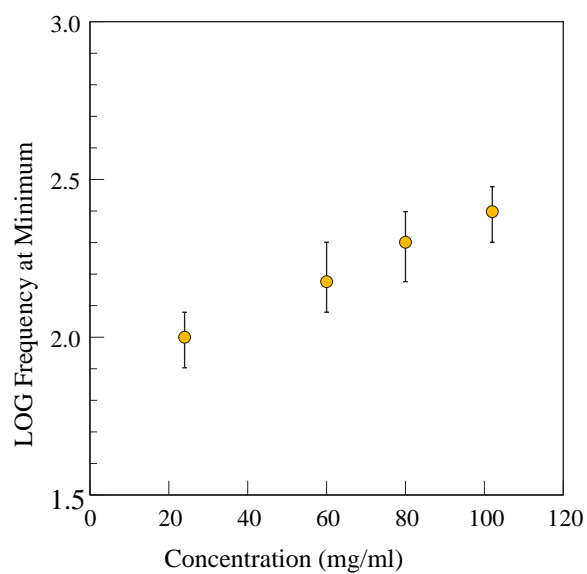


Figure N.18: DNA d.a. CaCl<sub>2</sub> : Frequency of Maximum of DS vs. Concentration

Figure N.19: DNA d.a. CaCl<sub>2</sub> : Magnitude of Minimum of DS vs. ConcentrationFigure N.20: DNA d.a. CaCl<sub>2</sub> : Frequency of Minimum of DS vs. Concentration

# Bibliography

- Arnold, W., Steele, R., and Mueller, H. (1958). On the magnetic asymmetry of muscle fibers. *Proc.Natl.Acad.Sci.USA*, 44:1–4.
- Bain, G. and Berry, J. (2008). Diamagnetic Corrections and Pascal's Constants. *J.Chem.Educ.*, 85:532.
- Bates, R., Staples, B., and Robinson, R. (1970). Ionic Hydration and Single Ion Activities in Unassociated Chlorides at High Ionic Strengths. *Analytical Chem.*, 42:867–871.
- Becker, J., Geacintov, N., Van Nostrand, F., and Van Metter, R. (1973). Orientation of chlorophyll in vivo. Studies with magnetic field oriented Chlorella. *Biochem.Biophys.Res.Comm.*, 51:597–602.
- Becker, J., Trentacosti, F., and Geacintov, N. (1978). A Linear Dichroism Study of the Orientation of Aromatic Protein Residues in Magnetically Oriented Bovine Rod Outer Segments. *Photochemistry and Photobiology*, 27:51–54.
- Bigio, I., Gosnell, T., and Mukherjee, P. (1993). Microwave absorption spectroscopy of DNA. *Biopolymers*, 33:147–150.
- Bondi, A. (1964). Van der Waals Volumes and Radii. *J.Phys.Chem.*, 68:441–451.
- Bone, S. and Small, C. (1995). Dielectric studies of ion fluctuation and chain bending in native DNA. *Biochimica et Biophysica Acta*, 1260:85–93.

- Bonincontro, A., Cametti, C., Di Biasio, A., and Pedone, F. (1984). Effect of ions on counterion fluctuations in low-molecular weight DNA dielectric dispersions. *J.Biophys.*, 45:495–501.
- Brandes, R. and Kearns, D. (1986). Magnetic Ordering of DNA Liquid Crystals. *Biochemistry*, 25:5890–5895.
- Chalazonitis, N., Chagneux, R., and Arvanitaki, A. (1970). Rotation des segments externes des photorecepteurs dans le champ magnetique constant. *C.R.Acad.Sci.Paris*, 271:130–133.
- Cole, R. and Cole, K. (1941). Dispersion and Absorption in Dielectrics. *J.Chem.Phys.*, 9:341.
- Davidson, D. (1961). Dielectric Relaxation in Liquids. *Can.J.Chem.*, 39:571.
- Edwards, G., Davis, C., and Saffer, J. (1984). Resonant microwave absorption of selected DNA molecules. *Phys.Rev.Lett.*, 53:1284–1287.
- Edwards, G., Davis, C., and Saffer, J. (1985). Microwave field-driven acoustic modes in DNA. *Biophys.J.*, 47:799–807.
- Emura, R., Ashida, N., Higashi, T., and Takeuchi, T. (2001). Orientation of Bull Sperms in Static Magnetic Fields. *Bioelectromagnetics*, 22:60–65.
- Finer, E. and Darke, A. (1975). Orientation of Poly-L-Lysine Hydrobromide by Magnetic Fields. *J.Chem.Soc.Farad.Trans.*, 1039:984–.
- Fischer, B., Walther, M., and Jepson, P. (2002). Far infrared vibrational modes of DNA components studied by terahertz time-domain spectroscopy. *Phys.Med.Biol.*, 47:3807–3814.
- Foster, K. R., Stuchly, M. A., Kraszewski, A., and Stuchly, S. S. (1984). Microwave dielectric absorption of DNA in aqueous solution. *Biopolymers*, 23:593–599.

- Glasstone, S., Laidler, K., and Eyring, H. (1941). *The theory of rate processes*. McGraw-Hill, New York.
- Globus, T., Woodward, D., and Samuels, A. (2002). Sub-millimeter-wave Fourier transform spectroscopy of biological macromolecules. *J.Appl.Phys.*, 91:6105–6113.
- Go, Y., Ejiri, S., and Fukada, E. (1969). Magnetic Orientation of Poly- $\gamma$ -benzyl-L-glutamate. *Biochim.Biophys.Acta*, 175:454–458.
- Grant, E., Sheppard, R., and South, G. (1978). *Dielectric behaviour of biological molecules in solutions*. Clarendon Press.
- Greenspan, L. (1977). Humidity Fixed Points of Binary Saturated Aqueous Solutions. *J.Res.Nat.Bur.Standards*, 81A:89.
- Grosse, C. (1989). Microwave absorption of suspensions of DNA type particles in electrolyte solution. *Alta frequenza*, 58:365–368.
- Guerra, C., Bickelhaupt, F., Snijders, J., and Baerends, E. (2000). Hydrogen Bonding in DNA Base Pairs: Reconciliation of Theory and Experiment. *J.Am.Chem.Soc.*, 17:4117–4128.
- Hasted, J. (1973). *Aqueous Dielectrics*. Chapman and Hall, London.
- Hayakawa, R., Sakamoto, M., and Wada, Y. (1978). Dielectric relaxation of DNA solutions. II. *Biopolymers*, 17:1507–1512.
- Hong, F., Mauzerall, D., and Mauro, A. (1971). Magnetic anisotropy and the orientation of retinal rods in a homogeneous magnetic field. *Proc.Natl.Acad.Sci.U.S.A.*, 68:1283–1285.
- Horseý, I. (2001). Design and Testing of Relative Humidity Sensor. Final year project.

- Kauzmann, W. (1942). Dielectric Relaxation as a Chemical Rate Process. *Rev.Mod.Phys.*, 14:12–44.
- Koneshan, S., Rasaiah, J., Lyndon-Bell, R., and Lee, S. (1998). Solvent Structure, Dynamics and Ion Mobility in Aqueous Solutions. *J.Phys.Chem.B*, 102:4193–4204.
- Manning, G. (1969). Limiting laws and counter-ion condensation in polyelectrolyte solutions. *J.Chem.Phys.*, 51:924–933.
- Manning, G. (1978). The molecular theory of polyelectrolyte solutions with applications to the electrostatic properties of polynucleotides. *Q.Rev.Biophysics*, 11:179–246.
- Marcus, Y. (1988). Ionic Radii in Aqueous Solutions. *Chem.Rev.*, 88:1475–1498.
- Maret, G. and Dransfeld, K. (1977). Macromolecules and Membranes in High Magnetic Fields. *Physica*, 86-88B:1077–1083.
- Maret, G., Schickfus, M., Mayer, A., and Dransfeld, K. (1975). Orientation of Nucleic Acids in High Magnetic Fields. *Phys.Rev.Lett.*, 35:397–400.
- Mashimo, S., Umehara, T., Kuwabara, S., and Yagihara, S. (1989). Dielectric study on dynamics and structure of water bound to DNA using a frequency range  $10^7$  -  $10^{10}$  Hz. *J.Phys.Chem.*, 93:4963–4967.
- Minakata, A. (1972). Dielectric properties of polyelectrolytes. *Biopolymers*, 11:1567–1582.
- Molinari, R., Cole, R., and Gibbs, J. (1981). Molecular weight dependence of the low frequency dielectric properties of aqueous solutions of gel-fractionated DNA. *Biopolymers*, 20:977–990.

- Morii, N., Kido, G., Suzuki, H., Nimori, S., and Morii, H. (2004). Molecular Chain Orientation of DNA Films Induced by Both the Magnetic Field and the Interfacial Effect. *Biomacromolecules*, 5:2297–2307.
- Nishizawa, J., Sasaki, T., and Suto, K. (2005). THz transmittance measurements of nucleobases and related molecules in the 0.4 to 5.8 THz region using a GaP THz wave generator. *Opt. Commun.*, 246:229–239.
- Odijk, T. (1979). Possible Scaling Relations for Semidilute Polyelectrolyte Solutions. *Macromolecules*, 12:688–693.
- Pethig, R. (1978). *Dielectric and Electronic Properties of Biological Materials*. John Wiley and Sons.
- Sakamoto, M., Hayakawa, R., and Wada, Y. (1979). Dielectric relaxation of DNA solutions. III. Effects of DNA concentration, protein contamination, and mixed solvents. *Biopolymers*, 18:2769–2782.
- Sakamoto, M., Kanda, H., Hayakawa, R., and Wada, Y. (1976). Dielectric relaxation of DNA in aqueous solutions. *Biopolymers*, 15:879–892.
- Schwan, H. (1966). Alternating Current Electrode Polarization. *Biophysik*, 3:181–201.
- Shen, Y., Upadhyaya, P., and Linfield, E. (2004). Vibrational spectra of nucleotides studied using terahertz time-domain spectroscopy. *Vib. Spectroscop.*, 35:111–114.
- Starkweather, H. (1990). Distribution of activation enthalpies in viscoelastic relaxations. *Macromolecules*, 23:328–332.
- Stokes, R. and Robinson, R. (1948). Ionic Hydration and Activity in Electrolyte Solutions. *J. Am. Chem. Soc.*, 70:1870–1878.
- Strzelecka, T., Davidson, M., and Rill, R. (1988). Multiple Liquid Crystal Phases of DNA at High Concentrations. *Nature*, 331:457–460.



- Strzelecka, T. and Rill, R. (1988). Solid-State 31-P NMR Studies of DNA Liquid Crystalline Phases. The Isotropic to Cholesteric Transition. *Nature*, 331:457–460.
- Sun, M., Pejanovic, S., and Mijovic, J. (2005). Dynamics of Deoxyribonucleic Acid Solutions as Studied by Dielectric Relaxation Spectroscopy and Dynamical Mechanical Spectroscopy. *Macromolecules*, 38:9854–9864.
- Suzuki, M. and Nakamura, H. (1996). Orientation of Sperm DNA under a Magnetic Field. *Proc.Jap.Acad.*, 71:36–38.
- Swicord, M. and Davis, C. (1982). Microwave absorption of DNA between 8 GHz and 12 GHz. *Biopolymers*, 21:2453–2460.
- Swicord, M. and Davis, C. (1983). An optical method for investigating the microwave absorption characteristics of DNA and other biomolecules in solution. *Bioelectromagnetics*, 4:21–42.
- Takashima, S. (1963). Dielectric dispersion of DNA . *J.Mol.Biol.*, 7:455–467.
- Takashima, S. (1989). *Electrical Properties of Biopolymers and Membranes*. Adam Hilger.
- Takashima, S., Gabriel, C., Sheppard, R., and Grant, E. (1984). Dielectric behavior of DNA solution at radio and microwave frequencies. *Biophysical J.*, 46:29–34.
- Takeuchi, T., Nakaoka, Y., Emura, R., and Higashi, T. (2001). Diamagnetic Orientation of Bull Sperms and Related Materials in Static Magnetic Fields. *J.Phys.Soc.Jap.*, 71:363–368.
- Thrane, L., Jacobsen, R., Jepsen, P. U., and Keiding, S. (1995). THz reflection spectroscopy of liquid water. *Cem.Phys.Letters*, 30:1893.

- Tohyama, K. and Miyata, N. (1974). Magnetic Alignment and Diamagnetic Anisotropy of Cholesteric Liquid Crystalline Poly- $\gamma$ -benzyl-L-glutamate. *Mol. Cryst. and Liq. Cryst.*, 29:35–42.
- Tomic, S., Babic, S., and Vuletic, T. (2007). Dielectric relaxation of DNA aqueous solutions. *Phys. Rev. E.*, 75:1–13.
- van der Touw, F. and Mandel, M. (1974). Dielectric increment and dielectric dispersion of solutions containing simple charged linear macromolecules. *Biophys. Chem.*, 2:218–230.
- Van Winkle, D., Chatterjee, A., Link, R., and Rill, R. (1997). Magnetic-field alignment of cholesteric liquid-crystalline DNA. *Physical Review E*, 55:4354–4359.
- Van Winkle, D., Davidson, M., Chen, W.-X., and Rill, R. (1990). Cholesteric Helical Pitch of Near Persistence Length DNA. *Macromolecules*, 23:4140–4148.
- Volger, J. (1960). Dielectric Properties of Solids in Relation to Imperfections. *Progress in Semiconductors*, 4:205.
- Wittlin, A., Genzel, L., and Kremer, F. (1986). Far infrared spectroscopy on oriented films of dry and hydrated DNA. *Phys. Rev. A.*, 34:493–500.
- Yanson, I., Teplitsky, A., and Sukhodub, L. (1979). Experimental studies of molecular interactions between nitrogen bases of nucleic acids. *Biopolymers*, 18:1149–1170.